EXPRESSION OF SELECTED CADHERINS IN ADULT ZEBRAFISH VISUAL

SYSTEM AND REGENERATING RETINA, AND MICROARRAY ANALYSIS

OF GENE EXPRESSION IN *PROTOCADHERIN-17* MORPHANTS

A Dissertation

Presented to

The Graduate Faculty of The University of Akron

In Partial Fulfillment

of the Requirements for the Degree

Doctor of Philosophy

Alicja Marlowe

August, 2022

EXPRESSION OF SELECTED CADHERINS IN ADULT ZEBRAFISH VISUAL

SYSTEM AND REGENERATING RETINA, AND MICROARRAY ANALYSIS

OF GENE EXPRESSION IN *PROTOCADHERIN-17* MORPHANTS

Alicja Sochacka-Marlowe

Dissertation

Approved: Accepted:

_____   _____
Advisor   Department Chair
Dr. Qin Liu   Dr. Stephen Weeks

_____   _____
Committee Member   Dean of the College
Dr. Richard Londraville   Dr. Mitchell S. McKinney

_____   _____
Committee Member   Interim Director, Graduate School
Dr. Brian Bagatto   Dr. Marnie Saunders

_____   _____
Committee Member   Date
Dr. Rolando J.J. Ramirez

_____
Committee Member
Dr. Zhong-Hui Duan

ABSTRACT

Cadherins are cell-adhesion molecules that play important roles in animal development, maintenance and/or regeneration of adult animal tissues. In order to understand cadherins' functions in adult vertebrate visual structures, one must study their distribution in those structures. First, I examined expression of *cadherin-6*, *cadherin-7*, *protocadherin-17* and *protocadherin-19* in the visual structures of normal adult zebrafish using RNA *in situ* hybridization, followed by studying expression of two Krüppel-like transcription factors (*klf6a* and *klf7*), that are known markers for regenerating adult zebrafish retinas and optic nerves, in normal adult zebrafish brain, normal and regenerating adult zebrafish retinas. Then, I investigated expression of these cadherins in regenerating adult zebrafish retinas using both RNA *in situ* hybridization and quantitative PCR. Finally, as the first step in elucidating molecular mechanisms underlying protocadherin-17 (one of the cadherins that I studied) function in zebrafish visual system development, I used DNA microarray analysis to study gene expression of zebrafish embryos with their *protocadherin-17* expression blocked by morpholino antisense oligonucleotides (these embryos are called *protocadherin-17* morphants).

The major findings include: 1) *cadherin-6*, *cadherin-7*, *protocadherin-17* and *protocadherin-19* were differently expressed in the retina and major visual

structures of normal adult zebrafish brain. 2) *klf6a* and *klf7* showed similar expression patterns in most visual structures in the adult fish brain, and in regenerating retinas, but *klf6a* appeared to be a superior regeneration marker based on RNA *in situ* hybridization. 3) These four cadherin molecules showed distinct expression patterns in the regenerating zebrafish retinas. 4) Several genes involved in vision and/or visual development were significantly down-regulated in the *protocadherin-17* morphants compared to control embryos.

My results suggest that these cadherins play differential roles in the maintenance and regeneration of the adult zebrafish visual system, and protocadherin-17 may function in the zebrafish visual system development via affecting expression of these genes involved in vision and/or visual development.

ACKNOWLEDGMENTS

My sincerest gratitude goes towards my advisor, Dr. Qin Liu, for giving me this excellent research opportunity. His knowledge, guidance and patience were essential for my success in the graduate school. I would like to express my appreciation to Dr. Richard Londraville for his advice with qPCR, microarray and the writing process. My earnest thanks go to Dr. Zhong-Hui Duan for her expertise and for teaching me about microarrays in the computational biology class. I would like to acknowledge Dr. Brian Bagatto, Dr. Rolando J. J. Ramirez and Dr. Jordan Renna for their valuable time and helpful suggestions.

I would like to thank my dear colleagues, Dr. Yun Chen, Dr. Sunil Bhattarai, Dr. Hope Ball, Dr. Mark Dalman, Dr. Mary Beth Wade, Dr. Jeremy Prokop and Dr. Reed Davis, who provided me with the valuable knowledge and advice. My deepest gratitude goes to the Dean of Students Office staff, Mike Strong and Rylie Crine, for their exceptional support and guidance during the dissertation writing process.

Special appreciation goes to my son Kuba, my parents Anna and Krzysztof, my brother Marcin, all of my grandparents and my friends. Thank you, from the bottom of my heart, for always believing in me.

TABLE OF CONTENTS

LIST OF FIGURES

FIGURE   PAGE

LIST OF TABLES

CHAPTER I

GENERAL INTRODUCTION

Cadherin superfamily

The development of multicellular organisms was possible because of

adhesion proteins binding them together (Suzuki 2000; Rokas 2008). Cadherins

are transmembrane proteins with binding properties that are mediated by their

extracellular domains that require Ca^{2+} ions (Boggon et al. 2002; Sotomayor et

al. 2014).The cadherin superfamily consists of over 100 members that are

present in all metazoans studied (Hulpiau and Van Roy 2009, 2011; Oda and

Takeichi 2011). Cadherins are important players in development, and they are

also involved in the maintenance and function in adult animals (Takeichi 1990;

Yagi and Takeichi 2000; Halbleib and Nelson 2006; Vestweber 2015; Suzuki and

Hirano 2016). Cadherins usually mediate homophilic cell-cell adhesion (Takeichi

1988; Cailliez and Lavery 2005). Based mainly on the number of the extracellular

domains and the distribution in genome, the cadherin superfamily is organized

into six subfamilies: classical cadherins, protocadherins, desmosomal cadherins,

Fat-cadherins, Flamingo/CELSR cadherins and cadherin-like adhesion

molecules (Takeichi 1990; Nollet et al. 2000; Yagi and Takeichi 2000; Hulpiau

and Van Roy 2009, 2011; Oda and Takeichi 2011; Brasch et al. 2012; Hirano and Takeichi 2012; Sotomayor et al. 2014).

A typical cadherin molecule consists of three domains (Figure 1.1): a large extracellular domain (EC) made of several homologous repeats, a short hydrophobic transmembrane domain and a cytoplasmic domain (Blaschuk et al. 1990). A hallmark of the cadherin superfamily is the presence of minimum two tandem ECs, each containing conserved calcium-binding residues. As three Ca^{2+} coordinated ions bind in between consecutive ECs, the linker region stabilizes its shape and trypsin cannot degrade the cadherin. The exact sequences between EC differ, but each is about 110 amino acids in length and its translated protein has a domain made of seven antiparallel β-strands (Brodt 1996; Brasch et al. 2012). Cadherins primarily interact with each other at the most distant domain from the plasma membrane, namely EC1. The cadherin interaction can be either between cadherins on the same cell (*cis*) or between cadherins on two opposing cells (*trans*). Cell-cell adhesion is achieved by *trans* interactions and *cis* interactions modulating strength of adhesion (Van Roy and Berx 2008; Brasch et al. 2012). Cadherin interactions are mostly homophilic (between the same type, e.g. cdh6 and cdh6) but heterophilic interactions (between different types, e.g. cdh2 and pcdh19) have also been reported (Emond et al. 2011). The transmembrane domain anchors the molecule to the cell membrane, while the cytoplasmic domain binds to other proteins including catenins that, in turn, bind to cytoskeletal proteins (e.g. actin, Yagi and Takeichi 2000; Vestweber 2015). In addition to acting as cellular "glues", cadherins are also involved in many

processes that affect cell survival, differentiation, migration, tissue growth, axonal extension, pathfinding, synaptic formation and stabilization (Yagi and Takeichi 2000; Wheelock and Johnson 2003; Halbleib and Nelson 2006; Clendenon et al. 2012; Hayashi et al. 2014; Stoeckli 2014; Missaire and Hindges 2015; Vestweber 2015). Mutations or malfunctions in cadherins result in various defects in developing animals (Kanzler et al. 2003; Ruan et al. 2006; Emond and Jontes 2008; Clendenon et al. 2012; Chen et al. 2013; Izuta et al. 2014), and numerous diseases in humans, including hereditary deafness (Usher syndrome), cardiovascular diseases and neuropsychiatric diseases (Resink et al. 2009; El-Amraoui and Petit 2010; Glover et al. 2012; Redies et al. 2012). Furthermore, altered expression of cadherins, especially E-cadherin (also called cadherin-1), has been found in all major forms of cancers (Berx and Van Roy 2009; Schmalhofer et al. 2009).
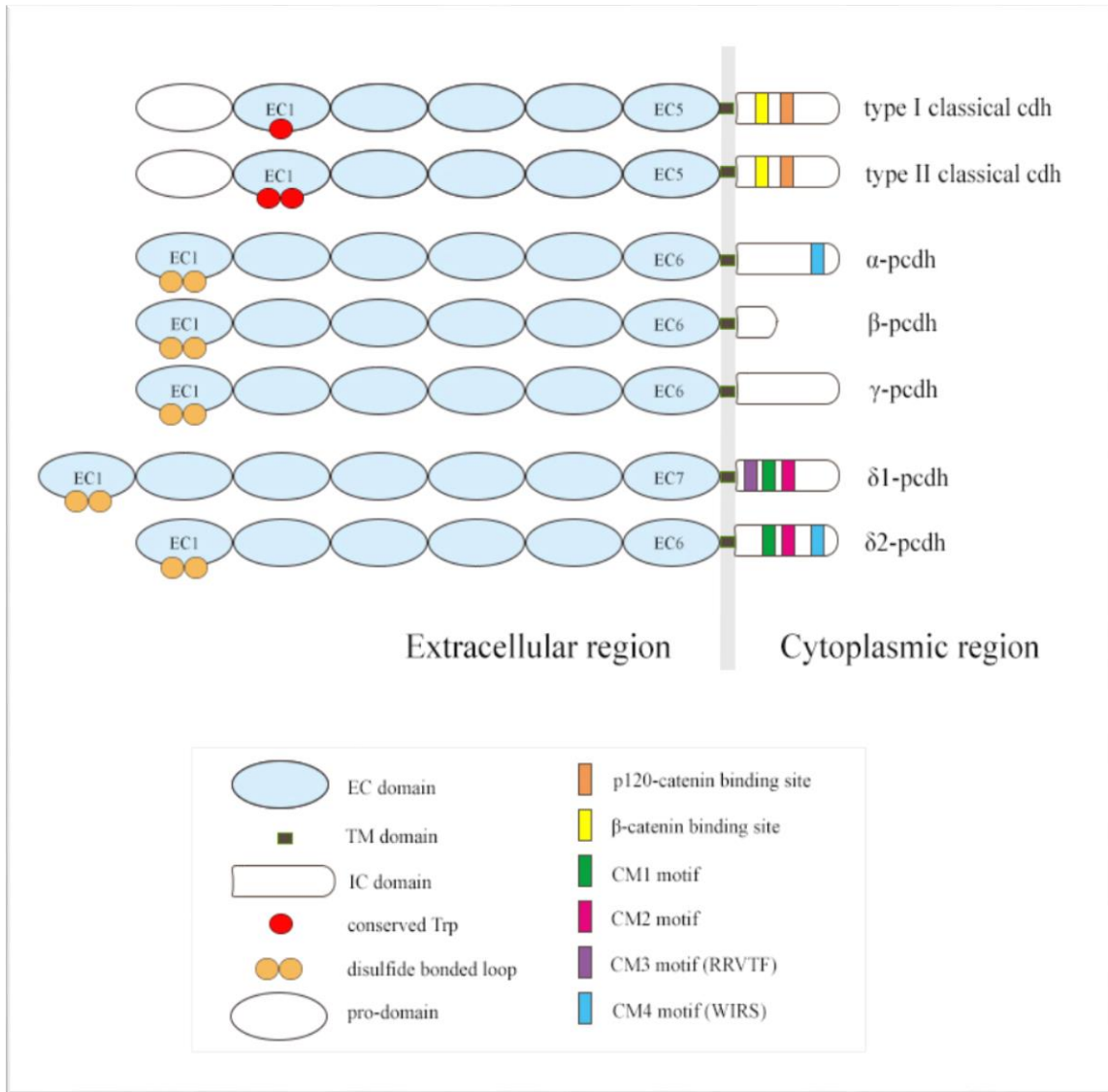
Figure 1.1. Domains of select members from classical cadherin and protocadherin subfamilies. Picture omits subfamilies desmosomal cadherins, Fat-cadherins, Flamingo/CELSR cadherins, and cadherin-like adhesion molecules. Only first and last EC domains are numbered for clarity. Adapted and modified from Morishita and Yagi (2007) and Hirano and Takeichi (2012). Abbreviations: EC – extracellular, TM – transmembrane, IC – intracellular/cytoplasmic.

Classical cadherins

The first cadherin was discovered by Masatoshi Takeichi (1977) who noticed that trypsin treatment permanently disrupted cell-cell adhesion, instead of only transiently. His trypsin solution also contained EDTA, which traps calcium. This made him realize the importance of calcium in cell adhesion. Further studies using cell aggregation assays of Chinese hamster V79 cells let Takeichi discover that cell adhesion can be calcium-dependent or calcium-independent, and the cell adhesion mediated by cadherins is calcium-dependent (Takeichi 1977, 2018; Okada 1996).

Cadherins were named after "calcium-dependent adherent protein" because in the presence of calcium they resist dissociation of cell aggregates by trypsin in vertebrate tissues (Hatta et al. 1985; Nose and Takeichi 1986). When calcium is absent, cell-cell connection mediated by cadherins degrades and thus cell complexes are more likely to dissociate. Ca^{2+} ions keep the EC of cadherins rigid and thereby protect it from proteolysis (Takeichi 1991).

The classical cadherins (e.g. cdh1, cdh2, cdh6) contain five extracellular EC repeats (Hirano et al. 1992; Yagi and Takeichi 2000; Lilien and Balsamo 2005). The intracellular portion (i.e. the cytoplasmic domain) of the cadherin interacts with p120-catenin that stabilizes and regulates availability of the cadherin. In addition, this domain also binds to beta-catenin/Armadillo, which in turn binds to alpha-catenin (which binds to actin cytoskeleton). The intracellular domains of the classical cadherins are more conserved, unlike the other regions of the molecule. The classical cadherins are divided into two groups based

mainly on presence of the conserved tryptophan (Trp) in the most distal extracellular domain (EC1): type-I (Trp2) and type-II (Trp2 and Trp4, Van Roy 2012). For example, each member of the type-I cadherins has a HAV tripeptide located in the EC1 (near the N-terminal), whereas each member of the type-II cadherins has a QIA tripeptide in this region. The type-I cadherins include cdh1 (E-cadherin), cdh2 (N-cadherin), cdh3 (P-cadherin) and cdh4 (R-cadherin), while the type-II include cdh6, cdh7, cdh8, cdh9 and cdh11 (Tanihara et al. 1994).

In addition to mediating strong homophilic cellular interactions, the classical cadherins also affect development and physiology via Wnt signalling pathways (Nelson and Nusse 2004; Agathocleous and Harris 2009; Heuberger and Birchmeier 2010). Interactions of classical cadherins are crucial for cell sorting in embryogenesis and morphogenesis of the majority of organs (Gumbiner 2005; Halbleib and Nelson 2006).

Type-I cadherins

Cadherin-1 (cdh1 or E-cadherin)

Cdh1 is the most studied and understood member of the cadherins (Hatta et al. 1985; Van Roy and Berx 2008). A PubMed search of "E-cadherin" returns over 35,000 publications and most of them are from the last 10 years. Cdh1 was isolated from epithelial tissues where it is strongly expressed, and thus was called E-cadherin (Yoshida and Takeichi 1982). Cdh1 expression in mouse embryos begins as early as the two-cell stage and its expression continues in the ectoderm of older embryos in most epithelial tissues (Larue et al. 1994). Cdh1

has a vital role during the early development of the mouse (Wheelock and Johnson 2003; Van Roy and Berx 2008; Van Roy 2012; Pieters et al. 2016). Two of the most important functions of cdh1 in adult animals seem to be maintenance of adult epithelial structures (e.g. adherens junctions) and role in cancer suppression (Vleminckx and Kemler 1999; Schmalhofer et al. 2009).

Similar cdh1 expression and function are found in zebrafish. Cdh1 is strongly expressed in epithelial tissues in developing zebrafish (Babb and Marrs 2004), and *cdh1* mutant zebrafish embryos show severe morphological defects and die early (Shimizu et al. 2005).

Cadherin-2 (cdh2 or N-cadherin)

The second most studied classical cadherin is cdh2 or N-cadherin. It is strongly expressed in the nervous system (Hatta et al. 1985). A search for "N-cadherin" in PubMed returns over 29,000 publications. Cdh2 expression starts in the neural precursor cells soon after gastrulation, while the entire ectoderm continues expressing cdh1, but on the dorsal region of the vertebrate embryo, neural precursor cells begin to express cdh2. These cdh2-expressing cells segregate from the cdh1-expressing cells, and begin their development from neural plate to neural tube, and the central and peripheral nervous systems (Takeichi 1987). At the molecular level, cdh2 stabilizes dynamics of adherens junctions (Bunse et al. 2013; Garg et al. 2015) and in rats cdh2 activates and regulates beta-catenin signaling in neuronal precursors (Zhang et al. 2010).

Cdh2 is expressed in developing chicken central nervous system (CNS) neurites (Redies et al. 1992), developing retina (Matsunaga et al. 1988), retinorecipient laminae (RL) in the optic tectum (Inoue and Sanes 1997), spinal cord (Lin et al. 2014), and neuromuscular system (Cifuentes-Diaz et al. 1994). Cdh2 is also broadly expressed in the developing mouse brain and olfactory system (Redies and Takeichi 1993; Akins et al. 2007). Furthermore, cdh2 is important for development of myocardium in mice embryos (Radice et al. 1997). Cdh2 is involved in establishing neuronal circuits (Obst-Pernberg et al. 2001). For example, cdh2 functions in axon guidance and target selection in *Xenopus* retinal ganglion cells (RGCs) (Riehl et al. 1996).

Zebrafish cdh2 was first isolated by Bitzur et al. (1994) who described its expression in the CNS of developing zebrafish. Cdh2 is also expressed in other zebrafish tissues, including the inner ear (Babb-Clendenon et al. 2006), olfactory system (Liu et al. 2004b), lateral line system and cranial ganglia (Liu et al. 2003; Kerstetter et al. 2004). Cdh2 plays an important role in CNS development, retinal development, inner ear development and lateral line system formation (Matsunaga et al. 1988; Lele et al. 2002; Liu et al. 2003; Novince et al. 2003; Babb-Clendenon et al. 2006).

Cadherin-4 (cdh4 or R-cadherin)

Cdh4 is another member of the type-I cadherin subfamily and was characterized by Suzuki et al. (1991). Cdh4 is expressed strongly in the nervous system, and was isolated for the first time from the chicken retina, hence the

name retinal cadherin (Inuzuka et al. 1991a, 1991b). Further studies examined cdh4 expression in the CNS of chickens and mice (Redies et al. 1992; Redies and Takeichi 1993, 1996; Miskevich et al. 1998; Hertel et al. 2012; Lin et al. 2014).

In developing chicken neural tube, cdh4 starts its expression after cdh2. Although some expression of both in the spinal cord is similar (Lin et al. 2014), the pattern of expression between them is different in developing CNS (brain and spinal cord), e.g. only cdh4 is detected in the tectoisthmic pathway (Inuzuka et al. 1991b; Redies et al. 1992, 1993). Cdh4 in developing chick is present in the optic tectum, nucleus rotundus and the cerebellum (Miskevich et al. 1998; Wöhrn et al. 1999; Becker and Redies 2003; Redies et al. 2011). In developing and adult mice, cdh4 is widely and strongly expressed in the embryonic olfactory system (Akins et al. 2007), in the parahippocampal area (Zhou et al. 2020), forebrain, amygdala, hypothalamus (Obst-Pernberg et al. 2001; Hertel et al. 2012), neocortex and cerebellum (Hertel and Redies 2011; Redies et al. 2011) and somatosensory cortex of the adult mouse (Krishna-K et al. 2011).

Functions of cdh4 in the nervous system are associated with the adhesive properties of this classical cadherin. Since the expression of cdh4 is more restricted than cdh2 in developing vertebrate brain, cdh4 is speculated to be involved in formation of nuclei and mediate selective fasciculation and/or pathfinding (segregation) of neurons forming functional circuits (Redies et al. 1993; Redies and Takeichi 1996; Wöhrn et al. 1999; Obst-Pernberg et al. 2001). Additionally, cdh4 is likely to play a role in establishing connectivity and

patterning of the cerebellum due to its specific expression pattern (Arndt et al. 1998).

In zebrafish, cdh4 expression was first studied by Liu et al. (1999b), showing its expression in visual structures (e.g. retina, optic nerve, optic tectum) of developing embryos. Additionally, cdh4 is present in other nervous structures including the olfactory bulb, telencephalon, tegmentum, cerebellum, hindbrain, spinal cord, cranial and lateral line ganglia of developing embryos (Liu et al. 2003, 2004b). Compared to cdh2, cdh4 expression in the developing zebrafish starts later (at least 15 hours) and is more restricted (Bitzur et al. 1994; Liu et al. 1999b; Liu and Londraville 2003). Interfering with cdh4 function using morpholino antisense oligonucleotide (MO) technology in embryonic zebrafish resulted in embryos with defects in the visual structures, e.g. reduced retinal ganglion cell (RGC) differentiation (Babb et al. 2005) and in the cranial and lateral line system (Wilson 2007).

In summary, results from studies of the classical type-I cadherins expression and function in several model organisms demonstrate that these cadherins control cell-cell adhesion, tissue morphogenesis, development of various tissues and organs, and are involved in maintaining adult structures.

Type-II cadherins

Cadherin-6 (cdh6 or K-cadherin)

Cdh6 is a type-II classical cadherin which was first isolated from rat brain by Suzuki et al. (1991) and later from fetal kidney tissue (Xiang et al. 1994).

Cdh6 is expressed in both nervous tissues (e.g. brain and retina) and non-nervous tissues (e.g. kidney) in developing zebrafish, *Xenopus* and mice (Suzuki et al. 1991; Cho et al. 1998; Mah et al. 2000; Liu et al. 2006, 2008a; Ruan et al. 2006).

In *Xenopus*, *cdh6* is expressed in neural crest cells, cranial ganglia, lateral line ganglia and dorsal root ganglia (David and Wedlich 2000). In the chicken neural tube, cdh6 regulates generation of dorsal interneurons that express Islet-1 (Park and Gumbiner 2015). *Cdh6* is detected in the spinal cord of the developing chicken since early stage 2.5E in neural crest and roof plate, and continues to be expressed in the floor plate and the lateral medial column (LMC) neurons till E10 (Lin et al. 2014). In the chicken neural tube, cdh6 regulates generation of dorsal interneurons in the spinal cord that express Islet-1 (Park and Gumbiner 2015). During mouse CNS development, *cdh6* expression is detected in restricted areas of the brain including the midbrain and hindbrain boundary (Inoue et al. 1997, 1998). Cdh6 is also expressed in cortical area of postnatal mice and therefore has been proposed to organize the cortical landscape by cell-sorting mechanism of classical cadherins (Egusa et al. 2015). Additionally, *cdh6* has a defined expression edge in the cortical plate, between the limb field and somatosensory barrel in mice at postnatal day 5 (P5, Terakawa et al. 2013).

The majority of studies on cdh6 have been concentrated on its expression and function in renal cells during development or cancer pathogenesis (Sancisi et al. 2013; Bringuier et al. 2015; Karthikeyan et al. 2016). Cdh6 also plays a role in the development of nephrons in *Xenopus* (Kubota et al. 2002), and interfering

with *cdh6* expression in mouse embryos causes defects in the kidney (Mah et al. 2000). Furthermore, cdh6 is involved in neural crest cell development by suppressing epithelial-to-mesenchymal transition: cdh6 expression is reduced in the neural crest cells before and for the period of their migration away from the dorsal neural tube (Clay and Halloran 2014).

In developing zebrafish CNS, *cdh6* is detected at the edge of the neural keel at 12 hpf, and later (at 18 hpf and 24 hpf) in dorsal telencephalon and regions of the diencephalon, dorsal regions of the spinal cord. *Cdh6* expression becomes increased as development proceeds, *cdh6* is found in regions of the dorsal thalamus, posterior hypothalamus and anterior cerebellum, and the midbrain and hindbrain boundary of 46-48 hpf embryos (Liu et al. 2006). Additionally, *cdh6* is expressed in neural crest cells, lateral line ganglia, cranial ganglia and dorsal root ganglia. Blocking *cdh6* function using morpholino technology resulted in the morphants (24 to 72 hpf) with smaller eyes, thoracic edema, smaller and misshaped cranial and lateral line ganglia (Liu et al. 2011b).

Cadherin-7 (cdh7)

Cdh7 is another member of the type-II classical cadherins, and was first isolated by Suzuki et al. (1991) from the rat brain. Cdh7 is found in developing ferret (*Mustela putorius furo*) blood vessels in the brain and in the lungs of adult mice (Moore et al. 2004; Krishna and Redies 2009).

Cdh7 is known to be expressed in the nervous system of developing vertebrates including zebrafish, chickens, rats and humans (Liu et al. 2007a,

2008b; Takahashi and Osumi 2008). Developing chicken has cdh7 expressed in the cerebellum (Redies et al. 2011), cerebellar cortex (Arndt et al. 1998), hindbrain, cranial motoneurons (Barnes et al. 2010) and in the spinal cord (Lin et al. 2014). Cdh7 was found in the embryonic mouse brain from E12-P15 (Faulkner-Jones et al. 1999) in the following structures: the amygdala (Hertel et al. 2012), hippocampus (Lefkovics et al. 2012), pontine nucleus during synaptogenesis (Kuwako et al. 2014) and in the primary somatosensory cortex (Lefkovics et al. 2012). In the adult mouse, cdh7 expression is limited to CNS structures including the cortex, hippocampus, amygdala and cerebellum (Faulkner-Jones et al. 1999; Moore et al. 2004; Hertel and Redies 2011; Krishna-K et al. 2011; Redies et al. 2011; Hertel et al. 2012; Lefkovics et al. 2012, 2012; Stoya et al. 2014). Developing marmoset (*Callithrix jacchus*) expresses cdh7 in the motor cortex, temporal neocortex and the thalamus (Matsunaga et al. 2015).

After interfering with *cdh7* function in chicken hindbrains *in ovo* (E2), growth of cranial motor axons were disturbed and neurites lost polarity and branched more (Barnes et al. 2010). *Cdh7* knockdown in developing mice disrupts axon connections in the pontine nucleus (Kuwako et al. 2014). In addition, cdh7 promotes axon growth and target finding, but suppresses axon branching in cultures of chick cranial motoneurons (Barnes et al. 2010).

In developing zebrafish, *cadherin-7* mRNA (*cdh7*) expression is found in both the brain and notochord (Liu et al. 2008b). *Cdh7* expression in zebrafish is first observed at 12 hpf in the neural keel. As development progresses, *cdh7* is found in the forebrain, midbrain and hindbrain, and its expression is reduced in 3

13

dpf embryos (Liu et al. 2007a). Interestingly, blocking *cdh7* function using specific morpholinos in embryonic zebrafish resulted in apparent defects mainly in the notochord, with the morphant embryos having curved and/or twisted bodies (Liu et al. 2008b).

Classical cadherins in the vertebrate visual system

Both the classical type-I cadherins and type-II cadherins are expressed in eyes of model organisms, including zebrafish (Liu et al. 1999b, 2001), *Xenopus* (Ruan et al. 2006), and mice (Faulkner-Jones et al. 1999; Xu et al. 2002); see Table 1.1.

Table 1.1. Expression of selective classical cadherins in the visual system of model organisms. Asterisks indicate expression in development and adult, otherwise the expression is solely during development. Abbreviations: (d)LGN – (dorsal) lateral geniculate nucleus, gcl – ganglion cell layer, inl – inner nuclear layer, onl – outer nuclear layer, opl – outer plexiform layer, RGC – retinal ganglion cell, V1 – primary visual cortex, V2 – secondary visual cortex.

Cdh	Expression in the visual structures	Model organism (Reference)
cdh1	cornea, epithelium of lens, eyelids, RGCs	mouse (Xu et al. 2002; De la Huerta 2013)
cdh2	inl, RGCs, superior colliculus, retinorecipient nuclei	mouse (Redies and Takeichi 1993; Honjo et al. 2000a; Xu et al. 2002; Osterhout et al. 2011)

	ipl, opl, optic nerve fiber (RGC), outer limiting membrane, nucleus rotundus, optic tectum	chicken (Matsunaga et al. 1988; Miskevich et al. 1998; Becker and Redies 2003)
	gcl, inl, onl	*Xenopus* (Simonneau et al. 1992)
	retinal precursor cells, ipl, opl, optic nerve, whole retina (4 day larvae)	zebrafish (Liu et al. 1999b, 2001; Liu and Londraville 2003)
	optic tectum	zebrafish* (Liu et al. 1999b, 2001)
cdh4	inner inl, middle inl, RGCs, V1, V2	ferret (Etzrodt et al. 2009; Krishna-K et al. 2009)
	amacrine and horizontal cells, mostly OFF-projecting RGCs, superior colliculus, retinorecipient nuclei, dLGN	mouse (Honjo et al. 2000a; Osterhout et al. 2011; De la Huerta 2013)
	RGCs, superior colliculus, nucleus rotundus	chicken (Inuzuka et al. 1991a; Miskevich et al. 1998; Becker and Redies 2003)

	gcl, inl, ipl, opl, optic tectum, outer limiting membrane, nucleus rotundus	zebrafish (Liu et al. 1999b, 2001)
	RGCs, inner inl, optic nerve, optic tectum	zebrafish* (Liu et al. 1999b, 2001)
cdh6	middle temporal visual area (MT, V5), LGN (V1)	marmoset (Matsunaga et al. 2014)
	horizontal cells, RGCs, V1	ferret (Etzrodt et al. 2009; Krishna-K et al. 2009)
	amacrine cells, mostly ON-OFF direction-selective RGCs (dsRGCs), RGCs, superior colliculus, retinorecipient nuclei	mouse (Honjo et al. 2000a; Osterhout et al. 2011; De la Huerta et al. 2012; De la Huerta 2013)
	RGCs, amacrine cells, optic nerve, optic tectum, retinorecipient nuclei, nucleus rotundus	chicken (Redies and Takeichi 1993; Wöhrn et al. 1998, 1999; Honjo et al. 2000b; Becker and Redies 2003)
	retina	*Xenopus* (David and Wedlich 2000)

	RGCs, inl, onl, optic nerve	zebrafish (Liu et al. 2008a)
cdh7	RGCs, displaced RGCs, horizontal cells, onl	ferret (Etzrodt et al. 2009)
	primary visual cortex (V1)	ferret* (Krishna-K et al. 2009)
	retina, retinorecipient nuclei	mouse (Faulkner-Jones et al. 1999; Osterhout et al. 2011)
	retina	rat (Takahashi and Osumi 2008)
	RGCs, inl, amacrine cells, optic nerve, retinorecipient nuclei, retinorecipient laminae, optic tectum, nucleus rotundus	chicken (Wöhrn et al. 1998, 1999; Becker and Redies 2003; Yamagata et al. 2006)
	retina, optic tectum, pretectal region	zebrafish (Liu et al. 2007a)

Cadherin-2 (cdh2) in the visual system

In developing *Xenopus*, *cdh2* is detected in the retina in tailbud stage (Nieuwkoop-Faber stage 20 to 40 NF); with reduced expression in tadpole stage (41-50 NF). Cdh2 is expressed throughout the developing chicken retina from embryonic day 4.5 untill hatching, with particularly strong expression in the outer nuclear layer (onl), gcl and inl (Matsunaga et al. 1988; Inuzuka et al. 1991a;

17

Miskevich et al. 1998). Cdh2 is also detected in the optic nerve, optic tract, optic tectum and in the tectofugal pathway and its target nuclei in the optic tectum of the developing chicken (Inuzuka et al. 1991a; Redies et al. 1993; Uchida et al. 1996; Inoue and Sanes 1997; Miskevich et al. 1998; Wöhrn et al. 1998). Cdh2 is expressed in both the ganglion cell layer (gcl) and inner nuclear layer (inl) of developing mouse retina, optic tract, and regions of the rodent brain receiving direct retinal projections, such as the superior colliculus, pretectal nucleus, anterodorsal and anteromedial nuclei of thalamus (Itaya 1980; Redies and Takeichi 1993; Obst-Pernberg et al. 2001; Xu et al. 2002).

Inhibiting cdh2 function by a dominant-negative cdh2 form or a cdh2 functional blocking antibody in *Xenopus* retina resulted in defective RGC differentiation or pathfinding of retinotectal projection (Riehl et al. 1996; Stone and Sakaguchi 1996).

The entire CNS of the developing zebrafish expresses cdh2 (Bitzur et al. 1994; Liu et al. 2001). The cdh2 expression is detected early in the optic primordium (20-24 hpf) and later all retinal precursor cells express cdh2 (Liu et al. 2001). Cdh2 expression is observed in the eye between 32-34 hpf, when RGCs start to differentiate (Schmitt and Dowling 1996; Hu and Easter 1999). At 50 hpf, cdh2 is localized in both the inner and outer plexiform layers, optic nerve, optic chiasm and optic tract, while its expression in the cellular retinal layers is reduced. In 3- and 4-day old larvae, cdh2 expression continues to be detected in the plexiform layers, optic nerve, optic chiasm and optic tract, and its expression in the cellular layers continues decreasing. In adult zebrafish retina, apparent

cdh2 expression is observed only in the outer plexiform layer and peripheral marginal zone (germinal zone, Liu et al. 2001). Zebrafish *cdh2* mutants have defective retinal lamination, reduced numbers of RGCs, amacrine cells and photoreceptors, with optic nerve pathfinding defects to the optic tectum (Masai et al. 2003).

In the optic tectum, strong cdh2 expression is present at as early as 24 hpf (Liu et al. 2004a). Cdh2 expression in the optic tectum is reduced somewhat in 34-80 hpf embryos, during which time RGC axons first arrive to the anterior part of the tectum at around 45 hpf and finish innervating the entire optic tectum by 72 hpf (Stuermer 1988; Burrill and Easter 1994). In 3- and 4-day old larvae, cdh2 expression becomes increased again in the optic tectum, but only in the superficial layer (including retinorecipient layer), and not in the cellular layer (Liu et al. 2001).

Cadherin-4 (cdh4) in the visual system

In the visual system, cdh4 was first characterized in the chicken retina by Inuzuka et al. (1991b). Interestingly, cdh4 was never found in RGCs or the optic nerve of the chicken (Redies et al. 1993; Miskevich et al. 1998; Wöhrn et al. 1998, 1999). However, cdh4 is expressed by the developing chicken's optic tectum, tectoisthmic and retinofugal pathways (Redies et al. 1993; Wöhrn et al. 1998). Cdh4 expression is detected in the gcl and inl of developing mouse embryos (P7, P14). Out of many RGC subtypes, cdh4 is found in five of them (De la Huerta 2013). Mouse brain visual structures that are cdh4-positive include

the lateral geniculate nucleus (LGN), the superior colliculus and the dorsal colliculus, a retinorecipient area (Redies and Takeichi 1993; Arndt et al. 1998; Vanhalst et al. 2005; De la Huerta 2013).

In zebrafish visual structures, cdh4 is first detected in an anteroventral region of the retina around 32 hpf (Liu et al. 1999b). As development proceeds, cdh4 is expressed by the RGC axons (36 hpf), gcl, inner half of the inl, optic nerve, optic tract and optic tectum (50 hpf). Similar cdh4 expression is also found in 3-4-day old larvae (Liu et al. 2001). Cdh4 expression is also found in the pretectum (a visual structure) of developing zebrafish (36 hpf to 4-day old). Blocking cdh4 function using morpholino technology resulted in the morphants with reduced eye size, reduced differentiation of retinal neurons (e.g. RGCs, amacrine cells, and photoreceptors), and abnormal development of the optic tectum (e.g. poorly developed, Babb et al. 2005).

Cadherin-6 (cdh6) in the visual system

Cdh6 is expressed in developing *Xenopus* in the gcl and onl of the retina, at stages examined (26, 32, 40, David and Wedlich 2000). Interfering with cdh6 function in *Xenopus* resulted in defective retinal development, including small eye size, likely caused by reduced proliferation of retinal cells, and misfolded neuroepithelium that caused retinal lamination defects (Ruan et al. 2006).

The chicken cdh6 was previously known as cdh6b (Arndt et al. 1998; Wöhrn et al. 1998, 1999; Honjo et al. 2000b; Becker and Redies 2003). A detailed study of cdh6 expression in developing chicken visual system by Wöhrn

20

et al. (1998) showed that cdh6 is expressed as early as E5 in a subset of RGCs and its expression is stronger in the central gcl until at least E14, when the displaced RGCs are found in the inl. Besides, cdh6 is present in a subset of amacrine cells in the inl and displaced amacrine cells in the gcl (starting at E9) and in the ipl (E11), until E18. In addition, cdh6 is also expressed in a subset of bipolar cells in opl (E11-E14) and in the outer portion of inl (E14) where most horizontal cells are located (Wöhrn et al. 1998). In the chicken optic pathway (optic nerve, optic chiasm and optic tract), cdh6 is first detected in the optic fibers at E5. Its expression is increased at E8-E18. Most retinal fibers projecting to mesencephalic nuclei and diencephalic nuclei express cdh6. At E11, other vision-related brain regions expressing cdh6 include nucleus lateralis anterior, ventral geniculate nucleus, external pretectal nucleus, nucleus of the basal optic root, area pretectalis, nucleus lateralis anterior of the thalamus, ventral lateral geniculate nucleus, and external pretectal nucleus (Wöhrn et al. 1998).

In the developing mouse retina, cdh6 expression is present in the gcl and inl (P7 mice, De la Huerta 2013). At P14, cdh6 continues to be expressed in the gcl, but only in a subset of RGCs. In the developing mouse brain, cdh6 expression is detected in the subsets of cells in the superficial layer of the superior colliculus (P14) and the middle-temporal visual area (both targets of non-primary visual pathway). Both the superior colliculus and the middle-temporal visual area are regions processing the motion perception (Osterhout et al. 2011; De la Huerta 2013).

Developing ferret retina expresses *cdh6* in the neuroblast layer (nbl) since E23, and the signal becomes restricted to its inner portion, that becomes gcl at E38 (Etzrodt et al. 2009). Once all three layers form at P13, *cdh6*-expressing cells continue to be detectable in small cells in the gcl and in the inner potion of inl, and this pattern continues until adulthood (P60). After birth (P2), *cdh6* is also observed in sparsely separated large RGCs located in gcl and in the displaced RGCs in the inner part of inl. Etzrodt et al. (2009) speculated that those large cells are not displaced RGCs, but another population of amacrine cells. For more expression of cdh6 in the visual system of model organisms, refer to Table 1.1. *Cdh6* is expressed in embryonic zebrafish retina during critical stages of its development (Liu et al. 2006). The earliest *cdh6* expression becomes detectable in a small anteroventral retina (where differentiating RGCs are located) of 34 hpf zebrafish embryos. Later in development (46-48 hpf), *cdh6* expression is found in the gcl and inner portion of inl where presumptive amacrine cells are located. Similar to cdh6 in the developing mouse retina, *cdh6* expression is detected in only a subset of RGCs. Blocking cdh6 function in developing zebrafish with morpholino technology resulted in reduced eye size, likely caused by reduced cell proliferation rates in the retina. Furthermore, differentiation of RGCs, amacrine cells and photoreceptors is also adversely affected (e.g. reduced number of these cells, decreased dendrites and/or axons, Liu et al. 2008a). These results are similar to those from the *Xenopus* study (see above).

Cadherin-7 (cdh7) in the visual system

In the developing chicken retina, cdh7 is first expressed at E2 (stage 18) when RGCs differentiate (Prada et al. 1991). Cdh7 is expressed in distinct populations of retinal cells, such as in bipolar cells and amacrine cells (Wöhrn et al. 1998). Cdh7 is expressed in inl (amacrine cells and some bipolar cells), ipl, certain RGCs, displaced RGC (characterized by large nuclei) and in the Müller glia (Wöhrn et al. 1998, 1998, 1998; Yamagata et al. 2006). Furthermore, ventral retina has higher density of cdh7-expressing cells than the dorsal retina (Yamagata et al. 2006). In the optic pathway of developing chicken, cdh7 is expressed in only few fibers and in retinorecipient laminae (SGFS-c) of the optic tectum (Wöhrn et al. 1998, 1999; Yamagata et al. 2006). In addition, cdh7 is found in the nucleus rotundus (in dorsal thalamus), a structure receiving visual cues from the optic tectum (Becker and Redies 2003). Moreover, the following retinorecipient structures in the developing chicken brain express cdh7: the anterior dorsolateral complex of the thalamus, external pretectal nucleus, griseum tectale, nucleus lateralis anterior, nucleus of the basal optic root, perirotundic area, superficial synencephalic nucleus of Rendahl, ventral geniculate nucleus and ventrolateral nucleus (Wöhrn et al. 1998).

Young mice express *cdh7* in the eye (E17-P13, Faulkner-Jones et al. 1999) with strong *cdh7* expression in gcl and inl (amacrine and horizontal cells) between P7 and P14 (De la Huerta 2013). The adult mouse eye has much higher cdh7 expression than that in the brain; cdh7 is found in subpopulations of cells in

gcl (displaced amacrine cells, confirmed by immunocytochemistry marker HPC-1) and in inner part of inl (in amacrine cells, Faulkner-Jones et al. 1999).

In the visual system of developing ferret retina, cdh7 is found in the inner layer of the optic cup, called the neuroblast layer (E23-P2), and further in all retinal layers: in gcl (E38-P60), all areas of inl (P13-P60) and briefly at P13 in onl (Etzrodt et al. 2009). For more expression of cdh7 in the visual system of model organisms, refer to Table 1.1.

In the developing visual system of zebrafish, *cdh7* is expressed first at 52 hpf in gcl and the inner portion of the inl (where amacrine cells reside) and becomes slightly reduced at 70 hpf (Liu et al. 2007a). *Cdh7* morphants exhibit a reduction of differentiating RGCs (Liu et al. 2008b).

Classical cadherins functions in human diseases

In humans, mutations in cadherins cause various diseases, including psychiatric and neural disorders (El-Amraoui and Petit 2010; Brayshaw and Price 2016). Several members of the classical cadherin family have been implicated in various diseases including obsessive-compulsive disorder (OCD, CDH2), macular pigmentary abnormalities (CDH3), autism spectrum disorder (CDH9, CDH10, CDH13), bipolar disorder (CDH7), CHARGE syndrome (CDH7), major depressive disorder, attention-deficit/hyperactivity disorder (ADHD, CDH13), schizophrenia (CDH13), addiction disorders (CDH13), severe intellectual disability (CDH15, M-cadherin), sensorineural deafness (CDH23) and Usher syndrome (CDH23) (Bhalla et al. 2008; Lasky-Su et al. 2008; Lesch et al. 2008;

24

Wang et al. 2009; Soronen et al. 2010; El-Amraoui and Petit 2010; Chapman et al. 2011; Børglum et al. 2014; Li et al. 2014; Salatino-Oliveira et al. 2015; McGregor et al. 2016; Galvez-Ruiz et al. 2020).

Protocadherins

The largest subfamily and the most recently discovered cadherins are the protocadherins (pcdhs), which have more than 80 members in mammals (Nollet et al. 2000). Using PCR with degenerate primers for EC of the classical cadherins, Suzuki and colleagues isolated two transcripts with similar classical cadherin EC domains but with differing intracellular domains (Sano et al. 1993). These two new cadherins were named pcdh42 and pcdh43 (Sano et al. 1993). Unlike the classical cadherins, the pcdhs have larger EC domains (e.g. δ-pcdhs have 6 or 7 ECs), and their cytoplasmic domains are less conserved, binding with proteins such as TAF1/Set and protein phosphatase 1 alpha (Yoshida et al. 1999; PP1α, Redies 2000; Redies et al. 2005; Hirano and Takeichi 2012). This is different from the classical cadherins with their cytoplasmic domain interacting with catenins (see above). Furthermore, genomic analysis reveals that each EC domain of the classical cadherins is encoded by multiple exons, while each EC domain of pcdhs is encoded by one large exon (about 2000 nucleotides long, Wu and Maniatis 1999; Frank and Kemler 2002). Since the pcdh EC sequences are found in multiple species of invertebrates and vertebrates, the term "protocadherins" was used, reasoning that they were the precursors to cadherins; proto in Greek means "first" (Sano et al. 1993). That idea assumes that pcdhs

underwent processes of duplication and diversification over the course of evolution, resulting in the formation of the new subfamily: the cadherins (Suzuki 1996). This hypothesis has been proven wrong by a recent phylogenetic analysis showing that pcdhs are conserved among the vertebrate species because protocadherin promoter motif sequence of the constant region is homologous between human and zebrafish (Wu and Maniatis 1999; Noonan et al. 2004). Due to possibly simpler nervous systems, invertebrate organisms *Drosophila melanogaster*, *Caenorhabditis elegans* and *Ciona savignyi* lack pcdh clusters in their genomes but several classical cadherins are present in those invertebrates, and are also conserved with the cadherins found in vertebrates, e.g. human, mouse, rat, zebrafish (Hill et al. 2001). Noonan et al. (2004) postulated that evolution of a more complex CNS in vertebrates was possibly supported by an emergence of clustered pcdhs.

Based on their genomic organization, pcdhs are divided into clustered and non-clustered pcdhs (Redies et al. 2005; Hulpiau and Van Roy 2009, 2011; Chen and Maniatis 2013). Figure 1.2 illustrates the classification of pcdhs. The clustered pcdhs (α-, β- and γ-pcdhs) are found concentrated in three genomic regions, while the non-clustered pcdhs (δ-pcdhs and unclassified pcdhs) are disseminated throughout various genomic locations (Wu and Maniatis 1999; Nollet et al. 2000).
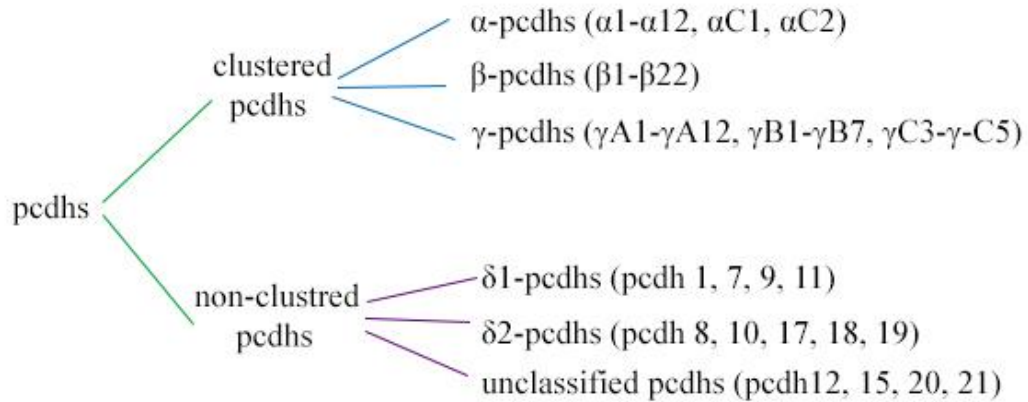
Figure 1.2. Classification of protocadherin family members. Adapted from Hayashi and Takeichi (2015). Zebrafish lacks β-pcdh cluster, and has additional set of α and γ cluster (Noonan et al. 2004).

Generally speaking, most classical cadherins are expressed in multiple tissues while pcdhs are mainly restricted to the CNS (Suzuki 2000; Wolverton and Lalande 2001; Wheelock and Johnson 2003; Chen and Maniatis 2013). The pcdhs have unique spatial and temporal distribution patterns during brain morphogenesis, and they participate in the formation of proper neuronal structures through neuronal migration and synapse formation (Frank and Kemler 2002; Nakao et al. 2008; Garrett and Weiner 2009; Hirayama and Yagi 2013; Coughlin and Kurrasch 2015). Moreover, classical cadherins mediate stronger cell-cell adhesion mainly through homophilic interactions, while pcdhs mediate weaker cell-cell adhesion through either homophilic or heterophilic interactions, likely affecting animal development mainly through regulating cell signaling (Obata et al. 1995; Frank et al. 2005; Reiss et al. 2006; Morishita and Yagi 2007; Hirano and Takeichi 2012; Peek et al. 2017).

Clustered pcdhs (α, β and γ-pcdhs)

The clustered pcdhs have similar genomic organization in humans and mice, while zebrafish lacks the β-pcdh cluster, but has an extra set of α-pcdh and γ-pcdh. In the genome, variable regions of exons (coding for EC, TM and part of CP domains) of α-pcdh and γ-pcdh genes are clustered together and are located next to constant exons (coding for the majority of CP domain). Transcripts of these clustered pcdhs are generated by alternative splicing of their 5' variable exons, combining with the 3' constant exons, resulting in many different isoforms, each made of a different variable region and the same constant region (Wu and Maniatis 1999; Blevins et al. 2011; Chen and Maniatis 2013; Hirayama and Yagi 2013). α-pcdhs show heterophilic binding via motifs Cys-X$_5$-Cys or RGD that are recognized and bound by β1-integrin (Mutoh et al. 2004; Morishita et al. 2006). However, homophilic *trans* interaction has also been documented in crystal structures of α-pcdh and β-pcdh (Goodman et al. 2016).

The clustered pcdhs were first described in humans by Wu and Maniatis (1999). They described them as cadherin-related neuronal receptors (CNRs), which corresponds to α-pcdh cluster. In the mammal CNS, clustered pcdhs are expressed mainly in numerous brain regions, including the cerebellum, hippocampus, neocortex and optic lobe (Hirano et al. 1999; Vanhalst et al. 2005; Cronin and Capehart 2007; Kim et al. 2007; Uemura et al. 2007; Wu and Jia 2020).

α-pcdhs are localized at synapses (young and adult neocortex), in the hippocampus, cerebellum and mitral cells of the olfactory bulb in adult mice

(Kohmura et al. 1998; Blank et al. 2004). Intracellularly, α-pcdhs interact with the tyrosine kinase Fyn, and are involved in long-term potentiation (LTP) and regulation of synaptic plasticity (Kohmura et al. 1998). Other binding partners in cytoplasm are neurofilament M, fascin, FAK, PYK2 and WRC (Chen et al. 2009; Kim et al. 2011; Sotomayor et al. 2014). Conserved cytoplasmic binding domain CM4 interacts with the cytoskeleton (Chen et al. 2014). Peptide CM4 is also called WIRS (WAVE-interacting receptor sequence) because it binds with the Wiskott-Aldrich syndrome family verprolin homologous protein (WAVE) from the WAVE regulatory complex (WRC). WRC complex controls dynamics of the actin cytoskeleton and comprises of actin regulator Nck-associated protein (Nap1), Wiskott-Aldrich syndrome protein family verprolin-homologous protein 1 (WAVE1), Abelson-interacting protein 2 (Abi2), hematopoietic stem/cell progenitor protein 300 (HSPC300), and cytoplasmic FMR1-interacting protein 1 (CYFIP1, Chen et al. 2014; Hayashi et al. 2014). In mice, reduced dendritic spines and simplified dendrites occur in *α-pcdh* knockout (Suo et al. 2012). Down-regulation of α-pcdh cluster adversely affects working memory in fear-conditioned learning in mice (Fukuda et al. 2008).

β-pcdhs are expressed at postsynaptic membranes in the mammal CNS (Junghans et al. 2008). Variable exons code for the whole protein and no cytoplasmic binding partners have been identified to date. Analysis of mouse mutants lacking the whole *β-pcdh* cluster provided us with important insights of their function in neuronal survival in the brainstem and the spinal cord interneurons (Hasegawa et al. 2016).

γ-pcdhs are expressed in dendrites, axons (Garrett and Weiner 2009) and subsets of excitatory synapses in embryonic rat hippocampal cell cultures (Banker and Goslin 1998; Tanaka et al. 2000; Phillips et al. 2003; Frank et al. 2005). Developing mice (E16 through P0) express γ-pcdhs in the brain, spinal cord and dorsal root ganglia, while in adult mice γ-pcdhs have high expression in the cortex, hippocampus and cerebellum (Wang et al. 2002). In developing avian brains, γ-pcdhs are found in areas in the fore-, mid- and hindbrain and in the spinal cord (Cronin and Capehart 2007). γ-pcdhs mediate homophilic interactions but the strength of their adhesion is not as strong as that of the classical cadherins (Fernández-Monreal et al. 2009). Cytoplasmic binding partners include kinases FAK, FYN, PKC (Chen et al. 2009; WAVE pathway, Keeler et al. 2015), microtubule-destabilizing protein SCG10 (Gayet et al. 2004; Sotomayor et al. 2014; Keeler et al. 2015, 2015), γ2-GABA$_A$ receptor (GABA signaling, Li et al. 2012b), Axin1 (Wnt pathway, Mah and Weiner 2016), programmed cell death 10 (PDCD10, apoptosis, Lin et al. 2010) and calmodulin-dependent protein kinase phosphatase (CaMKP, calcium signaling, Onouchi et al. 2015). γ-pcdhs are directly implicated in synaptic development of the spinal cord in mice (Weiner et al. 2005), although they are not required to initiate synaptogenesis (Phillips et al. 2003). Mice lacking the entire γ-pcdh cluster have abnormal axonal projections or smaller spinal cord due to extensive apoptosis of spinal interneurons (Wang et al. 2002; Hasegawa et al. 2016).

α-pcdh and γ-pcdh expression partially overlap in cultured hippocampus neurons. Heterotypical binding between α-pcdh and γ-pcdh forms a functional

protein complex that augments expression of α-pcdh proteins (Murata et al. 2004). Simultaneous knockdown of α-pcdh and γ-pcdh clusters in developing chickens increases apoptosis in the spinal cord (Han et al. 2010). Paired *α-pcdh* knockout with *γ-pcdh* RNAi knockdown causes reduction and simplification of dendrites in mice (Suo et al. 2012).

Clustered pcdhs in the vertebrate visual system

α-pcdhs

In young mice (P10-P14), α-pcdh is expressed in the lateral geniculate nucleus (LGN), the main target of RGC exons, and in the primary visual cortex (V1, Morishita et al. 2004). Deletion in the α-pcdh constant region in mice causes defects in the primary somatosensory cortical pathways, which is similar to posterior parietal cortex (PPC) lesions in mice (Yamashita et al. 2012). This result suggests that α-pcdhs are required for normal functioning of PPC where special recognition for somatosensory and visual information is integrated (Yoshitake et al. 2013).

β-pcdhs

In the developing mouse retina, β-pcdh is expressed in the post-synaptic membrane in the inner plexiform and outer plexiform layers, and in the outer segment of photoreceptors (Junghans et al. 2008). There are no published studies about β-pcdh gene cluster function in the visual system.

γ-pcdhs

In the developing chicken, γ-pcdhs are present in the optic tectum, suggesting its function in the formation of the visual circuitry (Cronin and Capehart 2007). There is no published information about γ-pcdhs expression in the chicken retina, nor in developing mouse retinas. In the adult mouse eye, γ-pcdhs are expressed at high levels (Frank et al. 2005). Specifically, γ-pcdhs are highly expressed in the inner plexiform layer and the outer plexiform layer (both comprised of synapses). Weaker expression is found in the outer segment of the photoreceptor layer, while the rest of the retinal layers have scattered expression of γ-pcdhs (Wang et al. 2002). Blocking all 22 γ-pcdhs in mice retina resulted in increased apoptosis in interneurons and RGCs (Lefebvre et al. 2008). However, neuronal signaling, synaptic formation, and layer-specific dendritic arborization appeared to be normal in mice without the γ-pcdh cluster. These results suggest that the γ-pcdhs are not essential for proper vision, but are important in regulation of neuronal populations during the early stages of retinal development (Lefebvre et al. 2008).

Additionally, deletion of either two (β-pcdh and γ-pcdh) or three (α-pcdh, β-pcdh and γ-pcdh) clusters increases neuronal death in the mouse retina (E18.5), and especially affects RGCs, amacrine cells and bipolar cells (Hasegawa et al. 2016).

Teleosts (including zebrafish) underwent a whole-genome duplication event in the ray-finned fish lineage (Amores et al. 1998). Unlike terrestrial vertebrates, teleosts have two α-pcdh and two γ-pcdh gene clusters, but lack

evolutionarily newer β-pcdh gene cluster (Noonan et al. 2004; Wu 2005). α-pcdh

and γ-pcdh are highly expressed in the developing zebrafish retina and in the

synaptic neuropil of the optic tectum (Biswas et al. 2012). Knockdown of *α-pcdhs*

causes neuronal apoptosis (Emond and Jontes 2008), which is similar to mice

(see above).

Non-clustered pcdhs (δ-pcdhs and unclassified pcdhs)

The non-clustered pcdhs are comprised of three subgroups: δ1-pcdhs

(pcdh1, pcdh7, pcdh9 and pcdh11), δ2-pcdhs (pcdh8, pcdh10, pcdh17, pcdh18

and pcdh19) and unclassified or non-categorized pcdhs (e.g. pcdh12, pcdh15,

pcdh20, pcdh21, Redies et al. 2005; Vanhalst et al. 2005; Morrow et al. 2008).

These subgroups differ mainly in the number of the EC homologous repeats, with

the δ1-pcdhs having seven EC repeats, while the δ2-pcdhs having six EC

repeats (Suzuki 2000). Additionally, different conserved motifs in the cytoplasmic

domains distinguish these subgroups: δ1-pcdhs have CM1, CM2 and CM3, while

δ2-pcdhs have CM1, CM2 and CM4/WIRS (Vanhalst et al. 2005). pcdh20 has

similarities with extracellular domains of δ-pcdhs, but it has truncated cytoplasmic

domain and lacks any of above CM motifs, therefore it is non-categorized

(Hulpiau and Van Roy 2009; Hayashi and Takeichi 2015). The conserved CM3

motif (RRVTF) in the δ1-pcdhs is important for binding with cytosolic

phosphatase PP1α, and functions possibly in synaptic plasticity (Yoshida et al.

1999; Munton et al. 2004; Redies et al. 2005; Kim et al. 2011). Another

conserved motif, CM4 or WIRS (present in pcdh9 and all δ2-pcdhs) recruits the

WAVE complex and regulates actin cytoskeleton polymerization (Chen et al. 2014; Hayashi et al. 2014). Protocadherins interact with many other intracellular binding partners that function as signal transducers in various mechanisms, and new molecules that interact with pcdhs have continuously been identified. In the δ1-pcdh subgroup, pcdh1 interacts with SMAD, pcdh7c interacts with protein phosphatase-1α (PP1α), and pcdh11Yc interacts with β-catenin (Yoshida et al. 1999; Chen et al. 2002; Hertel et al. 2008; Kim et al. 2011; Sotomayor et al. 2014; Faura Tellez et al. 2015). Studies on the δ2-pcdh subgroup revealed that pcdh8 binds with serine-threonine kinase (TAO2β), pcdh10 binds with the actin regulatory complex (Nap1/WAVE1), pcdh17 interacts with Nap1, WAVE1 and Abi1 (from WRC complex), pcdh19 interacts with Cyfip2, and pcdh18 binds to mouse disabled-1 (Homayouni et al. 2001; Yasuda et al. 2007; Nakao et al. 2008; Tai et al. 2010; Kim et al. 2011; Biswas et al. 2014; mDab1, Sotomayor et al. 2014). Additionally, molecular binding partners include C2kβ and Nlk1 (Wnt pathway, Kietzmann et al. 2012; Kumar et al. 2017), α1-GABAAR (GABA, Bassani et al. 2018) and non-POU-domain-containing octamer binding protein (NONO), a co-regulator of steroid hormone nuclear receptors (Pham et al. 2017). Lastly, molecular binding partners of unclassified cadherin-like molecules include Sans, Harmonin a (pcdh15) and Sans, Harmonin b, Myosin VIIa (Hirano and Takeichi 2012; cdh23, Sotomayor et al. 2014; Suzuki and Hirano 2016).

Most δ-pcdhs are present in all CNS subdivisions, from the forebrain to the spinal cord. In the brain, δ-pcdhs are expressed in the thalamus, sub-lamina regions of the cortex, cerebellum, hippocampus and basal ganglia (Hirano et al.

1999; Vanhalst et al. 2005; Kim et al. 2007, 2010; Uemura et al. 2007; Krishna-K et al. 2011; Redies et al. 2011; Lin et al. 2012, 2013).

δ1-pcdhs

Pcdh1 expression is not detected in embryonic rat brains but is highly expressed in the postnatal (P3) and adult rat brains (Sano et al. 1993; Kim et al. 2007). In zebrafish and *Xenopus*, pcdh1 ortholog is axial protocadherin (AXPC), which is found in the brain at the tailbud stage of *Xenopus* (Kim et al. 1998; Kuroda et al. 2002).

In developing *Xenopus*, expression of pcdh7 (NF-protocadherin) is found in the neural folds and neural tube. Pcdh7 used to be called BH-protocadherin due to its prominent expression in the brain (cerebral cortex) and heart of adult mice (Yoshida et al. 1998, 1999). In the developing mice (P1), pcdh7 is expressed in numerous brain regions including the insular cortex, temporoparietal cortex, perirhinal cortex, caudate-putamen, dorsal thalamus, hypothalamus, pretectal area, and amygdaloid complex (Vanhalst et al. 2005). Functional study of pcdh7 in developing *Xenopus* reveals that this protocadherin directs neurulation (helps to fold the neural tube) by interacting with TAF1 (Bradley et al. 1998; Heggem and Bradley 2003; Rashid et al. 2006).

Both pcdh9 and pcdh11 have similar wide expression in the developing mouse brain (Redies et al. 2005). In humans, PCDH9 is expressed in the same fetal and adult brain areas, including cerebral cortex (e.g. frontal and temporal

35

lobes), striatum, amygdala, hippocampus, thalamus, cerebellum, medulla and spinal cord (Strehl et al. 1998).

Humans have two copies of PCDH11, called PCDHX and PCDHY, and both are widely expressed in the fetal brain (Yoshida and Sugano 1999; Blanco et al. 2000), and in various brain regions in the adults (Blanco et al. 2000; Blanco-Arias et al. 2004).

In the developing zebrafish CNS, δ1-pcdhs (e.g. pcdh1a, pcdh1b, pcdh7a, pcdh7b and pcdh9) have similar expression patterns and are mainly found in a segmental fashion in the telencephalon and hindbrain (Blevins et al. 2011).

δ2-pcdhs

In mice, pcdh8 expression is detected in the brain of both embryos and adults (Makarenkova et al. 2005; Hertel et al. 2012; Stoya et al. 2014). The brain regions that express pcdh8 include the olfactory bulb, cerebral cortex, amygdala, hippocampus, parahippocampal region, inferior colliculus, hindbrain and spinal cord (Makarenkova et al. 2005). In embryonic rats (P3), expression of pcdh8 in brain comprises of regions such as the cerebral cortex, olfactory bulb, amygdaloid complex and hippocampal formation (Kim et al. 2007). Similar PCDH8 expression is found in human fetal and adult brains e.g. cerebral cortex, striatum, and hippocampus (Strehl et al. 1998).

Expression of both pcdh10, pcdh18 and pcdh19 was first described in rat brains by Wolverton and Lalande (2001). Pcdh10 (also called OL-protocadherin) expression is found in the olfactory system, limbic structures and cerebellum

36

(Hirano et al. 1999; Redies 2000; Luckner 2001; Kim et al. 2007). Pcdh10 is implicated to play roles in brain compartmentalization, axonal growth and target selection (Hirano et al. 1999; Lee et al. 2003; Uemura et al. 2007). Actin binding protein Nap-1 interacts with pcdh10 or pcdh18b to regulate axon motility (Nakao et al. 2008; Biswas et al. 2014).

Protocadherin-17 (pcdh17)

Protocadherin-17 (pcdh17) is a member of the non-clustered δ2-pcdh and was previously called PCDH68 (Nollet et al. 2000; Frank and Kemler 2002). Structures that express pcdh17 mRNA (*pcdh17*) in the developing rat (P3) brain include the olfactory bulb, cerebral cortex (e.g. frontal cortex, parietal cortex, motor and auditory cortices), amygdaloid complex, hippocampus, epithalamus, thalamus, hypothalamus and brain stem (Kim et al. 2007; Coughlin and Kurrasch 2015). *Pcdh17* expression in the developing mouse brain was similar to that of rats (Abrahams et al. 2007). *Pcdh17* expression is also detected in adult mouse brains. *Pcdh17*-positive adult structures include neocortex (e.g. primary somatosensory cortex), basal ganglia, hypothalamus, amygdala, hippocampal formation, ventral tegmental area and substantia nigra (Hertel and Redies 2011; Krishna-K et al. 2011; Hertel et al. 2012; Stoya et al. 2014; Yan et al. 2014; Coughlin and Kurrasch 2015). Additionally, immunostaining by Hertel et al. (2008) revealed scattered expression of pcdh17 in the ventral tegmental area (VTA), and in substantia nigra (Yan et al. 2014). In *pcdh17* mutant mice, defects in axonal extension and synaptogenesis are observed (Hoshina et al. 2013; Hayashi et al. 2014; Stoeckli 2014).

In a study using human midgestation cerebral tissue, Abrahams and coauthors found that *PCDH17* mRNA was present in the prefrontal cortex, anterior cingulate, thalamus, and ventromedial striatal neuroepithelium, which is somewhat similar to *pcdh17* expression in the developing mouse and rat brains (Abrahams et al. 2007). PCDH17 dysfunction has been linked to cognitive delay in humans (Redies et al. 2012). In individuals with schizophrenia, PCDH17 expression was increased in Brodmann's area 46 (Dean et al. 2007). PCDH17 misexpression accompanies the major mood disorders, such as bipolar disorder and major depressive disorder, while the overexpression in human cortical neurons *in vitro* decreases their spine density (Chang et al. 2018). Furthermore, results from several recent studies suggest that PCDH17 acts as a tumor suppressor (Haruki et al. 2010; Giefing et al. 2011; Hu et al. 2013).

Zebrafish and human pcdh17/PCDH17 proteins are 73.5% identical (Biswas and Jontes 2009; Liu et al. 2009). Pcdh17 in zebrafish has 4 exons, with the entire gene stretching 150 kb (kilobases) on chromosome 11 (Biswas and Jontes 2009). Paired CpG islands organized in a specific pattern upstream of the pcdh17 gene are likely the *cis*-regulatory elements involved in controlling its expression, and this CpG island organization is highly conserved in zebrafish and other teleosts (Haruki et al. 2010).

Pcdh17 is expressed in developing and adult zebrafish brains, including the visual system (Biswas and Jontes 2009; Liu et al. 2009). *Pcdh17* is first detected using RT-PCR at 6 hpf and its expression is maintained throughout development, at least untill 5 days post fertilization (dpf). In developing zebrafish

CNS, *pcdh17* is expressed in the anterior neural tube (14 hpf) and in the ventral portion of the spinal cord (18 hpf, Biswas and Jontes 2009). As development proceeds, *pcdh17* expression increases and at 24 hpf, it is expressed throughout the brain and spinal cord (Biswas and Jontes 2009; Liu et al. 2009). In the forebrain, *pcdh17* is strongly expressed in the ventral telencephalon and in ventrolateral diencephalon (Biswas and Jontes 2009; Liu et al. 2009). In the midbrain, *pcdh17* is found in a small cluster of cells in the tegmentum (Biswas and Jontes 2009). In the hindbrain, *pcdh17* is expressed in a rhombomeric pattern in the lateroventral hindbrain. In the spinal cord, *pcdh17* is found in ventral regions, especially in the anterior part of the spinal cord. In 34 hpf embryos, *pcdh17* expression is greatly increased in the CNS, including the lateroventral telencephalon, lateral regions of the dorsal and ventral thalamus, anterior hypothalamus, tegmentum, lateral to the midline regions of the hindbrain and in the spinal cord (Liu et al. 2009). A similar *pcdh17* expression is detected in the fore- and midbrain of 48 hpf embryos. In the hindbrain, *pcdh17* is present in two symmetric columns of cells located along the lateral margin of this region (Biswas, 2009). In 3-5 days old larvae, *pcdh17* expression is further increased in the dorsal and ventral thalamus, anterior hypothalamus, tegmentum and medulla oblongata (Biswas and Jontes 2009; Liu et al. 2009).

<u>Protocadherin-19 (pcdh19)</u>

Protocadherin-19 (pcdh19) is another member of the non-clustered δ2-pcdh family and was first characterized in the rat brain by Wolverton and Lalande (2001). *Pcdh19* is expressed mainly in the brain and visual system of developing

zebrafish, chickens, mice and rats (Vanhalst et al. 2005; Gaitan and Bouchard 2006; Emond et al. 2009; Liu et al. 2010; Tai et al. 2010). In *Xenopus*, pcdh19 is involved specifically in the morphogenesis of neural ectoderm (Heggem and Bradley 2003; Rashid et al. 2006). During chicken development, *pcdh19* is present in forebrain, midbrain and hindbrain, and spinal cord (Tai et al. 2010; Lin et al. 2012). Expression of *pcdh19* was also studied in young rats and found to be present at P3 in the structures such as cerebral cortex, thalamus, hypothalamus, midbrain (E9.5), hindbrain (E9.5) and in the spinal cord (E12.5, Kim et al. 2007; Coughlin and Kurrasch 2015). In developing mice, *pcdh19* expression is detected in neocortex (P5), amygdala (P5), entire striatum (P5), caudoputamen (P5), globus pallidus (P5), midbrain (E9.5) and spinal cord (E15.5 and E18.8, Gaitan and Bouchard 2006; Hertel and Redies 2011; Hertel et al. 2012; Lin et al. 2013). Interestingly, *pcdh19* expression gradient is the opposite of *pcdh17*, with stronger expression in the anterior brain, and progressively weaker expression in the posterior brain regions (Lin et al. 2013). Like *pcdh17*, *pcdh19* expression is maintained in the adult mouse brain. *Pcdh19*-expressing regions include neocortex (e.g. primary somatosensory cortex, piriform cortex), amygdala, hippocampal and parahippocampal formation, entire striatum and substantia nigra (Hertel and Redies 2011; Krishna-K et al. 2011; Hertel et al. 2012; Lin et al. 2013; Stoya et al. 2014).

Zebrafish pcdh19 is 70% identical to human PCDH19. The zebrafish pcdh19 gene is approximately 85 kb in size, contains 5 exons and is located on chromosome 14 (Emond et al. 2009). In developing zebrafish, *pcdh19* is

detected first at 8 hpf in the whole embryo (Emond et al. 2009). At 10-13 hpf, it is found in the neural keel. Its expression in the brain of 12-13 hpf embryos appears to be segmental, with stronger expression in the forebrain, and two segments in the hindbrain, one located anterior to the rhombomere 3, and the other between rhombomere 3 and rhombomere 5 (Liu et al. 2010). At 18 hpf, *pcdh19* expression is present throughout the CNS, with stronger expression in the ventral telencephalon and ventral diencephalon, and the tegmentum. Its expression in the spinal cord is weak, and *pcdh19* expression becomes stronger in both the brain and spinal cord of 24 hpf embryos (Emond et al. 2009; Liu et al. 2010). By 36 hpf, *pcdh19* expression becomes restricted, with strong expression confined to lateral telencephalon, dorsal diencephalon, dorsal tegmentum, dorsolateral hindbrain, and dorsal spinal cord (Liu et al. 2010). *Pcd19* expression in 50 hpf and 72 hpf embryos is similar to that at 36 hpf, except its expression domains become more restricted in the brain, and is not detected in the spinal cord at 72 hpf (Liu et al. 2010).

Functional studies showed that pcdh19 is involved in zebrafish early brain morphogenesis during neurulation (Emond et al. 2009). The general defects of *pcdh19* morphants are similar to *cdh2* morphants, in regards to the neural plate (anterior region in *pcdh19* morphants or posterior region of the neural plate defects in *cdh2* morphants, Biswas 2012). Although pcdh19 does not form strong adhesive interactions, the *cis* complex formed with cdh2 is able to mediate adhesion and these two cadherins work together to affect the brain development (Emond et al. 2011). Specifically, pcdh19 binds to Nap1 in its cytoplasmic

domain and interacts with cdh2 at the extracellular domain (Tai et al. 2010). The

downstream signaling of pcdh19 include proteins regulating Rho family GTPases

and microtubule cytoskeleton (Emond et al. 2021).

Unclassified pcdhs

Expression of unclassified pcdhs (e.g. pcdh15) was also examined in the

developing zebrafish CNS (Seiler et al. 2005). Two orthologs (pcdh15a and

pcdh15b) of the duplicated gene pcdh15 have distinct expression and functions

in zebrafish in hearing (i.e. *pcdh15a* mutant zebrafish show hearing defects).

Non-clustered pcdhs in the vertebrate visual system

In *Xenopus*, pcdh7 is expressed in RGCs, their axons, and in the optic

tectum (2 days and 18 hpf; at the time RGC axons enter the tectum). It

modulates RGC dendrite elongation, as well as RGC axonogenesis, when

growth cones of RGC axons reach their destination areas in the *Xenopus* brain

(Piper et al. 2008; Leung et al. 2013, 2015). Pcdh7c mediates initiation and

elongation of RGC axon by interacting with TATA-binding protein-associated

factor-1 (TAF1, Piper et al. 2008).

In the developing chicken visual system, *pcdh10* is expressed in the entire

retina, visual nuclei along the retinotectal pathway, and in the optic tectum

(Müller et al. 2004).

In P3 rat brains, pcdh7, pcdh8, pcdh11 and pcdh15 are expressed in the

superior colliculus; pcdh7 and pcdh20 are detected in the occipital cortex (i.e. the

primary visual cortex), while pcdh9 expression is detected in the occipital cortex and the accessory optic tract (Kim et al. 2007).

In E15 mouse retinas, pcdh9 is faintly expressed by RGCs, while pcdh11 is strongly expressed in all retinal layers (Vanhalst et al. 2005). In P1 mouse brains, similar expression (in terms of labeling intensities) of pcdh9 and pcdh11 is observed in the superior colliculus. In the occipital cortex, both pcdh7 and pcdh9 are expressed, but each showing a distinct expression pattern (Vanhalst et al. 2005). In the adult mouse, *pcdh10* expression is observed in the gcl and inl of the retina (Hirano et al. 1999), while pcdh10 is present (P7) in the ipl and optic nerve fiber layer (Aoki et al. 2003). RGC target areas of the mouse brain also express pcdh10. These areas include the suprachiasmic nucleus (SCN), dorsal lateral and ventrolateral geniculate nuclei, anterior pretectal and olivary pretectal nuclei (Aoki et al. 2003).

In human adults, PCDH8 and PCDH9 are found in the occipital lobe (Strehl et al. 1998). PCDH15 is expressed in the inner and the outer synaptic layers of the retina in both fetal and adult humans (Alagramam et al. 2001), and zebrafish *pcdh15b* morphants have defective photoreceptors (Seiler et al. 2005).

Developing zebrafish retina and optic tectum express several non-clustered pcdhs (e.g. pcdh9, pcdh18, pcdh17 and pcdh19, Kubota et al. 2008; Emond et al. 2009; Liu et al. 2009; Biswas et al. 2012; Chen et al. 2013), see below for more detailed information on expression of pcdh17 and pcdh19.

Protocadherin-17 (pcdh17) in the visual system

In the visual system of zebrafish, *pcdh17* is first detected at 18 hpf in the

anterior portion of the eye (Biswas and Jontes 2009), in a small anteroventral

retina of young embryos (26 hpf). This is where the first group of retinal neurons

(precursors of RGCs) begin to differentiate (Hu and Easter 1999; Liu et al. 2009;

Chen et al. 2013). From 34 hpf to 50 hpf, *pcdh17*-expressing domain in the retina

increases to almost the entire retina, except in the photoreceptor layer (Liu et al.

2009). In older embryos (72 hpf), *pcdh17* expression in the retina is reduced,

except in the outer portion of the inl (where horizontal cells reside). These results

suggest that pcdh17 may play differential roles in the development of diverse

retinal cell types (Biswas and Jontes 2009; Chen et al. 2013). In the brain of

embryonic zebrafish, *pcdh17* is detected in the pretectum and optic tectum, and

both are targets of RGC axons. Expression of *pcdh17* in the pretectum is

observed in both younger (34 hpf) and older embryos (50 hpf and 72 hpf). In the

optic tectum, apparent *pcdh17* expression is seen in 50 hpf embryos, and it

continues to be expressed in the optic tectum of 72 hpf embryos (Liu et al. 2009).

Pcdh17 expression in the optic tectum becomes undetectable in 5 dpf larvae

(Biswas and Jontes 2009). The stages of *pcdh17* expression in the optic tectum

(i.e. 50-72 hpf) coincide with the arrival of RGC axonal terminals and initial

synaptic formation between the RGC terminals and neurons in the optic tectum

(Vanegas 1983; Stuermer et al. 1990; Burrill and Easter 1994; Kita et al. 2015).

The *pcdh17* expression in the developing zebrafish is similar to that of

developing rats in that *pcdh17* is also detected in the pretectum and the superior

colliculus, the homologous structure of nonmammalian optic tectum (Kim et al. 2007).

Blocking *pcdh17* function using morpholino technology in developing zebrafish results in embryos (pcdh17 morphants) that are almost indistinguishable from normal embryos in gross morphology and size, except that the pcdh17 morphants have smaller eye size (Chen et al. 2013). Additional testing showed that the reduction of the eye size in the morphants results from decreased cell proliferation. Expression of regulatory molecules (e.g. crx, neuroD, otx5) in the morphants' retinas is greatly reduced compared to that in normal embryos, and differentiation of RGCs, amacrine cells and photoreceptors is disrupted (Chen et al. 2013).

Protocadherin-19 (pcdh19) in the visual system

In the visual system, pcdh19 is expressed in young mice at E12.5 and E15.5 in the retina (Gaitan and Bouchard 2006). P3 rat has high pcdh19 expression in brain regions that receive direct retinal inputs, including the superior colliculus, ventrolateral geniculate nucleus, anterior pretectal nucleus, anterodorsal and anteromedial thalamic nuclei (Kim et al. 2007).

In the visual system of the developing zebrafish, *pcdh19* expression is detected in the eye primordium at 12 hpf (Emond et al. 2009; Liu et al. 2010). It continues to be expressed in the entire eye in 18-24 hpf embryos, with more expression in the lens and marginal regions than in the central retina. *Pcdh19* expression in the eye is reduced more at 36 hpf, confined mainly to the lens and

retinal marginal zones. At 48 hpf, *pcdh19* signal is detected in the inner retina. *Pcdh19* expression is restricted to the gcl of older (50-72 hpf) embryos (Emond et al. 2009; Liu et al. 2010). In the brain, *pcdh19*-expressing cells are detected in the presumptive optic tectum region at 18 hpf, and the expression is higher in older embryos (24-72 hpf), with the strongest expression levels (judging by staining intensity) observed in the pretectum at 36 hpf (Liu et al. 2010).

Optic primordia (future eyes) of the zebrafish *pcdh19* morphants exhibit shape malformation as early as 12 hpf (Emond et al. 2009) and the visual circuitry is defective in *pcdh19* knockouts (Cooper et al. 2015).

Protocadherins functions in human diseases

Mutations of PCDHs cause several neurological and/or psychiatric disorders, such as late-onset Alzheimer's disease (*PCDH11*), Usher syndrome (*PCDH15*), bipolar disorder (*PCDH17*), schizophrenia (*PCDH8*, *PCDH17*), autism (*PCDH9*, *PCDH10*, *PCDH19*), Dravet syndrome (*PCDH19*), obsessive-compulsive disorder (*PCDH19*), X-linked epilepsy and mental retardation limited to females (EFMR; *PCDH19*), Huntington disease (*PCDH20*) and retinal dystrophy (*PCDH21*) (Dibbens et al. 2008; Morrow et al. 2008; Carrasquillo et al. 2009; Becanovic et al. 2010; Beecham et al. 2010; Henderson et al. 2010; Depienne et al. 2011, 2012; Redies et al. 2012).

Additionally, several non-neural diseases are connected to PCDHs, such as asthma (*PCDH1*), lung cancer (*PCDH7*), prostate cancer (*PCDH11*) (Rattner et al. 2001, 2004; Koppelman et al. 2009; Hu et al. 2012). Furthermore, PCDHs

act as tumor suppressors in humans, including PCDH8 and PCDH17 in breast

tissue (Yu et al. 2008; El-Benhawy et al. 2021), and PCDH LKC in liver, kidney

and colon tissues (Okazaki et al. 2002).

Regeneration of the vertebrate nervous system

Early attempts in understanding the vertebrate nervous system

regeneration were made by Langley (1895) in the autonomic nervous system of

cats, and by Sperry (1944) in the visual system in amphibians. In both studies,

the researchers observed reconnections of severed nerves with their respective

targets and restoration of their respective functions after experimental lesions of

the nerves.

The adult mammalian CNS has very limited regenerative capacity due to

the presence of specific growth inhibitory environment that impedes successful

CNS axonal outgrowth, and reduced intrinsic ability of the CNS neurons to

regenerate after injuries (Schwab and Thoenen 1985; Aguayo et al. 1991;

Goldberg et al. 2002). The inhibitory environment includes Nogo expressed by

oligodendrocytes, glial scars and chondroitin sulfate proteoglycans (Harel and

Strittmatter, 2006; Young, 2014). The intrinsic capability to regenerate depends

mainly on increased expression of molecules important for neuron survival and

axon outgrowth (Skene 1989). Mammalian CNS regeneration is still poor even

after blockage of the inhibitory factors, suggesting the importance of the intrinsic

factors in promoting successful regeneration in the CNS (So and Yip 1998;

Ferguson and Son 2011; Vajn et al. 2013).

In contrast to the CNS in mammals, the CNS in adult amphibians and teleost fish (e.g. zebrafish) is able to regenerate following injuries (Sperry 1948; Becker and Becker 2007; Brockerhoff and Fadool 2011; Fleisch et al. 2011). Again, both environmental and intrinsic factors are involved: the oligodendrocytes in these species are less inhibitive, little or no glial scars are present, and there is an up-regulation of molecules crucial for the neuron survival and axon outgrowth (Raymond and Hitchcock 2000). Nevertheless, not every developmental molecule is implicated in the regeneration mechanism because certain signaling mechanisms are different between those two processes (Benowitz et al. 2017, 2017).

The zebrafish has an extraordinary regenerative ability following injuries and therefore is a good model for the vertebrate regeneration studies (Liu and Londraville 2003; Becker and Becker 2007). The retina has been one of the favorite organs for studying CNS development, function, physiology and regeneration because it is peripherally localized (easily accessible), has a well-laminated structure with specific cell types localized mostly in a particular retinal layer (easy identification and isolation of cell types). Additionally, the retina and optic nerve are considered part of the CNS because they originate from the diencephalon during the embryonic development (Purves et al. 2001; Russek-Blum et al. 2009).

Following optic nerve lesions (e.g. crush or sever) in adult zebrafish, there is little cell death in RGCs as over 90% of these cells survive (Zou et al. 2013; Bollaerts et al. 2017). Regenerating retinal axons arrive at the anterior region of

the optic tectum (the major brain target of the retinal axons) by one week and innervate the entire tectal lobe by three weeks (Becker and Becker 2007; Zou et al. 2013). Molecular mechanisms underlying the successful retinal regeneration are still being investigated. Several molecules show marked increase following the optic nerve lesion. These molecules include: *klf6a*, *klf7* (Veldman et al. 2007), *GAP-43* (Benowitz et al. 2017, 2017), *alpha-tubulin* (Skene 1989; Bormann et al. 1998; Becker and Becker 2007), *reggie* (*flotillin*) (Stuermer 2010) and cadherins (e.g. cdh2 and cdh4, Liu et al. 2002). Functional studies show that klf6a/klf7, alpha-tubulin and reggie promote retinal axon outgrowth (Veldman et al. 2007, 2010; Munderloh et al. 2009). A recent study from our laboratory (unpublished) showed that blocking cdh2 function greatly reduced retinal axon regeneration in adult zebrafish, suggesting that this cadherin plays an essential role in successful retinal axon regeneration. The mammalian peripheral nervous system (PNS) regenerates significantly better than the CNS and one of the factors that may be responsible for that is an increased cdh2 expression (Squitti et al. 1999). Elevated cdh2 and cdh4 expression is also observed in regenerating cerebellum in adult zebrafish, and expression levels of these cdhs reduce to their pre-injury levels once the cerebellum is regenerated (Liu et al. 2004a).

Cadherins in regeneration

The expression patterns of cadherins is spatially and temporally controlled in nervous tissues of young, adult and regenerating vertebrates (Redies et al. 2011), including chickens (Shibuya et al. 1995), mice (Redies and Takeichi

1993), rats (Thornton et al. 2005) and zebrafish (Liu et al. 1999a, 1999b, 2002).

Expression of cadherins is elevated following injuries in fish, birds and mammals

(Squitti et al. 1999; Liu and Londraville 2003; Thornton et al. 2005). Increased

cadherin expression in mammals is only observed in the PNS, where there is a

successful nerve regeneration (Thornton et al. 2005), but not in the CNS (e.g.

optic nerve, Bates et al. 1999). Examples of cdh2 expression occurring in the

PNS injury are sciatic nerves of adult rats (Thornton et al. 2005) and young

chickens (Cifuentes-Diaz et al. 1994), and the ciliary ganglion of quail (Squitti et

al. 1999). A failure of nerve survival and subsequent regeneration is

accompanied with non-detectable expression change of few cell adhesion genes

(including cdh2) in the mouse optic nerve (Bates et al. 1999; Sharma et al. 2014;

Ribeiro et al. 2020). This is in contrast to the successful regeneration in adult

zebrafish CNS structures including the retina, optic nerve and cerebellum, which

coincides with increased cdh2 and cdh4 expression after lesions (Liu et al. 2002,

2004a).

Liu et al. (2002) studied expression of cdh2 and cdh4 in regenerating

retina, optic nerve and optic tectum of adult zebrafish. Injuries were either eye

stabbing or optic nerve crush. The authors showed that increased cdh2

expression (measured by immunohistochemistry and immunoblotting) was

observed as early as the second day after the injury, and cdh2 expression levels

continued to increase in the regenerating visual structures 3-days to 1-week

post-lesion. Increased cdh2 expression remained for 2 weeks following the

injuries, but returned to pre-lesion (normal/control) level 3 weeks after the lesion.

A similar expression profile was observed for cdh4 in the regenerating visual structures, except that the onset of its up-regulation was delayed 1-2 days compared to that of cdh2 up-regulation. The increased cdh2 expression in the regenerating adult zebrafish retina was confirmed using DNA microarray (Cameron et al. 2005).

Krüppel-like factors (Klfs) in regeneration

The family of Klfs belongs to a large group of proteins with characteristic DNA-binding zinc finger motif containing Cys_2-His_2 surrounding a zinc ion (Kaczynski et al. 2003; Lomberk and Urrutia 2005; McConnell and Yang 2010). A distinguishing feature of the Klf family is a set of highly conserved three zinc fingers in the C-terminus (McConnell and Yang 2010). The N-terminal of Klfs members contains domains interacting with co-activators and/or co-repressors (Kaczynski et al. 2003; Lomberk and Urrutia 2005; McConnell and Yang 2010). Classification of Klfs is mainly based on their variable N-terminal domains (Lomberk and Urrutia 2005; Presnell et al. 2015). Group 1 members (Klfs 3, 8, and 12) have PVALS/T N-terminal and are transcriptional repressors. Group 2 members (Klfs 1, 2, 4, 5, 6, and 7) are transcriptional activators, and all have the acidic activation domain and either inhibitory or S-rich domains. Group 3 members (Klfs 9, 10, 11, 13, 14, and 16) have a Sin3a-binding domain and are repressors. There are also some members that remain non-classified because they lack any of the above mentioned motifs (or domains) in their N-termini,

except containing the three zinc fingers in their C-termini (Klfs 15 and 17, Moore et al. 2009, 2011; McConnell and Yang 2010; Presnell et al. 2015).

The first Klf gene (Klf1) was discovered by Miller and Bieker (1993) in a murine red blood cell line. Each of the 16 Klfs discovered subsequently was named with increasing numbers (Kaczynski et al. 2003; e.g. Klf2, Klf3, etc. Lomberk and Urrutia 2005; McConnell and Yang 2010). Function of Klfs in axon intrinsic growth (Moore et al. 2009; Blackmore et al. 2012) and optic nerve regeneration were studied previously (Fleisch et al. 2011; Moore et al. 2011; Benowitz et al. 2017). In mice, all Klf members (except Klf1 and Klf17), are expressed in developing RGCs. Some members (e.g. Klf4 and Klf9) inhibit RGC axon regeneration, while others (Klf6 and Klf7, see more below) promote RGC axon regeneration (Moore et al. 2009, 2011).

Functions of Klfs in vertebrates are broad, impacting cell growth, differentiation, proliferation, migration, apoptosis, inflammation and regeneration (Bieker 2001; Kaczynski et al. 2003; Laub et al. 2005; McConnell and Yang 2010). The involvement of Klfs in cancer has been studied extensively (Bureau et al. 2009; Tetreault et al. 2013). Klfs are also involved in pathogenesis of neurological disorders, such as ischemic stroke (Yin et al. 2015).

Klf6

KLF6 was first identified from prostate cancer patients as a tumor suppressor in prostate cancer (Narla et al. 2001). KLF6 was further implicated in

several other cancers, such as gastric cancer, colorectal cancer and hepatocellular carcinoma (Reeves et al. 2004; Cho et al. 2005; Narla et al. 2007).

Klf6 expression in mouse embryos is first detected at E11.5 in mesenchyme, and later (E12.5) it is found in the nervous system, such as caudal hindbrain, dorsal root ganglia, and ventral horns of the spinal cord (Laub et al. 2001b). In addition to the above structures, Klf6 expression is also seen in the forebrain and midbrain at E16.5 (Laub et al. 2001a). In the mouse eye, Klf6 is first found in the lens pit at E10.5 and in the corneal epithelium at E15.5 (Nakamura et al. 2004). In RGCs, *Klf6* is first detected at E19 and its expression decreases steadily as mice develop, until P21 when there is over 8-fold decrease in its expression (Moore et al. 2009). In general, Klf6 expression in the developing mouse nervous tissues is more restricted than Klf7 (see below), but Klf6 is also found in non-neural tissues such as the developing heart, lung, kidney, autopod and hindgut (Laub et al. 2001b; Chu and Sadler 2009). Jeong et al. (2009) described wide Klf6 expression in the forebrain of the adult mouse.

Klf6 is involved in differentiation and cell cycle exit (Laub et al. 2001b, 2005). Klf6 functions as an activator of CPBP protein in mice and humans (Kaczynski et al. 2003). In addition, Klf6/KLF6 is a growth-enhancing molecule for neural axons (Moore et al. 2009).

The zebrafish *klf6a* gene located on chromosome 24 is orthologous to the mammalian *Klf6*/*KLF6* (mouse/human). *Klf6a* is found in developing zebrafish as early as 10.33 hpf (1 somite) in ventral mesoderm (Thisse et al. 2001). As the embryo develops, *klf6a* is found in the neural tube (16-18 hpf), telencephalon

(30-42 hpf), tectum and hindbrain nuclei (43-60 hpf), cranial ganglia (16-18 hpf), posterior lateral line ganglia (19-42 hpf), dorsal neurons (19-42 hpf, Thisse et al. 2001). Klf6a is not expressed in either developing or adult RGCs, but is expressed when their axons are crushed in adult fish (Veldman et al. 2010). *Klf6a* expression increases as soon as a couple of hours post-injury, and its expression intensifies further at 2-3 days (Veldman et al. 2007). *Klf6a* expression levels then decline until day 12-24 post lesion. There is no functional study of klf6a in zebrafish nervous system development. Klf6a, together with klf7 (see below), is implicated in promoting retinal axon regeneration in adult zebrafish (Veldman et al. 2007). In addition, klf6a is important in hematopoietic and vascular development (Xue et al. 2015).

Klf7

KLF7 in humans was first isolated from vascular endothelial cells using the degenerate primers PCR amplification, and was later found in many human tissues, but mainly in brain and spinal cord (Matsumoto et al. 1998). KLF7 has been implicated in the pathogenesis of type 2 diabetes (Kanazawa et al. 2005). Individuals with *de novo* KLF7 variants have neuromuscular and psychiatric complications related to autism and intellectual disability (Powis et al. 2018).

In developing mice, Klf7 expression is restricted to the nervous system (both CNS and PNS) and is found in neurons (e.g. dopaminergic) and neuroectodermal cells (Laub et al. 2001a, 2006; Caiazzo et al. 2010, 2011; Yin et al. 2015). Embryonic tissues expressing Klf7 include the olfactory bulb, dorsal

54

root ganglia, sympathetic ganglia and spinal cord. In postnatal mice, Klf7 is expressed in the olfactory system, cerebral cortex, hippocampus and mesencephalon (Laub et al. 2006; Caiazzo et al. 2011). In the adult mouse, Klf7 is found in the cerebellum and dorsal root ganglia, and weakly expressed in some other tissues (Laub et al. 2001a). In embryonic mice (E12-E19), Klf7 is expressed in RGCs. After birth (P1), Klf7 expression in the RGCs is slightly higher than at E19, but its expression levels decrease over 2-fold untill at least P21 (Laub et al. 2001a, 2005; Moore et al. 2009).

In *Klf7* null mutant mice, selective sensory neurons (e.g. olfactory neurons) are depleted (Lei et al. 2005; Laub et al. 2006; Caiazzo et al. 2011). Additionally, Klf7 functions in neurogenesis in cerebral cortex and hippocampus, likely through affecting genes important in neuronal differentiation (Laub et al. 2005; Caiazzo et al. 2010). Furthermore, *Klf7* mutants exhibit defects in retinal axons growth and pathfinding (Laub et al. 2005; Blackmore et al. 2012). The overexpression of *Klf7* promotes sciatic nerve (PNS) repair in 8-week-old mice and therefore this gene is involved in nerve regeneration (Wang et al. 2017). Klf7 expression in the adult mouse corticospinal tract (CST) is greatly decreased (Blackmore et al. 2012), leading the authors to propose that this down-regulation is one of the reasons injured CNS axons fail to regenerate. Overexpression of transactivation domain VP16 of Klf7 (VP16-klf7) helped to promote limited regeneration of injured axons (Blackmore et al. 2012).

The zebrafish *klf7* (*klf7b*) gene is located on chromosome 9 and is orthologous to the mammalian *Klf7*/*KLF7* (mouse/human). In zebrafish, *klf7* is

present in the olfactory bulb, diencephalon and cranial ganglia (Thisse and Thisse 2004; Li et al. 2010a; Xue et al. 2015). In the visual system of developing zebrafish (24-72 hpf), *klf7* is expressed in the gcl (Thisse and Thisse 2004; Laub et al. 2006; Veldman et al. 2007). Its expression in the gcl becomes almost undetectable in adult zebrafish, but it becomes greatly increased in RGC axons within hours post optic nerve crush, and its expression continues to increase and peaks at 6 days post-injury (Veldman et al. 2007). *Klf7* expression levels then decline and become almost the same as pre-injury at 24 days post lesion. In retinal explants, the axonal growth *in vitro* is affected in double knockdown of *klf6a* and *klf7*, but not in the individual knockdown of either protein, suggesting that they have redundant roles in promoting retinal axon regeneration and can compensate for each other in the process (Veldman et al. 2007).

Zebrafish as a model organism and its visual system

Zebrafish (*Danio rerio*, formely designated *Brachydanio rerio*) have been used as a model organism from the time when George Steisinger and his colleagues at The University of Oregon linked a mutation of *slc24a* gene in *golden* mutant (lighter skin pigmentation) between zebrafish and human (Streisinger et al. 1981). The choice of the zebrafish as a model organism is driven by several experimental advantages (Grunwald and Eisen 2002). Their development is fast and external. For example, most major organs are present by 24 hpf, and zebrafish can reach sexual maturity in 3-4 months. Additionally, embryos are transparent, allowing observation of internal structures in intact

embryos, thus the zebrafish is commonly used in developmental studies (Eisen 1996; Anderson and Ingham 2003; Schmidt et al. 2013). The low cost, high number of progeny (routinely >50 fertilized eggs per female each breeding), and easy maintenance of this model organism contribute to its popularity. Furthermore, the zebrafish genome is fully sequenced and easily accessible online (http://ncbi.nlm.nih.gov/genbank), and gene manipulation such as knockdown or knockout is relatively simple (Chen et al. 2013; Varshney et al. 2013). Over 70% protein-coding genes in human share the corresponding functional orthologs with zebrafish (Langheinrich 2003; Howe et al. 2013). Importantly, the molecular, cellular and physiological processes are similar between zebrafish and humans (Langheinrich 2003).

In addition, like other teleost fish and amphibians, zebrafish have the ability to regenerate damaged nervous tissues, including the retina and optic nerve. Moreover, the regenerating processes are faster (e.g. one week for the regenerating retinal axons to reach the optic tectum in adult zebrafish, but more than one month in goldfish) due to its smaller size and living in fresh water with higher temperatures (Hitchcock and Raymond 2004). The regeneration responses (such as axon outgrowth, tectal innervation and functional recovery) are delayed in aging zebrafish (5 months vs. 3 years), but are similarly successful (Bollaerts et al. 2017).

Given the above advantages of zebrafish, this model organism has been used to study development and regeneration, serving as an invaluable tool to model human diseases (Lieschke and Currie 2007; Santoriello and Zon 2012).

Zebrafish have been used to study the molecular and cellular mechanisms of wide spectrum of human diseases (developmental, skeletal, cardiovascular, hematopoietic, kidney diseases), in addition to human disorders (behavioral, neurological, psychiatric disorders; e.g. addiction), cancer and many others (Dooley and Zon 2000; Penberthy et al. 2002; Shin and Fishman 2002; Guo 2004; Lieschke and Currie 2007; Panula et al. 2010; Bakkers 2011; Chhetri et al. 2014). Importantly, zebrafish have been a model organism for the pathogenesis of human vision-related disorders/diseases including glaucoma, cataracts, ciliopathies, age-related macular degeneration (AMD), human congenital nystagmus (HCN) / infantile nystagmus syndrome (INS), human choroideremia (CHM) and Hermansky–Pudlak syndrome (Bibliowicz et al. 2011; Chhetri et al. 2014). In zebrafish, numerous behavioral tests for visual responses and its sensitivity may provide useful information for the research in human vision (Guo 2004). The similarities between eye anatomy of zebrafish and humans (shown in Figure 1.3) further justify the use of zebrafish as a model organism to study human vision-related disorders/diseases. Both are diurnal species and their vision is primarily mediated by cone photoreceptors in the retina during the day (Hughes et al. 1998; Bilotta and Saszik 2001). Although mice and rats are the two main mammal model organisms, both are nocturnal with their retinas containing much fewer cones (Carter-Dawson and Lavail 1979).

It should be pointed out that despite the advantages of zebrafish, there are apparent differences between the fish and humans. For example, some of their functional organs are different (e.g. lungs) and zebrafish lack a laminar

58

cerebral cortex. Furthermore, homologous genes may have partially redundant

functions because of evolutionary whole-genome duplication in zebrafish

(Rastogi and Liberles 2005; Kleinjan et al. 2008). Therefore, restraint and

carefulness are needed when extrapolating results from zebrafish to human

development and/or diseases (Maximino et al. 2015).
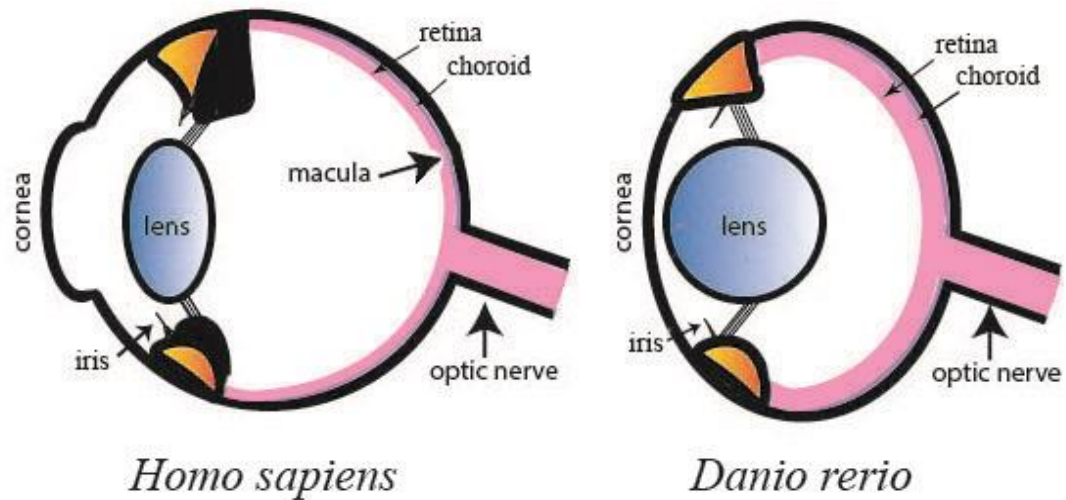
Figure 1.3. Comparison of the anatomy of zebrafish eye and human eye. The overall organizations of the two eyes are almost identical. The zebrafish eye has a slightly less round shape, smaller distance between the lens and cornea and lacks macula, compared to the human eye. Adapted and modified from Chhetri et al. (2014).

The advantages of using zebrafish as a model organism to study cellular

and molecular mechanisms involved in the retinal development, regeneration,

vision and visual disorders/diseases include similarity of the visual system

anatomy and physiology between zebrafish and humans, easy access and ease

of experimental manipulations, and robust and quick regeneration. The retina of

the zebrafish has the same major major cell types (one glial cell type and six

types of neurons with many subtypes, Figure 1.4) and laminar organization (three

cellular layers and two synaptic layers) as other vertebrates (Fadool and Dowling

2008). The three cellular layers contain the nuclei/cell body of various retinal

neurons and are the following: the outer nuclear layer (onl), the inner nuclear

layer (inl), and the ganglion cell layer (gcl). The outer nuclear layer hosts rod and

cone receptor cell bodies, the inner nuclear layer hosts nuclei of amacrine cells,

bipolar cells, horizontal cells and Müller glia, while the ganglion cell layer is a

location for cell bodies of retinal ganglion cells (RGCs) (Darby et al. 1990;

Bormann et al. 1998; Stenkamp 2007; Agathocleous and Harris 2009; Garrett

and Burgess 2011). The two plexiform layers are where cells from inl and onl

synapse with their respective nuclear layers: the outer plexiform layer is where

photoreceptors synapse with bipolar cells and horizontal cells, while the inner

plexiform layer is where bipolar cells and amacrine cells contact RGCs (Fadool

and Dowling 2008; Robles 2017). The inner plexiform layer can be further divided

to ON and OFF layers, based on where the ON and OFF bipolar cells terminate

(Robles 2017). A majority of somata residing in the gcl are RGCs, also called the

orthotopic ganglion cells. Certain populations of retinal neuron bodies are present

ectopically in the neighboring layers, and those include the displaced amacrine

cells (without axons) in the outer portion of gcl and the displaced ganglion cells

(Dogiel cells; with axons) in the inner portion of the inl or ipl (Rodieck 1979; Perry

1981; Frank and Hollyfield 1987a, 1987b). Both types of the displaced cells tend

to have a larger size, irregular distribution and they account for no more than few

percent of their respective populations in zebrafish (Hitchcock and Easter 1986;

Dunlop et al. 1992; Marc and Cameron 2002). Distribution of both types of

60

ectopic cell populations in zebrafish and goldfish is similar to some other

vertebrates. Frogs (*Hyla moorei* and *Xenopus laevis*) have only 0.6-1% of RGCs

displaced in the inl and 0.09% in the ipl (Hitchcock and Easter 1986; Toth and

Straznicky 1989; Darby et al. 1990; Dunlop et al. 1992), while rats and hamsters

have about 1% RGCs displaced in the inl (Perry 1981; Linden and Esberard

1987). The much bigger difference between zebrafish and mammals is observed

for the ectopic amacrine cells that account for around 50% of total cells in the gcl

in rats, over 40% in hamsters and similarly high percentages in wallabies (Perry

1981; Linden and Esberard 1987; Harman and Beazley 1989; Gao et al. 1997;

Takeda et al. 2000; Kielczewski et al. 2005; Nadal-Nicolas et al. 2015).
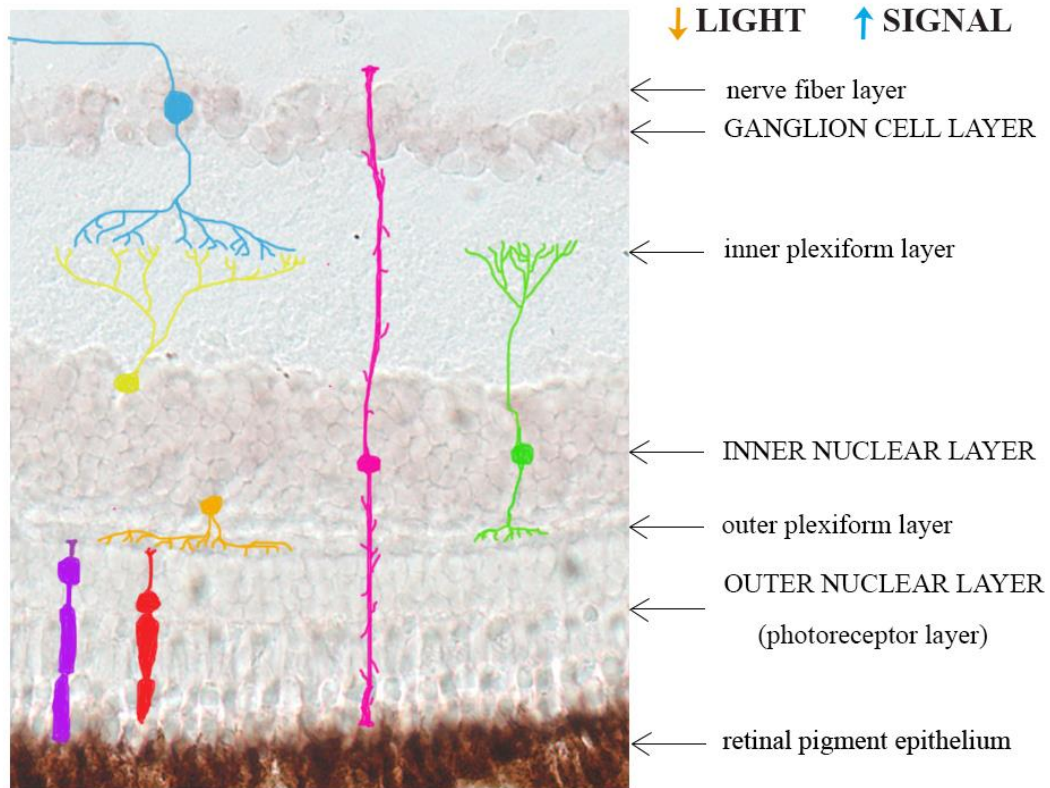
Figure 1.4. Major layers and neuron types in adult zebrafish retina. This is a high-magnified view of a zebrafish retina from a cross section with ganglion cell layer up. Major retinal neuron types are illustrated by pseudo-colored cell drawings with retinal ganglion cell in blue, amacrine cell in yellow, Müller cell in pink, bipolar cell in green, horizontal cell in orange, rod photoreceptor in purple, and cone photoreceptor in red. The terms in upper case letters depict layers containing primarily the cell bodies of the retinal neurons, while lower case letters depict layers containing primarily the axons and synapses of the retinal neurons. Adapted and modified from Goldsmith and Harris (2003).

The cell types residing in the vertebrate retina are generated from retinal progenitor cells (RPCs) in succession by specific timing of their final mitotic divisions (Stenkamp 2007; Centanin and Wittbrodt 2014). In zebrafish, this process happens from the outside of apical surface of the retina, to the inside (Hu and Easter 1999). The neurogenesis process produces each retinal layer in the precise 12-hour intervals. A simplified version of the development of the retinal cells in zebrafish is illustrated in Figure 1.5. The first generated layer is the

gcl, where the retinal ganglion cells differentiate from 28 to 36 hpf. Next, the inner

nuclear layer differentiates between 36 and 48 hpf. Lastly, the photoreceptor

layer generates two types of cells residing within: cones (from 48 to 60 hpf) and

rods (latter coming from a different neural lineage, Raymond 1985). By the end of

day 3, the zebrafish has generated and organized all types of the retinal cells in

layers and the RGC axons have reached and arborized their target areas of the

brain (see below, Sharma 1975; Burrill and Easter 1994; Arenzana et al. 2006).

This is when the visual system becomes functional and the embryo hatches

(Easter Jr and Nicola 1996).
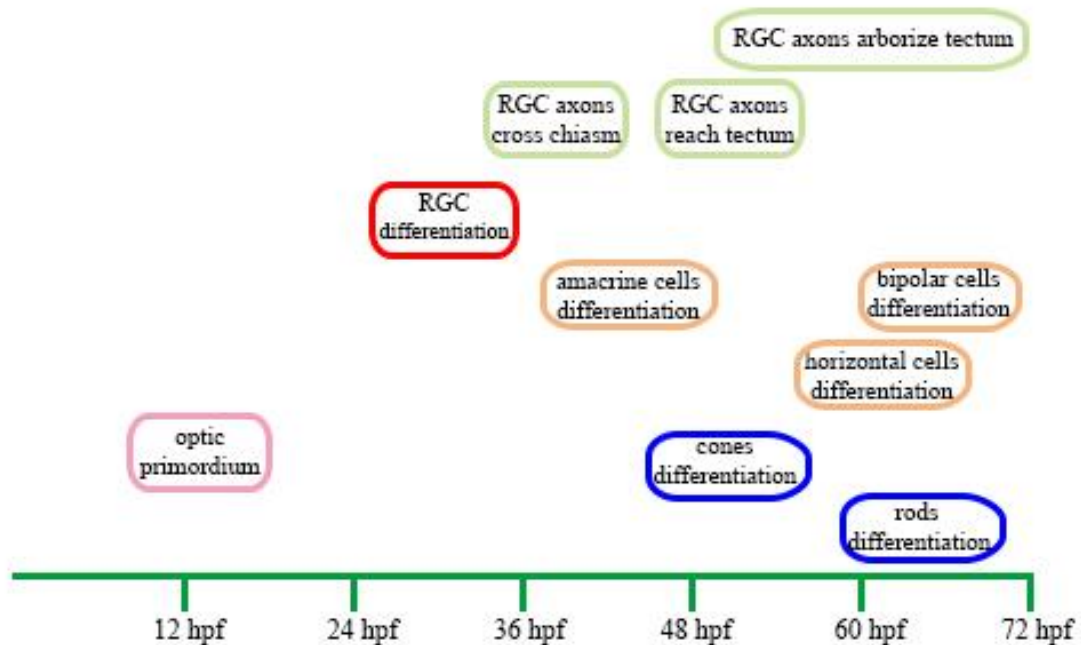
Figure 1.5. Timeline of neurogensis of retinal cell types and development of the visual pathway in zebrafish. Pink oval – origin of neural retina, red oval – cells in the gcl, orange ovals – cells in the inl, blue ovals – cells in the opl, green ovals – retinal ganglion cell developmental events outside of the eye. Abbreviations: hpf, hours post fertilization; RGC, retinal ganglion cell.

In vertabrates, RGC axons form the nerve fiber layer, join at the optic disk and exit the eye at the optic nerve head and project to their target visual fields in brain, forming terminal arbors. Teleost fish have nearly an equivalent number of retinorecipient areas in larvae (the arborization fields, AF) and in adults (the retinorecipient nuclei, Fraley and Sharma 1984; Meek 1990). In adult zebrafish, the visual fields are located in the midbrain (TeO), preoptic region (SCN, PPp), thalamus (VL, I, A, DP), pretectum (VAO, PSp, APN, CPN), the accessory optic system (periventricular group, PPd and the PPv, Burrill and Easter 1994); refer to list of Abbreviations at the end of Dissertation. In embryonic and larval zebrafish there are ten AFs (AF1-AF10) and each is numbered by its distance from the eye. AF10 is the first to be generated in development (48 hpf) and is targeted by 97% of RGC axons. The remaining axons target the AF9, which is generated next (52-54 hpf, Burrill and Easter 1994; Mueller 2012; Robles et al. 2014). Shortly after, bifurcated axon collaterals from RGC axons (that initially terminate in AF9 or AF10) make up the remaining AF1-8. By 72 hpf, all ten AFs are visible in the brain. Burrill and Easter (1994) identified visual larval structures with adult attributes and suggested the optic tectum (TeO) originates from AF10, the pretectal periventricular nuclei (PPd) develop from AF9. Additionally, the authors (Burrill and Easter 1994) paired all AFs with their possible adult counterparts, which were updated three decades later (Baier and Wullimann 2021), e.g. AF1 develops into the SCN and AF4 arborizes in the I.

In mammals, 90% of retinal projections in brain input the dorsal lateral geniculate nucleus (dLGN) of the thalamus, which in turn relays the information

64

to the primary visual cortex (V1). This pathway is called the geniculate pathway. The rest of the RGCs (extrageniculate pathway) target the superior colliculus (SC) and further signal to the caudal thalamic nuclei (e.g. pulvinar or lateroposterior complex) and then to the visual cortices (V2-V4) and the lateral amygdala (Doron and Ledoux 1999). The fish and amphibians lack geniculate and extrageniculate pathways, 97% of RGCs target the contralateral optic tectum (TeO, Northcutt 1983; Northcutt and Wullimann 1988; Mueller 2012). In humans, the retinal axons project to both sides, with the axons from the RGCs located in the temporal half of the retina projecting to the ipsilateral lateral geniculate nucleus, while those in the nasal side project to the contralateral lateral geniculate nucleus (Wurtz and Kandel 2006). The optic tectum of zebrafish (no LGN) is a homologous structure to the superior colliculus of mammals, as both structures are part of the mesencephalon/midbrain (Mueller 2012). In zebrafish, the retinal axons project mainly to the contralateral side of TeO in an inverted pattern: from dorsal-temporal of the retina to ventral-anterior of the optic tectum, and ventral-nasal of the retina to dorsal-posterior of the optic tectum (Stuermer 1988). Zebrafish and human RGC axons are myelinated, but the retinal part of the human axons is unmyelinated (Dezawa and Adachi-Usami 2000; Schweitzer et al. 2007; Münzel et al. 2014). Despite the differences in the visual system between zebrafish and humans, the comparable anatomy and physiology makes this fish an excellent model to study development and molecular aspects of neural circuits and regeneration (see below).

As discussed previously, there is a difference in the CNS regeneration ability between mammals and fish (Aguayo 1985; Sun and He 2010). A restricted ability of adult mammals to regenerate the injured CNS (caused by various extrinsic and intrinsic factors) contrasts the rapid regrowth of the injured axons and subsequent recuperation of neuronal functions in the teleost fish (Murray 1982; Skene 1989; y Cajal et al. 1991; Tsonis 2000; Poss et al. 2003; Sun and He 2010; Liu et al. 2011a; Lee-Liu et al. 2013; Alunni and Bally-Cuif 2016). The extrinsic factors (environmental) in mammals inhibiting axonal regeneration include the shortage of molecules that promote growth, coupled with the excess of molecules inhibiting growth (see above). The growth inhibitors comprise of those associated with glia (produced by oligodendrocytes) and chondroitin 6-sulfate proteoglycans (produced by astrocytes, Schwab and Thoenen 1985; Ferguson and Son 2011). The fish has a more robust CNS regeneration, partially due to absence or only very small amounts of inhibitory molecules produced by oligodendrocytes and astrocytes (Caroni et al. 1988). Studies showed that blocking inhibitory environmental factors had some effect on axonal regeneration in mammalian CNS (Fischer et al. 2004). More successful regeneration in mammalian RGC axons was observed when a peripheral nerve graft was attached to the injured RGC axons (Aguayo 1985; Vidal-Sanz et al. 1987; Robinson and Madison 2004). These findings suggest that the intrinsic factors (e.g. growth and/or survival factors produced by the regenerating neuron) of mammalian CNS may play more important role in the CNS ability to regrow its axons post-injury (Aguayo 1985; Vidal-Sanz et al. 1987; y Cajal et al. 1991; Yin

et al. 2003; Fischer et al. 2004). Mammals lose nearly all RGCs due to their atrophy and/or apoptosis that follow an optic nerve lesion (ONL), e.g. a rat loses 70-80% of axotomized RGCs in the first 7-9 days (and even more over the course of the next 15 months), a mouse loses 70% of injured RGCs axons in the first 7 days (85% at two weeks, and the rest over the next 3 months) (Allcutt et al. 1984; Levkovitch-Verbin et al. 2000; Takeda et al. 2000; Fischer and Leibinger 2012; Liu et al. 2014; Sharma et al. 2014; Nadal-Nicolas et al. 2015; Daniel et al. 2018; Sanchez-Migallon et al. 2018). Besides, neuronal death in the visual cortex (the contralateral superior colliculus) of mice is in the range of 28.9% $\pm$ 8.8% (4 weeks after optic nerve crush), while the normal (unoperated) eye loses approximately 20% of cells in the gcl (Liu et al. 2014). The frog, *Litoria (Hyla) moorei* is able to regenerate the optic nerve, despite the relatively high cell loss, accounting for 35-70% of RGC in the gcl and 36% of the displaced RGCs (Darby et al. 1990; Dunlop et al. 1992). In fish under similar circumstances, the cell survival rate is much higher; 80-90% RGCs survive in goldfish, while in zebrafish this number is 90% in the first two weeks (Murray 1982; Berry et al. 1988; Quigley et al. 1995; Zou et al. 2013). The rapid regeneration process in zebrafish allows half of RGCs arrive at the optic tectum by one week after axonal injury, the entire tectal lobe is innervated by three weeks, and a functional recovery is achieved by 2-4 weeks after the optic nerve lesion (Bernhardt 1999; McDowell et al. 2004; Becker and Becker 2007; Zou et al. 2013).

There is plethora of research on regeneration and gene expression patterns in vertebrates, including zebrafish (Liu and Londraville 2003; Hitchcock

and Raymond 2004; Saul 2008; Schuck et al. 2008; Moore et al. 2009; Gemberling et al. 2013; Benowitz et al. 2017). The regeneration of CNS in fish and PNS in mammals is successful, mainly because of molecules promoting cell survival of injured neurons, and stimulating axons to re-grow are produced soon after injuries. These intrinsic factors include cadherins (e.g. cdh2) and Klfs (e.g. klf6 and klf7; see above). There is a good correlation between cdh2 up-regulation following lesion and successful regeneration in fish CNS, chicken and quail PNS (see above). There is no detectable cdh2 up-regulation following optic nerve damage in mice, and virtually no regeneration in the optic nerve (Shibuya et al. 1995; Squitti et al. 1999; Liu et al. 2002; Ribeiro et al. 2020). Similarly, klf6 and klf7 are intrinsic factors promoting the axonal growth post-injury (Moore et al. 2011; Goldberg et al. 2013). Growth-promoting effects of klf6 and klf7 on damaged neural axons were demonstrated in both zebrafish (*in vitro*, Veldman et al. 2007) and mice (Moore et al. 2009; Goldberg et al. 2013).

There are no published results, to the best of my knowledge, on expression of *cdh6*, *cdh7*, *pcdh17* and *pcdh19* in the retina and brain visual structures of normal adult zebrafish. Nor there is any information available on the expression of these cadherins in the regenerating adult zebrafish retina. Similarly, information on *klf6a* and *klf7* expression in the brain visual structures of an adult zebrafish is lacking. Although a functional study on pcdh17 role in zebrafish retinal development was performed (see above), there is no information on molecular mechanisms involved in pcdh17-mediated retinal development.

Hypotheses

Based on expression and functional studies of selected cadherins in the visual system of embryonic and adult vertebrates, I hypothesized that *cdh6*, *pcdh17* and *pcdh19* would be expressed in the visual structures of adult zebrafish, and their expression would be up-regulated in the gcl following an optic nerve crush. RNA *In situ* hybridization and/or quantitative PCR were used to test these hypotheses. Information on expression of these cadherins in normal and regenerating adult zebrafish visual structures could provide foundation for the future functional studies of their roles in adult CNS maintenance and regeneration.

I hypothesized that both *klf6a* and *klf7* would be expressed in the visual structures of the adult zebrafish brain. *In situ* hybridization method was used to test this hypothesis. Information obtained from this study could help future studies investigating *in vivo* functional roles of these two Klfs in adult zebrafish vision.

I hypothesized that gene expression profiles, especially visual-related genes, of *pcdh17* morphants zebrafish embryos would be significantly different from those of normal zebrafish embryos. Morpholino antisense oligonucleotide technology and oligonucleotide microarray were used to test this hypothesis. Results from this study may help us in identifying molecular players involved in pcdh17-mediated regulation of zebrafish retinal development.

Information gathered in these studies could also provide insights into cdhs/pcdhs and Klfs functions in development and maintenance of visual system in other vertebrates, including humans.

CHAPTER II

CADHERIN-6, *CADHERIN-7*, *PROTOCADHERIN-17* AND *PROTOCADHERIN-19* EXPRESSION IN NORMAL VISUAL SYSTEM OF ADULT ZEBRAFISH

Introduction

Cadherin superfamily members are widely expressed in the developing vertebrates. The adhesive properties and/or activation of intracellular pathways upon binding of cadherin family members are the reason they are significant in the formation and further functioning of multicellular organisms (Nollet et al. 2000; Halbleib and Nelson 2006; Takeichi 2007; Van Roy 2012; Jontes 2016; Suzuki and Hirano 2016). The expression of several cdh and pcdh members is notable in the nervous system, especially during important stages of its development and during the formation of the neural circuits (Redies 1995, 2000; Redies and Takeichi 1996; Babb et al. 2001; Tai et al. 2010; Redies et al. 2011; Lefkovics et al. 2012; Pancho et al. 2020). The visual structures of developing model organisms, i.e. the developing mouse, chicken, *Xenopus* and zebrafish express numerous cdhs and pcdhs, and their expression patterns suggest that they are involved in the formation of the visual system (Liu et al. 2001, 2008a; Babb et al. 2005; Chen et al. 2013; De la Huerta 2013; Missaire and Hindges 2015). Moreover, misregulation of cdhs and pcdhs in the developing model

organisms causes defects in the visual system (Babb et al. 2005; Seiler et al. 2005; Ruan et al. 2006; Liu et al. 2008a; Chen et al. 2013). However, there are no published studies, to the best of my knowledge, on the expression and functions of cadherins in the visual system of the adult organisms. I am interested in examining expression of two type-II classical cadherins (*cdh6* and *cdh7*) and two non-clustered δ2-protocadherins (*pcdh17* and *pcdh19*) in the visual system of wildtype adult zebrafish, which can provide background knowledge on future studies that examine cdhs functions in adult and/or regenerating visual structures.

The visual system in zebrafish consists of dozen of types of neurons that reside in the retina and retinal targets in the brain, including the optic tectum (TeO, Wulliman et al. 2012; Baier and Wullimann 2021). In the zebrafish eye, the neuron cell bodies in the retina are located in three cellular layers, separated by two synaptic layers (Fadool and Dowling 2008). The most superficially situated are the cell bodies of the rod and cone photoreceptors in the outer nuclear layer (onl), synapsing in the outer plexiform layer (opl) with the horizontal and bipolar cells, whose bodies are located in the inner nuclear layer (inl). This layer also houses the amacrine cells, located in the inner portion of the inl. The bipolar cells are located in the middle portion of the inl, while the horizontal cells are located in the outer portion of the inl. The amacrine cells and bipolar cells synapse with dendrites of the retinal ganglion cells (RGCs) in the inner plexiform layer (ipl). Most of the RGCs are found in the retinal ganglion cell layer (gcl) and are situated in the innermost portion of the neural retina (Hitchcock and Raymond

2004; Stenkamp 2007; Fadool and Dowling 2008; Huberman et al. 2010). The RGC axons merge at the optic nerve head region (i.e., blind spot) to become the optic nerve (ON, *nervus opticus II*). The ONs from both eyes meet at the base of the hypothalamus, a region called the optic chiasm (CO). The collection of retinal axons becomes the optic tract (OT) after the optic chiasm. One part of the tract that projects dorsomedially is called the dorsomedial optic tract (DOT), while another part that projects ventrolaterally is called the ventrolateral optic tract (VOT). They reach the optic tectum in respective tectal regions and expand to cover the entire optic tectum (Wulliman et al. 2012; Baier and Wullimann 2021).

Like other teleost fish, the optic tectum is divided into six layers, starting from the most superficial layer: the stratum marginale (SM), stratum opticum (SO), stratum fibrosum et griseum superficiale (SFGS), stratum griseum centrale (SGC), stratum album centrale (SAC) and stratum periventriculare (SPV) (Vanegas 1983; Northmore 2011; Kolsch et al. 2021). The majority of retinal axons terminate in the superficial layers of the contralateral optic tectum, mainly arborize in the SFGS and in the outer portion of SO. The vast majority of cells in the optic tectum are located in the SPV, the deepest layer of the optic tectum (Stuermer 1988; Easter Jr and Nicola 1996; Kita 2015).

In addition to the optic tectum, retinal axons also project to other brain regions, most of which are located in the diencephalon (Baier and Wullimann 2021). They include those in the preoptic area (suprachiasmatic nucleus (SCN) and parvocellular preoptic nucleus, posterior part (PPp), those in the anterior thalamus (anterior thalamic nucleus (A), accessory pretectal nucleus (APN),

central pretectal nucleus (CPN), intermediate thalamic nucleus (I), parvocellular superficial pretectal nucleus (PSp), ventral accessory optic nucleus (VAO), and ventralateral thalamic nucleus (VL)), and those in the posterodorsal thalamus (periventricular pretectal nucleus, dorsal part (PPd) and periventricular pretectal nucleus, ventral part (PPv, Northcutt and Wullimann 1988; Northmore 2011; Baier and Wullimann 2021)).

There are also visual areas that do not receive retinal inputs directly, but are involved in the visual information processing via connections to other visual brain structures. These regions include the lateral zone of dorsal telencephalic area (Dl) that receives signals from the anterior thalamic nucleus (A), the dorsal posterior thalamic nucleus (DP) that receives visual information from the optic tectum and projects to the telencephalon, and the nucleus isthmi (NI) in the mid- and hindbrain boundary that are reciprocally connected to the optic tectum (Northcutt and Wullimann 1988; Northmore 1991, 2017; Hitchcock and Raymond 2004; Bakken and Stevens 2012; Wullimann 2020).

Little is known about cdhs and pcdhs expression and function in the visual system of adult vertebrates. As a first step in understanding their functions in the maintenance and physiology of visual structures of adult zebrafish, I investigated expression of *cdh6*, *cdh7*, *pcdh17* and *pcdh19* using RNA *in situ* hybridization method.

Materials and methods

Animals

Wild-type adult zebrafish (*Danio rerio*) used in this study were 12-18 months old and similar in length. Five animals of both sexes were used. Animals were housed in The University of Akron Research Vivarium (UARV). The fish were from our in-house colonies and maintained at 28°C in 14-hour light and 10-hour dark cycle in 10-gallon tanks, according to the Zebrafish Book (Westerfield 2007). After anesthetization in 0.03% (tricaine) ethyl 3-aminobenzoate methanesulfonate (MS-222, Sigma, St. Louis, MO), the fish were placed on ice in a 60 mm plastic petri dish and sacrificed by cervical transaction. The brains and retinas were quickly removed and placed immediately in 4% paraformaldehyde (PFA, by Fisher Scientifics, Waltham, MA) in 0.1M phosphate buffered saline (PBS, pH=7.4). Institutional Animal Care and Use Committee (IACUC) at The University of Akron approved all animal-related procedures (approval reference #15-07-08-LFD; copy in Appendix A).

Probe synthesis for RNA *in situ* hybridization (ISH)

The *in vitro* digoxigenin (DIG) RNA synthesis protocol (manufactuerer's manual, Roche, Indianapolis, IN) was used to generate antisense probes of each gene of interest for the detection of each *cdh* or *pcdh* mRNA in the tissues. Cloning of the cdh and pcdh genes was described in detail previously (Liu et al. 2006, 2007a, 2009, 2010). The zebrafish embryos (30-50 hpf) were used to obtain total RNA using TRIzol reagent (Life Technologies, Carlsbad, CA). cDNA

fragments were generated by using gene-specific primers in RT-PCR reactions

(Table 2.1), cloning into the pCRII-TOPO vector (Invitrogen, Carlsbad, CA), and

used as templates for generating antisense cRNA probes (Liu et al. 1999b).

Table 2.1. Zebrafish cdh genes and PCR primers used for generating cRNA probes. Vectors for molecular cloning were the following: pCRII-TOPO for cdh6 (Liu et al. 2006), pCRII-TOPO for cdh7 (Liu et al. 2007a), pCRII-TOPO for pcdh17 (Liu et al. 2009) and pCRII-TOPO for pcdh19 (Liu et al. 2010).

Gene name GenBank accession	Forward primer Reverse primer	Probe size
cdh6 AB 193290 1	5'-GCGGAAAAGATGAGGACTTG-3' 5'-CATCCACATCCTCGACACTG-3'	1131 nt
cdh7 XM 691001	5'-TGTTGGCAAGCTTCATTCTG-3' 5'-ACCGTGGGTCTATGTTCCTG-3'	1888 nt
pcdh17 XM 684743	5'-CTGTGTTTGAACAGCCCTCA-3' 5'-TTGCACCATCAGTGGGTTTA-3'	847 nt
pcdh19 BC 129243	5'-CAATGGCGAGGTGGTCTACT-3' 5'-CAACTCCAGCGTTTTTAGGG-3'	942 nt

Tissue processing for RNA *in situ* hybridization

After overnight fixation in 4% PFA at 4ºC, the eyes and brains were

washed three times for 10 minute each in 1xPBS with a constant slow agitation

(on a platform rocker) at room temperature (Barthel and Raymond 1990). The

washed tissues were subsequently placed in 20% sucrose (dissolved in PBS)

76

overnight at 4ºC (for cryoprotection). The next day (15-24 hours later), the eyes

and brains were placed in a mixture (1:1 v/v) of 20% sucrose and optimum

cutting temperature compound (Tissue-Tek® O.C.T. Compound, Sakura,

Netherlands) for 1 hour at room temperature on the platform rocker. Next, the

tissues were placed in the same solution in cylinder-shaped aluminum molds (15

mm in diameter, 25 mm in height, 2 or 3 eyes or brains in each mold), and

partially submerged into a mixture of crushed dry ice and 95% ethanol, until

frozen. The frozen tissue blocks were placed in labeled tissue sample bags and

stored at -80ºC until used for cryosectioning. The frozen tissues were cut using a

cryostat set to thickness of 14 µm for retinas and 16 µm for brains. The tissue

sections were collected on Fisher superfrost pre-treated glass slides (Fisher

Scientific, Waltham, MA). After drying at room temperature for about 1 hour, the

tissue slides were stored at -20ºC until processed for RNA *in situ* hybridization

(see below). Four sets of alternate-cross sections from each eye or brain were

collected and each set was usd for staining one *cdh* or *pcdh* probe (see below).

RNA *in situ* hybridization on tissue sections

Procedures for *in situ* hybridization on retinal tissue sections were

described previously in Barthel and Raymond (1993). Briefly, sectioned tissues

on slides were removed from the freezer and air-dried at room temperature. They

were treated with decreasing concentrations of ethanol. Then, the tissues were

briefly digested for 3 minutes with proteinase K (0.01 mg/ml, Roche) at 37ºC.

Next, the sections were incubated in 0.1 M triethanolamine (pH 8.0, Sigma, St.

77

Louis, MO), followed by washing in 0.1 M triethanolamine with 0.25% acetic anhydride (Fisher). Then, the sections were treated with increasing concentrations of ethanol, followed by air-drying at room temperature for about one hour. The sections were covered with 70 µl hybridization solution containing 2 µg/ml antisense cdh or pcdh cRNA probe, and placed in a hybridization oven (59ºC) overnight. Next day, the sections were washed in 2X SSC, followed by 50% formamide in 2X SSC (at the hybridization temperature). The tissue sections were treated with RNase A (Roche), washed in RNase buffer before incubation in a blocking solution (5% normal goat serum, 2 mg/ml BSA, 1% DMSO in PBS with Tween-20, PBST) for two hours at room temperature with constant agitation on the platform shaker. The sections were then treated with an anti-DIG antibody (conjugated to alkaline phosphatase, AB_514497, Roche) solution (diluted 1:5,000 in the blocking solution) overnight at 4ºC. Visualization of the signal was achieved by incubating the sections overnight in the dark at room temperature in a solution made from dissolving one tablet of 4-nitroblue tetrazolium chloride (NBT)/5-bromo-4-chloro-3- indolyl phosphate (BCIP, called NTB/BCIP tablet, Roche) in 10 ml of distilled water. Tissues were processed together and all paramaters were the same, except different cRNA probes were used.

Data analysis

Stained sections were observed under an Olympus BX51 compound microscope equipped with Normarski optics and connected to a SPOT digital

camera (SPOT Imaging Solutions, Sterling Heights, MI). Results were recorded as digital images and further processed using Photoshop 6.0 software (San Jose, CA).

Results

In the visual system of adult zebrafish, mRNAs for all four cadherins were detected but their expression patterns were unique. This section describes the spatial distribution of these mRNAs in the retina and in the visual structures located in the brain of intact adult zebrafish.

Cdh6, *cdh7*, *pcdh17* and *pcdh19* expression in the retina of normal adult zebrafish

Cdh6 expression was mainly detected in the inner nuclear layer (inl, Figure 2.1A). There was no obvious regional difference in *cdh6* expression within this layer, but some cells were more strongly labeled than others. Only a few faintly labeled cells were found in the retinal ganglion cell layer (gcl). Similar to *cdh6* expression in the retina, *cdh7* expression was mainly found in the inl (Figure 2.1B). Unlike *cdh6* expression in this layer, there appeared to be a regional difference in *cdh7* expression, with more strongly labeled cells in the inner portion of the inl. This region is primarily populated with amacrine cells in all vertebrate retinas examined (Hoon et al. 2014). *Pcdh17* expression in the gcl was more prominent (Figure 2.1C), compared to *cdh6* (Figure 2.1A) and *cdh7* (Figure 2.1B). In the inl, *pcdh17* was expressed uniformly with some cells labeled more strongly (Figure 2.1C). *Pcdh19* expression pattern in the retina looked

similar to *pcdh17*, except there seemed to be more *pcdh19*-positive cells in the

gcl (Figure 2.1D).
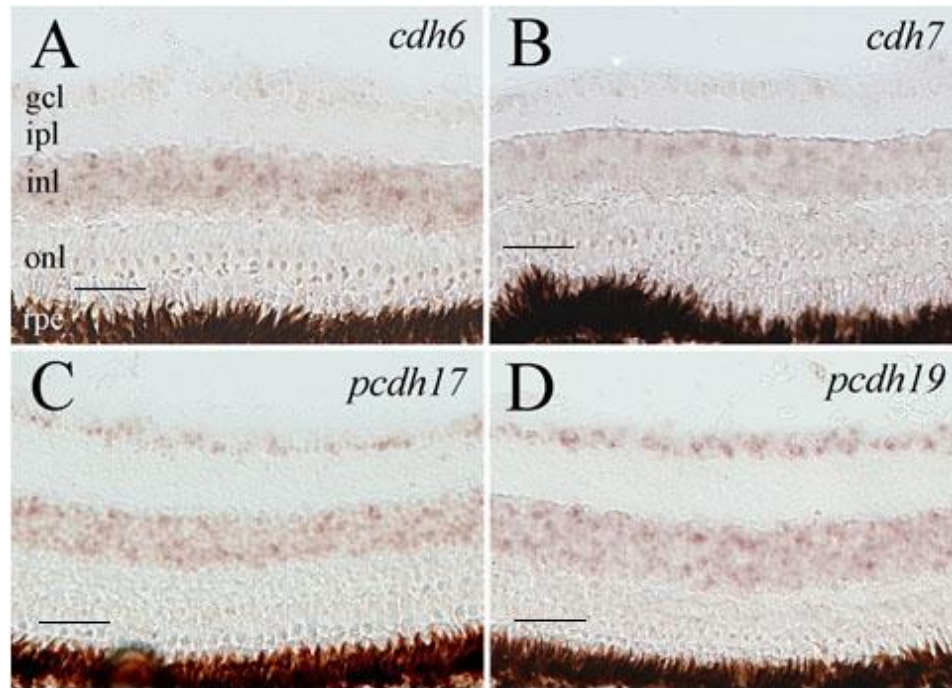
Figure 2.1. Expression of *cdh6*, *cdh7*, *pcdh17* and *pcdh19* in adult zebrafish retina. Images are cross-sections of the retina labeled with probes for *cdh6* (A), *cdh7* (B), *pcdh17* (C) and *pcdh19* (D). Scale bar = 50 µm. Abbreviations: gcl – ganglion cell layer, ipl – inner plexiform layer, inl – inner nuclear layer, onl – outer nuclear layer, rpe – retinal pigment epithelium.

Cdh6, *pcdh17* and *pcdh19* expression in the brain of normal adult zebrafish

The expression of cadherins in the visual structures of the adult zebrafish

brain was studied and *cdh7* was not detected. The expression of *pcdh19* was the

most prominent; therefore, it is described fist, followed by *pcdh17* and *cdh6* (that

showed the lowest expression). Their respective expression patterns are

described from anterior to posterior brain regions, and the section levels for

respective figures are shown in the schematic drawing of a lateral view of adult

zebrafish brain (Figure 2.2).
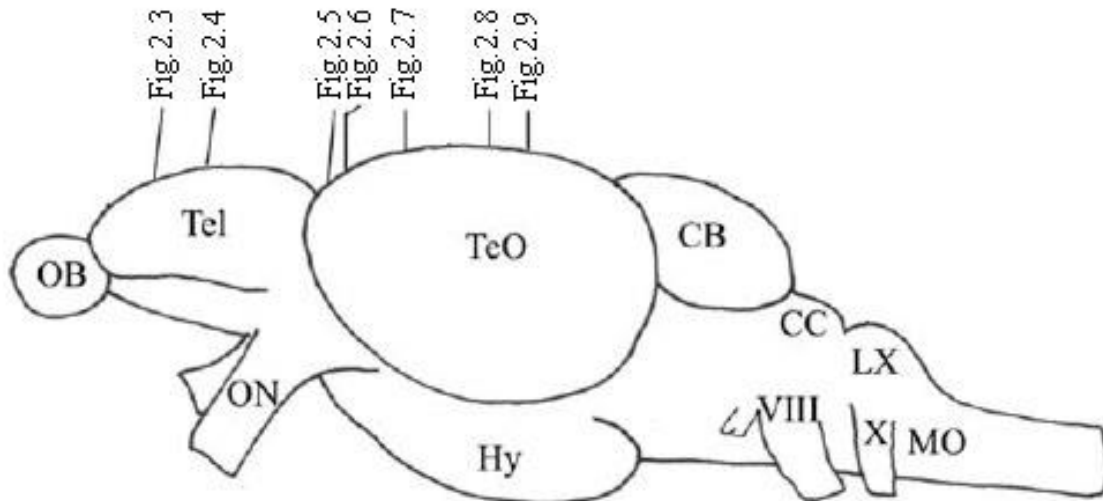
Figure 2.2. Schematic drawing of an adult zebrafish brain showing levels of cross-sections for examining *cdhs* and *pcdhs* expression. Lateral view, anterior to the left, dorsal to the top. Numbers represent respective figure numbers in this chapter. See Abbreviations for list of full terms.

Telencephalon

In the telencephalon, the visual structure that contained *pcdh19*-

expressing cells is the lateral zone of dorsal telencephalic area (Dl) (Figure 2.3

and Figure 2.4). In the precommissural telencephalon (Figure 2.3A, left panel,

Figure 2.3B and E), *pcdh19*-expressing cells appeared to be evenly distributed in

Dl, which was unlike *pcdh19* expression in the adjacent Dc (central zone of

dorsal telencephalic area) and Dm (medial zone of dorsal telencephalic area),

where only a few scattered *pcdh19*-expressing cells were found in Dc (Figure

2.3B and E), while most *pcdh19* expression was confined to the superficial layer

in Dm (Figure 2.3B). In the postcommissural telencephalon (Figure 2.4A, left panel and Figure 2.4B), *pcdh19* expression was more prominent in the superficial region of Dl, including the border region between Dl and Dc (Figure 2.4A, left panel).

In the precommisural telencephalon, *pcdh17* expression was mainly detected in the dorsomedial region of Dl, adjacent to Dm (Figure 2.3A, middle panel and Figure 2.3C). In the postcomissural telencephalon, expression levels of *pcdh17* were low in Dl (Figure 2.4A, middle panel and Figure 2.4C).

Cdh6 expression in the visual structures of the telencephalon was more limited than the *pcdhs*. In the precommisural telencephalon, weak *cdh6* expression was detected mainly in the superficial region of Dl (Figure 2.3A, right panel and Figure 2.3D and G). In the postcommisural telencephalon, no obvious *cdh6* was detected in Dl (Figure 2.4A, right panel and Figure 2.4D).
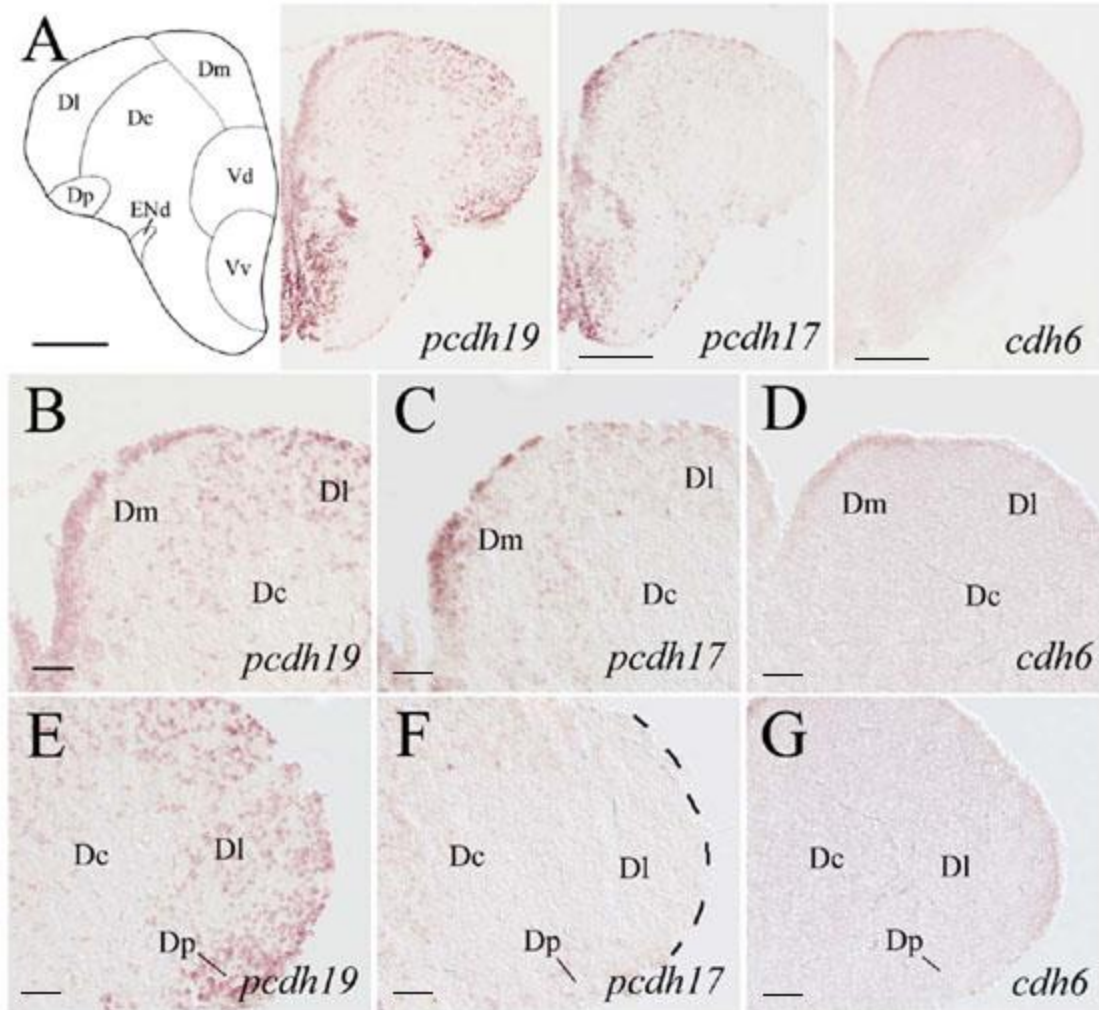
Figure 2.3. Expression *pcdh19*, *pcdh17* and *cdh6* in the precomissural telencephalon. Images in the top panels show lower magnification of adjacent brain regions from brain section shown in Figure 2.2. Images in the lower panels: B-D show higher magnifications of the dorsomedial regions of the dorsal telencephalon, while E-G show higher magnified views of the dorsolateral regions of the dorsal telencephalon shown in the top respective panels. Scale bar = 200 μm for panel A, 50 μm for panels B-G. See Abbreviations for list of full terms.
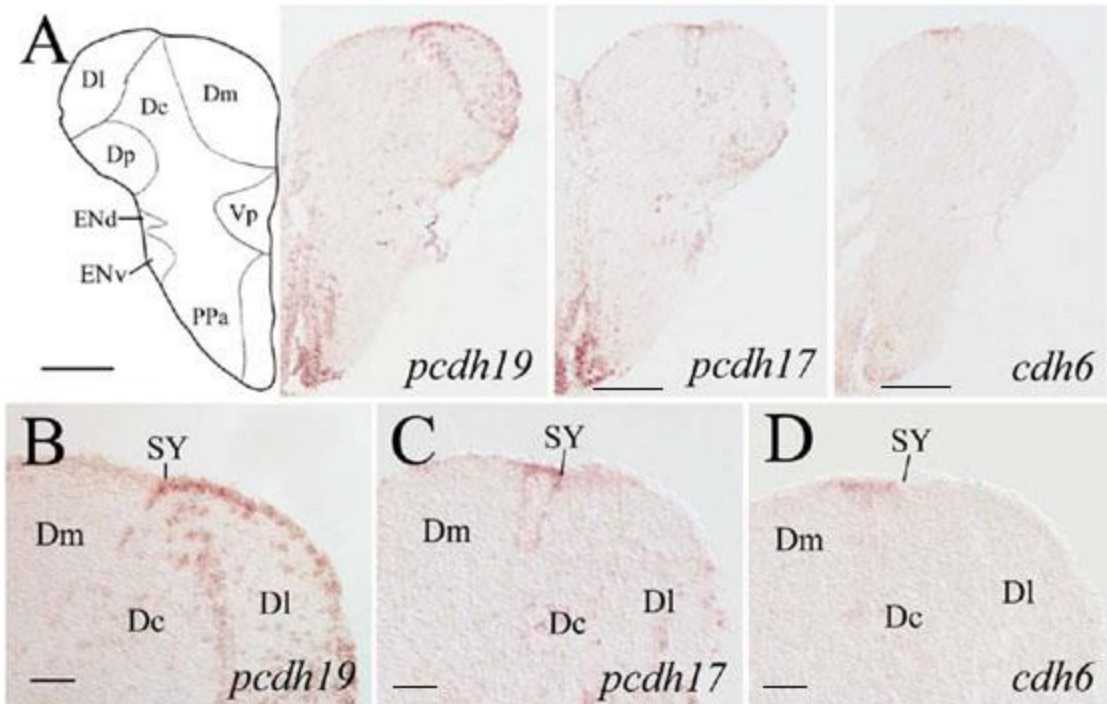
Figure 2.4. Expression of *pcdh19*, *pcdh17* and *cdh6* in the postcommissural telencephalon. Images in the top panels are low magnified views of adjacent brain at a level shown in Figure 2.2. Images in the lower panels show higher magnifications of the dorsal telencephalon region adjacent to the sulcus ypsiloniformis (SY) shown in their respective top panels. Scale bar = 200 μm for panel A, 50 μm for panels B-D. See Abbreviations for list of full terms.

The preoptic area

The posterior part of the parvocellular preoptic nucleus (PPp) and suprachiasmatic nucleus (SCN) are two of the nuclei in the preoptic area of vertebrates that receive direct inputs from retinal axons. All three cadherin family members were expressed in these two nuclei. *Pcdh19* was strongly expressed in both PPp and SCN (Figure 2.5A, left panel and Figure 2.5B). Most cells in PPp appeared to contain *pcdh19* mRNA, but those in the ventral half of PPp were more strongly labeled than those in the dorsal half of PPp. Compared to PPp,

there were fewer *pcdh19*-expressing cells in the SCN, with these cells displaying

patchy distribution.

Pcdh17 exhibited almost the exact same pattern of expression in the PPp

and SCN of the preoptic area (Figure 2.5A, middle panel and Figure 2.5C) as

pcdh19, while *cdh6* expression in these two nuclei was much weaker compared

to that of the two *pcdhs* (Figure 2.5A, right panel and Figure 2.5D).
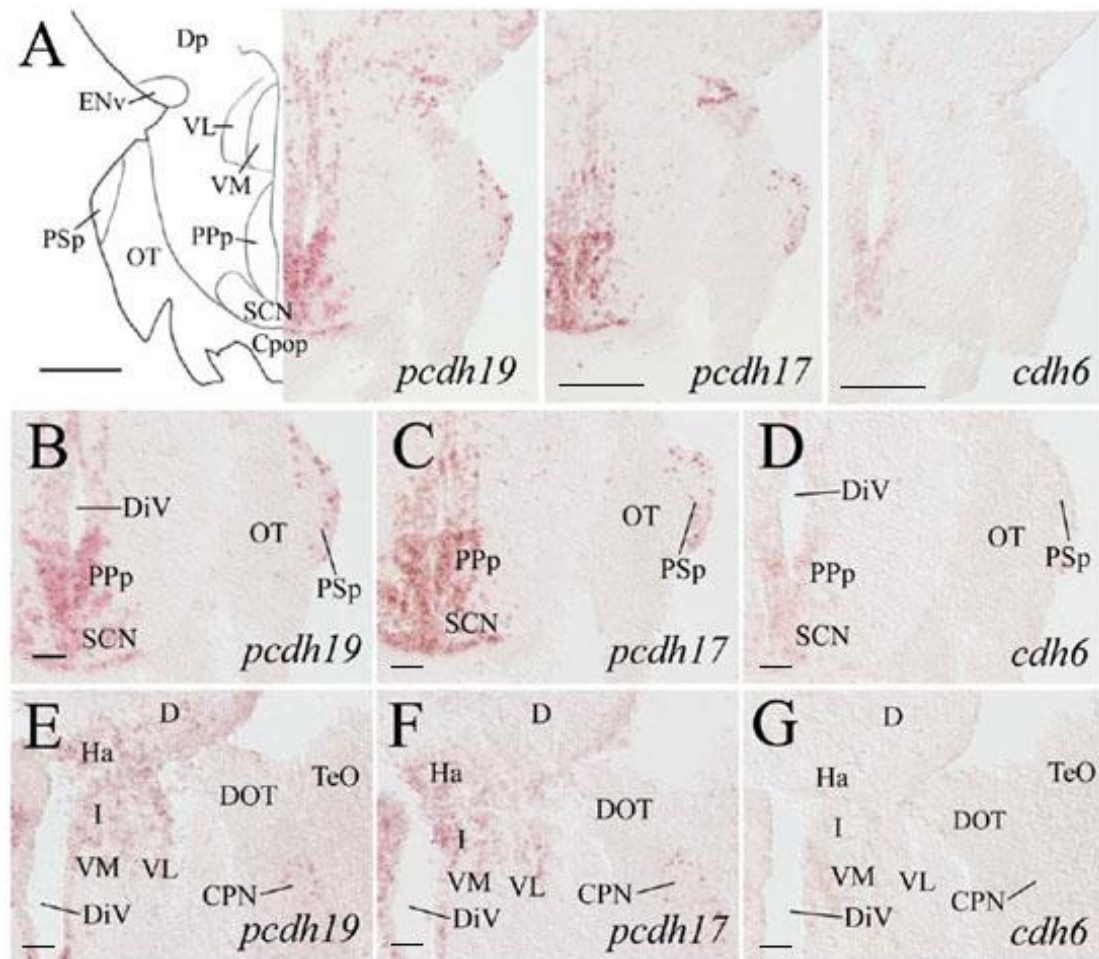
Figure 2.5. Expression of *pcdh19*, *pcdh17* and *cdh6* in the posterior preoptic area, ventral thalamus and pretectum. Top panel images show low magnifications of the brain from adjacent sections at a level indicated in Figure 2.2. Images B-D represent higher magnifications of the posterior preoptic areas and the suprachiasmatic nucleus (SCN) shown in the top panels. E-G are sections 100-150 μm located posterior to those shown in B-D, showing epithalamus and ventral thalamus. Scale bar = 200 μm for the panel A, 50 μm for panels B-G. See Abbreviations for list of full terms.

Diencephalon

In the diencephalon, where many visual structures are located, the three cadherin mRNAs were differentially expressed (Figure 2.5, Figure 2.6 and Figure 2.7). Adjacent to the midline in the anterior thalamus, *pcdh19*-expressing cells were detected in the intermediate thalamic nucleus (I, Figure 2.5E), anterior thalamic nucleus (A) and ventrolateral thalamic nucleus (VL, Figure 2.6A and D). The ventral accessory optic nucleus (VAO, Figure 2.6A), central pretectal nucleus (CPN) and accessory pretectal nucleus (APN) in the more lateral regions of the anterior thalamus also contained a few *pcdh19*-expressing cells (Figure 2.6D). *Pcdh17* was also expressed in these nuclei in the anterior thalamus (Figure 2.5F, Figure 2.6B and E), but its expression in the A, VL, CPN and APN appeared to be less than *pcdh19*, and its expression was not detected in the VAO.

The parvocellular superficial pretectal nucleus (PSp), a visual structure located in the anterolateral thalamus, also contained *pcdh19* and *pcdh17* (Figure 2.5B and C). Moreover, both *pcdh19*- and *pcdh17*-expressing cells were found mainly in the superficial regions of this nucleus. In the posterior thalamus, *pcdh19* expression was detected in dorsomedially located nuclei that receive retinal inputs: the periventricular pretectal nucleus, dorsal part (PPd) and ventral parts (PPv, Figure 2.7B). *Pcdh19* was also detected in the posterior thalamic nucleus (DP) that receives visual inputs from the optic tectum. As in the anterior thalamus, *pcdh17* expression pattern was similar to that of *pcdh19* in the posterior thalamus, except that expression level of *pcdh17* was somewhat lower,

based on the staining intensity, than *pcdh19* in the three dorsomedially located nuclei (Figure 2.7C).

Cdh6 expression in the diencephalon was considerably limited and it was only faintly expressed in the A in the anterior thalamus, and the DP of the dorsal posterior thalamus (Figure 2.6C and Figure 2.7D).
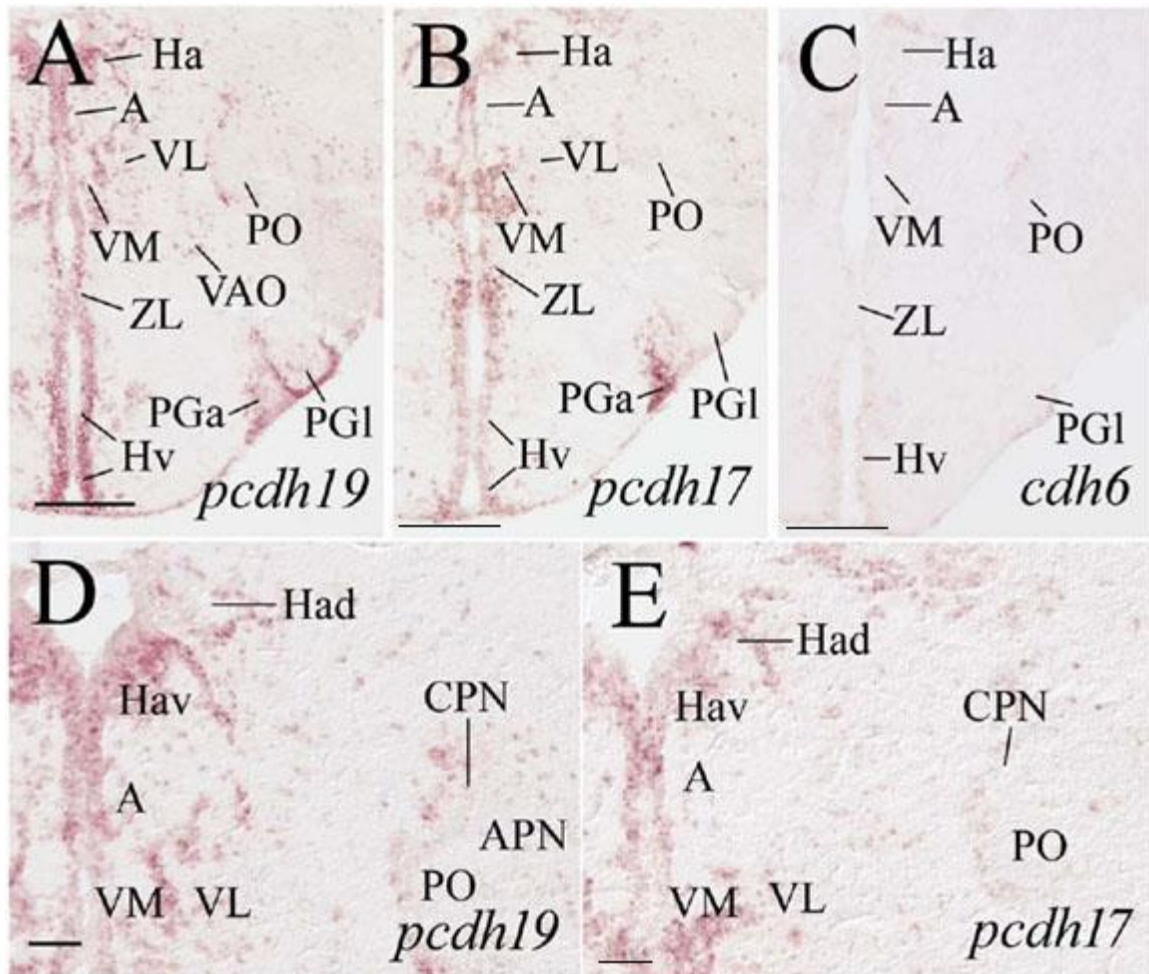
Figure 2.6. Expression of *pcdh19*, *pcdh17* and *cdh6* in the thalamic and pretectal regions. Images in top panel show low magnifications of adjacent brain sections from a level shown in Figure 2.2. Images D and E represent higher magnifications of the habenular, ventral thalamic and pretectal regions of their respective images in the top panels. Scale bar = 200 μm for the top panels, 50 μm for the lower panels. See Abbreviations for list of full terms.
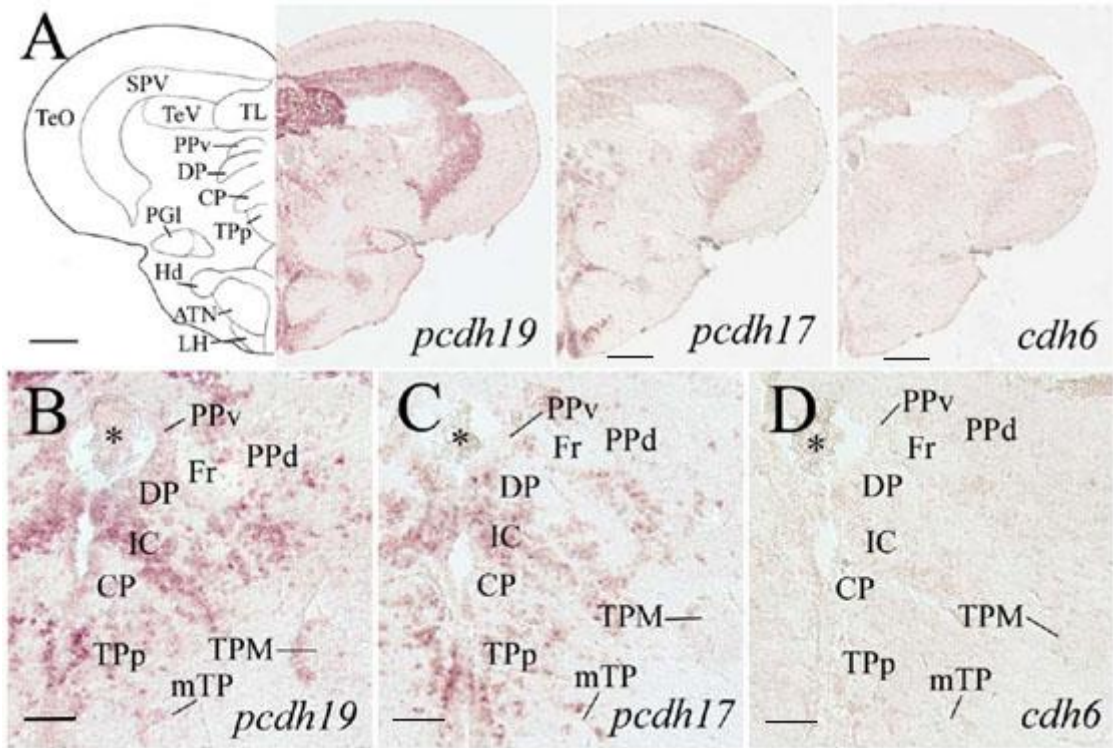
Figure 2.7. Expression of *pcdh19*, *pcdh17* and *cdh6* in the dorsal thalamus, pretectum and optic tectum. Images in the top panels show low magnifications of adjacent sections from a level shown in Figure 2.2. B-D: Magnified views of the dorsal thalamus and periventricular pretectum from their respective images in the top panels. Asterisks point to groups of cells in the diencephalic ventricle. Scale bar = 200 µm for the top panels, 50 µm for the lower panels. See list for abbreviations.

Mesencephalon and isthmus

The mesencephalon includes the optic tectum (TeO), which is the main target of RGCs. As mentioned in the introduction, the TeO is organized into six layers, with the stratum fibrosum et grieseum superficiale (SFGS) and stratum opticum (SO) as the main retinal-recipient layers, and stratum periventriculare (SPV) containing the vast majority of the tectal cells. It appeared that almost all cells in the SPV were *pcdh19*-expressing, and some cells (more in the dorsal region of the SPV) were more strongly labeled than others (Figure 2.7A left

panel, Figure 2.8A). The SFGS, the major retinal-recipient region in the optic

tectum also contained many *pcdh19*-expressing cells (Figure 2.8A). Only a few

scattered *pcdh19*-expressing cells were detected in the remaining optic tectum

(Figure 2.8A).

The SPV also contained *pcdh17*-expressing cells (Figure 2.8B). Its

expression in the SPV was similar to that of *pcdh19*, but less strongly labeled.

There was no obvious *pcdh17* expression in any of the tectal layers above the

SPV. *Cdh6* expression in the optic tectum (Figure 2.8C) was somewhat similar to

that of *pcdh17*, except the labeling was weaker than *pcdh17*.

Figure 2.8. Expression of *pcdh19*, *pcdh17* and *cdh6* in the optic tectum. Higher magnifications of adjacent sections of the medial optic tectum are from images shown in the top panels in Figure 2.2. Scale bar = 50 µm. See Abbreviations for list of full terms.

Pcdh19-expressing cells were also detected in the nucleus isthmi (NI), a

visual structure in the boundary of the mid-hindbrain, and reciprocally connected

with the optic tectum (Figure 2.9A). It appeared that cortex cells in the dorsal and

lateral regions were more intensely labeled than other *pcdh19*-expressing cells in

the structure. The NI also contained *pcdh17*-expressing (Figure 2.9B) and *cdh6*-

expressing cells (Figure 2.9C), but due to their weak labeling, it was difficult to

describe their staining characteristics.
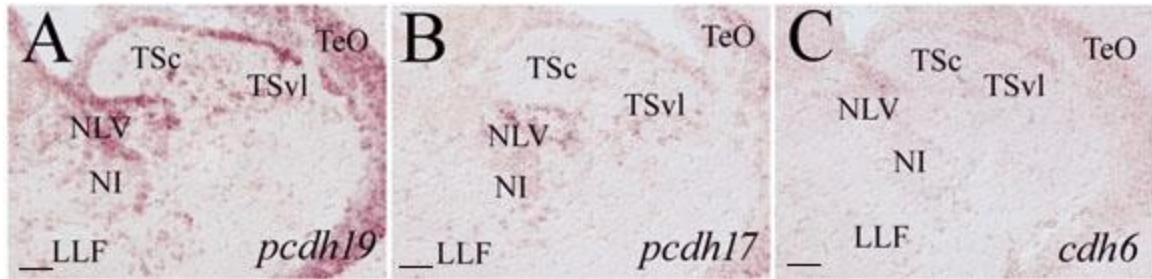
Figure 2.9. Expression of *pcdh19*, *pcdh17* and *cdh6* in the isthmus. Higher magnifications of adjacent sections of the medial optic tectum from images shown in the top panels in Figure 2.2. Scale bar = 50 μm. See Abbreviations for list of full terms.

Expression of *pcdh19*, *pcdh17* and *cdh6* in the visual structures of the adult zebrafish brain is summarized in Table 2.2.

Table 2.2. Summary of *pcdh19*, *pcdh17* and *cdh6* expression in normal adult zebrafish brain visual structures. The number of plus signs indicates staining intensities: +++, strong; ++, moderate; +, weak; +/-, barely detectable; -, no labeling detected. Asterisks indicate that the staining is limited to superficial regions. See Abbreviations for list of full terms.

	pcdh19	*pcdh17*	*cdh6*
A	+	+	+/-
APN	+	+	-
CPN	+	+	-
DI	++	+	+*
DP	+++	++	-
I	++	++	+/-
NI	+	+	+/-
PPd/PPv	++	+	-
PPp	++	++	+/-

PSp	+	+	-
SCN	++	++	-
TeO	+++	++	+
VAO	+	-	-
VL	+	+	-

Discussion

Cadherin expression has been studied primarily in developing model organisms, and information on cadherin expression in adult organisms is scarce. This study characterized unique spatial expression of two type-II classical cdhs and two non-clustered δ2-pcdhs in the adult zebrafish's visual system. *Pcdh19* was the the most prominently and widely expressed, while *pcdh17* expression patterns were similar but had less staining intensity, and/or with fewer stained cells. *Cdh6* expression was much more restricted in the the visual structures of the brain, and the positive cells were much less stained. *Cdh7* was expressed in the retina, but was not detected in the brain.

Continued expression of those cadherins in adult zebrafish visual structures suggests that not only do cadherins play roles in the development of the visual system, but also that they may be involved in the maintenance and/or normal function of the visual structures in adult vertebrates.

Expression of *cdh6*, *cdh7*, *pcdh17* and *pcdh19* in the retina of adult zebrafish and comparison with developing zebrafish

In embryonic zebrafish, *cdh6* is mainly expressed in the gcl and inl (Liu et al. 2006), which is comparable to its expression in the adult zebrafish retina. However, a more detailed comparison of their expression patterns reveals some obvious differences between the developing and adult zebrafish (Liu et al. 2006). There appeared to be more *cdh6*-expressing cells that are more intensly labeled in the developing retina, than in the adult retina. Moreover, in the inl (at 46-48 hpf, when inl develops), *cdh6*-expressing cells are mainly found in the inner portion of this layer (Liu et al. 2006), while in the adult retina, the entire inl contained many *cdh6*-expressing cells. These differences in their expression patterns, if confirmed by immunocytochemical studies, suggest that cdh6 plays similar (in a subset of RGCs and amacrine cells) and different functions (in other cells types such as bipolar cells and horizontal cells) during embryonic development and adult stage.

Expression of *cdh7* in the adult zebrafish retina was analogous to its expression in the developing zebrafish retina (Liu et al. 2007a), except that its expression in the gcl was much reduced in the gcl of adult retina. If similar cdh7 protein expression pattern is observed in the developing and adult zebrafish retina, my results sugget that cdh7 plays a more important role during gcl development than its function in gcl maintenance and/or physiology, while it is implicated in both the development and maintenance of the amacrine cells.

In the adult retina, *pcdh17* is expressed by cells in both the gcl and inl, so this expression pattern is similar to developing zebrafish retinas at 34-50 hpf,

when *pcdh17*-expressing cells are uniformly located in all retinal layers (Liu et al. 2009). In addition, the adult retina is comparable to 72 hpf embryonic zebrafish retina, as *pcdh17* is present in an area of inl where horizontal cells are localized, and also no *pcdh17* is found where the photoreceptor cells reside (in the onl). Nonetheless, *pcdh17* expression in the 72 hpf retina is apparently different from that of both the early retina and adult retina, with its expression solely confined to the outer portion of the inl (Biswas and Jontes 2009; Liu et al. 2009). This dynamic change of *pcdh17* expression in the developing retina and adult retinas suggest that this non-clustered pcdh plays differential roles in the development of the retina and subsequent maintenance and/or physiological function of the retinal cells.

Expression of *pcdh19* in adult zebrafish is detected in the gcl and inl, which is somewhat similar to its expression in the eye primordia at 12 hpf and the entire retina of 18 and 24 hpf embryos (Liu et al. 2010). *Pcdh19* expression in embryos becomes almost undetectable in the retina of 36 hpf embryos, but reappears in the gcl of 50 hpf and 72 hpf embryos (Emond et al. 2009; Liu et al. 2010). These expression patterns suggest that *pcdh19* is involved in the early eye and retinal development (12-24 hpf), later in the gcl formation (50-72 hpf), and in the maintenance and/or physiological function of the adult zebrafish retina.

Overall, it was surprising to observe a wide and strong expression of these *cdhs* and *pcdhs* in the adult zebrafish retina, because expression of classical cadherins (cdh2 and cdh4; mRNA and protein) is greatly reduced in the adult zebrafish retina (Liu et al. 1999b, 2001). On the other hand, it is noteworthy to

report that expression of each of the four *cdhs*/*pcdhs* in the adult retina was unique, which is similar to that of most cdhs in developing organisms. Analysis of the single-cell transcriptome of RGCs from both embryonic and adult zebrafish confirmed expression of *cdh6*, *pcdh17* and *pcdh19* mRNAs (Kolsch et al. 2021). These results suggest that these cdhs and pcdhs play diverse roles and are significant in the maintenance and/or physiology of the adult retina.

Expression of *cdh6*, *cdh7*, *pcdh17* and *pcdh19* in the brain visual structures of adult zebrafish and comparison with developing zebrafish

In the embryonic zebrafish of 34-48 hpf, almost all retinal axons project to the optic tectum (arborization field 10, AF10, Burrill and Easter 1994). By 72 hpf, the retinal axons have been detected in most of the brain visual structures in the preoptic area, diencephalon and midbrain (e.g. suprachiasmatic nucleus, pretectal nuclei and optic tectum, Burrill and Easter 1994; Baier and Wullimann 2021). The expression of *cdh6* in the visual structures of an embryonic (24-48 hpf) brain is limited and weak, confined mainly to the pretectum and anteroventral optic tectum (Liu et al. 2006). This is somewhat similar to *cdh6* expression in an adult's brain visual structures: it is faintly expressed in the main cellular layer (SPV, stratum periventriculare) of the optic tectum. The apparent difference in *cdh6* expression between embryonic and adult brain visual structures is the higher level of expression (based on staining intensity) in the pretectum of 48 hpf embryos than in an adult fish. The locally restricted and weak expression of *cdh6* in both the embryonic and adult brain visual structures suggests that this cadherin plays a limited role in the development of this system.

94

In embryonic zebrafish, *cdh7* is expressed along the optic pathway: the anterior hypothalamus (where future preoptic and suprachiasmatic nuclei will form), in the pretectum and in the optic tectum (Liu et al. 2007a). Unlike the other cadherins studied here, *cdh7* was not detected at all in the adult zebrafish brain. It is possible that cdh7 proteins are only involved in development of the brain visual structures, and are not required for the structure and/function of the adult brain.

Developing zebrafish brains have strong and wide *pcdh17* expression (Liu et al. 2009). The visual regions in the anterior hypothalamus, pretectum and the major retinal target (i.e. optic tectum) express *pcdh17* from 24 hpf to 72 hpf. This expression pattern is similar to that in the adult zebrafish brain, suggesting that this pcdh plays a role in both the development and maintenance of brain visual structures.

Compared to *pcdh17*, expression of *pcdh19* in the developing zebrafish brain appears to be wider in younger embryos (18-24 hpf), but slightly more restricted in older embryos (50-72 hpf, Liu et al. 2010). *Pcdh19* is strongly expressed in the entire optic tectum at 18 hpf. In contrast, apparent *pcdh17* expression in the optic tectum is observed in much older embryos (50-72 hpf). *Pcdh19* expression in the pretectum and optic tectum is strong throughout the developmental stages examined (18-72 hpf). This pattern of expression is similar to its expression in the adult visual structures, suggesting that this pcdh functions both early, before the arrival of retial axons, and later during the innervation and arborization of the brain structures, and it is also involved in the maintenance of

the visual structures. It is interesting to note that pcdh19 expression in the young zebrafish is somewhat similar to that of cdh2 (i.e. N-cadherin), and it is demonstrated that these two cadherins work together to promote the formation of the zebrafish central nervous system, including the visual structures (Biswas et al. 2010; Emond et al. 2011).

Comparing *cdh6*, *cdh7*, *pcdh17* and *pcdh19* expression in the retina of adult zebrafish and other model organisms

The majority of studies examining the expression of cadherins and protocadherins focus on the developing vertebrates, only few studies used the adult animals. This section compares retinal expression of *cdh6*, *cdh7*, *pcdh17* and *pcdh19* in the adult zebrafish to other adult model organisms. In cases where the adult expression is not available (e.g. chicken, mouse), the information on developing retinas is used.

In adult ferrets (*Mustela putorius furo*), *cdh6* is detected in the gcl and inl (Etzrodt et al. 2009), which is similar to *cdh6* expression in the adult zebrafish retina. Unlike the zebrafish retina, where most cells in the inl are *cdh6*-expressing and there is only a few faintly labeled cells in the gcl, there are more cells expressing *cdh6* in the gcl than in the inl of the ferret retina. Moreover, the *cdh6*-expressing cells in both ferret gcl and inl are similarly stained. Furthermore, *cdh6* expression in the ferret inl is confined to the innermost region where amacrine cells reside. There is no published data on cdh6 expression in adult mouse retina. *cdh6* mRNA (using RNA *in situ* hybridization method) and cdh6 protein (using immunohistochemistry method) are found in a subset of amacrine

cells of P0-42 mouse retina (Honjo et al. 2000a; Kay et al. 2011). Additionally, a subset of retinal ganglion cells, the ON-OFF direction-selective RGCs in developing mouse retina, is shown to contain *cdh6*/cdh6 (Kay et al. 2011; Osterhout et al. 2011; De la Huerta 2013). These results are similar to *cdh6* expression in adult zebrafish in that it is expressed in only a few cells in the gcl, and in the inner portion of the inl where the amacrine cells reside. Unlike the mouse retina, *cdh6* is expressed in the entire inl of adult zebrafish retina.

Cdh7 is expressed in both the gcl and inl in adult zebrafish, which is similar to *cdh7* expression in the gcl of both adult ferrets (based on their morphology, Etzrodt et al. 2009) and mice (Faulkner-Jones et al. 1999). Also similarly to adult zebrafish and ferrets, *cdh7* expression is stronger in the inner portion of the inl. Unlike *cdh7* expression in adult zebrafish, where only a few weakly labeled cells are *cdh7*-expressing in the gcl, *cdh7* is strongly expressed in many cells in the gcl of adult ferrets. Some *cdh7*-positive cells in the inner portion of the inl of the adult ferret retina are likely displaced RGCs. Since displaced RGCs in zebrafish are very rare (~1%), it is more likely that most *cdh7*-expressing cells in the inner portion of the inl were the amacrine cells in zebrafish. There is no published information on cdh7 expression in adult chicken retinas, but developing chicken retinas expressed cdh7 in several retinal layers including the ipl, inl and opl (Wöhrn et al. 1998). Specifically, similar to the adult zebrafish, cdh7 is expressed by the amacrine cells of developing chicken retinas (Wöhrn et al. 1998).

The only available report on *pcdh17* expression in adult vertebrate eyes is for the ferret (Etzrodt et al. 2009). As in the adult zebrafish, *pcdh17*-expressing cells are detected in both the gcl and inl. But unlike *pcdh17* expression in the adult zebrafish retina where no pcdh17 expression is detected in the onl, all cells in the onl of the ferret retina appear to be *pcdh17*-expressing.

Pcdh19/*pcdh19* expression data in the retina of the adult model organisms is absent in literature. Developing retinas in mice (Gaitan and Bouchard 2006) express *pcdh19* in the same layers (gcl and inl) as in the adult zebrafish. In developing chick retinas, pcdh19 is expressed by cells in the gcl and in the optic nerve (Tai et al. 2010).

Comparing *cdh6*, *cdh7*, *pcdh17* and *pcdh19* expression in the brain visual structures of adult zebrafish and other model organisms

As in the previous section, the expression of *cdh6*, *cdh7*, *pcdh17* and *pcdh19* in the adult zebrafish is compared with other adult model organisms in the visual structures of the brain. Similarly, if there is no available data for cdh/pcdh in the brain of adult organisms, its expression in developing brains is briefly compared to that in the adult zebrafish brain.

In adult mammals (mouse and marmoset), *cdh6* is detected in the primary visual cortex (V1), the main mammalian structure processing visual information, that receives its visual inputs primarily from the dorsal lateral geniculate nucleus (dLGN, an important retinal-recipient target area in the thalamus). Although the nonmammals lack a structure homologous to V1, the optic tectum of nonmammals serves similar functions in processing the visual information. In

both mammal species, *cdh6* is expressed in cells in the deepest layer (VI) of the

visual cortex (Krishna-K et al. 2009; Matsunaga et al. 2014). Cells in this layer

receive inputs from other cortical layers, and process complex visual information.

In most nonmammals there is only one major cellular layer in the optic tectum, so

it is difficult to compare functional similarities of the six (cellular)-layered

mammalian visual cortex with the optic tectum of the nonmammals. Therefore, I

can only state that *cdh6* is expressed by subset of cells in the major brain visual

structure of adult zebrafish, mice and marmoset. There are no published data on

cdh6 expression in adult chicken brains. In developing chickens, *cdh6* is detected

in the optic tectum (Wöhrn et al. 1999) and in several retinorecipient areas of the

brain, including the anterior thalamic nucleus (A, Wöhrn et al. 1998).

The adult zebrafish visual areas (and brain in general) had no detectable

cdh7 expression and that finding is consistent with information available from

adult mice (Faulkner-Jones et al. 1999) and rats (Takahashi and Osumi 2008). A

recent study by Kolsch et al. (2021) further confirms this result by showing the

adult zebrafish optic tectum lacks *cdh7* input from RGCs.

Adult ferrets (Krishna-K et al. 2009) and mice (Yan et al. 2014) have

pcdh17 expression in the visual (occipital) cortices, and this is similar to the adult

zebrafish (see above). *Pcdh17* expression data in the other brain visual

structures, e.g. the superior colliculus (SC) is available only for the developing

mouse (Visel et al. 2004; Hoshina et al. 2013) and rat (Kim et al. 2007). The SC

in mammals receives direct retinofugal projections and is a homologous structure

(based on the majority of direct retinal inputs it receives and the location in the

midbrain) to the optic tectum (TeO) in fish and birds (Vanhalst et al. 2005; Kim et al. 2007; Coughlin and Kurrasch 2015, 2015; Ito and Feldheim 2018). The SC relays visual information (along with dLGN, see above) to other brain regions, e.g. the primary visual cortex (V1). Similarly to adult zebrafish, developing rats (Kim et al. 2007) strongly express *pcdh17* in the deep cellular layers of the SC, while expression in that area is reduced in developing mice (Visel et al. 2004).

 Pcdh19-expressing cells are also found in the visual cortex of adult ferrets (Krishna-K et al. 2009) and this expression is limited to only a few cells in deep layers of the V1. This is different from *pcdh19* expression in the adult zebrafish, where the vast majority of cells in the optic tectum are *pcdh19*-expressing. In adult mice, *pcdh19* is detected in the superficial and in the deep layers of the secondary visual cortex (V2, Yan et al. 2014), a structure receiving signals from V1, which does not have a homologous structure in fish. There are no published studies on pcdh19 expression for adult rats. Strong *pcdh19* expression is detected in various brain visual structures in developing rats (Kim et al. 2007). These structures include the superior colliculus, occipital cortex, dLGN, APN and SCN. This wide *pcdh19* expression in the brain visual structures of developing rats is similar to its expression in the visual centers in adult zebrafish. Finally, pcdh19 expression is observed in the optic tectum of embryonic chicks (Tai et al. 2010). Similar to adult zebrafish, pcdh19 is expressed in the retinal-recipient layers (including the SFGS) of the developing chick, but unlike the zebrafish, there are only few scattered cells in the SPV in the chick optic tectum that are pcdh19-positive.

CHAPTER III

KLF6A AND *KLF7* EXPRESSION IN NORMAL VISUAL SYSTEM AND IN

REGENERATING OPTIC NERVE OF ADULT ZEBRAFISH

Introduction

Klf genes are homologous to the *Drosophila* Krüppel gene, which

regulates the fly's embryonic patterning (Rosenberg et al. 1986; Kaczynski et al.

2003; Pearson et al. 2008). Klfs belong to a family of transcription factors with

conserved three C_2H_2-type DNA-binding domains near carboxyl terminal and

include three tandem zinc fingers (Cys_2/His_2) with conserved linker

(TGEKP(Y/F)X) regions (Dang et al. 2000; Bieker 2001; Iuchi 2001; McConnell

and Yang 2010). Klfs bind in GC- and CACCC- regions in the promoter regions

of their target genes (Miller and Bieker 1993; Conkright et al. 1999) and activate

or repress gene transcription (Pearson et al. 2008; Moore et al. 2011).

In vertebrates, Klfs are widely expressed in most of the tissues and

organs, including CNS and PNS (Laub et al. 2001a, 2001b, 2006; Oates et al.

2001; Pearson et al. 2008; Moore et al. 2009, 2011). In the visual system of

zebrafish, *klf7* is expressed only in the developing RGCs (Veldman et al. 2007).

The zebrafish homolog of mammal *Klf6* is *klf6a* (Xue et al. 2015). It is absent in

developing and adult zebrafish RGCs but is present in the TeO at 42-48 hpf

(Thisse et al. 2001; Veldman et al. 2007). However, following the optic nerve injury and through the regeneration period, Veldman et al. (2007) observed robust up-regulation of *klf6a* and *klf7* in RGCs of the zebrafish. The levels of both *klfs* are elevated at day 1 after injury, peak at 2-6 days, continue to increase at 12 days and return to a baseline by 24 days after the injury. *Klf6* function is hypothesized to be limited to the retinal axon regeneration, while *klf7* modulates both the regeneration and development of RGCs (Veldman et al. 2007). Veldman et al. (2007) used the term klf7a, although the primers for cRNA clones match gene named krüppel-like factor 7 (ubiquitous), like (klf7l). This gene was re-named klf7b in 2011 by Zebrafish Nomenclature Committe in ZFIN.org database (http://zfin.org/action/nomenclature/history/ZDB-GENE-041014-171). I will use the term klf7 in this dissertation.

Klfs studies are mainly focused on their expression in the non-nervous tissues in mammals with few reports describing non-mammalian CNS (Veldman et al. 2007; Bureau et al. 2009; Antin et al. 2010; Moore et al. 2011). Zebrafish is a widely used model organism to investigate development and regeneration processes. There are no published studies on *Klf6*/*klf6a* and *Klf7*/*klf7* describing their expression in the visual structures in the adult vertebrate brain. I measured *klf6a*/*klf7* expression in regenerating adult zebrafish retinas using qPCR and RNA *in situ* hybridization.

I hypothesized that *klf6a* and *klf7* are differentially expressed in the visual centers of the adult zebrafish brain, because only *klf7* is expressed in the embryonic retina (Veldman et al. 2007). I tested this hypothesis by using RNA *in*

situ hybridization method. Since *klf6a* and *klf7* appear to be sensitive and reliable markers for regenerating nervous tissues, I wanted to confirm the qPCR data from the optic nerve regeneration study conducted by Veldman et al. (2007), using mainly *in situ* hybridization. If confirmed, I could use *klf6a* and/or *klf7* as regeneration markers in my study of *cdhs* and *pcdhs* expression in regenerating adult zebrafish retinas (Chapter IV).

Materials and methods

Animals

Adult wild-type zebrafish (*Danio rerio*) used for the gene expression and the optic nerve lesion study were 12-18 months old and similar in length, and fish from both sexes were used. Animals were housed in The University of Akron Research Vivarium (UARV). The fish were bred in-house for several generations and maintained according to the Zebrafish Book (Westerfield 2007) in constant conditions at 28°C in 14-hour light and 10-hour dark cycle in 10-gallon tanks, 20-30 fish per tank. Six animals were used for studying *klf6a* and *klf7* expression in the normal adult zebrafish visual brain structures, and 35 animals were used for examining *klf6a* and *klf7* expression in the regenerating retinas. Institutional Animal Care and Use Committee (IACUC) at The University of Akron approved all animal-related procedures (approval reference #15-07-08-LFD; copy in Appendix A).

Optic nerve lesion surgery

The procedures were carried out according to the protocol for optic nerve lesion (ONL) described in detail previously (Liu and Londraville 2003). Briefly, adult zebrafish were anesthetized using tricaine methanesulfonate (MS-222, 0.03%, Sigma, St. Louis, MO) at room temperature. Each fish was placed in a 60 mm plastic petri dish, with its body wrapped in wet paper towel and left side upwards, under a dissecting microscope. In order to rotate the eye and expose the optic nerve to be crushed, the superficial membrane (also called outer cornea) covering the left eye was removed. Next, the posterior half of the eye was pulled partially out of the eye socket using a fine-tipped tweezers to expose the left optic nerve. The visible optic nerve was crushed using another pair of fine-tipped forceps. The fish was quickly returned to the recovery container. The nerve injury procedure lasted approximately 2 minutes, and most fish recovered within 2 minutes after being returned to tank and began to swim. The fish was allowed to survive for various days and was harvested at the following time points: 1-day, 2-day, 3-day, 1-week (also for qPCR), 2-weeks and 3-weeks. A total of 35 fish were used, 5 fish for each time period, except for the 1-week time point where 10 animals were used (5 for *in situ* hybridization and 5 for qPCR). These time points were selected because they are the crucial phases of the optic nerve regeneration in zebrafish (McCurley and Callard 2010). At each sampling interval, the fish were anesthetized at room temperature using 0.05% MS-222. For *in situ* hybridization, fish were placed on ice (in a 60 mm plastic petri dish) and both eyes and brains were quickly removed and placed in 4%

paraformaldehyde (PFA, 1X RNAse-free phosphate buffered saline, PBS, pH=7.4) on ice. To harvest tissues for qPCR, retinas were quickly removed, placed in a sterile and RNase-free 2 ml centrifuge tube, and quickly frozen on dry ice. Some fish were excluded from the study due to a possible damage of the ophthalmic blood vessels running along the optic nerve (Alvarez et al. 2007), causing the eye degeneration or fish death. After exclusion of fish from the operated group, 3 or 4 fish were used to study each regeneration interval. For each fish, the left retina was the experimental tissue, and the right retina was the control.

Probe synthesis for RNA *in situ* hybridization (ISH)

Full length *klf7* cDNAs (GenBank Accession BC124329) and *klf6a* (GenBank Accession NM_201461) from zebrafish were generously provided by Dr. Daniel Goldman from The University of Michigan. A detailed procedure for the molecular cloning of the zebrafish *klf6a* and *klf7* is described in Veldman et al. (2010). Those cDNAs were used as templates to generate antisense cRNA probes using gene-specific primers (Table 3.1). Endonucleases (BamHI) linearized DNAs that were further purified using electrophoresis (MinElute Gel Extraction Kit, Qiagen, Valencia, CA). Finally, those linearized cDNAs served as templates to synthesize digoxigenin (DIG)-labeled antisense cRNA probes using either T7 or Sp6 RNA polymerase (Roche, Indianapolis, IN).

Table 3.1. Zebrafish *klf* genes and PCR primers used for generating cRNA probes. pCS2+vector was used in molecular cloning (Veldman et al. 2010).

Gene name GenBank accession	Forward primer Reverse primer Amplicon size
klf6a NM_201461	5′-GAGAGACAATTGATGGATGTTCTACCAATGTGC-3′ 5′- GAGAGACTCGAGTCAGAGGTGCCTCTTCATGTG-3′ 834 bp
klf7 BC124329	5′-GAGAGAGAATTCATGGACGTGTTGGCGAATTAC-3′ 5′- GAGAGACTCGAGTTAGATATGTCGCTTCATGTG-3′ 888 bp

Tissue processing for RNA *in situ* hybridization

After overnight fixation in 4% PFA at 4ºC, the eyes and brains were washed three times for 10 minute each in 1xPBS with a constant slow agitation (on a platform rocker) at room temperature (Barthel and Raymond 1990). The washed tissues were subsequently placed in 20% sucrose (dissolved in PBS) overnight at 4ºC (for cryoprotection). The next day (15-24 hours later), the eyes and brains were placed in a mixture (1:1 v/v) of 20% sucrose and optimum cutting temperature compound (Tissue-Tek® O.C.T. Compound, Sakura, Netherlands) for 1 hour at room temperature on the platform rocker. Next, the tissues were placed in the same solution in cylinder-shaped aluminum molds (15 mm in diameter, 25 mm in height, 2-3 eyes or brains in each mold), and partially

submerged into a mixture of crushed dry ice and 95% ethanol, until frozen. The frozen tissue blocks were placed in labeled tissue sample bags and stored at -80ºC until used for cryosectioning. The frozen tissues were cut using a cryostat set to thickness of 14 µm for retinas and 16 µm for brains. The tissue sections were collected on Fisher superfrost pre-treated glass slides (Fisher scientific, Waltham, MA). After drying at room temperature for about 1 hour, the tissue slides were stored at -20ºC until processed for RNA *in situ* hybridization (see below). Two sets of alternate-cross sections from each eye or brain were collected for each set staining one *Klf* probe (see below).

RNA *in situ* hybridization on tissue sections

Procedures for *in situ* hybridization on retinal tissue sections were described previously in Barthel and Raymond (1993). Briefly, sectioned tissues on slides were removed from the freezer and air-dried at room temperature. They were treated with decreasing concentrations of ethanol. Then, the tissues were briefly digested for 3 minutes with proteinase K (0.01 mg/ml, Roche) at 37ºC. Next, the sections were incubated in 0.1 M triethanolamine (pH 8.0, Sigma, St. Louis, MO), followed by washing in 0.1 M triethanolamine with 0.25% acetic anhydride (Fisher). Then, the sections were treated with increasing concentrations of ethanol. Next, they were air-dried at room temperature for about one hour. The sections were covered with 75 µl hybridization solution containing 2 µg/ml antisense *klf6* or *klf7* cRNA probe, and placed in a hybridization oven (59ºC) overnight. Next day, the sections were washed in 2X

SSC, followed by 50% formamide in 2X SSC (at the hybridization temperature). The tissue sections were treated with RNase A (Roche), washed in RNase buffer before incubation in a blocking solution (5% normal goat serum, 2 mg/ml BSA, 1% DMSO in PBS with Tween-20, PBST) for two hours at room temperature, with constant agitation on the platform shaker. The sections were then treated with an anti-DIG antibody (conjugated to alkaline phosphatase, AB_514497, Roche) solution (diluted 1:5,000 in the blocking solution) overnight at 4ºC. Visualization of the signal was achieved by incubating the sections overnight in dark at room temperature, in a solution made from dissolving one tablet of 4-nitroblue tetrazolium chloride (NBT)/5-bromo-4-chloro-3- indolyl phosphate (BCIP, called NTB/BCIP tablet, Roche) in 10 ml of distilled water. Tissues were processed together and all paramaters were the same, except different cRNA probes were used.

Data analysis

Stained sections were observed under an Olympus BX51 compound microscope equipped with Normarski optics and connected to a SPOT digital camera (SPOT Imaging Solutions, Sterling Heights, MI). Results were recorded as digital images and further processed using Photoshop 6.0 software (San Jose, CA).

Absolute quantitative real-time PCR (qPCR)

In order to quantify the amount of *klf7* mRNA copies in tissues, the purified *klf7* cDNA in vector was used to generate a reference called the standard curve. First, the mass of single plasmid (vector with *klf7* gene insert) was calculated by multiplying its length in bp (base pairs) by 1.096×10^{-21} g/bp. This formula was derived from the estimation that 1 bp of dsDNA (double-stranded DNA) molecule has the average molecular weight of 660 g/mole and the Avogadro's number of 6.022×10^{23} molecules (bp) per 1 mole (Applied Biosystems). Next, the mass of a single plasmid was multiplied by the *klf7* gene copy number (10^7-10^2) needed in each reaction. Once a known amount of linearized plasmid was serially diluted, it was run on the same 96-well plate as the samples during qPCR reaction (see below) and used next to generate the standard curve. Efficiency of assays was calculated using the formula: efficiency = ($10^{-1/slope}$-1) (Yuan et al. 2007).

Retinas were harvested as described above and homogenized using the BeadBug microtube homogenizer (MIDSCI, Valley Park, MO). TRIzol reagent (Life Technologies, Carlsbad, CA) was used to isolate total RNA according to the manufacturer's protocol. Traces of genomic DNA were removed using Turbo DNA-free kit (Ambion, Austin, TX). RNA concentration was measured with Qubit 2.0 fluorometer (Life Technologies). Equal amounts (500 ng) of total RNA from each sample was reverse-transcribed to cDNA using Quanta Biosciences qScript cDNA SuperMix containing blend of oligo (dT) and random primers (Quanta Biosciences, Gaithersburg, MD). cDNA synthesis was also performed with negative control of no reverse transcriptase. The cDNA was further purified and

concentrated using precipitation in 0.1 volume of sodium acetate, pH 5.2 (final concentration of 0.3 M) and two volumes of 100% ethanol.

Klf7 gene-specific primers and hydrolysis probe (Integrated DNA Technologies) were designed to span the exon-exon boundary using NCBI Primer-BLAST tool and were further checked against the whole *Danio rerio* database for specificity (Table 3.2). Samples were loaded on 96-well plate on ice, under the sterile hood and sealed with adhesive tape and subsequently centrifuged for 5 minutes at 300 g in 4ºC. qPCR was performed in an Applied Biosystems AB 7300 cycler (Applied Biosystems, Waltham, MA) under the following conditions: one cycle of UDG enzyme activation at 50ºC for 2 minutes, one cycle of AmpliTaq Gold UP enzyme activation at 95ºC for 10 minutes, 40 cycles of denaturation at 95ºC for 15 seconds and annealing at 60ºC for 1 minute. The amplification was carried out in triplicate in a volume of 20 μl containing TaqMan Gene Expression Master Mix with ROX (Life Technologies), gene-specific primers (forward and reverse, 500 nM working concentration) and hydrolysis probe (250 nM working concentration, PrimeTime Primer Probe Mix, Integrated DNA Technologies; Table 3.2), 3 μl cDNA template (25 ng/μl) or 5μl standard (six serial dilutions of plasmid). No template and no reverse transcriptase controls were run in duplicate along with the samples. Sequence Detection System (SDS) software from Applied Biosystems was used to analyze amplicons and calculate mRNA copies in each sample. The PCR product specificity was confirmed by staining with ethidium bromide solution (EtBr) on the

gel electrophoresis and visualized band product of correct size (131 nucleotides).

Klf7 mRNA copy number/total RNA was calculated using the standard curves.

Table 3.2. Primer and probe sequences of *klf7* gene for absolute qPCR probes.

Gene name	klf7	Amplicon size
Forward primer	5'-CACATCAGAGGACACATACAGG-3'	
Reverse primer	5'-GCACTTAAAAGGCTTGGCG-3'	131 nt
Probe	5'-ACGAGGCACTACCGCAAACACA-3'	

Results

The staining patterns and intensity of *klf6a* and *klf7* cRNA probes were comparable between all the retinas and brains examined. This section describes the spatial distribution of mRNA from both *Klfs* in the intact and injured retina, and in the intact visual structures located in the brain of an adult zebrafish. *Klf7*-expressing cells were more prevalent in the brain, and therefore are described first.

Klf7 and *klf6a* expression in the retina of normal adult zebrafish

Expression of either *klf7* or *klf6a* in normal (wild-type/uninjured) retinas was not detectable (Figure 3.1). This result is consistent with what was presented by Veldman et al. (2007).
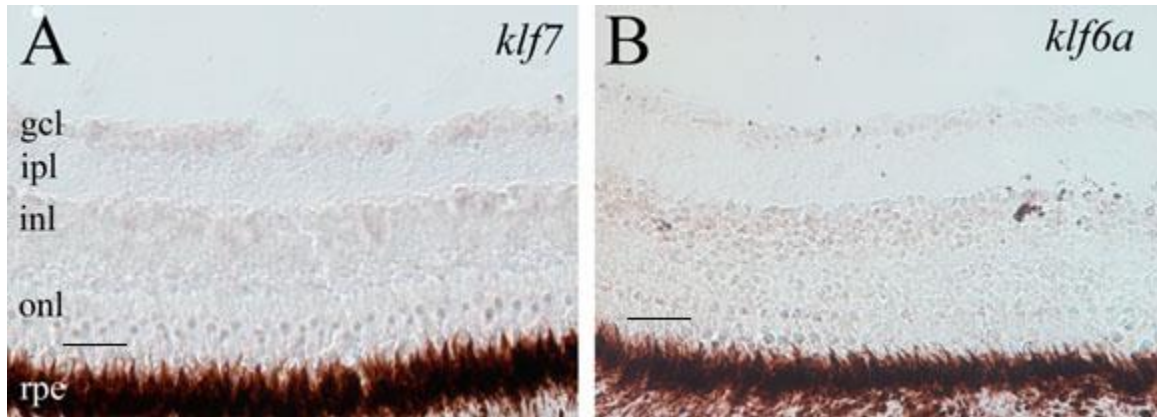
Figure 3.1. Expression of *klf7* and *klf6a* in adult zebrafish retina. Scale bar = 50 µm. See Abbreviations for list of full terms.

Klf7 and *klf6a* expression in the brain visual structures of normal adult zebrafish

Klfs expression patterns in the visual areas of the adult zebrafish brain are described from anterior to posterior brain regions, and the section levels for respective figures are shown in the schematic drawing of a lateral view of adult zebrafish brain (Figure 3.2).
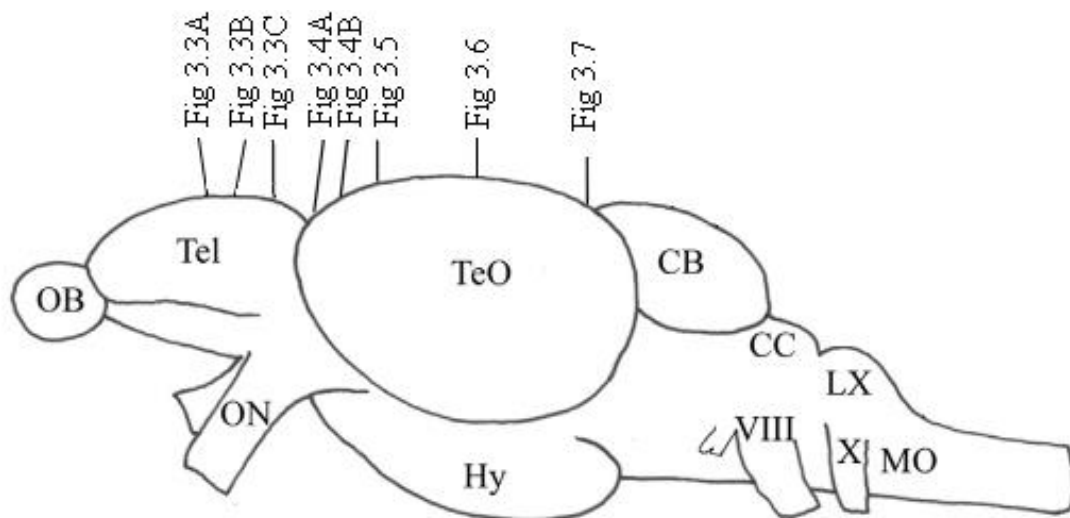
Figure 3.2. Schematic drawing of an adult zebrafish brain showing levels of cross-sections for examining *Klfs* expression. Lateral view, anterior to the left, dorsal to the top. Numbers represent respective figure numbers in this chapter. See Abbreviations for list of full terms.

Telencephalon

In the dorsolateral zone (Dl) of the telencephalon, expression of both *Klf* genes was comparable in the intensity and spatial distribution (Figure 3.3). In Dl of the precomissural part of the telencephalon, expression of both *klf7* and *klf6a* was confined mainly to the most exterior (superficial) region, and scarcely found in the remaining portion of Dl (Figure 3.3A, middle and right panels). Expression of these two *Klfs* in the telencephalon slightly posterior to the above level was also similar, although there were more positive cells in the superficial region, the dorsal region bordering the medial zone of the dorsal telencephalic area (Dm), next to the sulcus ypsiloniformis (SY), and the border region between Dl and posterior zone of the dorsal telencephalic area (Dp) contained strongly labeled cells (Figure 3.3B, D and E). In more caudal section of the telencephalon, posterior to the anterior commissure (Figure 3.3C), expression of both *klf7* (Figure 3.3F) and *klf6a* (Figure 3.3G) was similar in Dl in general, with more staining in the superficial regions. However, there appeared to be slightly more *klf7* labeling in the dorsal half of the Dl than its ventral half (Figure 3.3F), while no such difference was observed for *klf6a* staining (Figure 3.3G).
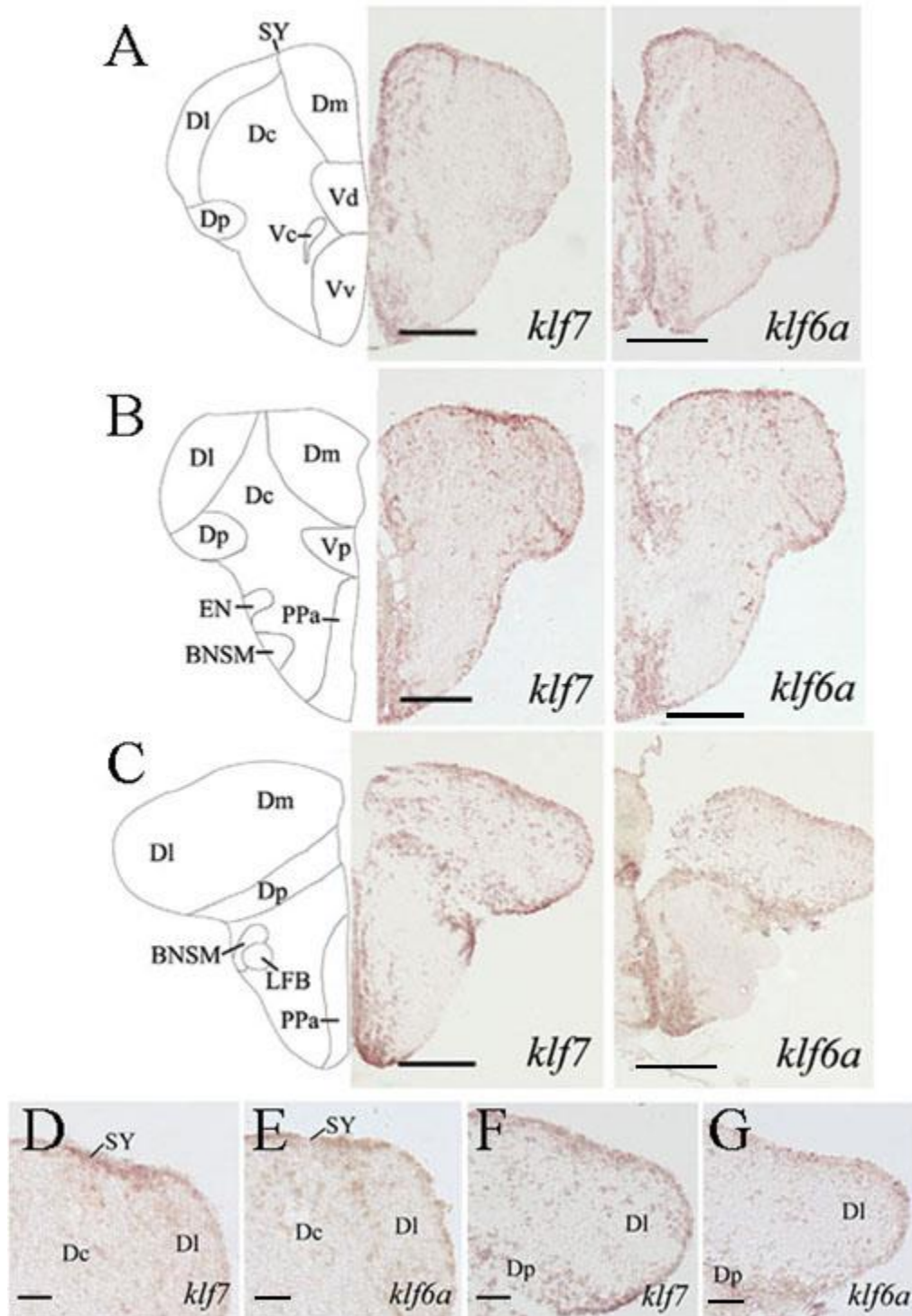
Figure 3.3. Expression of *klf7* and *klf6a* in anterior and post anterior-commisure telencephalon of adult zebrafish. Panels A and B depict anterior telencephalon and panel C shows post anterior-commisure telencephalon. The images shown in the top panels correspond to brain regions at a level shown in Figure 3.2. Pictures D and E show higher magnification of B, and pictures F and G show higher magnifications of dorsal telencephalon in panel C. Scale bar = 200 μm for A-C, 50 μm for D-G. See Abbreviations for list of full terms.

114

The preoptic region and diencephalon

In the preoptic area, both *Klfs* were expressed in two important visual structures of that region: PPp and SCN (Figure 3.4A). In PPp, *Klf*-positive cells were found adjacent to diencephalic ventricle (DiV), and *klf7*- and *klf6a*-expressing patterns in PPp looked similar (Figure 3.4C and D). Their expression in SCN appeared similar for these two *Klfs* in that stronger labeled cells were mainly detected in the midline. A difference in their expression was that *klf7*-expression was also obvious in lateral regions of this nucleus, while *klf6a* expression was more concentrated along the midline. Moreover, *klf6a*-expressing cells were more strongly labeled that those of *klf7*-expressing cells.

In the diencephalon, both *Klfs* were present in several visual nuclei (Figure 3.4). In the anterior thalamic nucleus (A), *klf7* expression was apparently higher (Figure 3.4C and E) than *klf6a* expression (Figure 3.4D and F). Both PSm and PSp contain faintly labeled *klf7*- (Figure 3.4C) and *klf6a*-expressing cells (Figure 3.4D). Similar faint labeling was also seen in both APN and CPN for both *Klfs* (Figure 3.4E and F). In the posteriodorsal thalamus, both *klf7* and *klf6a* expression was observed in PPv and DP (Figure 3.5B and C). Although their expression in PPv appeared to be similar, *klf6a* expression in DP was stronger than *klf7* expression, based on the staining intensities.
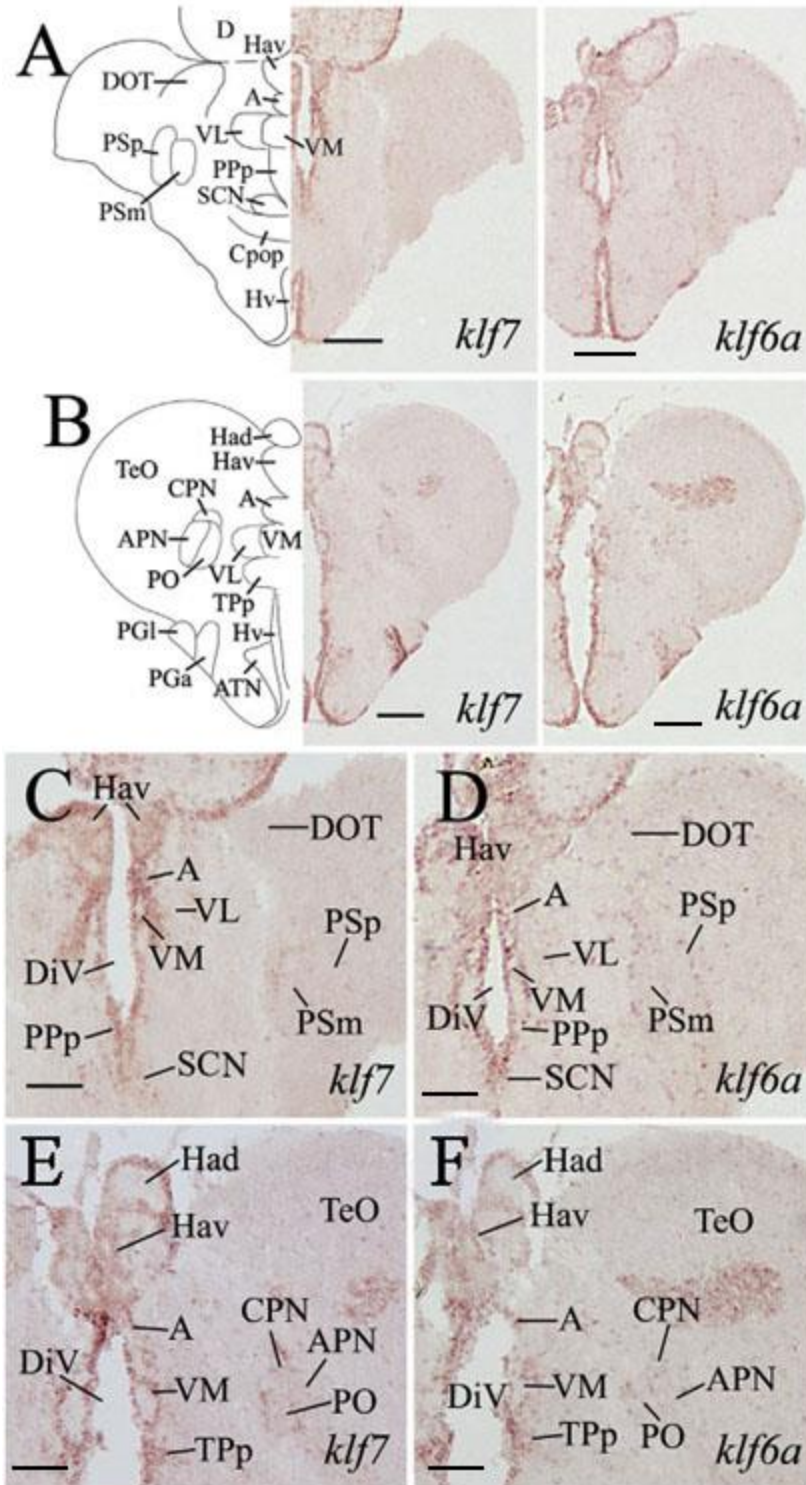
Figure 3.4. Expression of *klf7* and *klf6a* in preoptic area, habenular, pretectal regions and diencephalon of adult zebrafish. The images shown in the top panels correspond to brain regions at a level shown in Figure 3.2. Pictures C and D show higher magnification of panel A, and pictures E and F show a higher magnification of panel B. Scale bar = 200 μm for A-B, 50 μm for C-F. See Abbreviations for list of full terms.
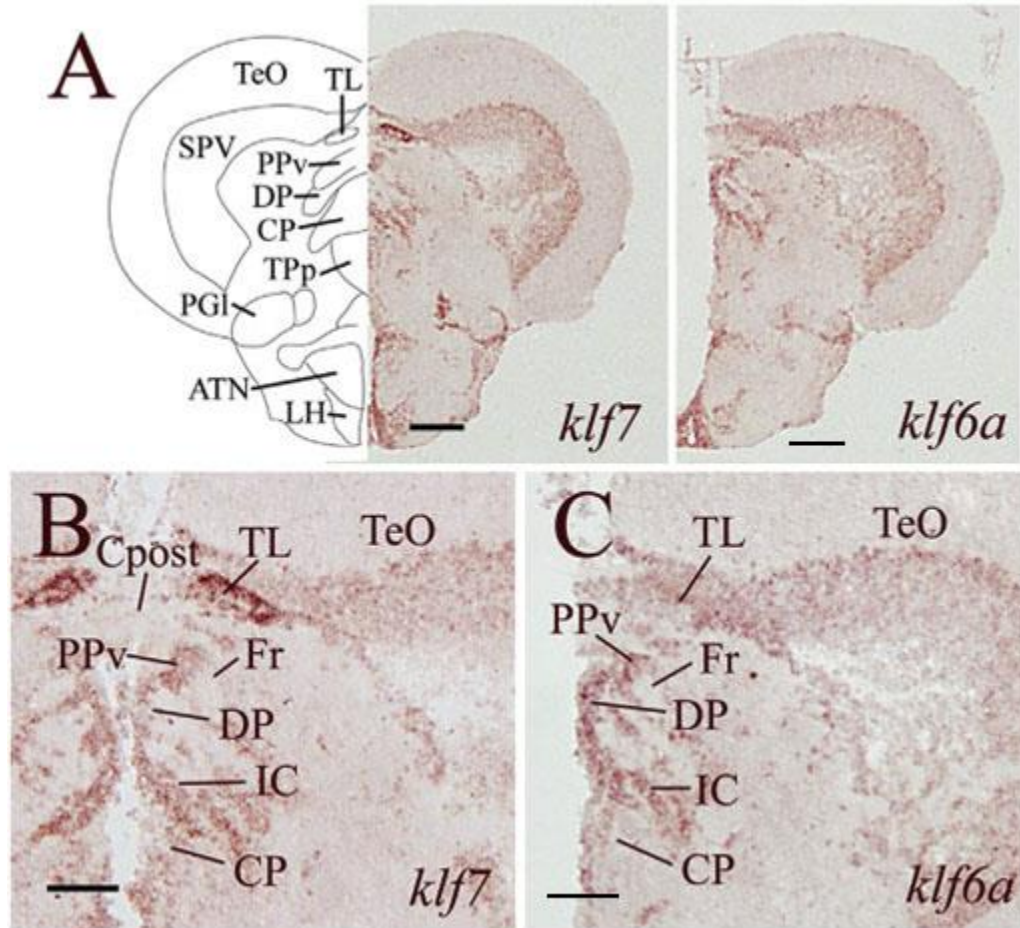
Figure 3.5. Expression of *klf7* and *klf6a* in posterior diencephalon of adult zebrafish. The image shown in the panel A corresponds to brain regions at a level shown in Figure 3.2. Pictures B and C show higher magnification of panel A. Scale bar = 200 μm for A, 50 μm for D-G. See Abbreviations for list of full terms.

Mesencephalon and isthmus

In the TeO of the mesencephalon, both *klf7* and *klf6a* were strongly and uniformly expressed in the SPV layer (Figure 3.5, Figure 3.6, Figure 3.7). No *klf7* or *klf6a*-expressing cells were detected in other layers of the TeO. Both *Klfs* were expressed in the nucleus isthmi (NI), with *klf7*-expressing cells located more in the dorsal 1/3 of the nucleus (Figure 3.7B), and *klf6a*-expressing cells mainly in

117

the periphery of the nucleus (Figure 3.7C). Moreover, expression of *klf7* was

slightly stronger, based on staining intensities, than *klf6a* expression.
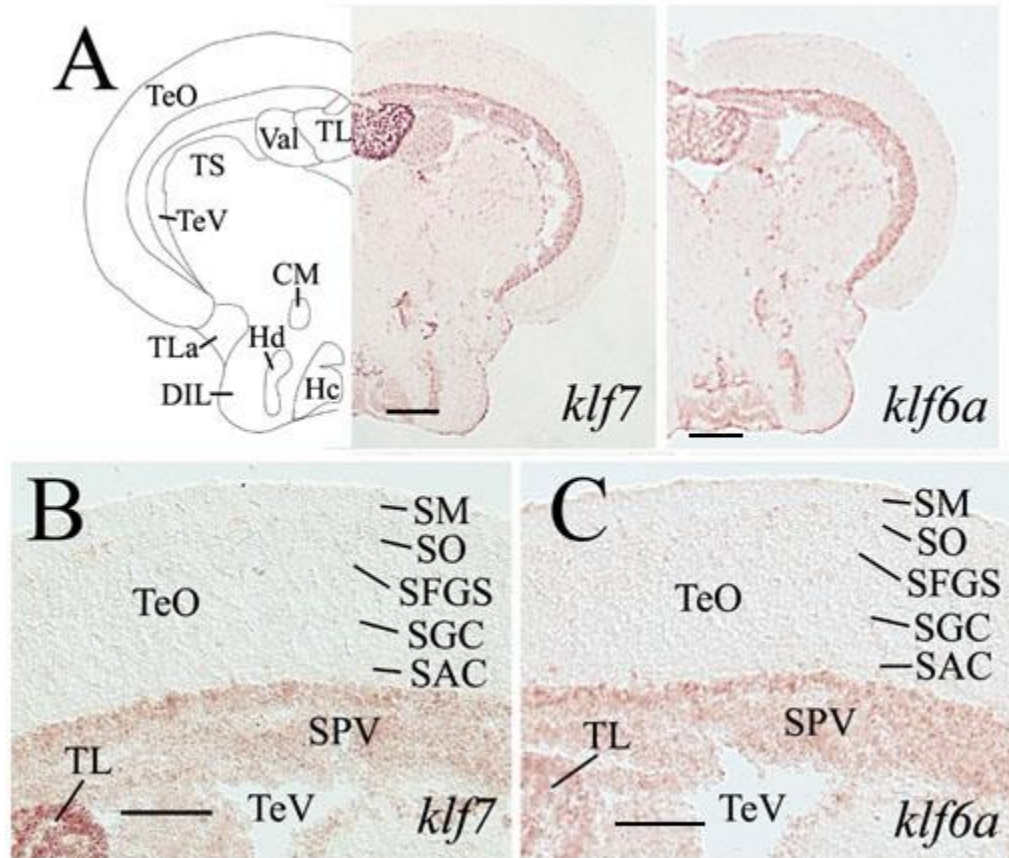
Figure 3.6. Expression of *klf7* and *klf6a* in the optic tectum of adult zebrafish. The image shown corresponds to brain regions at a level shown in Figure 3.2. Pictures B and C show higher magnification of panel A. Scale bar = 100 μm. See Abbreviations for list of full terms.
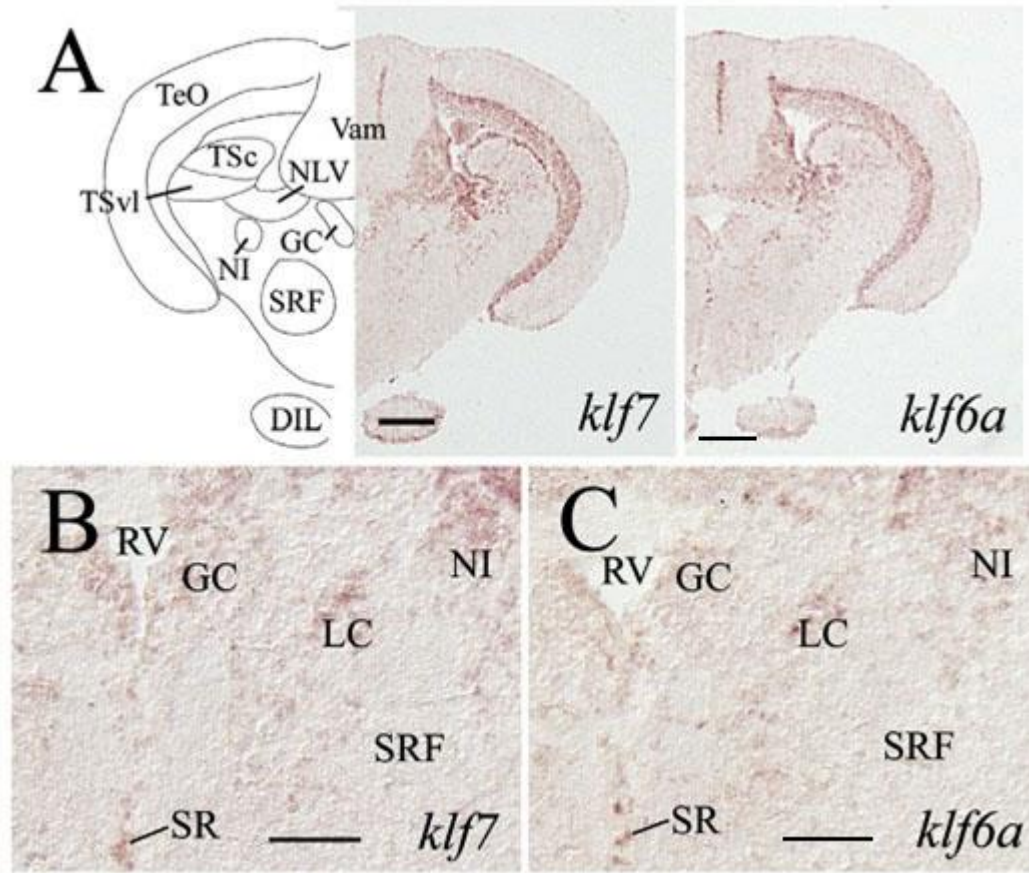
Figure 3.7. Expression of *klf7* and *klf6a* in the dorsal tegmentum, isthmus, torus semicircularis and anterior medulla of adult zebrafish. The image shown in panel A corresponds to brain regions at a level shown in Figure 3.2. Pictures B and C show higher magnification of panel A. Scale bar = 200 μm for A, 100 μm for B and C. See Abbreviations for list of full terms.

*Klf7* and *klf6a* expression in the visual structures of the adult zebrafish brain is summarized in Table 3.3.

Table 3.3. Summary of *klf7* and *klf6a* expression in normal adult zebrafish brain visual structures. Staining intensities (labeling) are indicated by the number of plus signs: ++, strong; +, weak to moderate; +/-, barely detectable. See Abbreviations for list of full terms.

	klf7	*klf6a*
A	++	+
APN	+/-	+/-
CPN	+	+/-
DI	+	+
DP	+	++
NI	+	+
PPv	++	+
PPp	++	+
PSp	+/-	+/-
SCN	+	+
TeO	++	++

Klf7 and *klf6a* expression in the retina after the optic nerve crush in adult zebrafish

Before this study, changes in the expression of *Klfs* in regenerating adult zebrafish retina were documented mainly using relative qPCR method (Veldman et al. 2007). This study provides information about expression patterns of *klf7* and *klf6a* in regenerating retinas of adult zebrafish using RNA *in situ* hybridization method, allowing direct visualization of changes in *Klfs* expression to confirm the idea that *klf7* and *klf6a* are robust and reliable markers of the

120

retinal axon regeneration. Three or 4 fish (6 or 8 retinas) were used to examine *Klfs* for the spatial gene expression on day one through three weeks after optic nerve crush. The gene expression patterns were similar within the control and experimental groups.

Klf6a mRNA of control retinas was not detectable (Figure 3.8A). One day after the optic nerve injury, *klf6a* was detected in the gcl, and slightly increased in the inl, seen as a few scattered *klf6a*-expressing cells in the innermost region of the inl (Figure 3.8B). The *klf6a* expression in the gcl appeared to be slightly increased in retinas of 2-3 days post lesion (Figure 3.8C and D). Again, a few scattered *klf6a*-expressing cells were found in the innermost portion of the inl. One week after the injury to the optic nerve, *klf6a* expression became apparently stronger (based on staining intensities) in the gcl (Figure 3.8E). At 2 weeks post ONL, *klf6a* signal in the gcl remained strong, while its expression pattern in the inl was similar to that in earlier periods (Figure 3.8F). By 3 weeks post-injury, the expression of *klf6a* returned to that in normal/control retinas (Figure 3.8G).
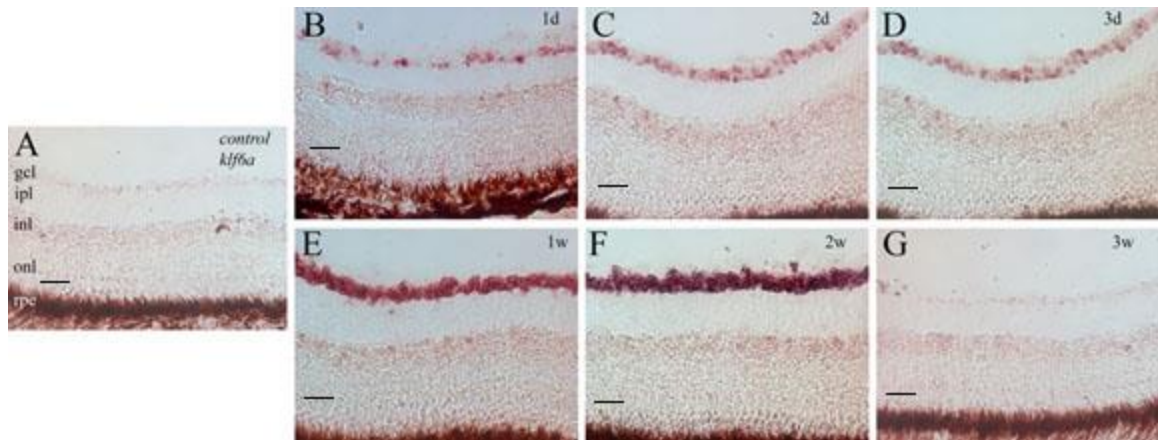
Figure 3.8. Expression of *klf6a* in control and regenerating adult zebrafish retinas. In control retinas (panel A), *klf6a* mRNA is not detectable with *in situ* hybridization. One day through two weeks after ONL (panels B-F), *klf6a* mRNA signal increases mainly in the gcl and returns to the baseline levels at 3 weeks (panel G). Scale bar = 50 µm. See Abbreviations for list of full terms.

Klf7 mRNA expression was absent in control retinas (Figure 3.9A). Weak *klf7* expression was detected in the gcl 1 day post ONL (Figure 3.9B), and its expression was increased in retinas 2 days after the lesion (Figure 3.9C). The *klf7* expression was even stronger in the gcl of retinas 3 days after the optic nerve crush (Figure 3.9D). In 1-week post-surgery retinas, *klf7* expression appeared to be slightly less intense compared to that of 3-day tissues (Figure 3.9E). This pattern was maintained in the retinas of 2-week post ONL (Figure 3.9F). Expression of *klf7* returned to that of normal/control retinas 3 weeks post optic nerve lesion (Figure 3.9G). Unlike *klf6a* expression in the regenerating retina, there was no *klf7* expression detected outside the gcl.
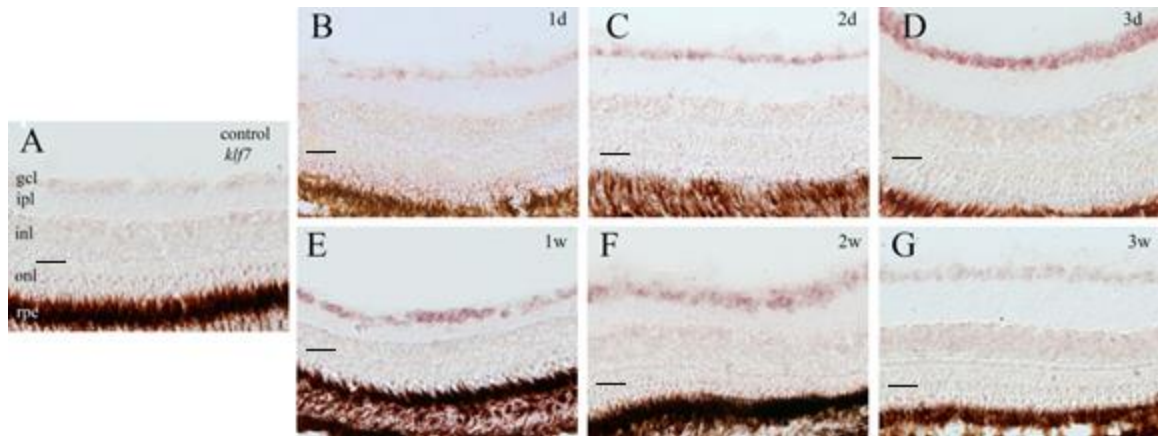
Figure 3.9. Expression of *klf7* in control and regenerating adult zebrafish retinas. In control retinas (panel A), *klf7* mRNA is not detectable with *in situ* hybridization. One day through two weeks after ONL (panels B-F), *klf7* mRNA signal increases only in the gcl and returns to the baseline levels at 3 weeks (panel G). Scale bar = 50 µm. See Abbreviations for list of full terms.

Expression of *klf7* was also tested by qPCR and a 9.3-fold change was observed in whole retinas 1-week post ONL (Figure 3.10). This increase shown by RNA *in situ* hybridization and qPCR result is consistent with a previous study by Veldman et al. (2007), who used the laser-dissected RGCs. Per 1 ng total RNA, the *klf7* mRNA copy number in the normal retina was 88 and one week post-lesion the copy number was increased to 820. The plotted standard curve in Figure 3.10 was used to read the exact mRNA copy number of *klf7* gene in tissue and also to verify the efficiency and specificity of the gene target. The efficiency was 102.74%, the correlation efficiency was 0.979512, and therefore the obtained data was reliable.

RNA *in situ* hybridization is a powerful technique for the spatial detection of mRNA in the specific areas of the sectioned or whole-mount sample, but the quantification of expression is not as straightforward as in qPCR. Amplification in qPCR renders this method more sensitive, and technically a single copy of

mRNA can be detected. *In situ* hybridization using DIG probe visualization has lower limit of detection than qPCR as there is no amplification step. As mentioned earlier, *klf7* did not appear to be detected visually in the normal/control adult retinas with *in situ* hybridization method, but based on qPCR method, these whole retinas had 88 copies/ng total RNA of *klf7* present. This small discrepancy is likely due to the aforementioned higher sensitivity of the qPCR method over RNA *in situ* hybridization.
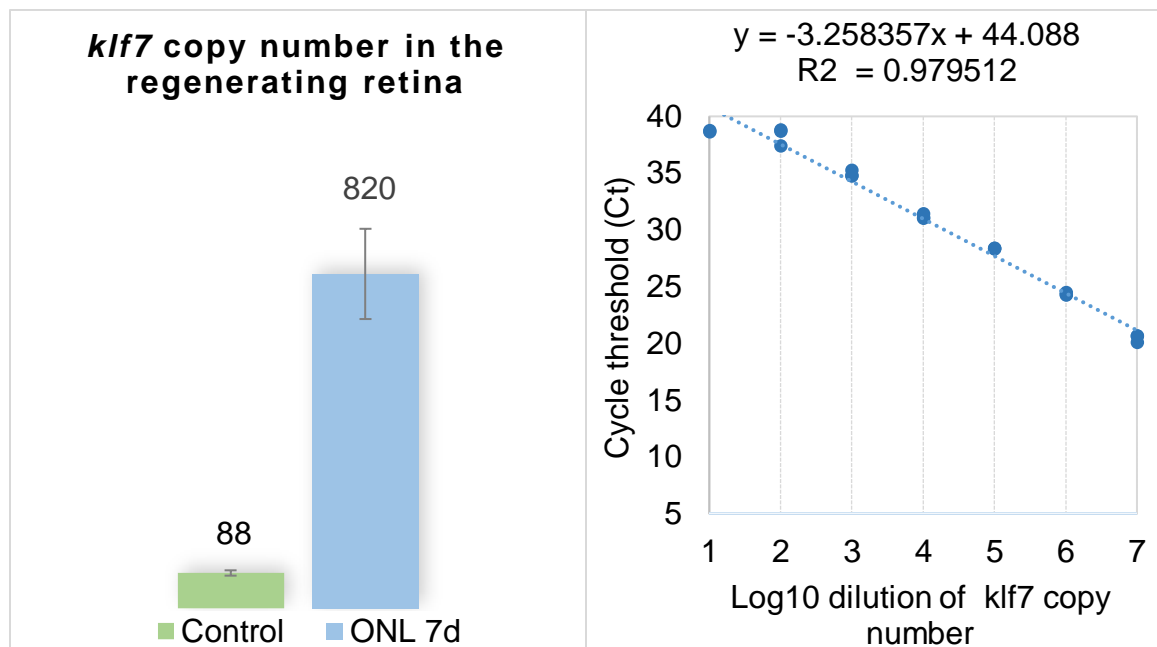
Figure 3.10. Expression of *klf7* in control and regenerating retinas at one week after ONL. On the left: *klf7* was increased by over nine-fold in eyes with crushed optic nerves comparing to control, and reached over 800 mRNA copies. Five retinas per group were used. Error bars represent standard deviation. Copy numbers are per 1 ng total RNA. Two-tailed T-test=0.003003382. On the right: *klf7* standard curve with 102.74% efficiency, calculated with formula: efficiency = $(10^{-1/slope}-1)$ (Yuan et al. 2007).

Discussion

Expression of *klf6a* and *klf7* in the retina and brain visual structures of adult zebrafish and comparison with developing zebrafish visual system

There are only a few published studies on *klf6a* and *klf7* expression in the developing zebrafish, but these reports focus on non-neural tisssues (e.g. Xue et al. 2015) and images of their expression in the brain are not shown or are out of focus (e.g. Zhao et al. 2010), therefore making it difficult to assess the spatial distributions of these two *Klfs*. Thisse et al. (2001) published *in situ* hybridization images of *klf6a* in ZFIN. One of which is an image of 50-72 hpf embryo showing *klf6a* expression in the optic tectum. Its expression in the telencephalon and diencephalon is too faint and/or unfocused, therefore unclear. *Klf7* expression along with many other genes was examined in developing zebrafish in Li et al. (2010b) and in Thisse and Thisse (2004), showing its expression detected in the telencephalon, the diencephalon (e.g. pretectum), the optic tectum and in the retina (42-72 hpf). Its expression is strong in 48-72 hpf embryos, but much reduced in 120 hpf embryos. Due to the small size of the images provided, it is difficult to see exact locations of brain regions that contain *klf7*-expressing cells in this study. In the retina, the region that is *klf7*-positive appears to be the gcl. Moreover, there is no detailed description of *klf7* expression in the brain, except in stating that it is detected in the diencephalon, dorsal thalamus and hindbrain of developing zebrafish brain. As mentioned earlier, Veldman and colleagues found no *klf6a* expression in developing zebrafish retinas, but reported *klf7* expression in the gcl of 48 hpf embryonic retinas (Veldman et al. 2007, 2010). Therefore,

klf6a expression in the retinas of both developing and adult zebrafish is similar, with no detectable expression using *in situ* hybridization method. These results suggest that *klf6a* is unlikely to be involved in either the development or maintenance of zebrafish retina. Its expression in the developing optic tectum suggests that it may participate in the formation of this structure, as well as that of other brain regions (e.g. hindbrain) that express this *Klf*. Since *klf7* is expressed in the gcl of developing zebrafish during critical stages of retinal ganglion cell (RGC) differentiation, and *klf7* is expressed in the pretectum and optic tectum of developing zebrafish when RGCs axons grow into these visual structures, it is reasonable to speculate that this *Klf* plays a role in RGC differentiation, pathfinding and/or synapse formation.

In general, expression patterns of *klf6a* and *klf7* are similar in the visual structures of adult zebrafish: both are expressed by most of the visual structures along the optic pathway, and in structures that receive visual inputs. It is surprising that neither of these *Klfs* is detected in the control adult retina at levels detectable by RNA *in situ* hybridization, since qPCR indicated *klf7* is expressed in the adult retina, but with the low copy number (88/ng of total RNA). It is known that qPCR is more sensitive, and therefore was able to detect and visualize the lower number of *klf7* mRNA copies. It is possible that *klf6a* has similar low expression in adult zebrafish retinas, but qPCR experiments are required to validate that. More likely though, strong expression of these two *Klfs* in the visual brain structures is a reflection of their overlapping functions in the maintenance of

all brain structures that express them. As shown in Bhattarai et al. (2016), these two *Klfs* are present in many sensory and motor regions of the brain.

Comparison of *klf6a* and *klf7* expression in the adult visual system between zebrafish and mouse

An immunocytochemical study of klf6 expression in the adult mouse forebrain showed that this Klf is expressed widely in the telencephalon (cerebral hemispheres and olfactory bulbs) and diencephalon (Jeong et al. 2009). Although klf6 in adult mice is detected in numerous brain regions such as the cerebral cortex, amygdala, hippocampus, thalamus and hypothalamus, which homologous zebrafish brain regions also contain *klf6a* (Bhattarai et al. 2016), there is no description of klf6 expression in visual brain structures, except in the laterodorsal thalamic nucleus and the geniculate nucleus. The laterodorsal thalamic nucleus receives visual inputs. For the geniculate nucleus, authors in the paper (Jeong et al. 2009) did not specified it as either the lateral geniculate nucleus, which is the main relay center for retinal inputs, or medial geniculate nucleus, which is a major auditory brain structure. Therefore, I cannot comment further about its expression in the geniculate nucleus. The similarities of Klf6/*klf6a* expression in CNS of both mice and zebrafish imply that this transcription factor has a conserved function in adult vertebrate organism CNS maintenance. It is still unclear if this Klf has a similar function in the visual structures in brain, since the available data in mice is not detailed enough.

There are no available reports, to the best of my knowledge, on Klf6/*Klf6* expression in the retina of other adult organisms that were non-operated. It would

be interesting to see if this Klf is also not expressed, or expressed at low levels in these retinas. The most interesting difference between zebrafish and mouse retinas is a lack of klf6-expressing cells in RGCs of zebrafish embryo (Thisse et al. 2001) and in adult here, contrasted with the apparent klf6 expression in embryonic (from E19) and postnatal mouse (until P21, Moore et al. 2009). In the optic chiasm of embryonic mice (E16), more klf6-expressing cells are in the ipsilateral RGCs, than in contralateral RGCs (while all RGC in zebrafish cross at the optic chiasm, Wang et al. 2016). In zebrafish, klf6a is only found in the gcl in the glaucoma pathology model (Veth et al. 2011), and after RGC axons are injured, which is followed by the successful nerve regeneration (Veldman et al. 2010) and in this study. Interestingly, mammalian retinal axons that do not regenerate do not seem to express klf6.

There is only one published report on Klf7/*Klf7* expression in the adult mouse brain (Laub et al. 2001a). Apparent *Klf7* expression is detected only in the cerebellum of the adult mouse brain. Based on the data from zebrafish and mice, Klf7/*klf7* expression in the adult vertebrate brain is species-specific, therefore this Klf may serve different functions in the brain of different adult vertebrates. There is no published data available for Klf7/*Klf7* expression in the retina of other adult vertebrates.

Patterns of *klf6a* and *klf7* expression in the retina after the optic nerve lesion

Previous reports implicated Klfs in promoting retinal axon regeneration in adult zebrafish (Veldman et al. 2007) and mice (Moore et al. 2009). Veldman et

128

al. (2007), using mainly qPCR method, reported the increased *klf6a* and *klf7*

expression as early as one day after optic nerve lesion, peaking at 2-4 days and

4-8 days post ONL (respectively), and by 3 weeks expression of both *Klfs*

became similar to control retinas. My results, using mainly *in situ* hybridization,

generally agree with the findings by Veldman et al. (2007). Moreover, my qPCR

data of *klf7* expression in 1-week post ONL tissue (9.3-fold increase) matches

relatively well with their data at 6 days after ONL (12-fold increase). However,

there is an apparent difference in the expression levels of these two *Klfs* at the

time point around 2-weeks after ONL. Data from Veldman et al. (2007) shows

that expression levels of both *Klfs* at 12 days after ONL are significantly declined

from the week before (point of *klf7* peak expression and the second-highest fold

change for *klf6a*), and are only about 1.5-2 fold higher than the control levels. On

the contrary, based on staining intensities, my results at 14 days after ONL show

that *klf6a* maintains its peak levels and continues similar expression from the

previous week, while *klf7* is still strongly expressed but at slightly lower levels

than a week before. This difference may be partially due to different

methodologies used in these studies, but further studies (e.g. absolute qPCR to

estimate the actual number of mRNA copies using our tissues) may be needed to

confirm the rest of the relative qPCR results.

The polymerase chain reaction (PCR) method was developed by Kary

Mullis in 1987 (Mullis and Faloona 1987). Further development of reverse

transcription of mRNA allowed for development of the quantitative PCR (qPCR)

in 1993 (Higuchi et al. 1993). This highly sensitive method allows monitoring the

gene amplification in real time, by using the fluorescent detectors and hence measuring gene expression levels with high accuracy. Relative qPCR is the commonly used technique for the comparison of transcribed genes between two conditions, calculated as a fold change, and uses endogenous control(s) called reference gene(s) for normalization (Wong and Medrano 2005). Absolute qPCR is less frequently used method, as it requires more initial preparation and additonal reagent use for a reference called the standard curve. A standard curve is constructed by amplifying in qPCR reaction the known copy numbers of i.e., linearized plasmids containing the gene of interest, which are diluted over the several orders of magnitude. The advantages of this method include the ability to learn the copy number of transcribed gene per 1 ng of total RNA from sample, and therefore allows for comparisons not only between two conditions, but also between distinct organs or species during separate experiments (VanGuilder et al. 2008). The absolute qPCR in my study here accessed the baseline transcription of *klf7* gene as 88 mRNA copy number per 1 ng of total RNA in the adult retinas. The relative qPCR method would not be able to provide this information, as the values calculated between two conditons are arbitrary. In addition, 88 mRNA copy number per 1 ng of total RNA appeared to be below the limit of detection for *in situ* hybridization method, based on *klf7* gene expression. The relative qPCR method relies on the assumption that the ratio of reference gene expression is the same between conditions tested. The relative qPCR from Veldman et al. (2007) relied on glyceraldehyde-3-phosphate dehydrogenase (GAPDH) as a reference gene, which was deemed unsuitable due to its

variability of expression in adult zebrafish tissues (including eyes) and in developing zebrafish (important to mention as certain genes expressed during regeneration recapitulate their developmental expression, Tang et al. 2007). It is possible that discrepancies between expression levels at around 2 weeks after ONL between techniques used in my *in situ* hybridization and relative qPCR stem from the changed expression of GAPDH normalization gene, therefore affecting the relative fold changes at certain time points.

A major advantage of using *in situ* hybridization in studying gene expression is its ability to provide detailed spatial information on expression of the gene of interest. This allowed me to detect scattered, but obvious *klf6a*-expressing cells in the inner portion of the inl. The significance of this is that these cells, although located in a postion mostly occupied by the amacrine cells, are likely the displaced retinal ganglion cells (displaced RGCs) in the zebrafish retina. Therefore, it provides a novel way of identifying displaced RGCs not only in zebrafish, but also in other vertebrate organisms. The likely reason that there are no obvious labeled *klf7* cells in the inner portion of the inl of the regenerating retinas in my study is that the staining intensity of *klf7* in the retina is much less intense compared to that of *klf6a*. This intensity difference is unlikely due to my processing of retinal tissues, because staining intensities of both *klfs* probes are similar in the fish adult brain tissues. Moreover, such difference in tissue staining with these two *Klfs* probes is also observed by Veldman et al. (2007) in their 3-day post-surgery retinas (the only time point where *in situ* hybridization was performed in that study). Therefore, another novel finding of my study is that

klf6a is a better marker for regenerating retinas than *klf7* using *in situ* hybridization method.

The up-regulated expression of both *Klfs* is not surprising because 90% of the RGCs in teleost fish survive after their axons sustain injury and the first regenerating RGC axons appear in the retina at 1-day post-injury (dpi). Those retinal axons grow towards the optic tectum and establish the initial tectal connections by about 14 dpi (Bhumika et al. 2015), all these processes correlate with an obvious up-regulation of *klf7* and *klf6a*. Since both *Klfs* returned to the baseline levels by the time most of the tectal lobe is covered with regenerating axon terminals (by 21 days post-injury), it is unlikely they are players in a process of the synaptic refinement which takes place in the next few weeks.

CHAPTER IV

CADHERIN-6, *CADHERIN-7*, *PROTOCADHERIN-17* AND *PROTOCADHERIN-19* EXPRESSION IN REGENERATING ADULT ZEBRAFISH RETINA

Introduction

Cadherins are a superfamily of adhesion molecules that are important in formation and functioning of the multicellular organisms, including vertebrates (Hulpiau and Van Roy 2009, 2011; Oda and Takeichi 2011; Suzuki and Hirano 2016). Most of the cadherin superfamily members are expressed during the nervous system development, while some continue to be detectable in the nervous structures of adult animals (Takeichi 1990; Yagi and Takeichi 2000; Halbleib and Nelson 2006; Vestweber 2015). Moreover, some cadherins are even more strongly expressed during the vertebrate central nrvous system (CNS) regeneration (e.g. cdh2 and cdh4, Liu et al. 2002, 2004a). Briefly, there is a good correlation between up-regulation of cdh2 and the successful nerve regeneration in the zebrafish CNS or mammalian peripheral nervous system (PNS). Furthermore, cdh2 promotes the optic axon regeneration following the optic nerve crush (ONL) in adult zebrafish (Liu et al. 2002; Liu and Londraville 2003). These findings suggest that cadherins are key promoting molecules for nervous system regeneration in vertebrates. Developing zebrafish visual structures also

express multiple cadherin superfamily members, for example type-II classical cadherins (*cdh6*, *cdh7*) and clustered δ-protocadherins (*pcdh17*, *pcdh19*), and those genes are known to be involved in the visual system development of vertebrates (Wöhrn et al. 1999; Honjo et al. 2000a; Liu et al. 2006, 2008b, 2009; Ruan et al. 2006; Krishna-K et al. 2009; Tai et al. 2010, 2010; Chen et al. 2013; Cooper 2017). Moreover, expression of these cadherins in the visual system of adult zebrafish (see results of Chapter II) is different from that in the embryos. Successful regeneration of vertebrate nervous structures requires combined functions of multiple molecules (e.g. GAP-43, klf6a, klf7, cdh2) (Blackmore and Letourneau 2006; Veldman et al. 2007; Rasmussen and Sagasti 2016). In order to determine functions of cdh6, cdh7, pcdh17 and pcdh19 in the optic nerve regeneration, their expression in the regenerating retina must be examined first. There are no published studies that examine expression patterns of these cadherin molecules in regenerating visual structures of any adult vertebrate. Current study was conducted to accomplish this goal using RNA *in situ* hybridization and qPCR.

Materials and methods

Animals

Adult wild-type zebrafish (*Danio rerio*) of both sexes were 12-18 months old and similar in length. Animals were housed in The University of Akron Research Vivarium (UARV). The fish were bred in-house for several generations and maintained in constant conditions at 28°C in 14-hour light and 10-hour dark

cycle in 10-gallon tanks, according to the Zebrafish Book (Westerfield 2007).

Institutional Animal Care and Use Committee (IACUC) at The University of Akron

approved all animal-related procedures (approval reference #15-07-08-LFD;

copy in Appendix A).

Optic nerve lesion surgery

Based on the previous knowledge on zebrafish optic nerve regeneration,

cdh2 and cdh4 expression in regenerating zebrafish visual system (Liu et al.

2002; Liu and Londraville 2003), and my findings of *klf6a* and *klf7* expression in

the regenerating zebrafish optic retina (Chapter III), I decided to examine *cdh6*,

cdh7, *pcdh17* and *pcdh19* expression in the regenerating retina of adult zebrafish

at the following stages: 1-day, 2-day, 3-day, 1-week, 2-weeks and 3-weeks

following the optic nerve crush (McCurley and Callard 2010).

The procedures were carried out according to the protocol for the optic

nerve lesion (ONL) described in detail previously (Liu and Londraville 2003).

Briefly, adult zebrafish were anesthetized using tricaine methanesulfonate (MS-

222, 0.03%, Sigma, St. Louis, MO) at room temperature. Each fish was placed in

a 60 mm plastic petri dish, with its body wrapped in a wet paper towel and left

side upwards, under a dissecting microscope. In order to rotate the eye and

expose the optic nerve to be crushed, the superficial membrane (also called

outer cornea) covering the left eye was removed. Next, the posterior half of the

eye was pulled partially out of the eye socket using a fine-tipped tweezer to

expose the left optic nerve. The exposed optic nerve was crushed using another

pair of fine-tipped forceps. The fish was quickly returned to the recovery container. The nerve injury procedure lasted approximately 2 minutes and most fish recovered within 2 minutes of being returned to tank, and began to swim. At each sampling interval, the fish were anesthetized at room temperature using 0.05% MS-222. For *in situ* hybridization, fish were placed on ice (in a 60 mm plastic petri dish) and eyes were quickly removed and placed in 4% paraformaldehyde (PFA, 1X RNAse-free phosphate buffered saline, PBS, pH=7.4) on ice. To harvest tissues for qPCR, retinas were quickly removed, placed in a sterile and RNase-free 2 ml centrifuge tube, and quickly frozen on dry ice.

The optic nerve crush surgery was performed on the left optic nerve of each fish and right eye was used as a control. Six animals had surgery per each stage, except the 1-week time point when 12 fish underwent surgery. For 1-week after ONL, tissues from 4 fish were used for *in situ* hybridization and tissues from 4 fish were used for qPCR, while for the remaining survival stages, tissues from 4 fish were used for *in situ* hybridization. The reason more fish were operated on but fewer fish were used for the experiment was due to the eye degeneration exhibited in several fish. This occurs ocassionally in some operated fish, possibly due to accidental damage to the ophthalmic blood vessels that run along the optic nerve (Alvarez et al. 2007).

Probe synthesis for RNA *in situ* hybridization (ISH)

An *in vitro* digoxigenin (DIG) RNA synthesis protocol (manufactuerer's manual, Roche, Indianapolis, IN) was used to generate the antisense probes of each gene of interest for the detection of each *cdh* or *pcdh* mRNA in tissues. Cloning of the *cdh* and *pcdh* genes was described in detail previously (Liu et al. 2006, 2007a, 2009, 2010). The zebrafish embryos (30-50 hpf) were used to obtain total RNA using TRIzol reagent (Life Technologies, Carlsbad, CA). cDNA fragments were generated by using gene-specific primers by RT-PCR (Table 4.1), cloned into the pCRII-TOPO vector (Invitrogen, Carlsbad, CA), and used as templates for generating antisense cRNA probes (Liu et al. 1999b).

Table 4.1. Zebrafish *cdh* genes and PCR primers used for generating cRNA probes. The following molecular cloning vectors were used: pCRII-TOPO for *cdh6* (Liu et al. 2006), pCRII-TOPO for *cdh7* (Liu et al. 2007a), pCRII-TOPO for *pcdh17* (Liu et al. 2009) and pCRII-TOPO for *pcdh19* (Liu et al. 2010).

Gene name GenBank accession	Forward primer Reverse primer	Probe size
cdh6 **AB 193290 1**	5'-GCGGAAAAGATGAGGACTTG-3' 5'-CATCCACATCCTCGACACTG-3'	1131 nt
cdh7 **XM 691001**	5'-TGTTGGCAAGCTTCATTCTG-3' 5'-ACCGTGGGTCTATGTTCCTG-3'	1888 nt
pcdh17 **XM 684743**	5'-CTGTGTTTGAACAGCCCTCA-3' 5'-TTGCACCATCAGTGGGTTTA-3'	847 nt

| pcdh19 | 5'-CAATGGCGAGGTGGTCTACT-3' | 942 nt |
| BC 129243 | 5'-CAACTCCAGCGTTTTTAGGG-3' | |

Tissue processing for RNA *in situ* hybridization

After overnight fixation in 4% PFA at 4ºC, the eyes were washed three times for 10 minute each in 1xPBS with a constant slow agitation (on a platform rocker) at room temperature (Barthel and Raymond 1990). The washed tissues were subsequently placed in 20% sucrose (dissolved in PBS) overnight at 4ºC (for cryoprotection). The next day (15-24 hours later), the eyes and brains were placed in a mixture (1:1 v/v) of 20% sucrose and optimum cutting temperature compound (Tissue-Tek® O.C.T. Compound, Sakura, Netherlands) for 1 hour at room temperature on the platform rocker. Next, the tissues were placed in the same solution in cylinder-shaped aluminum molds (15 mm in diameter, 25 mm in height, 2 or 3 eyes or brains in each mold), and partially submerged into a mixture of crushed dry ice and 95% ethanol, until frozen. The frozen tissue blocks were placed in labeled tissue sample bags and stored at -80ºC until used for cryosectioning. The frozen tissues were cut using a cryostat set to thickness of 14 µm. The tissue sections were collected on Fisher superfrost pre-treated glass slides (Fisher scientific, Waltham, MA). After drying at room temperature for about 1 hour, the tissue slides were stored at -20ºC until processed for RNA *in situ* hybridization (see below). Four sets of alternate-cross sections from each eye or brain were collected and each set was used for staining one *cdh* or *pcdh* probe (see below).

RNA *in situ* hybridization on tissue sections

Procedures for *in situ* hybridization on retinal tissue sections were described previously in Barthel and Raymond (1993). Briefly, sectioned tissues on slides were removed from the freezer and air-dried at room temperature. They were treated with decreasing concentrations of ethanol. Then, the tissues were briefly digested for 3 minutes with proteinase K (0.01 mg/ml, Roche) at 37ºC. Next, the sections were incubated in 0.1 M triethanolamine (pH 8.0, Sigma, St. Louis, MO), followed by washing in 0.1 M triethanolamine with 0.25% acetic anhydride (Fisher). After the sections were treated with increasing concentrations of ethanol, they were air-dried at room temperature for about one hour. The sections were covered with 70 µl hybridization solution containing 2 µg/ml antisense *cdh* or *pcdh* cRNA probe, and placed in a hybridization oven (59ºC) overnight. Next day, the sections were washed in 2X SSC, followed by 50% formamide in 2X SSC (at the hybridization temperature). The tissue sections were treated with RNase A (Roche), washed in RNase buffer before incubation in a blocking solution (5% normal goat serum, 2 mg/ml BSA, 1% DMSO in PBS with Tween-20, PBST) for two hours at room temperature with constant agitation on the platform shaker. The sections were then treated with an anti-DIG antibody (conjugated to alkaline phosphatase, AB_514497, Roche) solution (diluted 1:5,000 in the blocking solution) overnight at 4ºC. Visualization of the signal was achieved by incubating the sections overnight in dark at room temperature in a solution made from dissolving one tablet of 4-nitroblue tetrazolium chloride (NBT)/5-bromo-4-chloro-3- indolyl phosphate (BCIP, called NTB/BCIP tablet,

Roche) in 10 ml of distilled water. Tissues were processed together and all paramaters were the same, except different cRNA probes were used.

Data analysis

Stained sections were observed under an Olympus BX51 compound microscope equipped with Normarski optics and connected to a SPOT digital camera (SPOT Imaging Solutions, Sterling Heights, MI). Results were recorded as digital images and further processed using Photoshop 6.0 software (San Jose, CA).

Absolute quantitative real-time PCR (qPCR)

In order to quantify the amount of cadherin mRNA copies in tissues, the purified cDNA for each cadherin gene in vector was used to generate standard curves that served as a reference. First, the mass of single plasmid (vector with *cdh6*, *cdh7*, *pcdh17* and *pcdh19* gene insert) was calculated by multiplying its length in bp (base pairs) by 1.096×10^{-21} g/bp. This formula was derived from the estimation that 1 bp of dsDNA (double-stranded DNA) molecule has the average molecular weight of 660 g/mole and the Avogadro's number of 6.022×10^{23} molecules (bp) per 1 mole (Applied Biosystems). Next, the mass of a single plasmid was multiplied by each cadherin gene copy number (10^7-10^2) needed in each reaction. Once a known amount of linearized plasmid was serially diluted, it was used to generate the standard curve by running it on the same 96-well plate

as the samples during qPCR reaction (see below). Efficiency of assays was calculated using the formula: efficiency = $(10^{-1/slope}-1)$ (Yuan et al. 2007).

Retinas were harvested as described above and homogenized using the BeadBug microtube homogenizer (MIDSCI, Valley Park, MO). TRIzol reagent (Life Technologies, Carlsbad, CA) was used to isolate total RNA according to the manufacturer's protocol. Traces of genomic DNA were removed using Turbo DNA-free kit (Ambion, Austin, TX). RNA concentration was measured with Qubit 2.0 fluorometer (Life Technologies). Equal amounts (500 ng) of total RNA from each sample were reverse-transcribed to cDNA using Quanta Biosciences qScript cDNA SuperMix containing blend of oligo (dT) and random primers (Quanta Biosciences, Gaithersburg, MD). cDNA synthesis was also performed with negative control of no reverse transcriptase. The cDNA was further purified and concentrated using precipitation in 0.1 volume of sodium acetate, pH 5.2 (final concentration of 0.3 M) and two volumes of 100% ethanol.

Cadherin gene-specific primers and hydrolysis probe (Integrated DNA Technologies) were designed to span the exon-exon boundary using NCBI Primer-BLAST tool and were further checked against the whole *Danio rerio* database for specificity (Table 4.2). Samples were loaded on 96-well plate on ice, under the sterile hood and sealed with adhesive tape and subsequently centrifuged for 5 minutes at 300 g in 4ºC. qPCR was performed in an Applied Biosystems AB 7300 cycler (Applied Biosystems, Waltham, MA) under the following conditions: one cycle of UDG enzyme activation at 50ºC for 2 minutes, one cycle of AmpliTaq Gold UP enzyme activation at 95ºC for 10 minutes, 40

cycles of denaturation at 95ºC for 15 seconds and annealing at 60ºC for 1

minute. The amplification was carried out in triplicate, volume of each reaction

was 20 µl and contained TaqMan Gene Expression Master Mix with ROX (Life

Technologies), gene-specific primers (forward and reverse, 500 nM working

concentration), hydrolysis probe (250 nM working concentration, PrimeTime

Primer Probe Mix, Integrated DNA Technologies; Table 4.2), and 3 µl cDNA

template (75 ng/µl) or 5 µl standard (six serial dilutions of plasmid). No template

and no reverse transcriptase controls were run in duplicate along with the

samples. Sequence Detection System (SDS) software from Applied Biosystems

was used to analyze amplicons and calculate mRNA copies in each sample. The

PCR product specificity was confirmed by staining with ethidium bromide solution

(EtBr) on the gel electrophoresis and visualized band products of correct size

(106 bp for cdh6, 140 bp for cdh7, 102 bp for pcdh17 and 150 bp for pcdh19).

mRNA copy number/total RNA for each cadherin gene was calculated using the

standard curves.

Table 4.2. Primer and probe sequences of *cdh* genes for absolute qPCR.

Gene name	*cdh6*	Amplicon size
Forward primer	5'-GCTCCACAACAGTCAACATTAG-3'	
Reverse primer	5'-GATCCTACCTTGGTGAGTTCTG-3'	106 bp
Probe	5'-TCACCGATATCAACGACAACGCCC-3'	
Gene name	*cdh7*	
Forward primer	5'-ATCTTCTAGTAATCCAGGCCAAAG-3'	

Reverse primer	5'-AGGCACAGCAAACTGATAGG-3'	140 bp
Probe	5'-ACGGACGTTAATGACAACCCTCCC-3'	
Gene name	*pcdh17*	
Forward primer	5'-AGGTGCCTGAGAACAACATC-3'	
Reverse primer	5'-AGGGTAGGAGAGAATAGGACAC-3'	102 bp
Probe	5'-AGGGTAGGAGAGAATAGGACAC-3'	
Gene name	*pcdh19*	
Forward primer	5'-CTACGTGACCGTCAACTCAAA-3'	
Reverse primer	5'-CCATCCTTCGCAGACACTTTA-3'	150 bp
Probe	3'-AAGCCCTGACGCCGTATATTTCGC-5'	

Results

Cdh6, *cdh7*, *pcdh17* and *pcdh19* expression in the retina of adult zebrafish after optic nerve crush

Expression of *cdh6*, *cdh7*, *pcdh17* and *pcdh19* in both normal and lesioned retinas was examined at one day, two days, three days, one week, two weeks and three weeks after the optic nerve crush from both normal (i.e. unoperated or control) and lesion groups. Expression of *klf6a* and *klf7* (see Chapter III) in retinas from the same batch of tissues from selective stages (e.g. one week after the optic nerve lesion) was used to confirm the successful lesion of optic nerve (Figure 4.1, see Chapter III). In general, the expression pattern for each *cdh* or *pcdh* gene was similar among regenerating retinas from the same time point, and similar among all stages of control retinas. Only one image from

normal retinas was shown in each figure and one image from regenerating

retinas of each stage was used for each figure in the result (see below).
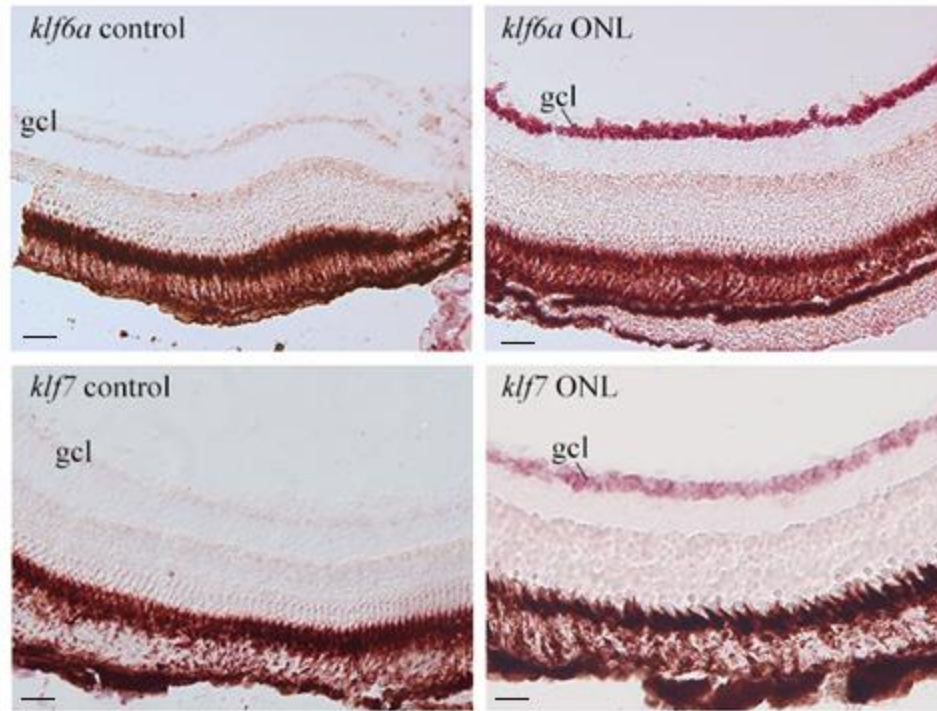

Figure 4.1. Confirmation of the successful optic nerve lesion using *klf6a* and *klf7* staining. Expression of *klf6a* and *klf7* is greatly elevated at one week (1w) post lesion (ONL), shown in images on the right column, compared to the control retina shown in the left column. Scale bar = 50 μm.

Compared to *cdh6* expression in the normal retina (Figure 4.2A),

expression in the retinas of 1-day, 2-day and 3-day post optic nerve lesion (ONL)

was similar, in that it was mainly observed in the inl (Figure 4.2B-D). *Cdh6*

expression in the gcl remained the same (i.e. little or no change) until 1-week

(1w) after ONL, when a few scattered cells in the gcl became *cdh6*-positive

(arrows in Figure 4.2E). A similar *cdh6* expression pattern was also detected in

retinas of two weeks (2w) post ONL, except that there seemed to be fewer

labeled cells in the gcl (arrow in Figure 4.2F). Moreover, the intensity of *cdh6*

expression in the inl appeared to decrease at 1 and 2 weeks after injury (Figure

4.2E and F). *Cdh6* expression returned to the control pattern in the retinas from 3

weeks post ONL (Figure 4.2G).
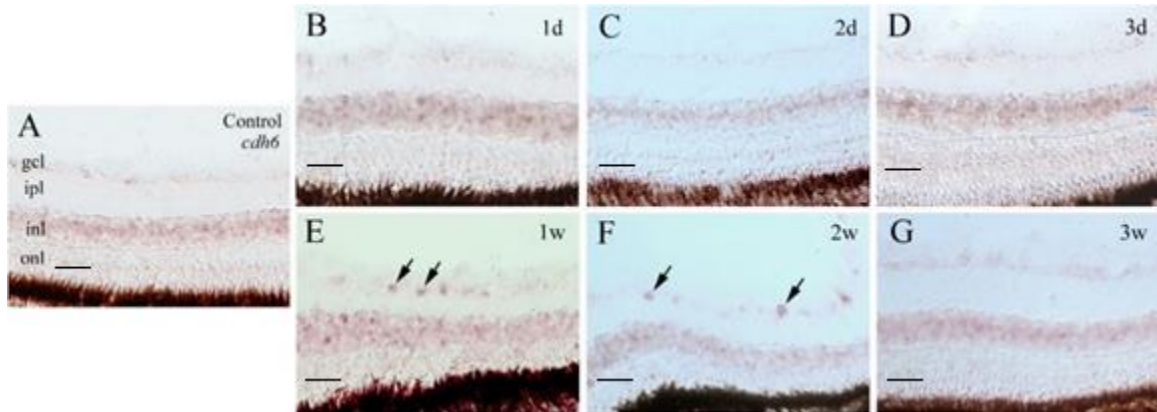
Figure 4.2. Expression of *cdh6* in zebrafish retinas in normal and ONL animals.
In control retinas (panel A), *cdh6* mRNA is detectable in the inl with *in situ*
hybridization. No changes are observed within the first three days after ONL
(panels B-D). During 1 and 2 weeks post ONL, *cdh6* mRNA signal decreases
slightly in the inl, while appears to be expressed in few scattered cells in the gcl
(panels E-F). At 3 weeks (panel G), *cdh6* labeling returns to the baseline levels.
Arrows point to *cdh6*-labeled cells in the gcl. Scale bar = 50 µm. See
Abbreviations for list of full terms.

In comparison to *cdh7* expression in normal retina (Figure 4.3A), the *cdh7*

expression in retinas at 1-day, 2-day and 3-day after ONL was very similar, with

some weakly labeled cells confined to the inner portion of the inl, but not the

innermost layer (Figure 4.3B-D, Chapter II). One week after the injury, increased

cdh7 expression, based on the staining intensity, was detected in few scattered

cells in the most inner region of the inl (arrows in Figure 4.3E). At 2 weeks after

ONL, the *cdh7* expression was similar to that of 1 week, except that the staining

intensity of some *cdh7*-expressing cells was reduced (Figure 4.3F). *Cdh7*

expression in retina returned to the same levels as control at 3 weeks after ONL

(Figure 4.3G).
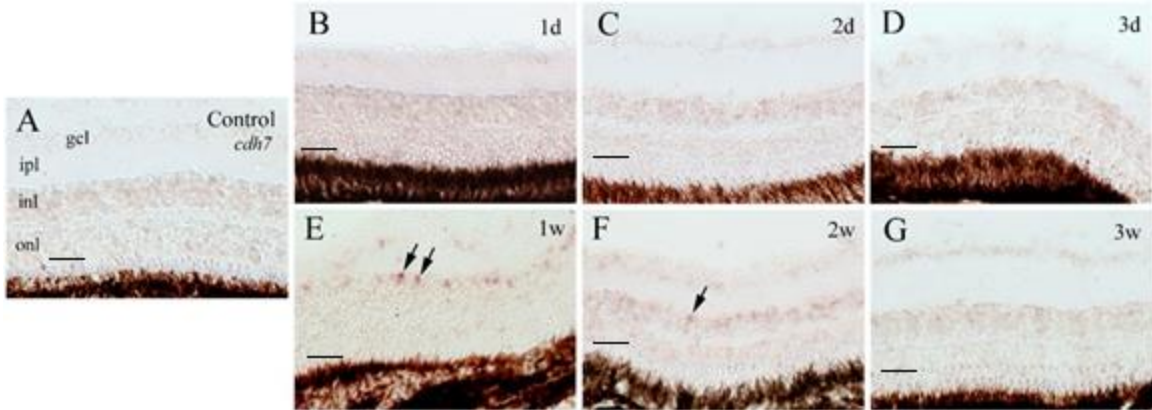
Figure 4.3. Expression of *cdh7* in zebrafish retinas in normal and ONL animals. In control retinas (panel A), *cdh7* mRNA is weakly detectable in the inner portion of the inl with *in situ* hybridization. No changes are observed within the first three days after ONL (panels B-D). During 1 and 2 weeks post ONL, *cdh7* mRNA appears to be expressed in few scattered cells in the inner part of the inl (panels E-F). At 3 weeks (panel G), *cdh7* labeling returns to the baseline levels. Arrows point to *cdh7*-labeled cells. Scale bar = 50 µm. See Abbreviations for list of full terms.

Pcdh17 expression in control retina was observed in the gcl and inl (Figure 4.4A). Many cells in the gcl, and most cells in the inl were *pcdh17*-positive. A change in *pcdh17* expression was detected in one day post ONL retinas (Figure 4.4B): its expression in the gcl was reduced compared to that in the control retina (Figure 4.4A). This reduction in *pcdh17* expression was even more apparent in retinas from 2 and 3 days, and 1-week post ONL fish (Figure 4.4C-E). No constant and apparent changes in *pcdh17* expression were found in other regions (e.g. the inl) of the retina in those tissues. *Pcdh17* expression patterns returned to the control pattern in retinas from 2 and 3 weeks post ONL (Figure 4.4F and G).
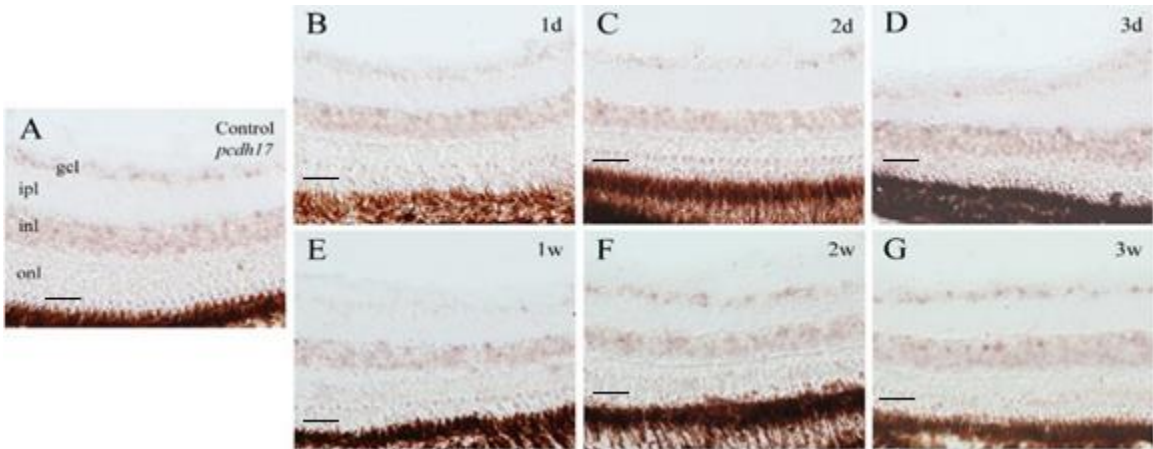
Figure 4.4. Expression of *pcdh17* in zebrafish retinas in normal and ONL animals. In control retinas (panel A), *pcdh17* mRNA is detectable in the gcl and inl with *in situ* hybridization. The expression is reduced in the gcl from 1 day to 1 week after ONL (panels B-E). At 2 weeks (panel F), *pcdh17* labeling returns to the baseline levels and remains the same at 3 weeks post ONL (panel G). Arrows point to *pcdh17*-labeled cells. Scale bar = 50 μm. See Abbreviations for list of full terms.

A comparable reduction of gene expression pattern of retinas with lesioned optic nerve was observed for *pcdh19* (Figure 4.5). *Pcdh19* expression in control retinas was mainly confined to the gcl and inner half of the inl (Figure 4.5A). At one day following the lesion, an obvious reduction in *pcdh19* signal was observed in the gcl (Figure 4.5B) and the decrease was also detected in the gcl of 2 days, 3 days and 1 week ONL fish (Figure 4.5C-E). There was no consistant and obvious change in *pcdh19* expression in the inl. *Pcdh19* expression returned to control levels in 2 and 3 weeks post lesion tissues. *Pcdh19* expression returned to control levels in 2 and 3 weeks post lesion tissues (Figure 4.5F and G).
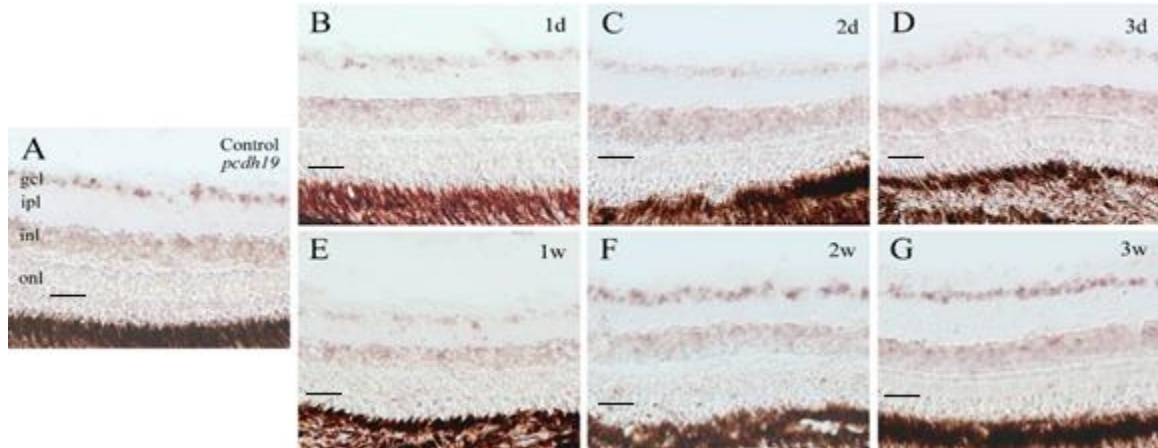
Figure 4.5. Expression of *pcdh19* in zebrafish retinas in normal and ONL animals.In control retinas (panel A), *pcdh19* mRNA is detectable in the gcl and inner region of inl with *in situ* hybridization. From 1 day through 1 week after ONL (panels B-E), *pcdh19* mRNA signal decreases significantly in the gcl. At 2 weeks (panel F), *pcdh19* labeling returns to the baseline levels and remains similar at 3 weeks post ONL (panel G). Arrows point to *pcdh19*-labeled cells. Scale bar = 50 µm. See Abbreviations for list of full terms.

In order to quantify the expression of cadherins in the retinas, I performed qPCR on selected control and lesioned tissues. A concentration of 75 ng/µl of RNA from normal and lesioned retinas was used to generate cDNA. The known amount of mRNA for each *cadherin*/*protocadherin* gene was serially diluted (10-10^6) and amplified in the qPCR reaction. The average of three amplicon cycle thresholds (Ct) for each diluted gene sample was plotted against the log10 dilution, resulting in the standard curve serving as a reference for the number of cadherin mRNA copies in the studied tissues (Figure 4.6). The standard curves for *cdh6*, *cdh7* and *pcdh19* had reliable efficiencies (96.3%, 92% and 99%, respectively) and excellent correlation efficiencies (0.991446, 0.988867 and 0.997059, respectively). There was no amplification for *pcdh17* fragment to generate the standard curve, possibly due to primers not working.
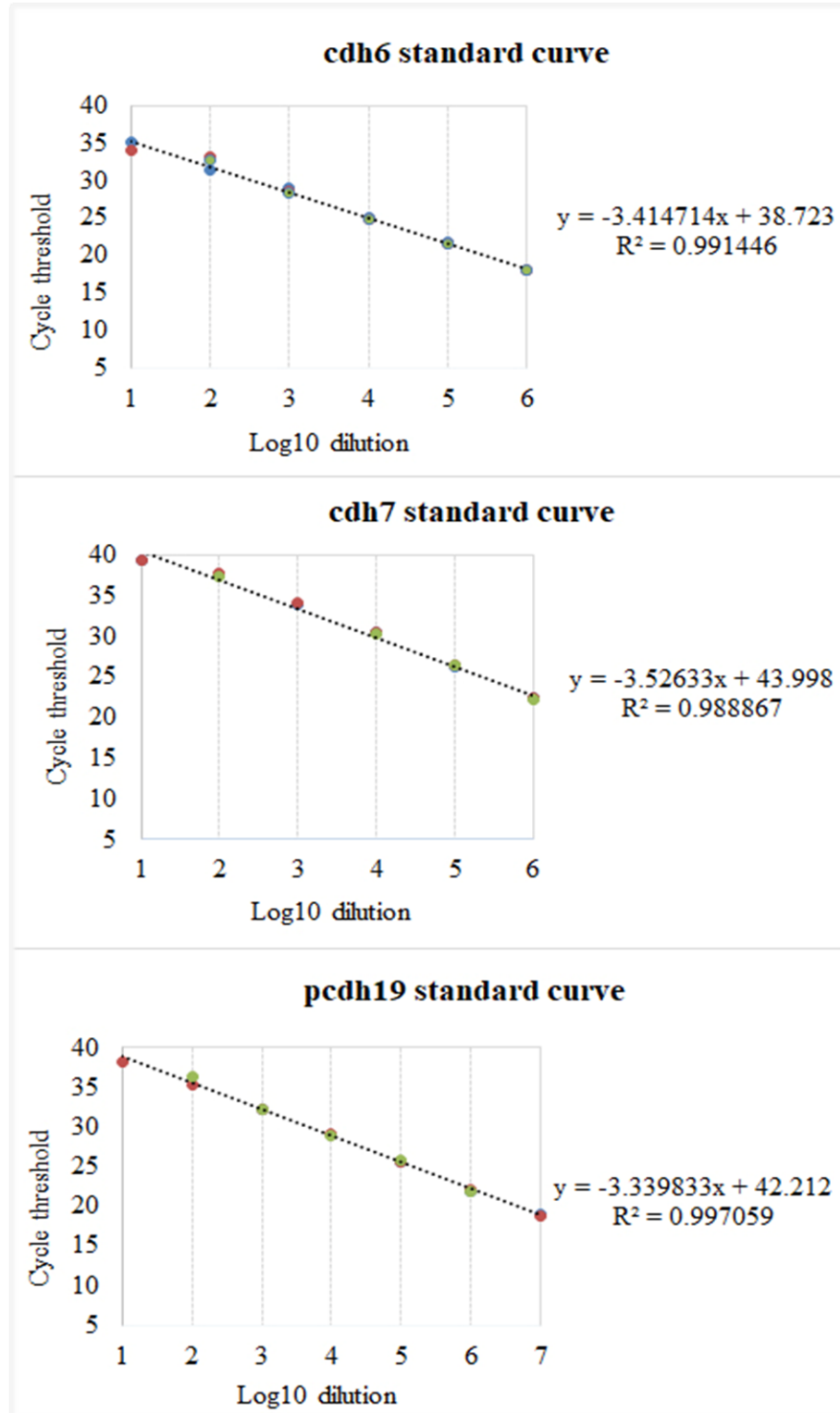
Figure 4.6. Standard curves for *cdh6*, *cdh7* and *pcdh19*. Log10 serial dilution is depicted on x-axis and cycle threshold on y-axis. Samples in triplicate were further used to obtain linear trendline. The reaction efficiency was calculated and was the following: *cdh6* (96%), *cdh7* (92%) and *pcdh19* (99%).

The data from 7-day post ONL is reliable for the reason that the tissue was processed along with *klf7* gene used as a marker for the successful lesion, and the observed increase in the copy number in ONL samples correlates well with the data published before (see Results in Chapter III).The copy number of *cdh6*, *cdh7* and *pcdh19* mRNA in the control retina and the retina 1-week post ONL is depicted in Figure 4.7. The gene expression of all three cadherin family members did not change enough to account to a fold change between the control and experimental retinas. Similar *cdh6* gene expression levels were detected between the control and lesioned tissues, increasing slightly in the experimental sample. The opposite outcome was observed for *cdh7* and *pcdh19* gene expression since the copy numbers were reduced in the retina where the optic nerve was crushed 7 days prior, in comparison to the control retina. The reduction of gene expression in the lesion sample was even more noticeable in the case of *pcdh19*. Examining the abundance of cadherins in terms of copy number, *pcdh19* was the most highly expressed of all three genes, accounting for 335 mRNA copies/ng in the normal retina and 290 mRNA copies/ng in the ONL retina. On the other hand, in both experimental conditions, *cdh6* expression was the scarcest (14 and 15 mRNA copies/ng, respectively) and was about five times lower than the copy number of *cdh7* (88 and 74 mRNA copies/ng, repectively) and more than twenty times lower than the copy number of *pcdh19* (Figure 4.7).

Cadherin copy number in the regenerating retina

■ control ■ ONL 7d

| | cdh6 | cdh7 | pcdh19 |
| control | 14 | 88 | 335 |
| ONL 7d | 15 | 74 | 290 |
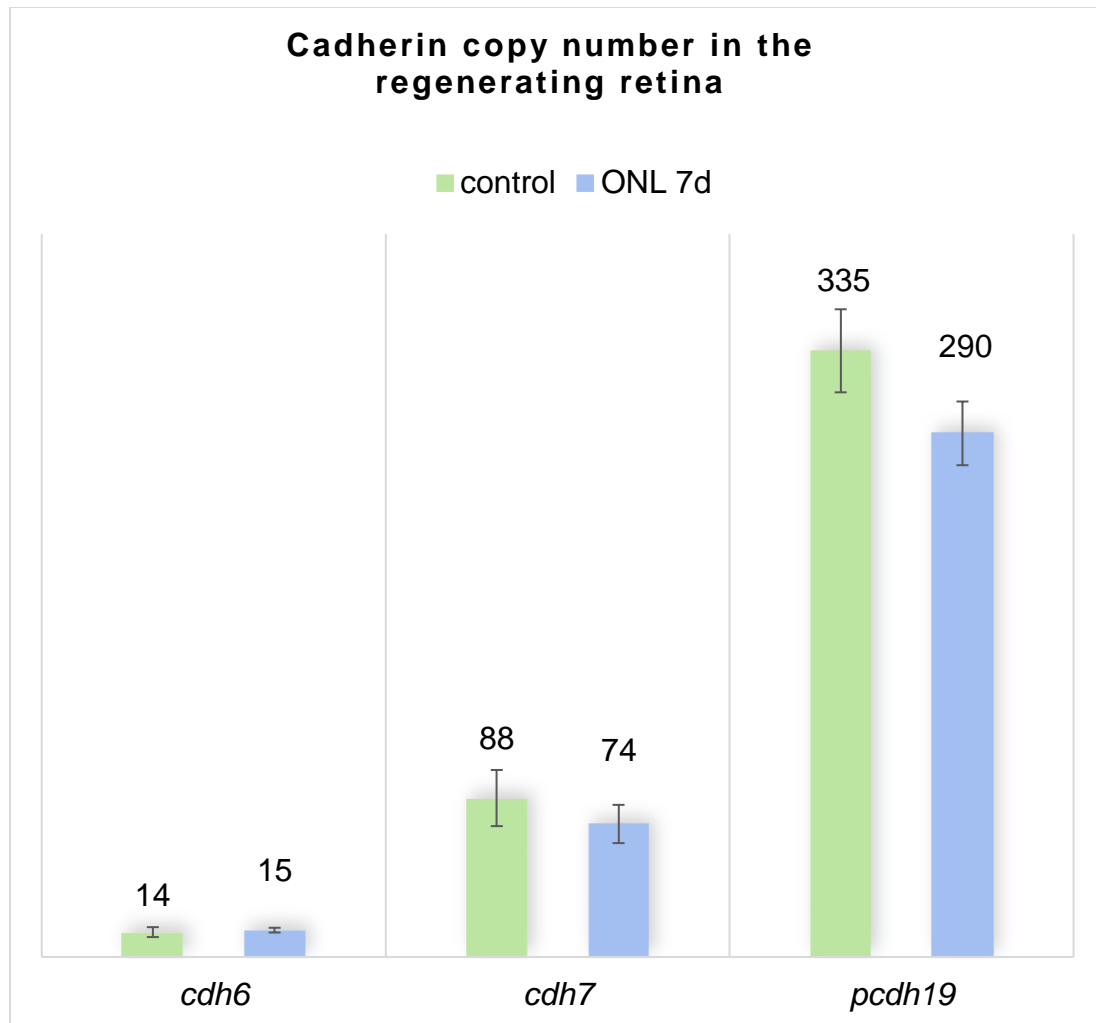
Figure 4.7. Copy number of *cdh6*, *cdh7* and *pcdh19* mRNA in retinas of normal and 7-day post optic nerve crush in adult zebrafish.The error bars represent the standard deviation. Copy numbers are per 1 ng total RNA. Sample size n=4. The copy number between conditions for each gene were not significant (paired two-tailed T-test were the following: p-value=0.567032901 for cdh6, 0.620700672 for cdh7, 0.100820611 for pcdh19), but copy numbers between each gene were statistically significant (1-way ANOVA p-value=0.00119).

Discussion

The optic nerve regeneration is a model system to study regeneration in

the nervous system, especially in the vertebrate CNS because of its accessibility

and regenerative potential in nonmammal vertebrates. Unlike mammals,

zebrafish fully regenerates its optic nerve and achieves functional recovery (Ferguson and Son 2011; Zupanc and Sîrbulescu 2011; Kato et al. 2013; Zou et al. 2013; Rasmussen and Sagasti 2016; Yin et al. 2019).

In this study, I showed that two classical type-II cadherins (*cdh6* and *cdh7*) and two δ2-protocadherins (*pcdh17* and *pcdh19*) exhibited differential expression patterns in the regenerating adult zebrafish retinas. *Cdh6* displayed an increased expression in selected cells in the gcl, while *cdh7* had increased expression in a few cells located in the innermost region of the inl of the regenerating retinas. On the other hand, the two protocadherins (*pcdh17* and *pcdh19*) showed decreased expression in the gcl of the regenerating retinas. My results suggest that these cadherins may play different roles in the retinal regeneration. The decreased expression of both *pcdh17* and *pcdh19* in the gcl of the regenerating retina was surprising, because previous studies by Liu and colleagues showed that expression of both cdh2 and cdh4 was greatly increased in the gcl of regenerating adult zebrafish retinas (Liu et al. 2002) and cerebella (Liu et al. 2004a). Consequently, it is likely that certain cadherins (e.g. cdh2 and cdh4) stimulate the retinal axon regrowth, whereas others (e.g. *pcdh19*) hamper the retinal axon outgrowth, or that the down-regulation of some cadherins is necessary to promote the successful regeneration of the optic nerve.

Different patterns of *cdh6*, *cdh7*, *pcdh17* and *pcdh19* expression in the adult zebrafish retina after optic nerve lesion

Expression of some genes in vertebrates recapitulates developmental programs during regeneration, while other genes appear to be regeneration-

specific genes (Franklin and Hinks 1999; Fausett 2007; Veldman et al. 2007; Brockerhoff and Fadool 2011; Cuenca et al. 2014). Cadherin family members are acknowledged to be involved in the retinal and/or brain development in vertebrates (including zebrafish); therefore, they likely contribute to the regenerating process. An increased cdh2 expression post-injury is associated with the successful nervous tissue regeneration in the fish optic nerve (Liu et al. 2002, 2004a), fish cerebellum (Liu et al. 2004a), rat sciatic nerve (Thornton et al. 2005) and quail ciliary ganglion (Squitti et al. 1999). In mice, cdh2 is not up-regulated in regenerating RGCs (Bates et al. 1999), while *cdh2* knockout results in the lowered RGC survival after the optic nerve crush (Ribeiro et al. 2020). In zebrafish, *cdh2* knockdown suppresses specification and subsequent regeneration of the RGCs and amacrine cells following their chemical injury, by affecting basal migration of Müller glia from their normal location in the inner half of the inl to the gcl (Nagashima et al. 2013). Since 90% of RGCs survive axonal injury (ONL) in zebrafish, the small amount of new cells are likely originating from the de-differentiated Müller glia (Nagashima et al. 2013). Furthermore, an unpublished study in our lab (Bahattarai dissertation research) showed that optic nerve regeneration was severely disrupted in adult zebrafish whose optic nerves were crushed with the cdh2 morpholino antisense oligonucleotide (*cdh2*MO) electroporated into regenerating RGCs (personal communications). Importantly, this *cdh2*MO had been shown to phenocopy zebrafish *cdh2* mutants (Lele et al. 2002).

The increased expression of *cdh6* was mainly found in a few scattered cells in the gcl, suggesting that up-regulation of this gene is not required for a successful optic nerve regeneration in the vast majority of RGCs, while it may promote regeneration of the axons of the RGCs that exhibit an increased *cdh6* expression. Only a subset of cells in the gcl of developing zebrafish retina are *cdh6*-expressing (Liu et al., 2006a), and cdh6 plays a role in zebrafish retinal development (Liu et al., 2008). Similarly to developing mouse retina, only a subset of cells in the gcl are cdh6-positive (cdh6 protein expression was examined), and all these cdh6-expressing retinal cells mediate non-image forming visual circuit (Osterhout et al. 2011). It is possible that the *cdh6*-expressing cells in both the developing and regenerating zebrafish serve a similar function in zebrafish.

Cdh7 is expressed by a subset of cells in the gcl, and most cells in the inner portion of the inl in a developing zebrafish (Liu et al., 2006b). In an adult retina, fewer cells in both the gcl and the inner portion of the inl contain *cdh7* (Figure 4.3A and Figure 2.1B from Chapter II). A few scattered cells in the inner portion of the inl showed apparent increase in their *cdh7* expression, similar to the few *cdh6*-expressing cells in the gcl (see above). The identity of these *cdh7*-expressing cells is unknown, but they are likely the displaced retinal ganglion cells. This is similar to the increased *klf6a* expression in the inner portion of the inl (Chapter III). It will be interesting to see if these cells can be double-labelled by both cdh7 and klf6a markers, if suitable antibodies against their respective proteins are available. Another reason for my speculation that these cells are the

displaced RGCs is that in developing chicken displaced RGCs in the inl are also *cdh7*-positive (Wöhrn et al. 1998). Again, like cdh6, cdh7 may not be involved in the retinal axon regeneration for most RGCs, but may participate in the regeneration of retinal axons for selected subset of retinal neurons (i.e. the displaced RGCs).

It is surprising that expression of both *pcdh17* and *pcdh19* was greatly reduced in the gcl of the regenerating retina, because expression of both cdh2 and cdh4 is significantly increased in the regenerating retina of adult zebrafish (Liu et al. 2002). These results suggest that down-regulation of both pcdh17 and pcdh19 is necessary for the successful optic nerve regeneration. Type-I classical cadherins, such as cdh2 and cdh4, are known to mediate stronger cell-cell adhesion, while pcdhs mediate weaker cell-cell adhesion, and may be more involved in regulating cellular functions via mediating cell-cell signaling and/or recognition (Takeichi 1990; Suzuki 1996; Halbleib and Nelson 2006; Suzuki and Hirano 2016). The cytoplasmic domain of the type-I classical cdhs is linked to the actin cytoskeleton through α- and β-catenins (Hirano and Takeichi 2012), while the cytoplasmic domain of δ-pcdhs interacts with proteins involved in signal transduction pathways, such as SMAD (Faura Tellez et al. 2015), protein kinases (TAO2β, Yasuda et al. 2007), protein phosphatases (Yoshida et al. 1999), cytoplasmic FMR1-interacting protein 1 (CYFIP1, Chen et al. 2014; Hayashi et al. 2014), C2kβ and Nlk1 (Wnt pathway, Kietzmann et al. 2012; Kumar et al. 2017).

It is interesting that the result of disrupting cdh2 function or pcdh19 function during embryogenesis causes similar defects in the zebrafish CNS

(Emond et al. 2009; Biswas 2012), and cdh2 and pcdh19 are shown to work together (forming heterodimers) to regulate CNS formation during embryogenesis (Emond et al. 2011). However, during the optic nerve regeneration, expression of these two members of the cadherin superfamily shows the opposite patterns, with significantly increased cdh2 expression (at the protein level, Liu et al. 2002) and greatly reduced *pcdh19* expression (my results). If the *pcdh19* expression is confirmed at the protein level (using pcdh19 antibodies), my results suggest that they may play different roles in development and regeneration.

The discrepancies between my RNA *in situ* hybridization results (e.g. clear change in *pcdh19* expression in the gcl at 1 week after optic nerve crush) and the qPCR data (e.g. no significant change in *pcdh19* expression 1 week after surgery) are likely due to the fact that ISH on tissue sections allows observation of regional differences in gene expression, while qPCR provides quantitative data on expression from the entire retinal tissue. There are far more cells and *cdh*/*pcdh*-expressing cells in the inl than those in the gcl, therefore they likely mask changes in *cdh*/*pcdh* expression in the gcl. I am confident that if I were able to isolate the gcl of the control and regenerating retinas (e.g. using laser dissection), and compared their *cdh*/*pcdh* expression, I would have gotten similar results (e.g. reduced *pcdh19* expression in the gcl) with both methods.

CHAPTER V

IDENTIFICATION OF DIFFERENTIALLY EXPRESSED GENES IN ZEBRAFISH

PROTOCADHERIN-17 MORPHANTS

Introduction

Cadherins are a diverse superfamily of calcium-dependent

transmembrane proteins comprised of more than 100 members (Nollet et al.

2000; Hirano and Takeichi 2012). Cadherins are present in organisms ranging

from *Drosophila* to mammals and function in the development of variety of

tissues and organs, as well as maintenance of adult structures (Van Roy and

Berx 2008; Hirano and Takeichi 2012; Suzuki and Hirano 2016). Cadherins

include classical cadherins, protocadherins, and desmosomal cadherins. Most

works have focused on studying expression and functions of the classical

cadherins in the development of model organisms (e.g. zebrafish, chicken and

mouse, Hirano and Takeichi 2012). A typical classical cadherin (e.g. cadherin-1,

also called E-cadherin) is made of a large extracellular domain (EC) consisting of

five homologous repeats, a transmembrane domain (TM), and a cytoplasmic

(intracellular) domain (IC) that is more conserved than the other domains of the

molecule. The cytoplasmic domain of classical cadherins interacts with catenins

(e.g. α- and β-catenins) that bind to other intracellular proteins, including actin

157

(Hirano and Takeichi 2012). The protocadherin (pcdh) subfamily contains more members (> 80 in mammals) than any other cadherin subfamily (Yagi 2008). Members of the pcdh subfamily can be grouped into clustered (i.e. α-pcdh, -β and γs) and non-clustered (i.e. δ-pcdhs). δ-pcdhs (e.g. pcdh17) also contain three domains, but their EC domain consists of 6 or 7 homologous repeats, while their IC domain is less conserved (Redies et al. 2005; Vanhalst et al. 2005).

Results from recent functional studies of δ-pcdhs (e.g. OL-pcdh, pcdh10, pcdh17 and pcdh19) convincingly demonstrated that these molecules play crucial roles in development of the vertebrate central nervous system (CNS, reviewed by Suzuki and Takeichi 2008; Kim et al. 2011; Hirano and Takeichi 2012). In mice, pcdh17 controls assembly of vesicles in presynapses in the corticobasal ganglia (Hoshina et al. 2013) and mediates collective axon extension in a subset of amygdala neurons (Hayashi et al. 2014). In developing zebrafish with reduced *pcdh17* expression, development of the eye in general is severely disrupted, in particular the differentiation of retinal cells (Chen et al. 2013). Moreover, expression of *PCDH17* is increased in Brodmann's area 46 in individuals with schizophrenia (Dean et al. 2007).

Cadherins and protocadherins play important roles in animal development through interactions with other molecules, and since the eye defects are the major phenotype in *pcdh17* morphants, I hypothesized that expression of genes related to the vertebrate eye development would be greatly changed in the *pcdh17* morphants. I tested this hypothesis using single-channel microarray, a technique useful in estimating the change in expression of thousands of genes

158

between two conditions. I found that several genes expressed in the photoreceptor layer and those important for the photoreceptor development had reduced expression in the morphants. Therefore, my results confirm that *pcdh17* exerts its effect on the photoreceptor cells by decreasing their growth and/or slowing down their differentiation. Understanding molecular mechanisms underlying pcdh17 function in zebrafish, a model organism for the study of vertebrate development, visual system and human brain disorders (Dooley and Zon 2000; Bilotta and Saszik 2001; Penberthy et al. 2002; Ward and Lieschke 2002; Santana et al. 2012; reviewed by Schmidt et al. 2013; Stewart et al. 2014), may help to gain insight into δ-pcdhs function in the vertebrate CNS development in general.

Materials and methods

Animals

Zebrafish embryos were obtained by breeding a colony of wild-type adult (6-12 months) zebrafish, maintained at The University of Akron Research Viviarium (UARV), as described in the Zebrafish Book (Westerfield 2007). The adult fish were maintained in 10-gallon tanks at 28°C at a 14-hour light /10-hour dark cycle. Embryos for whole-mount *in situ* hybridization were raised at 28°C in PTU- (1-phenyl-2-thiourea, 0.003%) supplemented water (1:1 filtered fish tank water: embryo water) to prevent melanization (Karlsson et al. 2001). Institutional Animal Care and Use Committee (IACUC) at The University of Akron (IACUC)

approved all animal-related procedures (approval reference #12-9A; copy in Appendix B).

Microinjection

A splice-blocking *pcdh17* morpholino (*pcdh17*sMO, designed to bind to the exon/intron 1 boundary: 5'-ATA TAA GTT GTC GCT CCT ACC TGT A-3', Chen et al. 2013) was synthesized by Gene Tools (Philomath, OR). Specificity of the *pcdh17*sMO was previously demonstrated by RT-PCR, showing inclusion of intron 1 (Morcos 2007) in morphants' mRNA leading to a premature stop codon 123 nucleotides downstream of exon 1 (Chen et al. 2013). Gross morphological defects (mainly reduced eye size, compared to embryos injected with a 5 bp-mismatch *pcdh17*sMO or uninjected embryos) seen in these embryos were indistinguishable from embryos injected with a translation-blocking *pcdh17* morpholino (Chen et al. 2013).

Zebrafish embryos were mounted in grooves of 1.5% agarose gel injection plates containing 0.01% (w/v) methylene blue (Sigma Aldrich) in fish tank water. The IM300 pheumatic microinjector (Narishige, East Meadow, NY) was used to inject 1-2 nl (1.5-3 ng) of *pcdh17*sMO suspended in Danieau buffer (58 mM NaCl, 0.7 mM KCl, 0.4 mM MgSO4, 0.6 mM Ca(NO3)$_2$, 5.0 mM HEPES, pH 7.6) into 1-4 cell stage embryos. Injected embryos were allowed to develop in separate 400 ml plastic containers at 28.5ºC in water bath. The animal survival rate was about 80%, similar to uninjected control embryos. Dead embryos were promptly removed from the container. When the embryos reached desired stage

(72 hpf), they were anesthetized in 0.05% MS-222 (Tricain) and euthanized in 0.2% MS-222. Whole embryos were processed for total RNA isolation (for microarray and qPCR), or fixed in 4% paraformaldehyde overnight at 4ºC (for whole-mount RNA *in situ* hybridization, WISH).

RNA isolation

The tissue samples (pooled 50 embryos of 72 hpf for each biological replicate) from control (uninjected) and experimental condition (embryos injected with *pcdh17*sMO) were processed side by side. The anesthetized embryos were homogenized using the BeadBug microtube homogenizer (MIDSCI, Valley Park, MO). Total RNA was extracted using TRIzol Reagent (Life Technologies, Carlsbad, CA) according to the manufacturer's instructions. The genomic DNA was removed using Turbo DNA-free kit (Ambion, Austin, TX). RNA was concentrated and washed with MinElute Gel Extraction Kit RNA (Qiagen, Valencia, CA) cleanup protocol. The RNA concentration was quantified with Qubit 2.0 fluorometer (Life Technologies). RNA Integrity Number (RIN) was measured with the Agilent 2100 Bioanalyzer (Agilent Technologies, Palo Alto, CA). Only high-quality RNA samples (> 500-600 ng/µl and RIN ≥ 9) were used for microarray and qPCR.

Microarray

The total RNA was sent to The University of Michigan Comprehensive Cancer Center's Microarray Core Facility (Ann Arbor, MI) for biotinylated cDNA

synthesis (Ambion WT kit), hybridization on arrays and microarray chip scan. Four morphant (three biological and two technical replicates) and six control (five biological and two technical replicates) samples (batches, each containing 50 embryos) were independently hybridized with Zebrafish Gene 1.1 ST Array Strips (Affymetrix, Santa Clara, CA) and scanned using Affymetrix Gene Atlas System (software version: 1.0.4.267; Affymetrix). Array chips type ZebGene-1_1-st-v1 were built on danRer7/ Zv9 zebrafish genome assemblies and each contained 1,255,682 probes, covering expression of 59,302 zebrafish genes.

Microarray (.CEL) files (raw probe intensities) from each single-channel microarray were imported into Partek® Genomics Suite 7.0 (Partek, St. Louis, MO) to further analyze the hybridization represented as the intensity value for each oligonucleotide probe. All probe-level intensities were corrected for GC content, reducing the effects caused by intensity of probes. Data was analyzed using Robust Multi-Array Average (RMA) algorithm that removed the added variability of probe intensities between arrays, from processes of sample labeling, hybridization and scanning. The background correction removed affinities for perfect matches (PM) for probes, while the quantile normalization normalized probe level intensity between all chips (Irizarry et al. 2003). Subsequently, the relative fold changes (FC) and the log2 transformation was calculated for the probesets on each array, and Quality Control/Quality Assurance (QA/QC) metrics were viewed as a box plot showing the similar intensity distribution among arrays.

Affymetrics gene transcript probesets identifiers (probeset IDs) were further annotated with the corresponding gene symbols (Entrez Gene identifiers), based on zebrafish Zv9 (July 2010; Wellcome Trust Sanger Institute) genome assembly. Probesets without matching gene identifiers were filtered, reducing 75,212 initial transcript probesets to 25,450 gene transcript-matching probesets. ANOVA 1-way analysis was used to calculate the probability values for all fold changes between two experimental conditions: one contrast for the experimental treatment. *Post hoc* analysis for multiple testing was performed. This method is called the false detection rate (FDR, Benjamini and Hochberg 1995) and it controls for the detection of false positives, also known as the type-I error (occurring when a null hypothesis is erroneously rejected).

Genes with the following cut-off criteria were deemed significant: log2 fold change (FC) of $\leq$ -0.5 or $\geq$ 0.5 and adjusted p-value $\leq$ 0.05 FDR, and are further referred as differentially expressed genes (DEGs). Hierarchical clustering of DEGs for each sample was achieved by standardized normalization, where the genes were shifted to a mean of zero and scaled to standard deviation of one. DEGs (using Entrez Gene identifiers) were further analyzed using Fisher exact test in Partek® Gene Ontology (GO) Enrichment to identify significantly changed GO terms, and independently in Partek® Pathway (connected to KEGG – Kyoto Encyclopedia of Genes and Genomes, http://www.genome.jp/kegg) to identify the pathways containing significantly changed DEGs in the morphants.

Relative quantitative PCR (qPCR) validation of microarray

Relative quantitative PCR on selective genes with high fold changes and/or genes related to the visual system was performed to validate the gene expression estimates from the microarray. The following genes were selected: *opn1sw2*, *grk1b* and *grk7a* (important in phototransduction), *prph2a* (important in visual perception and retinal degeneration), *rbp4l* (involved in retinal development), *cdhr1a* and *pcdh17* (significantly changed cadherin superfamily genes), and finally, *hbbe3* (responsible for heme and oxygen binding in the embryo, a highly up-regulated gene). Gene-specific primers (Integrated DNA Technologies, Coralville, IA) were designed to span exon-exon boundaries using NCBI Primer-BLAST tool and checked against the whole *Danio rerio* database for specificity (Table 5.1).

Table 5.1. Primer sequences of selected genes for relative qPCR.

Gene name	F primer R primer	Amplicon size
rpl13a	5'-CACAAAATTGTGGTGGTGAG-3' 5'-GGTTGGTGTTCATTCTCTTG-3'	106 bp
grk7a	5'-ATGCTAAGAAGGAGAAGGTG-3' 5'-GCAAAGTTGATGGACTTGAA-3'	199 bp
grk1b	5'-TGTTGAATTACCACCAGGAA-3' 5'-AAGCGTGAAGTAGTCTACAG-3'	118 bp
cdhr1a	5'-CCAATCAGAGAGACTGTACC-3'	162 bp

	5'-GCATGGGATTTTCCCTACTA-3'	
opn1sw2	5'-TACGTCATGTTCCTCTTCTG-3'	164 bp
	5'-ATTACCACCACCATCTTTGT-3'	
prph2a	5'-ATGGTGGAATGATGAACACT-3'	185 bp
	5'-GATGTCAGTGAAGGTCTCTT-3'	
rbp4l	5'-GTTTTACAGTCAAGGACGAC-3'	141 bp
	5'-CAGTCATGGTTCCATCATCA-3'	
hbbe3	5'-CGATTCAGAACATCTTTGCC-3'	112 bp
	5'-TTTCCAAACCCACCAAAGTA-3'	
pcdh17	5'-GACAGCGATCAGGACACTAATAA-3'	129 bp
	5'-CTCCGTGCAGTTCAAACAATC-3'	

Equal amounts of total RNA from each condition (described in the section above) were synthesized to cDNA using high-capacity cDNA RT kit (Life Technologies) with oligo (dT) primers. Three null controls were included in cDNA synthesis step: no template, no primer, and no reverse transcriptase. Next, cDNA was purified and concentrated by precipitation in 0.1 volume of sodium acetate, pH 5.2 (final concentration of 0.3 M) and two volumes of 100% ethanol.

Quantitative real-time PCR (qPCR) was carried out on Applied Biosystems AB 7300 cycler (Applied Biosystems, Waltham, MA) with intercalating dye SYBR green fluorescent label. The cycles entailed an initial denaturation at 95ºC for 10 minutes and 40 cycles of 95ºC for 15 seconds, 59ºC for 1 minute. Each cDNA sample was diluted over six orders of magnitude to calculate the PCR

amplification efficiency. With 100% amplification efficiency, the amount of product

doubles in each qPCR cycle. The calibration curves were plotted on a graph: the

sample diluted by log10 on x-axis and Ct on y-axis, and used to calculate the

efficiency using the formula: efficiency = $(10^{-1/slope}-1)$ (Yuan et al. 2007). Samples

were loaded under the sterile hood to 96-well plate on ice, and subsequently

sealed with adhesive tape, then centrifuged for 5 minutes at 300 g in 4ºC. The

amplification was carried out in triplicate in a volume of 20 µl using of 2x

FastStart Universal SYBR Green Master with Rox passive dye (Roche,

Indianapolis, IN), forward and reverse specific primers (200 nM each working

concentration, Table 5.1) and a cDNA template (25 ng/µl). No template and no

reverse transcriptase controls were run in duplicate along with the samples. A

single peak was observed for all qPCR products using the dissociation curve

analysis (Applied Biosystems® SDS Software v1.4.1). Each PCR product

specificity was confirmed by staining with ethidium bromide solution (EtBr) on gel

electrophoresis and confirmation of the band size. Relative gene expression was

calculated using comparative $2^{-\Delta\Delta CT}$ method (Livak and Schmittgen 2001) and

data normalization used ribosomal protein L13a (*rpl13a*) as a reference gene

(Tang et al. 2007). The primer sequences are in Table 5.1. The statistical

significance of Ct differences between biological replicates and between

experimental conditions was calculated using two-tailed T-test.

Whole-mount RNA *in situ* hybridization (WISH)

Procedures for the synthesis of digoxigenin-labeled (DIG) cRNA probes (Liu et al. 1999b) and whole-mount *in situ* hybridization were described previously (Barthel and Raymond 1990, 1993). cDNAs used to generate cRNA probes were kindly provided by Pamela Raymond at The University of Michigan. For each cRNA probe, control embryos (uninjected) and experimental (*pcdh17* morphants) were processed at the same time, side by side.

The fixed (in 4% PFA) embryos were washed twice for 10 minutes each in 1xPBS with a constant slow agitation (on a platform rocker under the ventilation hood) at room temperature. Next, the embryos were washed in 70% methanol (Met; in DEPC water) for 10 minutes, then washed three times, 5 minutes each, in 100% methanol. The embryos were stored in 100% methanol at -20°C until used for whole-mount *in situ* hybridization (WISH). For WISH, the embryos were placed in 75% MetOH, 25% PBST (PBS with Tween-20) for 5 minutes, then in 50% MetOH, 50% PBST for 5 minutes, which was followed by placing the embryos in 25% MetOH, 75% PBST for 5 minutes. The embryos were washed four times in PBST for 5 minutes each. All the above steps were carried out in 1.5 ml RNAse-free centrifuge tubes at room temperature. Subsequently, the embryos were treated with proteinase K (0.01 mg/ml, Roche) for 20 minutes at room temperature. Then, the embryos were rinsed in PBST for 5 minutes, re-fixed in 4% paraformaldehyde for 20 minutes at room temperature. Next, the embryos were washed 5 times in PBST for 5 minutes each. For the pre-hybridization step, the embryos were placed in new 1.5 ml RNAse-free centrifuge

tubes in a hybridization solution without any cRNA probe for 1 hour at 58ºC.

Meanwhile, the antisense cRNA probe was heated to 80ºC for 10 minutes and

then quickly placed on ice. The hybridization buffer was then replaced with

hybridization solution containing the cRNA probe for each gene, with the probe

concentration at 0.5 µg/ml. Hybridization of embryos happened overnight at

59ºC. The next day, the embryos were washed for 1 hour in 50% formamide/2X

SSCT, followed by two 10-minute washes in 2X SSCT and for 30 minutes in 0.2X

SSCT (all at the hybridization temperature). Then, the embryos were washed for

10 minutes each in decreasing concentrations of 0.2X SSCT, in PBST (75% 0.2X

SSCT/25% PBST, 50% 0.2X SSCT/50% PBST, 25% 0.2X SSCT/75% PBST,

100% PBST). For the blocking step, the embryos were incubated in a blocking

solution (5% normal goat serum, 2 mg/ml BSA, 1% DMSO in PBST) for two

hours at room temperature with constant agitation on the platform shaker. Finally,

the embryos were treated with an anti-DIG antibody (conjugated to alkaline

phosphatase, AB_514497, Roche, Indianapolis, IN), diluted 1:5,000 in the

blocking solution, overnight at 4ºC with constant agitation. For

immunocytochemical detection of the digoxigenin-labeled cRNA probes, an anti-

digoxigenin Fab fragment antibody conjugated to alkaline phosphatase (Roche)

was used, followed by a color reaction step using NBT/BCIP tablets (Roche).

After the color reaction, the embryos were fixed in 4% paraformaldehyde for 20

minutes, washed three times in PBST for 5 minutes each. In order to make them

transparent, the embryos were placed in 50% glycerol (in PBS) for 2-3 hours.

They were stored at 4ºC until the microscopy step (see below).

Microscopy

Stained whole-mount embryos were observed with an Olympus BX51 compound microscope equipped with a SPOT digital camera (Diagnostic Instrument Inc., Sterling Heights, MI). The images were slightly adjusted for contrast and sharpness using Adobe Photoshop 6.0 software (San Jose, CA).

Results

In order to identify genes that might be involved in *pcdh17*-mediated eye development, I performed the microarray analysis using total RNA from 72 hpf zebrafish morphants. This stage of zebrafish embryos was chosen because most of the major types of retinal cells are present, and smaller eye along with perturbed differentiation of the retinal cells (especially the retinal ganglion cells and photoreceptors) are the major defects observed in the *pcdh17* morphants at this stage (Chen et al. 2013).

Gene expression profiles of *pcdh17* morphants

Pcdh17 expression in embryos was reduced by the splice-blocking zebrafish *pcdh17* morpholino, previously shown to alter splicing of *pcdh17* mRNA (i.e. introducing premature stop codons in the exon 1 of the gene, Chen et al. 2013). The *pcdh17*sMO was previously validated using the 5 bp-mismatch morpholino for the dose specificity and by PCR for the successful intron inclusion in target mRNA. Based on gross morphology and measurements, embryos injected with the *pcdh17*sMO are indistinguishable from those injected with the

translation-blocking *pcdh17* morpholino (*pcdh17*atgMO), and uninjected controls are indistinguishable from those co-injected with *pcdh17*sMO and *pcdh17* mRNA (complete rescue, Chen et al. 2013). The use of the lowest dose of the antisense morpholino resulting in the experimental defects limits the likelihood of morpholino interacting with off-target RNA (Moulton 2017). The gross size and morphology of the resulting embryos were similar to those described in our previous publication (Chen et al. 2013), with the embryos having similar size and shape as those of control embryos, but smaller eyes (Figure 5.11). Embryos of 72 hpf were used for microarray, qPCR and *in situ* hybridization experiments.

The principal components analysis (PCA) was performed to assess the clustering patterns of all samples, as well as possible presence of outliers. This analysis indicated that the gene expression profile of the *pcdh17* morphants was significantly different from that of control embryos. PCA mapping revealed that 60.4% dissimilarities in the gene expression originated from variations between biological sample groups, while 24.3 % dissimilarities originated from within-group differences (Figure 5.1).
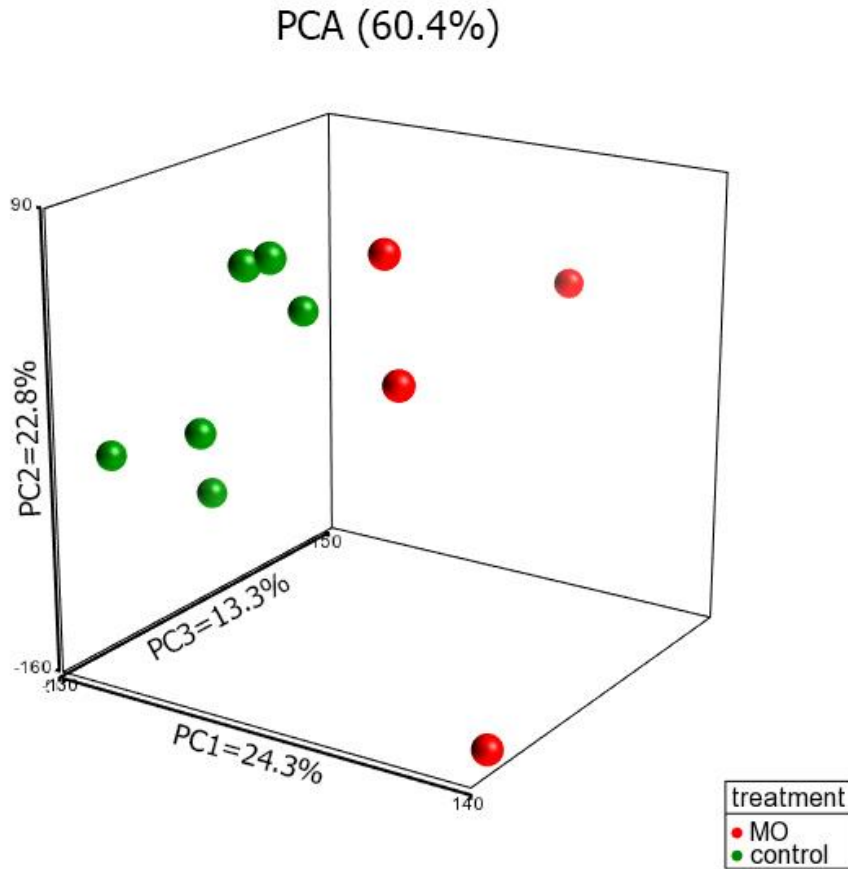
Figure 5.1. PCA (Principal Components Analysis) scatter plot. Graph delineates that differences in the gene expression between *pcdh17* morphants and control microarray samples can be explained by 60.4% intergroup (between treatments) dissimilarities and 24.3% intragroup (within a treatment) dissimilarities. A total of 10 microarray samples (4 from the morphants, 6 from control) are shown on this three-dimensional graph.

Out of the 75,212 gene-level probes (probesets) on the Affymetrix

zebrafish 1.1 ST microarray strip, 25,450 had gene transcript annotation. The

statistical analysis found 72 differentially expressed genes (DEGs) with fold

changes ≥ ±0.5 and FDR adjusted p-value < 0.05 between *pcdh17* morphants

and control embryos. The majority of these genes had a decreased expression

(49 genes, 67% of the total), while 23 genes (33% of the total) showed an

increased expression. The volcano plot visualizes annotated gene transcripts on

array based on their log2 FC and p-value (Figure 5.2). All DEGs sorted by their

significance values are listed in Table 5.2. Post-import quality check on the

distribution of 75,212 probeset intensities from microarrays (n=10) is pictured in

Appendix C and in Figure 5.1.
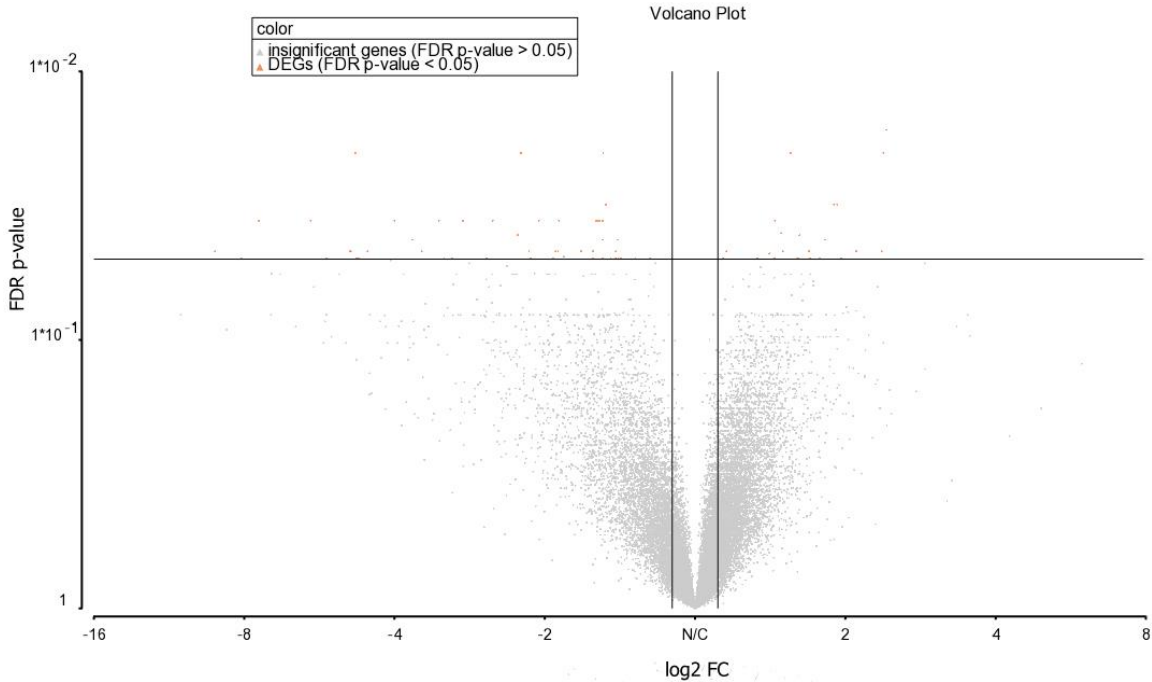
Figure 5.2. Transcripts on microarray depicted on the volcano plot. The log2 fold changes of 25,450 filtered genes on array are displayed on y-axis, with the cut-off significance ±0.5 fold change. The FDR adjusted p-value is plotted on the x-axis with the 0.05 cut-off significance. Two vertical lines on the graph indicate the mark at -0.5 and +0.5 log2 fold changes, while one horizontal line indicates the mark at 0.05 for FDR p-value. Seventy-two genes (DEGs: differentially expressed genes depicted as orange triangles) displayed significant expression changes in *pcdh17* morphants compared to control (uninjected) animals. Twenty-three up-regulated genes have log2 fold changes within the 1.14 and 2.42 range and are located above the horizontal line and to the right of the vertical line. Forty-nine down-regulated genes have log2 fold changes within the -9.15 and -1.23 range and are located above the horizontal line and to the left of the vertical line. Insignificant genes are marked in grey and are below the horizontal line.

Differentially expressed genes in *pcdh17* morphants

Differentially expressed genes (DEGs) are sorted by their probability values in Table 5.2. As expected, *pcdh17* gene was down-regulated in the morphants by 2.04 log2 fold change in comparison to control zebrafish (Table 5.2). *Pcdh17* is expressed in the eyes of zebrafish (Liu et al. 2009; Chen et al. 2013), and morphant eyes are smaller than control animals.

The most significant and also highest up-regulated gene in the morphants was *dusp27* (dual specificity phosphatase 27), an enzyme present in the optic tectum in zebrafish (24-30 hpf), skeletal muscle, liver and functioning in maturation of myofibers (Fero et al. 2014). Other most significantly changed genes function in ion binding such as *fxyd6* (FXYD domain containing ion transport regulator 6), in calcium binding such as *scpp9* (secretory calcium-binding phosphoprotein 9) and *dld* (deltaD). Genes encoding some transcription factors were also some of the most significantly changed genes in the morphants. They include *lhx5* (LIM homeobox 5) and *hes2.2* (hes family bHLH transcription factor 2, tandem duplicate 2).

The up-regulated genes in *pcdh17* morphants are expressed in muscles (*her13*, *dld*, *nr6a1a*, *scfd2*) and in brain (*foxi1*, *neurog1*, *nkx2.1*, *lhx5*, *otpa*), with most of their encoded proteins functioning in the nucleus (*foxi1*, *neurog1*, *her13*, *nkx2.1*, *nr6a1a*, *lhx1b*, *lhx5*, *scml2*, *scml2*, *lmx1bb*). Genes encoding transcription-related proteins include *neurog1*, *her13*, *nkx2.1*, *nr6a1a*, *lhx1b*, *scml2* and *otpa*. Genes expressed in the eyes that were positively up-regulated in *pcdh17* morphants include: *hes2.2* (hes family bHLH transcription factor 2,

tandem duplicate 2; likely a transcription repressor), *psmd4b* (proteasome 26S subunit ubiquitin receptor, non-ATPase 4b; involved in proteasome assembly) and *lhx5* (LIM homeobox 5; a transcription factor important in eye development).

The most down-regulated gene in *pcdh17* morphants was *slc1a2a* (solute carrier family 1 glial high affinity glutamate transporter, member 2a). This gene was annotated to two probesets on an array and their log2 FCs were -9.14773 and -7.4856. *Slc1a2a* is expressed in the zebrafish brain and retina. Previous studies (Niklaus et al. 2017; Breuer et al. 2019) showed that in the retina, it is detected in the photoreceptor layer (outer nuclear layer, onl; 72 hpf and 5 dpf to adult), in the outer plexiform layer (opl) and inner nuclear layer (inl; 5 dpf to adult), and functions as a glutamate transporter in the nervous system. Mutations in its human ortholog *SLC1A* are found in people with epileptic encephalopathy (Myers et al. 2016; Guella et al. 2017). Other genes that are expressed in the eye and have reduced expression in the morphants were the following: *slc1a2a*, *zgc:73075/ rcvrn3*, *cplx4a*, *slc51a*, *gabra6a*, *rbp4l*, *cx35b*, *rgra*, *sh3gl2*, *spock3c*, *syngr3a*, *dpp6b*, *kcnip3a*, *syngr3b*, *ndufa4*, *spag1a* and *LOC100000094* (predicted *lbhl*). The rest of the down-regulated genes include those that are primarily expressed in the brain (e.g. *grapb*, *fxyd6*, *si:dkey-221l4.11/cldn23l*), and in other organs (e.g. *c3a.2*, *nr1h4*). Locations of these down-regulated genes in the cell are either extracellular (*LOC569340/ impg1a*, *ttr*, *c3a.2*, *rbp4l*,), or on the cell/plasma membrane (*pcdh17*, *gdpd3b*, *gabra6a*, *cx35b*, *fxyd6*, *plppr3b*, *si:dkey-221l4.11/cldn23l*, *asic4a*, *slc1a2a*, *irbp*, *grk7a*, *usp21*, *gdpd3b*, *rgra*). The functions of genes negatively affected by *pcdh17* knockdown include signal

transduction (*zgc:73075/ rcvrn3*, *spock3*), neurotransmitter transport (*cplx4a*) and calcium ion binding (*pcdh17*, *zgc:73075/ rcvrn3*, *spock3*, *kcnip3a*, *necab2*). Expression of *LOC100000094* (predicted *lbhl*, limb bud and heart-like) gene regulating the photoreceptor development (Li et al. 2015) was also significantly down-regulated in the morphants.

The eye-specific genes with some of the greatest down-regulation in *pcdh17* morphants are genes involved in the eye development and/or "phototransduction" KEGG pathway. They include *grk1b* (G protein-coupled receptor kinase 1 b), *grk7a* (G protein-coupled receptor kinase 7a), *rgra* (retinal G protein-coupled receptor a), *irbp* (interphotoreceptor retinoid-binding protein), *LOC569340* (interphotoreceptor matrix proteoglycan 1), and *rbp4l* (retinol binding protein 4, like). Lower transcript levels in genes normally expressed in the eye included many genes with partially known or predicted functions. Those include the following: *rbp4l* (retinol binding protein 4, like) predicted to transport retinol through transmembrane, z*gc:73075/ rcvrn3* (recoverin 3) expressed in the double cones and regulating cone opsin recovery in dim light conditions by control of Ca^{2+} in light response, *gabra6a* (gamma-aminobutyric acid type A receptor subunit alpha6a) also expressed in the onl of developing zebrafish and functioning as a receptor for inhibitory neurotransmitter $GABA_A$, and *asic4* (acid-sensing (proton-gated) ion channel family member 4a), which is similarly expressed in the gcl and onl and implicated in neuronal communication (Paukert et al. 2004; Vina et al. 2015; Zang et al. 2015; Monesson-Olson et al. 2018). Additionally, two genes with reduced expression have human orthologs

implicated in retinal pathologies: *rgra* (retinal G protein-coupled receptor a),

assumed to be a part of the G protein-coupled receptor signaling pathway and

cellular response to light stimulus in phototransduction, and is othologous to

human RGR (retinal G protein-coupled receptor), gene implicated in retinitis

pigmentosa (Morimura et al. 1999). Human ortholog IMPG1 (interphotoreceptor

matrix proteoglycan 1) is associated with vitelliform macular dystrophy (Meunier

et al. 2014) and retinitis pigmentosa (Olivier et al. 2021), and in the morphants

this gene (*LOC569340*, XM_003200660, *impg1a*, interphotoreceptor matrix

proteoglycan 1a), predicted to be involved in visual system development, was

reduced.

Table 5.2. Differentially expressed genes (DEGs) in 72 hpf *pcdh17*MOs. The cut-off significance is based on FC ±0.5 and ≤0.05 FDR adjusted p-value. The complete list of 72 DEGs is sorted by their probability values. Sample size = 10.

Gene Symbol	RefSeq	log2 fold change	p-value	FDR p-value
dusp27	XM_003197607	2.41751	6.49E-07	0.016518
fxyd6	NM_199847	-2.23206	1.87E-06	0.020111
scpp9	NM_001145245	-4.79417	3.50E-06	0.020111
lhx5	NM_131218	1.55249	3.95E-06	0.020111
hes2.2	NM_001045353	2.385	4.36E-06	0.020111
zgc:136872	NM_001040251	-1.52754	4.74E-06	0.020111
dld	NM_130955	1.89708	9.50E-06	0.031272
syngr3b	NM_001100441	-1.50891	1.09E-05	0.031272

psmd4b	NM_001017624	1.92724	1.11E-05	0.031272
rbp4l	NM_199965	-2.54198	1.51E-05	0.035968
pfkpa	XM_002666597	-1.87325	1.65E-05	0.035968
slc1a2a	NM_001190305	-7.4856	1.73E-05	0.035968
zgc:73075 (rcvrn3)	NM_200825	-5.88554	1.97E-05	0.035968
slc51a	NM_001004546	-3.25967	2.09E-05	0.035968
pcdh17	NM_001160822	-2.05565	2.24E-05	0.035968
usp21	XM_005162129	-3.99971	2.45E-05	0.035968
kcnip3a	NM_200819	-1.53092	2.59E-05	0.035968
dpp6b	NM_001115122	-1.55292	2.64E-05	0.035968
syngr3a	NM_001020591	-1.56754	2.87E-05	0.035968
scml2	XM_003199502	1.44574	2.88E-05	0.035968
spock3	XM_009307619	-1.57708	2.99E-05	0.035968
LOC101886585	XR_223248	-2.91716	3.11E-05	0.035968
fam124b	XM_009291410	1.48924	3.62E-05	0.040054
abtb2	XM_682789	1.6197	3.94E-05	0.040746
cx35b	NM_194420	-2.26458	4.00E-05	0.040746
c3a.2	NM_131243	-3.67944	4.57E-05	0.04235
nkx2.1	NM_131776	1.81889	4.62E-05	0.04235
glipr1b	NM_200575	-1.53052	4.76E-05	0.04235
ndufa4	NM_213025	-1.42624	4.83E-05	0.04235
cplx4a	NM_001077300	-4.88955	6.04E-05	0.04676
LOC560023	XM_683417	-2.15089	6.17E-05	0.04676

neurog1	ENSDART000000 78563	2.10405	6.21E-05	0.04676
lhx1b	NM_131207	1.69003	6.25E-05	0.04676
LOC569340 (impg1a)	XM_003200660	-4.91048	6.47E-05	0.04676
grapb	NM_001030080	-1.60069	6.78E-05	0.04676
slc1a2a	XM_005166477	-9.14773	6.90E-05	0.04676
foxi1	NM_181735	2.36386	7.03E-05	0.04676
wu:fe17e08	XM_002665275	1.15623	7.28E-05	0.04676
LOC100000094 (lbhl)	XM_001336435	-3.52757	7.36E-05	0.04676
si:dkey-221l4.11 (cldn23l)	XM_001332989	-1.69175	7.49E-05	0.04676
scfd2	NM_001013564	1.49957	7.77E-05	0.04676
sh3gl2	NM_201116	-1.90231	7.77E-05	0.04676
fbp2	NM_001004008	-1.88133	8.00E-05	0.04676
si:zfos-411a11.2	XM_001923562	-4.52699	8.08E-05	0.04676
necab2	NM_001030195	-1.4417	8.28E-05	0.046839
otpa	NM_001128703	1.4099	8.63E-05	0.04774
rab3b	XM_680562	-1.83159	9.05E-05	0.04903
LOC564234	XM_687578	1.44315	9.48E-05	0.049742
ptk7a	ENSDART000000 98461	1.60355	9.72E-05	0.049742

efhc1	NM_200967	1.69842	9.95E-05	0.049742
grk7a	NM_001031841	-4.72498	9.97E-05	0.049742
asic4a	NM_214787	-1.42501	1.08E-04	0.049781
LOC100537764	XR_222889	-1.22945	1.08E-04	0.049781
ttr	NM_001005598	-4.76461	1.09E-04	0.049781
spag1a	NM_001089406	-1.40906	1.12E-04	0.049781
nr6a1a	NM_131256	1.77577	1.13E-04	0.049781
gabra6a	NM_200731	-3.18194	1.14E-04	0.049781
nr1h4	NM_001002574	-1.44093	1.20E-04	0.049781
irbp	NM_131451	-5.48152	1.20E-04	0.049781
vmo1a	XM_001332044	1.13896	1.21E-04	0.049781
rgra	NM_001017877	-2.13478	1.24E-04	0.049781
scg3	NM_200757	-1.47592	1.28E-04	0.049781
grk1b	NM_001017711	-8.11259	1.29E-04	0.049781
lmx1bb	NM_001025167	1.33289	1.32E-04	0.049781
plppr3b	XM_005155961	-1.92465	1.33E-04	0.049781
si:ch211-132f19.7	XM_009293165	-3.0695	1.34E-04	0.049781
her13	NM_001017901	1.96392	1.34E-04	0.049781
gdpd3b	XM_690578	-2.61568	1.36E-04	0.049781
gpx3	NM_001137555	-1.60413	1.39E-04	0.049781
abcb10	XM_001343182	-1.31728	1.39E-04	0.049781
wu:fc66h01 (trabd2a)	NM_001302230	1.60762	1.40E-04	0.049781

fmn2a	XM_001333025	-1.52925	1.41E-04	0.049781

DEGs from all ten samples were hierarchically clustered to visualize the expression profiles of genes in all samples (Figure 5.3). Hierarchical clustering helps to identify a possible functional relation between genes clustered together in a tree. Dendrogram displays four morphant samples clustered together and showing visibly distinct expression patterns from six control samples from the second cluster.

Down-regulated *pcdh17* (in *pcdh17* morphants) was clustered with three genes that are also normally expressed in 72 hpf zebrafish embryos, and include *syngr3a* (synaptogyrin 3a; located on synaptic membrane), *si:ch211-132f19.7* (also located on the cell membrane, involved in signal transduction) and *grapb* (GRB2-related adaptor protein b, possibly functioning in protein phosphorylation). The exact function of *syngr3a* in zebrafish is unknown, but in humans, SYNGR3 ortholog is expressed in different regions of the brain (mainly the cerebral cortex and cerebellum) and in the horizontal cells of the retina (primarily), bipolar cells , rod and cone photoreceptor cells, and is known to interact with SLC6A3 (Thul et al. 2017). In mice, *syngr3* is expressed in retina (Magdaleno et al. 2006; Diez-Roux et al. 2011). The second gene clustered with *pcdh17* was gene *si:ch211-132f19.7*, also with unknown function in zebrafish. Its human ortholog is ADCY8 (adenylate cyclase 8). Gene *si:ch211-132f19.7* is expressed in the murine retina ganglion cell layer (gcl) during development (Visel et al. 2004; Nicol et al. 2006; Kashyap et al. 2014; Manoli and Driever 2014). The third clustered gene was

grapb, and its human ortholog is GRAP which is involved in the autosomal

recessive nonsyndromic deafness (Li et al. 2019).

The most significantly up-regulated gene in the morphants was *dusp27*

(Table 5.2), and it clustered with transcription factors (TF) including *scml2* (sex

comb on midleg-like 2), *foxi1* (forkhead box i1), *lmx1bb* (LIM homeobox

transcription factor 1, beta b), *nkx2.1* (NK2 homeobox 1), *her13* (hairy-related 13)

and *otpa* (orthopedia homeobox a). *Lmx1bb*, *nkx2.1* and *her13* are specifically

expressed in the nervous system, while *otpa* is involved in the visual processing

(Webb et al. 2011; Fernandes et al. 2012; Burzynski et al. 2013; Manoli and

Driever 2014; Wang et al. 2019). Other genes from this cluster included

wu:fc66h01 (also known as *trabd2a*, TraB domain containing 2A; predicted to

negatively regulate Wnt signaling, Zhang et al. 2012), *psmd4b* (proteasome 26S

subunit, non-ATPase 4b, predicted to be involved in proteasome assembly, Liu et

al. 2019) and *fam124b* (family with sequence similarity 124B, possibly involved in

neurodevelopmental disorders, Batsukh et al. 2012).
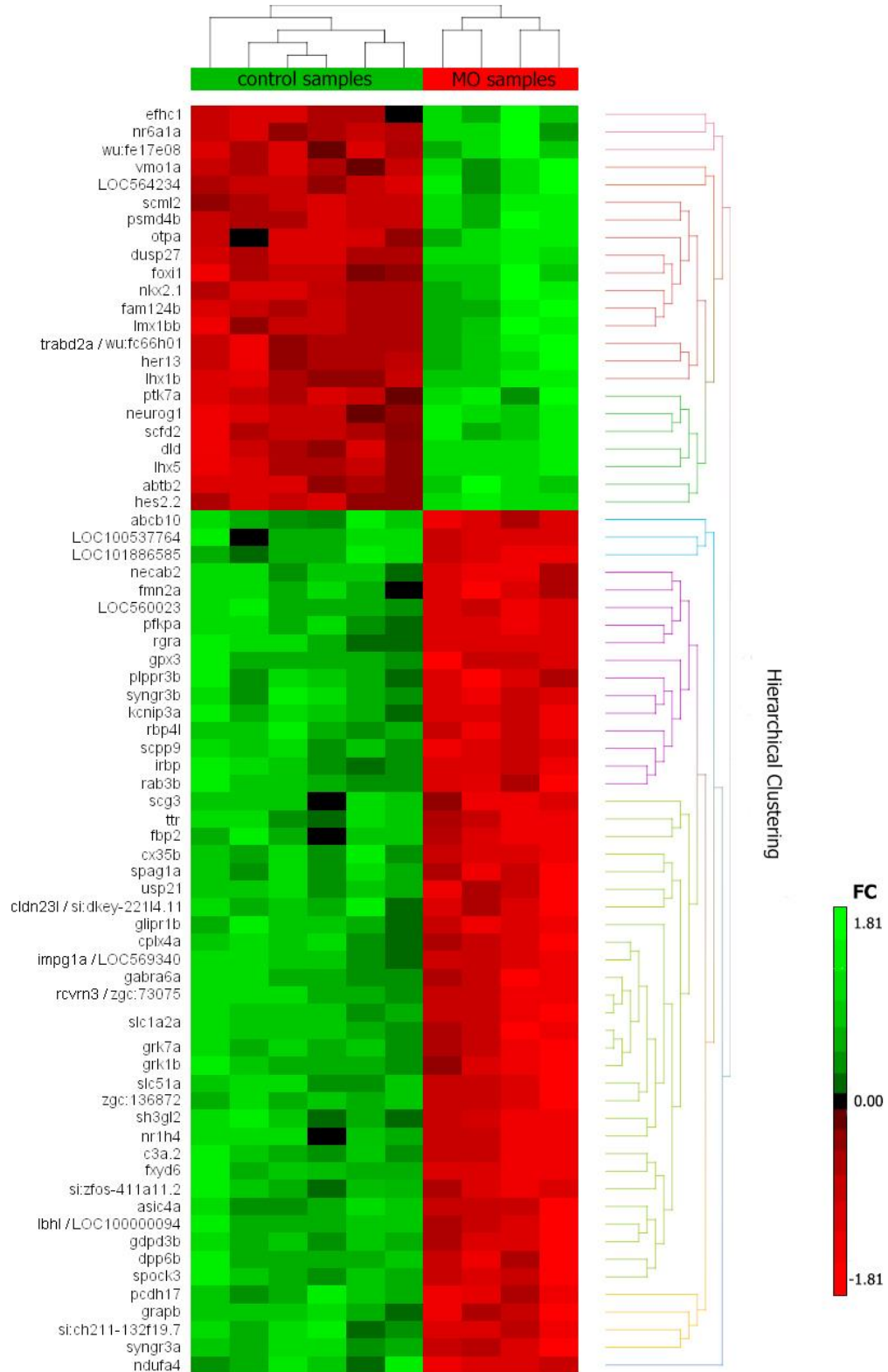
Figure 5.3. Heatmap of DEGs in *pcdh17* MOs representing similar expression patters. Relatively up- (green) and down-regulated (red) genes are hierarchically clustered between zebrafish *pcdh17* morphants (4 microarray samples, right column) and controls (6 microarray samples, left column).

Gene ontology enrichment

Gene ontology (GO) analysis (Partek Genomics Suite) was performed to identify the categories of enrichment for differentially expressed genes in the *pcdh17* morphants. Gene ontology is the systemic mapping of genes according to their functionality, by the use of controlled and specific terms describing gene functions. The Gene Ontology Consortium constructed three extensive non-overlapping and independent ontologies to describe genes (and gene products): "cellular component", "molecular function" and "biological process" (Ashburner et al. 2000; Consortium 2019). These classifications cover information units shared between all the living organisms. The definitions of GO terms and their gene associations are available on http://geneontology.org. In each independent ontology, the GO term describes a specific aspect of gene (or gene product) function and is part of a directed acyclic graph helping to visualize its relationship to the broader GO terms. The most common use of GO analysis is to understand the biological relevance of large amount of data from high-throughput experiments (-omics platforms, e.g. microarray).

Seventy-two DEGs were annotated with 205 GO terms with p-value ≤0.05 (listed in Appendix D, including unique GO IDs) and 46 GO terms with p-value ≤0.01 (listed in Figure 5.4 and Figure 5.5). The "over-represented" genes, occurring more often than by chance from each category were sorted based on their significance (Figure 5.4 and Figure 5.5). Three broad categories of GO help to interpret biological changes and their location in the treatment condition. The "cellular component" GO domain marked in yellow on Figure 5.4 indicates the

changes in *pcdh17* morphants occuring on the cell membrane (e.g., GO terms "transport vesicle membrane", "exocytic/synaptic vesicle membrane") and in the presynapse (e.g., "presnapse" and "synaptic vesicle membrane"). Another GO domain called "biological process" indicated that response to *pcdh17* knockdown was particularly tied to neuron/cell differentiation and CNS development (e.g. "neuron and cell differentiation", "forebrain neuron development") and to vision ("cone photoresponse recovery", "response to light stimulus"). From the molecular perspective ("molecular process" GO domain), changes resulting from the *pcdh17* knockdown were especially tied to kinases activity ("rhodopsin kinase activity", "G protein-coupled receptor kinase activity"), and the activity of transcription factors ("DNA-binding transcription factor activity", "RNA polymerase II transcription regulatory region", "regulatory region nucleic acid binding").

Enriched GO terms in *pcdh17* morphants dominate processes related to the central nervous system development and functioning of the visual system, including the activity of the transcription factors (Figure 5.4). GO term "neuron differentiation" was the most enriched (significant, based on adjusted p-value) in *pcdh17* morphants, and included six up-regulated genes (*lhx1*, *lhx5*, *dld*, *neurog1*, *otpa* and *lmx1bb*) and one down-regulated *pcdh17* gene (Figure 5.5). Other top significant GO terms related to vision include "cone photoresponse recovery", "rhodopsin kinase activity" and "G protein-coupled receptor kinase activity", and were annotated to two (down-regulated in the morphants) opsin genes (*grk7a* and *grk1b*). Transcription factor genes (under four significantly enriched GO terms) comprised of "DNA-binding transcription factor activity, RNA

184

polymerase II-specific", "DNA-binding transcription factor activity" and "transcription regulator activity", and included mostly up-regulated genes (*lhx5*, *hes2.2*, *nkx2.1*, *neurog1*, *lhx1b*, *foxi1*, *otpa*, *nr6a1a*, *lmx1bb* and *her13*), while only one gene was down-regulated (*nr1h4*).
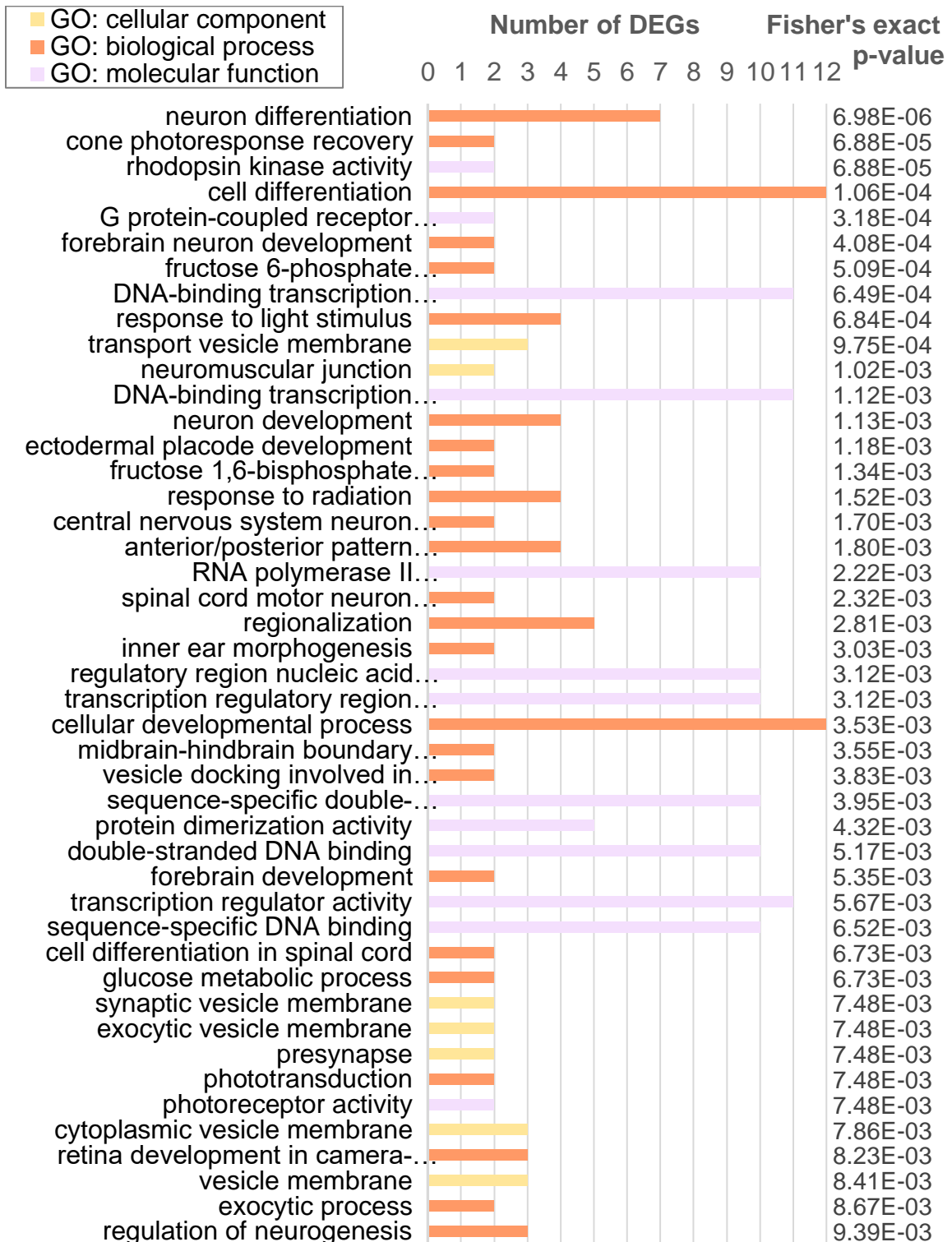
Figure 5.4. Significant GO terms mapped to DEGs in *pcdh17* MOs. Three separate ontologies (main GO domains) are labeled in orange (biological process), purple (molecular function) and yellow (cellular component) on a barplot. X-axis lists the number of DEGs, y-axis lists each GO term and its significance.
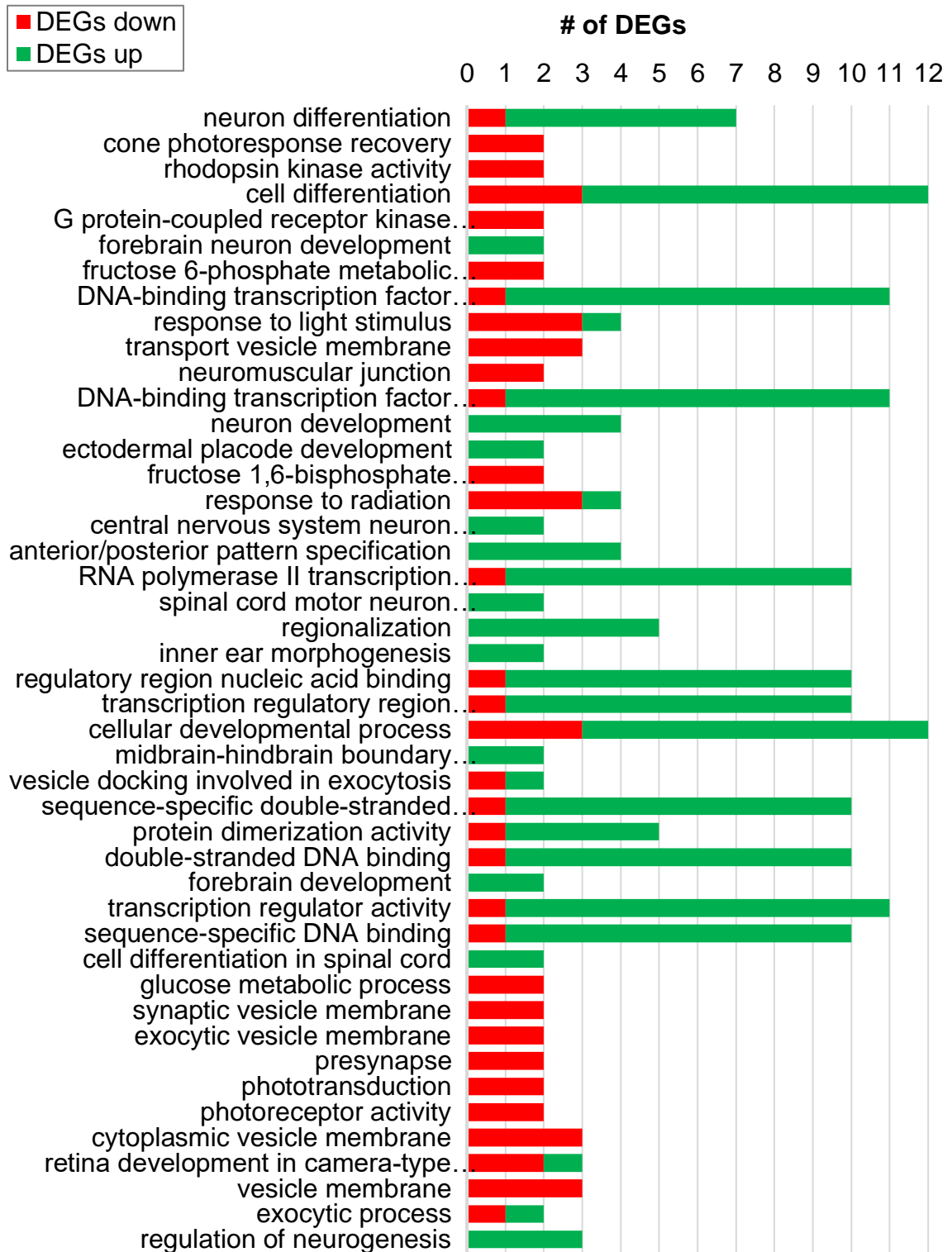
Figure 5.5. Gene changes within enriched GO terms in *pcdh17* MOs. GO terms are sorted by their significance. Down-regulated genes in the morphants are labeled in red and up-regulated genes are labeled in green.

KEGG pathway enrichment

The KEGG (Kyoto Encyclopedia of Genes and Genomes) database

includes known molecular pathways. The pathways that contain differentially

expressed genes are shown below as KEGG pathway enrichment analysis.

Pcdh17 morphants had three overrepresented pathways with adjusted p-value ≤

0.01 (Table 5.3). Two carbohydrate metabolism pathways (pentose phosphate

and fructose mannose metabolism) include both shared and similarly down-

regulated *pfkpa* (-1.87 log2 FC) and *fbp2* (-1.88 log2 FC) DEGs (Figure 5.6 and

Figure 5.7). The third most significantly enriched pathway was the

phototransduction pathway including two down-regulated DEGs (*grk1b* and

grk7a) in the morphants (Figure 5.8). In light conditions, kinases *grk1b* (-8.11

log2 FC) and *grk7a* (-4.72 log2 FC) require G protein to phosphorylate the opsin

in cones (Rinner et al. 2005; Wada et al. 2006).

Table 5.3. Significant KEGG pathways in *pcdh17*MOs. The list includes the
overrepresented patways with p-value ≤0.01.

KEGG Pathway Name	KEGG ID	Fisher's exact p-value	DEG #	DEG % in pathway
Pentose phosphate pathway	dre00030	0.002829	2	6
Fructose and mannose metabolism	dre00051	0.00418381	2	5
Phototransduction	dre04744	0.00439765	2	5
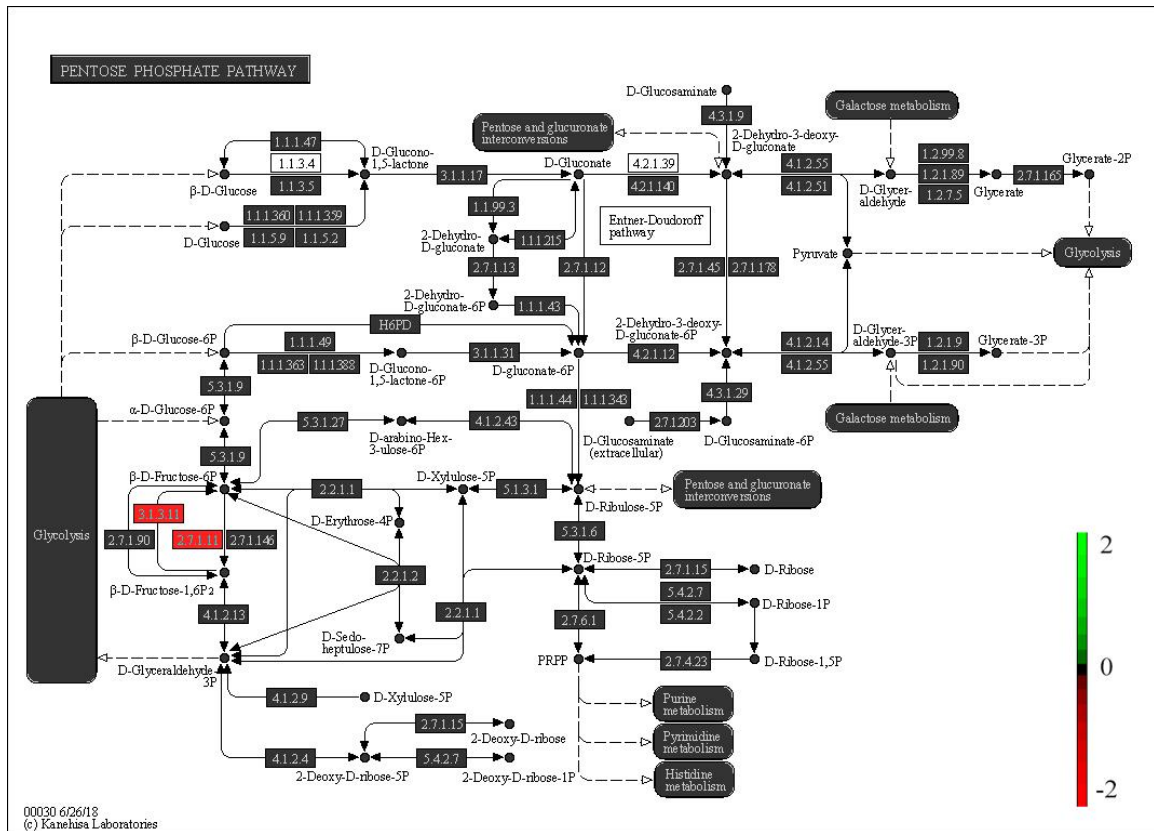
Figure 5.6. Pentose phosphate pathway in *pcdh17*MOs. DEGs that are down-regulated are *fbp2* (3.1.3.11) and *pfkpa* (2.7.1.11). Colored scale shows log2 fold changes: green for up-regulation and red for down-regulation in the morphants.
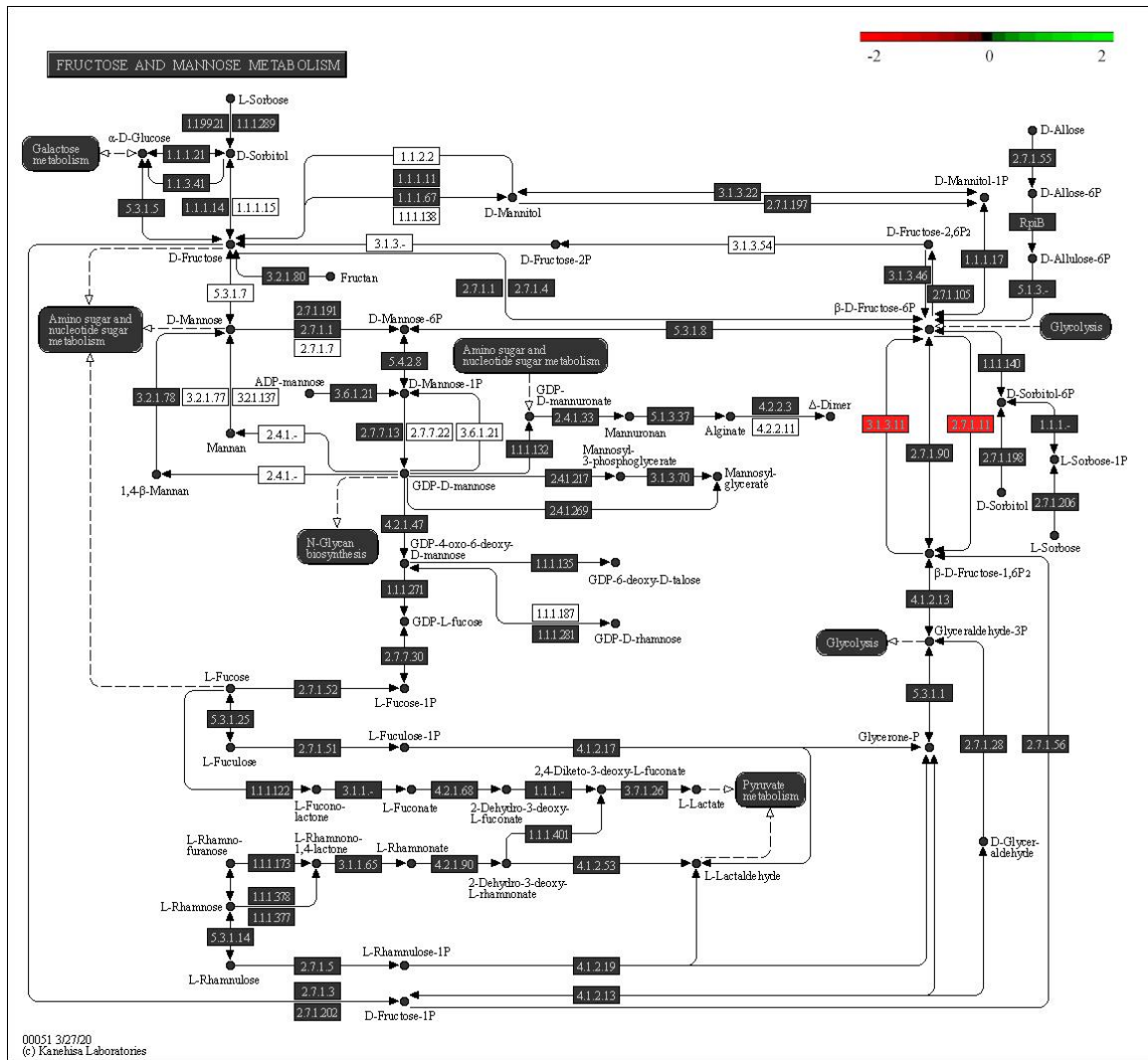
Figure 5.7. Fructose and mannose metabolism pathway in *pcdh17* MOs. DEGs that are down-regulated are *fbp2* (3.1.3.11) and *pfkpa* (2.7.1.11). Colored scale shows log2 fold changes: green for up-regulation and red for down-regulation in the morphants.
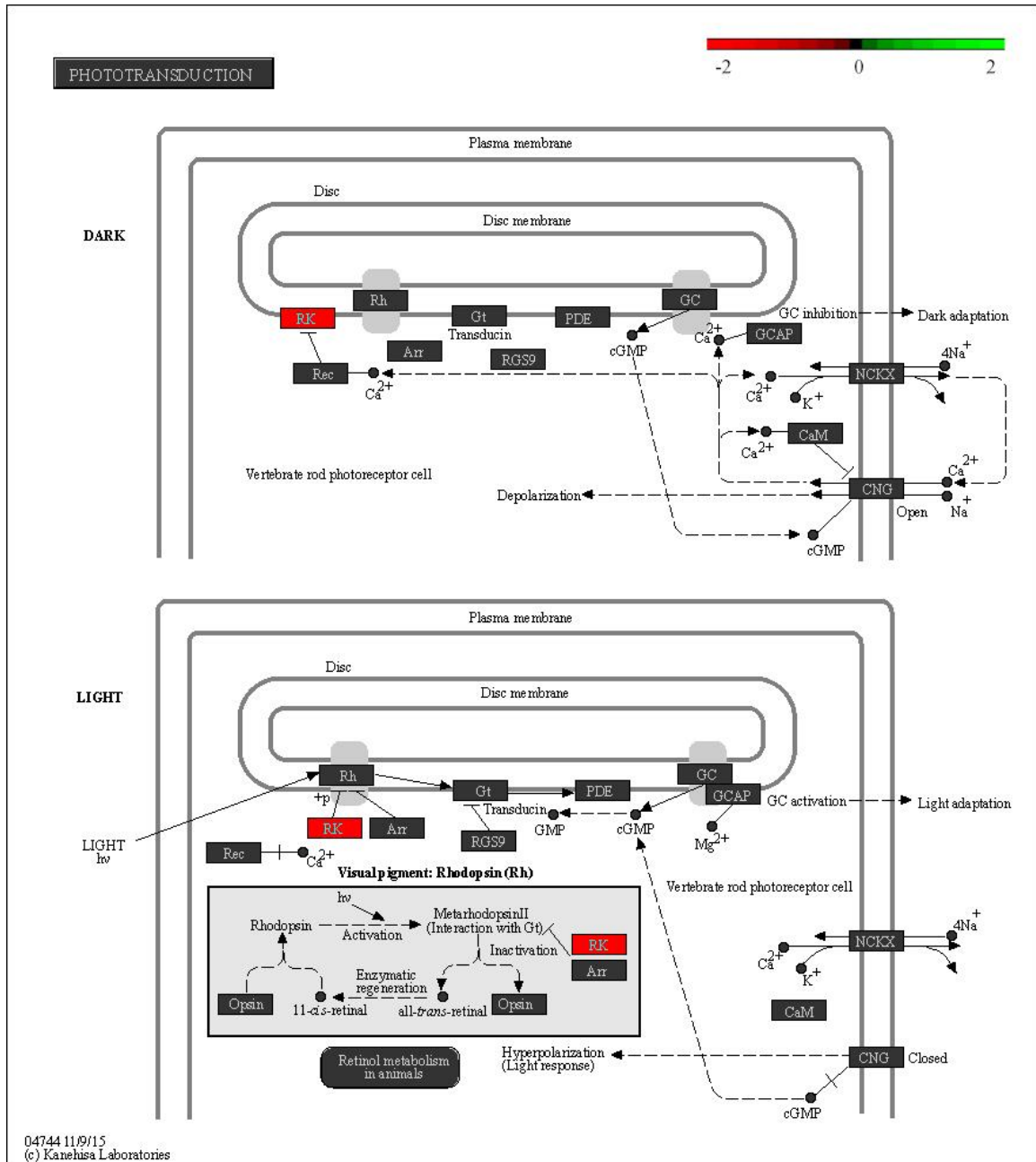
Figure 5.8. Phototransduction pathway in *pcdh17* MOs. DEGs that are down-regulated are opsin kinases: *grk1b* and *grk7a* (RK), both expressed in cone photoreceptors in zebrafish. Colored scale shows log2 fold changes: green for up-regulation and red for down-regulation in the morphants.

191

qPCR verification of the microarray results

The microarray results were verified using quantitative PCR (qPCR). Relative mRNA levels were measured by the comparative method (Livak and Schmittgen 2001) for 8 genes (Figure 5.9 and Figure 5.10). Several genes with high fold changes from the microarray analysis and/or genes with functions related to the visual system were chosen: *opn1sw2*, *grk1b* and *grk7a* (important in phototransduction), *prph2a* (important in visual perception and retinal degeneration), *rbp4l* (involved in retinal development), *cdhr1a* and *pcdh17* (significantly changed cadherin superfamily genes) and finally, *hbbe3* (responsible for heme and oxygen binding in the embryo, a highly up-regulated gene). The qPCR amplification efficiency for each gene was in the target range of 90-110% and is listed here: 101% efficiency for *rpl13a*, 99% for *prph2a*, 98% for *hbbe3*, 98% for *grk1b*, 97% for *pcdh17*, 96% for *cdh1a*, 92% for *opn1sw2*, 91% for *grk7a* and 90% for *rbp4l*.

In order to calculate concordance in the gene expression changes between the microarray and qPCR data, the Pearson correlation coefficient was calculated, resulting in r = 0.850167694 which was converted to a t-statistic, further used to calculate a p-value p = 0.00749257. The result indicates strong correlation in pairs between two methods and therefore the high reliability and accuracy of microarray.
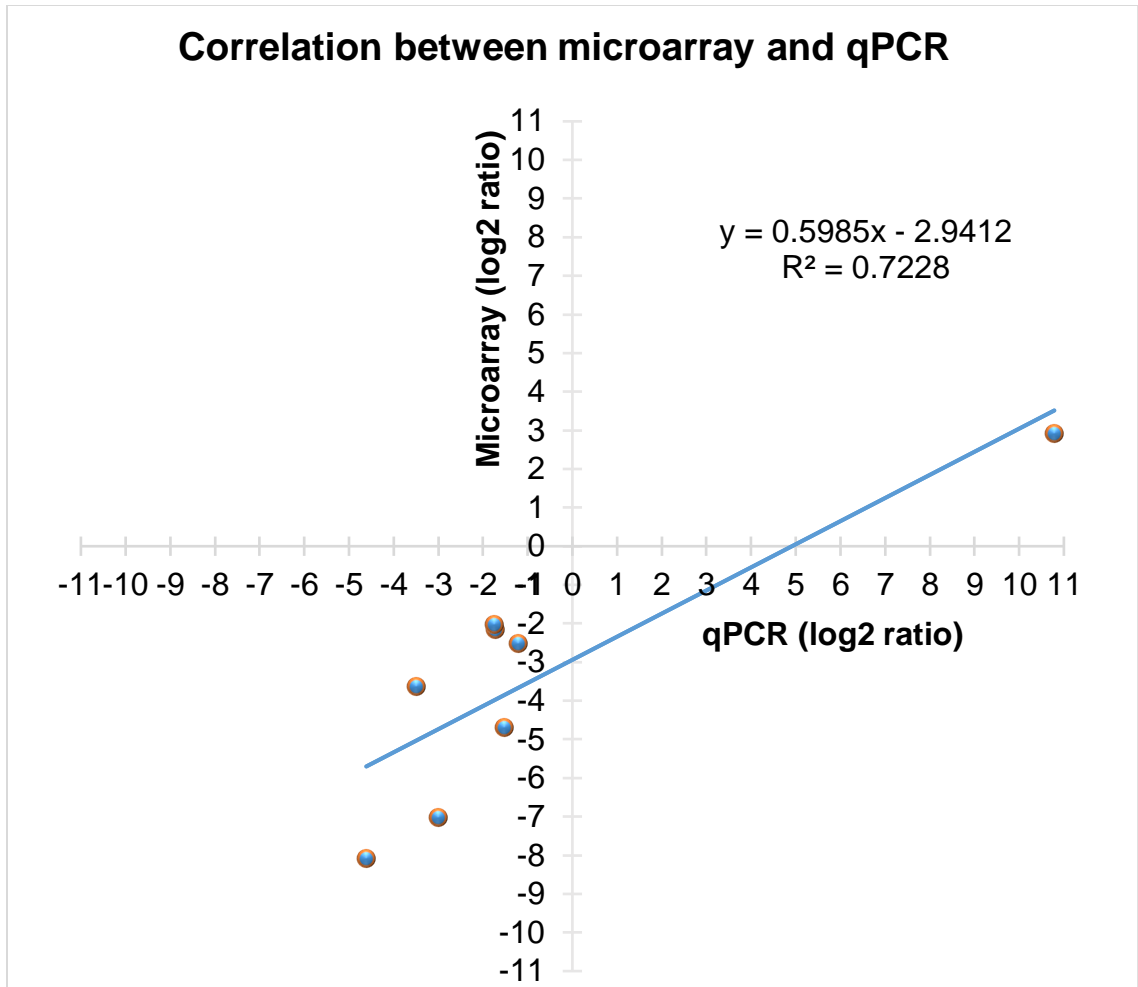
Figure 5.9. Correlation between microarray and qPCR. Fold change (log2 transformed) between microarray (x-axis) and qPCR (y-axis) for eight genes. Coefficient of determination R^2 indicates the calculated model is strong. Pearson p-value = 0.00749257.

The fold changes of genes tested by both microarray and qPCR are depicted on Figure 5.10. Expression changes for all genes matched the direction of changes between qPCR and microarray. The degree of changes for most genes (e.g. *opn1sw2*) matched well between the microarray and qPCR data, while only one (*hbbe3*) exhibited several folds of difference, but all had the same directional changes (Figure 5.10).
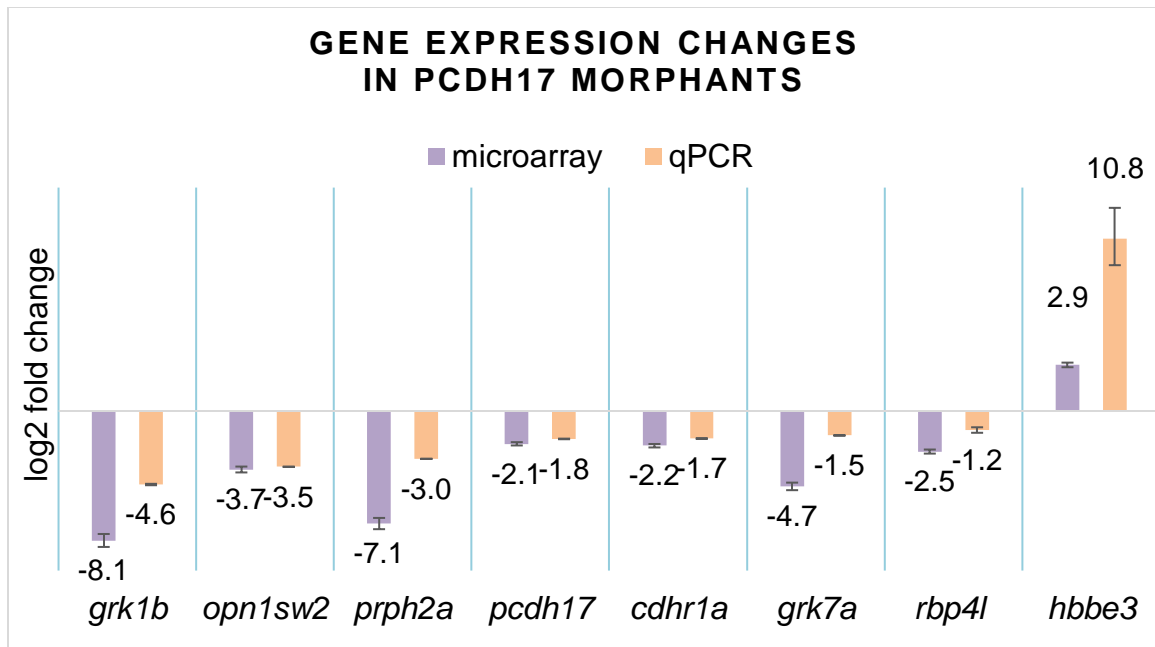
Figure 5.10. Gene expression fold changes between *pcdh17* MO and control embryos. Barplot depicts the log2 fold changes from microarray and qPCR (y-axis) for each selected gene (x-axis). qPCR confirms results from microarray, as the direction of gene expression between both is the same, while the magnitude of change is also very similar. Most of the genes above are down-regulated. Error bars show standard deviation. Paired T-test p-value=0.02651569.

RNA *in situ* hybridization verification of the microarray results

In order to provide spatial and morphological context and to further validate the microarray data of the *pcdh17* morphants and control embryos, expression of five genes, *gnat1*, *gnat2*, *irbp*, *rho* and *uvo* (*opn1sw1*) was visualized using whole-mount RNA *in situ* hybridization (WISH). The patterns of expression for all five genes examined by WISH matched well with the results of the microarray. These genes were chosen because they are highly expressed by developing zebrafish photoreceptors (Raymond et al. 1995; Stenkamp et al. 1998; Brockerhoff et al. 2003). Although both the control and morphant embryos had similar size and shape in their heads and bodies (Figure 5.11), expression of

these five genes (based mainly on the staining intensity and/or expression domain size) was different.
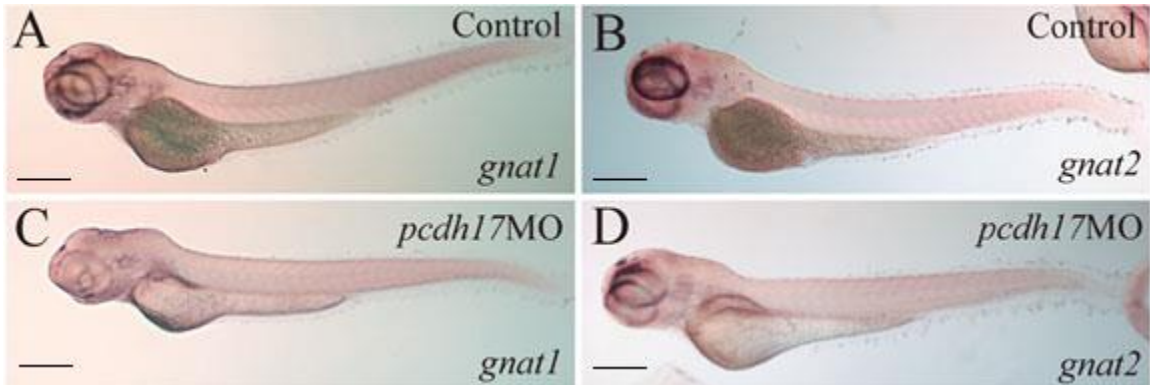
Figure 5.11. The effects of blocking *pcdh17* on zebrafish development using *in situ* hybridization. All panels are lateral views with anterior to the left and dorsal up of 72 hpf embryos. *Pcdh17* morphants and control embryos appear similar in size and shape. Scale bar = 250 μm.

Expression of *irbp*, *gnat1* and *gnat2* was prominently reduced in the morphants (Figure 5.12 detected by ISH; log2 FCs in microarray were -5.5, -3.9 and -3.3, respectively). The expression of *uvo* and *rho* was moderately reduced in morphants, shown on Figure 5.13 detected by ISH; log2 FCs in microarray were -2.7 and -2.4, respectively. Larger changes of gene expression in *pcdh17* morphants of *gnat1* were observed only in the ventral portion of the retina in the photoreceptor layer and the outer portion of the inl. *Gnat2* and *irbp* mRNA expression in the morphants became restricted mainly to a small patch on the ventral portion of the retina (Figure 5.12). Moderate reduction in *rho* and *uvo* expression was observed in the *pcdh17* morphants (Figure 5.13), where the reduction of the signals was mainly restricted to the posterior half of the retina.
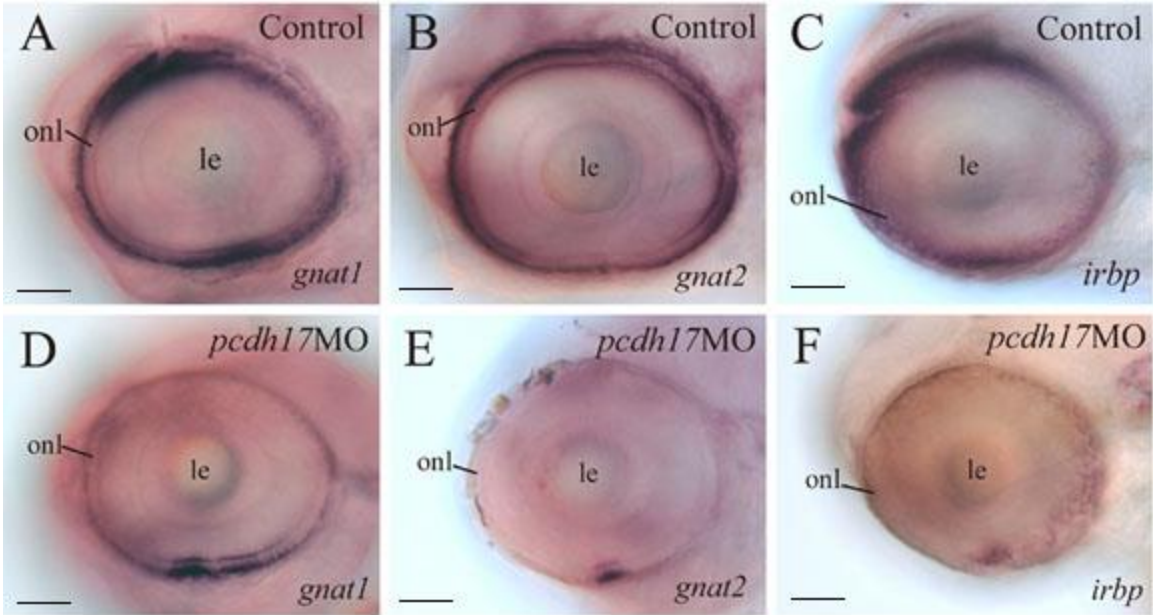
Figure 5.12. Expression of *gnat1*, *gnat2* and *irbp* in *pcdh17*MOs is greatly decreased. Each panel represents lateral view on whole-mount eye from 72 hpf embryos, anterior to the left and dorsal up. The morphant eyes (panels D, E and F) show much reduced gene expression compared to the control eyes (panels A, B and C). Scale bar = 50 μm. Abbreviations: lens (le) and outer nuclear layer (onl), hours post fertilization (hpf).
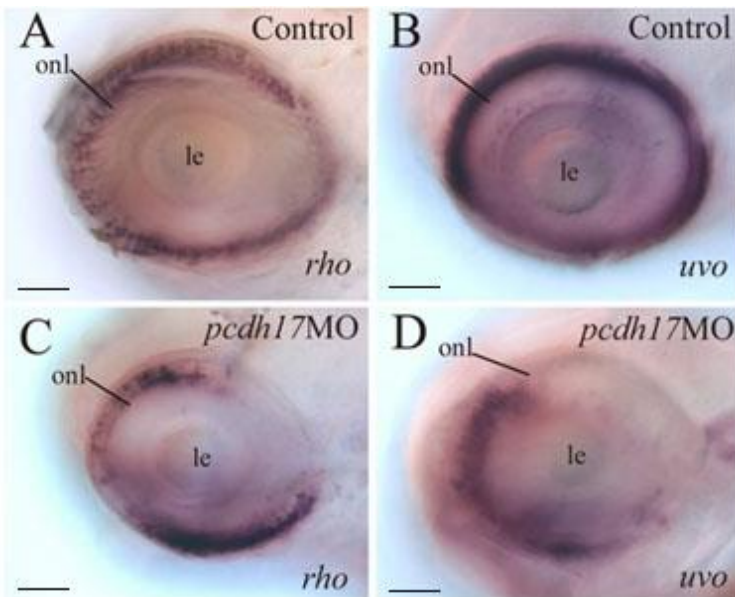
Figure 5.13. Expression of *rho* and *uvo* (*opn1sw1*) in *pcdh17*MOs is moderately decreased. All images illustrate lateral view on whole-mount eyes from 72 hpf embryos, where anterior is to the left and dorsal is up. The morphant eyes (panels C and D) show much moderately reduced gene expression compared to the control eyes (panels A and B). Scale bar = 50 μm.

The pineal gland in teleost fish contains photoreceptors that express similar genes as the photoreceptors in the retina (Robinson et al. 1995; Forsell et al. 2001; Falcon et al. 2003; Liu et al. 2007b). In order to find out if *pcdh17* is involved in development of photoreceptors in the pineal gland, expression of *gnat1* (rod cell-specific), *gnat2* (cone cell-specific) and *irbp* (photoreceptor cell-specific) was tested using *in situ* hybridization (Figure 5.14). The levels of mRNA for those three genes were similar between control and morphant embryos, which was unlike the down-regulation of these genes in the *pcdh17* morphants' eyes. This result suggests that pcdh17 selectively affects photoreceptors development in the retina.
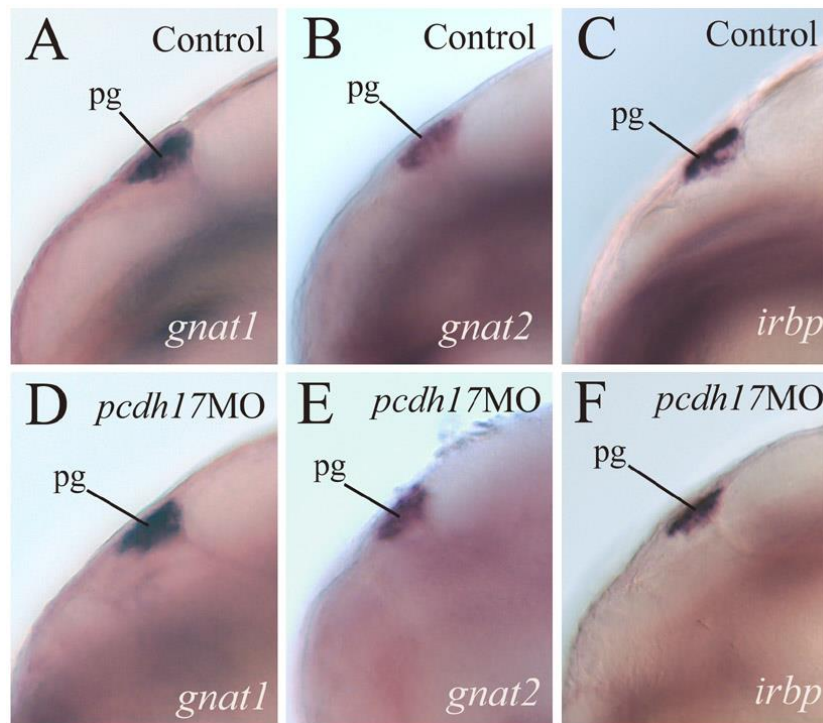
Figure 5.14. Expression of eye-related genes was not affected in the pineal gland of *pcdh17*MOs. Each panel shows lateral views of the anterodorsal region of whole-mount heads with anterior to the left and dorsal up. Abbreviations: pg = pineal gland.

Discussion

The study was the first investigation of transcriptomics in zebrafish with disrupted *protocadherin-17* expression via morpholino oligonucleotide. Zebrafish as a vertebrate model organism is a favorite model for developmental studies, as their maturation occurs rapidly and externally from the mother. The fully sequenced genome and easiness of genetic manipulation contribute to the great advantages of this model organism and its use for gene knockdown and knockout (Varshney et al. 2013, 2015; Holtzman et al. 2016). Pcdh17 is known to have an important function in the eye development (Chen et al. 2013). This study focuses on analyzing the transcriptome using the microarray of the 72 hpf *pcdh17* morphants zebrafish. My research reveals significant changes in the expression of a variety of genes including those involved in eye development and vision in the *pcdh17* morphants, which provides possible mechanisms underlying pcdh17 function in zebrafish eye development. The microarray data was validated with relative qPCR and RNA *in situ* hybridization, demonstrating repeatability and sensitivity of the used assays.

Like RNA sequencing (RNAseq), the oligonucleotide microarray technology used here is a reliable method for the transcriptional profiling between samples, offering measurements of gene relative ratios between sample sets (Dasgupta et al. 2017; Derda et al. 2018; Tuttle et al. 2019; Qian and Zhou 2020). Microarray technology was sufficient to identify the fold changes within the "whole transcriptome" based on most recent danRer7 and Zv9 zebrafish genome assembly, covering expression of 59,302 genes. The advantage of microarray

over RNAseq was a lower cost and more available at the time access to software analysis. The limitation of microarray is its lower dynamic range and predefined set of genes, unlike RNAseq technology which allows detection of alternatively spliced genes. Recent studies identified differential *pcdh17* expression in a variety of samples using these technologies: a microarray study in patients with myocardial infarction (Derda et al. 2018), RNAseq studies in leukemia (Huang et al. 2021), in lung cancer (Sun et al. 2021), in different breeds of pigs muscles (Piorkowska et al. 2018) and in mice hippocampal interneurons (Que et al. 2021). In the developing mouse brain, *pcdh17* is shown to participate in neuronal circuit formation and function, and is down-regulated during the nuclear translocation of the DSCAM/L1 (Sachse et al. 2019). RNAseq of developing zebrafish indicated reduced *pcdh17* expression in claudin-h (*cldnh*) knockdown (Lu et al. 2020).

pcdh17 morpholino knockdown is specific

This study was carefully designed and followed the morpholino validation from the previous published study by Chen et al. (2013), according to the guidelines for the morpholino use in zebrafish (Moulton and Moulton 2017; Stainier et al. 2017; Zimmer et al. 2019). Based on the gross morphology and immunocytochemical studies, zebrafish embryos injected with the splice-blocking morpholino (sMO) resembled those injected with the translation-blocking morpholino (atgMO). Furthermore, embryos injected with the 5-base mismatch sMO were indistinguishable from uninjected embryos. Finally, embryos injected with either the splice-blocking MO or translation-blocking MO show a similar

defect (i.e. small eyes) as those injected with *in vivo*-sMO (into the eye at 25-26 hpf). The effect of the sMO on *pcdh17* mRNA was tested by RT-PCR, showing that *pcdh17* mRNA in the morphants contained a premature stop codon 123 nucleotides downstream of the exon 1 (due to inclusion of part of intron 1, Chen et al. 2013). In addition, terminal UTP nick-end labeling (TUNEL) experiment proved that this *pcdh17*sMO did not cause significantly higher apoptosis in the morphant retina (Chen et al. 2013), a mechanism stipulated to be a non-specific effect of morpholino use (Robu et al. 2007; Gerety and Wilkinson 2011). Taken together, I am confident that the *pcdh17*sMO used in this study is highly specific in reducing pcdh17 function, and the changed gene expression in the *pcdh17* morphants (revealed by the microarray analysis) was likely caused by the selectively reduced *pcdh17* function in the morphants.

This knockdown study provides comprehensive information about *pcdh17* transcriptome. CRISPR-Cas9 knockout of extracellular portion of *pcdh17* in zebrafish has shown axon clumping in the spinal motor neurons (Asakawa and Kawakami 2018). The authors suspected functional redundancy by other protocadherins masking the phenotype of their mutant. There have been many recent published studies (Dasgupta et al. 2017; Niklaus et al. 2017; Richardson et al. 2019; Tuttle et al. 2019; Lu et al. 2020; Harding et al. 2021) in zebrafish using morpholino technique, because gene knockdown allowed to better analyze the functional implications of gene loss over the gene knockout (Bosze et al. 2018, 2020). Moreover, multiple studies confirmed that the morphants phenocopied the mutants's phenotypes and molecular-level changes in at least

50% of animals (Wyatt 2011; Taylor et al. 2015). Genetic compensation

mechanism that is likely to occur during the gene knockout may mask the genetic

changes and phenotype outcomes researchers seek to unveil (Rossi et al. 2015;

El-Brolosy and Stainier 2017; El-Brolosy et al. 2019; Peng 2019). Researchers

often observe more drastic phenotypes with the morpholino use, while the

knockouts have genetic compensation mechanisms that reduce severity, but

perhaps do not uncover all gene functions (Cooper 2017). The genetic

compensation tends to happen between genes belonging to the same family

(such as pcdh subfamily), therefore it is possible that this mechanism applies to

the phenotypes of *pcdhs* knockouts. Several protocadherins are up-regulated in

zebrafish *pcdh10a* knockout, but only pcdh10b is suspected to compensate for

the loss of the gene (Williams 2018).

Interestingly, the majority of the morphants embryos that were allowed to

survive over 72 hpf died (Alicja's personal communication with Dr. Qin Liu). Most

likely, they were not able to find food due to impaired vision; therefore, a

behavioral study needs to be performed in the future to confirm this speculation.

The transcriptional profiles suggest pcdh17 functions in eye development by affecting phototransduction pathway

Cadherins play important roles in vertebrate CNS development including

retinal development (reviewed in Chapter I). It was previously demonstrated by

our laboratory that pcdh17 is important in zebrafish eye development (Chen et al.

2013). However, the molecular mechanism underlying pcdh17 function in the eye

development is not known. This study identified transcriptional profile of zebrafish

with reduced *pcdh17* expression. Some of the genes responding to *pcdh17* knockdown are part of the phototransduction pathway, while others are involved in the development of the photoreceptors and their functions.

The transcriptional profile of 72 hpf zebrafish with *pcdh17* knocked down matched the gross morphological defects, where changes were primarily observed in the eye and the gene expression was mainly down-regulated. The transcript-level response to *pcdh17* knockdown was predominantly within the vision category, described as the enriched KEGG "phototransduction pathway" (Figure 5.8) and the enriched GO: "cone photoresponse recovery", "rhodopsin kinase activity" and "G protein-coupled receptor kinase activity" (Figure 5.4 and Figure 5.5), based on statistically enriched group of significantly down-regulated opsin genes (*grk7a* and *grk1b*). The eye of 72 hpf zebrafish is one of the biggest organs and the reduction of its size in the morphants (Figure 5.11) likely resulted from reduced genes activities from two interfaced pathways: "pentose phosphate pathway" (Figure 5.6; causing lower nucleotide synthesis) and glycolysis (Figure 5.7; "fructose and mannose metabolism pathway").

Pcdh17 morphants had mild morphological defects mainly limited to the eye compared to zebrafish embryos with disrupted classical cadherins expression, such as *cdh2*, *cdh4* and *cdh6* (Lele et al. 2002; Malicki et al. 2003; Masai et al. 2003; Babb et al. 2005; Liu et al. 2008a). Expression of photoreceptor-specific genes in *cdh2* and *cdh4* morphants was studied previously (Liu et al. 2007a). *Cdh2* mutant and morphant embryos display reduced expression of photoreceptor-specific genes as well as disrupted retinal

lamination (Malicki et al. 2003; Masai et al. 2003), while *pcdh17* morphants have reduced expression of photoreceptor-specific genes (not as severe as those in *cdh2* mutants or morphants), but without retinal lamination defect (Chen et al. 2013). In the present study, the reduction of photoreceptor-specific genes in 72 hpf zebrafish *pcdh17* morphants was confirmed using the microarray technique, and further validated using qPCR and whole-mount RNA *in situ* hybridization.

The photoreceptors in zebrafish retina are made of one rod and four cone types (cone-dominant) and their development was affected based on the lower transcript levels in the *pcdh17* morphants. Cone cell-specific genes included opsin genes *opn1sw1* (UV-sensitive, short single cones) and *opn1sw2* (blue-sensitive, long single cones), G protein receptor kinases *grk7a, grk1b* and transducer gene *gnat2*, while the rod cell-specific genes that were down-regulated were *rho* (rod opsin) and *gnat1*. Both *gnat1* and *gnat2* are genes involved in G protein-coupled receptor signaling during the phototransduction. Lastly, expressed in all photoreceptor cells *irbp* (interphotoreceptor retinoid-binding protein gene) plays a role in mediating protein transport through the interphotoreceptor matrix (crucial for retinal cycle) and in the photoreceptor development (Stenkamp et al. 1998). The expression of *gnat1*, *gnat2* and *irbp* is greatly reduced in the eye of *cdh2* mutant *glass onion*, *cdh2* morphants, and *cdh4* morphants (Babb et al. 2005; Liu et al. 2007b). Moreover, expression of *rho* (rod cell opsin) and *opn1sw1* (uvo, uv-opsin) was found to be down-regulated in the *pcdh17* morphant eyes, but not as much reduced as in *cdh2* mutants/morphants (Liu et al. 2007b). The difference in the severity of the retinal

203

defects likely resulted from different expression patterns of these cadherins, with cdh2 strongly expressed in most retinal cells in the early retina, whereas pcdh17 is expressed at lower levels (based on staining intensity) later in development and with more restricted expression domains.

The genes shown to increase expression in the *pcdh17* morphants included several repressory neural fate transcription factor genes, suggesting pcdh17 is necessary in proper retinal development. The stunted retinal cell proliferation was possibly cased by inhibitory effects on Wnt signaling from increase of gene wu:*fc66h01* (*trabd2a,* likely down-regulating Wnt signaling, Zhang et al. 2012) or the transcription factor important in eye development, lhx5 (LIM homeobox 5). The common feature of smaller eye is observed between *lhx5* and *pcdh17* morphants, and lhx5 gain of function in zebrafish inhibits Wnt signaling (Peng and Westerfield 2006). Likely, the reduction in proliferation of the amacrine cells in the *pcdh17* morphants resulted from activation of Notch pathway because their up-regulated genes (*dld*, *otpa*, *neurog1*, *lbhl* and genes from bHLH family) are known to interact. The transmembrane ligand dld binds to receptor Notch and acts upstream of otpa in dopaminergic neuron specification (Mahler et al. 2010; Taylor et al. 2015) and the dopaminergic cells in retina of zebrafish and mammals are the amacrine cells. Notch signaling targets basic helix-loop-helix (bHLH) family, and higher levels of *her13* (orthologous to human HES6; hes family bHLH transcription factor 6) and *hes2.2* (orthologous to human HES2; hes family bHLH transcription factor 2), a transcription repressor, likely reduced genes promoting the eye development. Notch pathway activation is

associated with regulator of otx2-mediated photoreceptors differentiation (Li et al. 2015), *lbhl* (XM_001336435; predicted LBH regulator of Wnt signaling pathway, like) that was down-regulated in the morphants here. *Pcdh17* and *lbhl* morphants share the transcriptional reduction of several photoreceptor-specific genes (*opn1sw1*, *opn1sw2*, *gnat1*, *gnat2*, *irbp*, *rho*, *neuroD* and *crx*) at the same developmental stage, and such reduction is restricted to the retina location (see below) (Chen et al. 2013; Li et al. 2015). Consequently, it is likely *lbhl* was co-regulated with *pcdh17*. What is more, these two morphants maintained normal mRNA expression of several photoreceptor-specific genes (*gnat1*, *gnat2* and *irbp*) in the pineal gland, compared to controls. In fish and amphibians, the pineal gland is a circadian clock regulator and contains the pineal photoreceptor cells, which differentiate earlier than retinal photoreceptors (Ekstrzm and Meissl 1997; Li et al. 2012a). Simiar absence of transcriptional changes in the pineal photoreceptors, in addition to disturbed cone development is seen in *cplx4a* (complexin 4a) morphants (Vaithianathan et al. 2013). *Cplx4a* is a presynaptic protein involved in the neurotransmitter release and was down-reglated in the *pcdh17* morphants.

Two significatly enriched genes from KEGG phototransduction (*grk1b* and *grk7a*) could be functionally related with *slc1a2a* (solute carrier family 1 glial high affinity glutamate transporter, member 2b), based on the their similar gene transcription patterns from the unbiased method of the hierarchical clustering. *Slc1a2a* was the highest down-regulated gene (Table 5.2) in the *pcdh17* morphants. This gene was previously named *EAAT2b* and is expressed in

developing zebrafish in the onl, opl, onl and inl, and functions as a glutamate transporter in the nervous system (Niklaus et al. 2017; Breuer et al. 2019). It is possible that pcdh17 is co-expressed with syngr3a, judging by their similar expression levels from the hierarchical clustering. While function of *syngr3a* is unknown in zebrafish, human ortholog SYNGR3 interacts with SLC6A3 (Thul et al. 2017), also from the solute carrier family as glutamate transporter *slc1a2a.* Previous studies in 5 dpf zebrafish indicated that *slc1a2a* morphants (Niklaus et al. 2017) has the reduced opl, a layer that connects photoreceptors with other cells in the retina. Therefore, it is probable that those orthologs interact in zebrafish.

The majority of *pcdh17*-regulated gene transcripts were down-regulated (Figure 5.2) and appeared to be vision-related, while up-regulated transcripts were repressory transcription factors, confirming the null hypothesis that *pcdh17* knockdown slowed the eye development and/or reduced its functionality. It is likely that a consequence of *pcdh17* knockdown reflects a direct role for pcdh17 in the differentiation of retinal cells (especially photoreceptors), but not the pineal gland photorecptors. It is possible that there was an indirect consequence of interfering with synaptic transmission. The results may help future functional studies in elucidating molecular mechanism of *pcdh17* function in eye formation, because the genes from the affected pathways are valid candidates for the future hypothesis testing as the possible down-stream genes in a signaling mechanism. Additionally, genes with similar clustering patterns to *pcdh17* are good

candidates for the gene function prediction, as many DEGs have unknown or only predicted function in the databases.

Integrated Bioscience

During the recent few decades, biology has relied more on computer science for the storage and annotation of huge databases in genomics, transcriptomics, proteomics and metabolomics (Lucitt et al. 2008; Consortium 2011, 2019; Vesterlund et al. 2011; Palmblad et al. 2013; Robinson et al. 2014; Wu and Kim 2016). Moreover, the computer science is crucial in the implementation of algorithms that allow the mining, analysis and interpretation of biological data and significance. Microarray and RNA sequencing (RNAseq) are techniques used in transcriptomics and produce vast amount of data. The large amount of data obtained from such techniques needs to be pre-processed (e.g. normalized), undergo quality controls and statistical analysis. The goal is to use this data to indicate the genes and pathways that are differentially changed between the experimental conditions (Tarca et al. 2006; Slonim and Yanai 2009; Robinson et al. 2014). The results are often further validated by other methods (e.g., microarray with qPCR), and compared with the available knowledge, and/or used to form new hypotheses, which could be further tested *in vivo*, *in vitro* or *in silico*. Merging the sub-disciplines of science that rely on the knowledge of computational methods and biology, require specialists who are able to interpret the information and determine if it has a biological relevance. Combining the knowledge and background of two or more fields is the general premise of the

Integrated Bioscience, with the goal of communicating ideas and solving scientific questions effectively, and discovering areas that blend these fields to ensure better learning about the living systems and/or organisms.

My research integrates biology with the computational biology. From the biology standpoint, the research involved answering questions on molecular mechansims of gene function by examination and comparison of gene expression between control zebrafish embryos and embryos with reduced *pcdh17* function. In the class "Computational Biology", I learned to understand several methods of computer science for analysis of microarrays and the process of using algorithms to select the relevant data. I was able to learn sufficient bioinformatics to allow me to analyze, summarize and interprete the microarray data, which would not have been possible if I had not being trained as an integrated biologist.

REFERENCES

Abrahams, B. S., D. Tentler, J. V. Perederiy, M. C. Oldham, G. Coppola and D. H. Geschwind (2007). Genome-wide analyses of human perisylvian cerebral cortical patterning. *Proceedings of the National Academy of Sciences* 104:17849–17854

Agathocleous, M. and W. A. Harris (2009). From progenitors to differentiated cells in the vertebrate retina. *Annual Review of Cell and Developmental Biology* 25:45–69

Aguayo, A. J. (1985). Axonal regeneration from injured neurons in the adult mammalian central nervous system. Pages 457–484. Interventive Strategies for Central Nervous System Repair. Guilford New York

Aguayo, A., M. Rasminsky, G. Bray, S. Carbonetto, L. McKerracher, M. Villegas-Perez, M. Vidal-Sanz and D. Carter (1991). Degenerative and regenerative responses of injured neurons in the central nervous system of adult mammals. *Philosophical Transactions of the Royal Society of London: Biological Sciences* 331:337–343

Akins, M. R., D. L. Benson and C. A. Greer (2007). Cadherin expression in the developing mouse olfactory system. *Journal of Comparative Neurology* 501:483–497

Alagramam, K. N., H. Yuan, M. H. Kuehn, C. L. Murcia, S. Wayne, C. S. Srisailpathy, R. B. Lowry, R. Knaus, L. Van Laer, F. Bernier, S. Schwartz, C. Lee, C. Morton, R. Mullins, A. Ramesh, G. Van Camo, G. Hagemen, R. Woychik and R. Smith (2001). Mutations in the novel protocadherin PCDH15 cause Usher syndrome type 1F. *Human Molecular Genetics* 10:1709–1718

Allcutt, D., M. Berry and J. Sievers (1984). A quantitative comparison of the reactions of retinal ganglion cells to optic nerve crush in neonatal and adult mice. *Developmental Brain Research* 16:219–230

Alunni, A. and L. Bally-Cuif (2016). A comparative view of regenerative neurogenesis in vertebrates. *Development* 143:741–753

Alvarez, Y., M. L. Cederlund, D. C. Cottell, B. R. Bill, S. C. Ekker, J. Torres-Vazquez, B. M. Weinstein, D. R. Hyde, T. S. Vihtelic and B. N. Kennedy (2007). Genetic determinants of hyaloid and retinal vasculature in zebrafish. *BMC Developmental Biology* 7:1–17

Amores, A., A. Force, Y.-L. Yan, L. Joly, C. Amemiya, A. Fritz, R. K. Ho, J. Langeland, V. Prince, Y.-L. Wang, M. Westerfield, M. Ekker and J. Postlethwait (1998). Zebrafish hox clusters and vertebrate genome evolution. *Science* 282:1711–1714

Anderson, K. V. and P. W. Ingham (2003). The transformation of the model organism: a decade of developmental genetics. *Nature Genetics* 33:285–293

Antin, P. B., M. Pier, T. Sesepasara, T. A. Yatskievych and D. K. Darnell (2010). Embryonic expression of the chicken krüppel-like (KLF) transcription factor gene family. *Developmental Dynamics* 239:1879–1887

Aoki, E., R. Kimura, S. Suzuki and S. Hirano (2003). Distribution of OL-protocadherin protein in correlation with specific neural compartments and local circuits in the postnatal mouse brain. *Neuroscience* 117:593–614

Arenzana, F., M. J. Carvan III, J. Aijon, R. Sanchez-Gonzalez, R. Arevalo and A. Porteros (2006). Teratogenic effects of ethanol exposure on zebrafish visual system development. *Neurotoxicology and Teratology* 28:342–348

Arndt, K., S. Nakagawa, M. Takeichi and C. Redies (1998). Cadherin-defined segments and parasagittal cell ribbons in the developing chicken cerebellum. *Molecular and Cellular Neuroscience* 10:211–228

Asakawa, K. and K. Kawakami (2018). Protocadherin-mediated cell repulsion controls the central topography and efferent projections of the abducens nucleus. *Cell Reports* 24:1562–1572

Ashburner, M., C. A. Ball, J. A. Blake, D. Botstein, H. Butler, J. M. Cherry, A. P. Davis, K. Dolinski, S. S. Dwight, J. T. Eppig, M. Harris, P. I.-T. L. Hill, A. Kasarskis, S. Lewis, J. Matese, J. Richardson, M. Rinwald, G. Rubin and G. Sherlock (2000). Gene Ontology: tool for the unification of biology. *Nature Genetics* 25:25

Babb, S. G., J. Barnett, A. L. Doedens, N. Cobb, Q. Liu, B. C. Sorkin, P. C. Yelick, P. A. Raymond and J. A. Marrs (2001). Zebrafish E-cadherin: Expression during early embryogenesis and regulation during brain development. *Developmental Dynamics* 221:231–237

Babb, S. G., S. M. Kotradi, B. Shah, C. Chiappini-Williamson, L. N. Bell, G. Schmeiser, E. Chen, Q. Liu and J. A. Marrs (2005). Zebrafish R-cadherin

(Cdh4) controls visual system development and differentiation. *Developmental Dynamics* 233:930–945

Babb, S. G. and J. A. Marrs (2004). E-cadherin regulates cell movements and tissue formation in early zebrafish embryos. *Developmental Dynamics* 230:263–277

Babb-Clendenon, S., Y. Shen, Q. Liu, K. E. Turner, M. S. Mills, G. W. Cook, C. A. Miller, V. H. Gattone, K. F. Barald and J. A. Marrs (2006). Cadherin-2 participates in the morphogenesis of the zebrafish inner ear. *Journal of Cell Science* 119:5169–5177

Baier, H. and M. F. Wullimann (2021). Anatomy and function of retinorecipient arborization fields in zebrafish. *Journal of Comparative Neurology* 529:3454–3476

Bakken, T. E. and C. F. Stevens (2012). Visual system scaling in teleost fish. *Journal of Comparative Neurology* 520:142–153

Bakkers, J. (2011). Zebrafish as a model to study cardiac development and human cardiac disease. *Cardiovascular Research* 91:279–288

Banker, G. and K. Goslin (1998). Culturing Nerve Cells. MIT press

Barnes, S. H., S. R. Price, C. Wentzel and S. C. Guthrie (2010). Cadherin-7 and cadherin-6B differentially regulate the growth, branching and guidance of cranial motor axons. *Development* 137:805–814

Barthel, L. K. and P. A. Raymond (1990). Improved method for obtaining 3-microns cryosections for immunocytochemistry. *Journal of Histochemistry & Cytochemistry* 38:1383–1388

Barthel, L. K. and P. A. Raymond (1993). Subcellular localization of alpha-tubulin and opsin mRNA in the goldfish retina using digoxigenin-labeled cRNA probes detected by alkaline phosphatase and HRP histochemistry. *Journal of Neuroscience Methods* 50:145–152

Bassani, S., A. W. Cwetsch, L. Gerosa, G. M. Serratto, A. Folci, I. F. Hall, M. Mazzanti, L. Cancedda and M. Passafaro (2018). The female epilepsy protein PCDH19 is a new GABAAR-binding partner that regulates GABAergic transmission as well as migration and morphological maturation of hippocampal neurons. *Human Molecular Genetics* 27:1027–1038

Bates, C. A., C. G. Becker, J. A. Miotke and R. L. Meyer (1999). Expression of Polysialylated NCAM but Not L1 or N-Cadherin by Regenerating Adult Mouse

Optic Fibers in Vitro. *Experimental Neurology* 155:128–139

Batsukh, T., Y. Schulz, S. Wolf, T. I. Rabe, T. Oellerich, H. Urlaub, I.-M. Schaefer and S. Pauli (2012). Identification and characterization of FAM124B as a novel component of a CHD7 and CHD8 containing complex. *PloS One* 7:e52640

Becanovic, K., M. A. Pouladi, R. S. Lim, A. Kuhn, P. Pavlidis, R. Luthi-Carter, M. R. Hayden and B. R. Leavitt (2010). Transcriptional changes in Huntington disease identified using genome-wide expression profiling and cross-platform analysis. *Human Molecular Genetics* 19:1438–1452

Becker, C. G. and T. Becker (2007). Growth and pathfinding of regenerating axons in the optic projection of adult fish. *Journal of Neuroscience Research* 85:2793–2799

Becker, T. and C. Redies (2003). Internal structure of the nucleus rotundus revealed by mapping cadherin expression in the embryonic chicken visual system. *Journal of Comparative Neurology* 467:536–548

Beecham, G. W., A. Naj, J. R. Gilbert, J. L. Haines, J. D. Buxbaum and M. A. Pericak-Vance (2010). PCDH11X variation is not associated with late-onset Alzheimer disease susceptibility. *Psychiatric Genetics* 20:321

Benjamini, Y. and Y. Hochberg (1995). Controlling the false discovery rate: a practical and powerful approach to multiple testing. *Journal of the Royal Statistical Society: Series B (Methodological)* 57:289–300

Benowitz, L. I., Z. He and J. L. Goldberg (2017). Reaching the brain: Advances in optic nerve regeneration. *Experimental Neurology* 287:365–373

Bernhardt, R. (1999). Cellular and molecular bases of axonal regeneration in the fish central nervous system. *Experimental Neurology* 157:223–240

Berry, M., L. Rees, S. Hall, P. Yiu and J. Sievers (1988). Optic axons regenerate into sciatic nerve isografts only in the presence of Schwann cells. *Brain Research Bulletin* 20:223–231

Berx, G. and F. Van Roy (2009). Involvement of members of the cadherin superfamily in cancer. *Cold Spring Harbor Perspectives in Biology* 1:a003129

Bhalla, K., Y. Luo, T. Buchan, M. A. Beachem, G. F. Guzauskas, S. Ladd, S. J. Bratcher, R. J. Schroer, J. Balsamo, B. R. DuPont, J. Lilien and A. K. Srivastava (2008). Alterations in CDH15 and KIRREL3 in patients with mild to severe intellectual disability. *The American Journal of Human Genetics* 83:703–713

Bhattarai, S., A. Sochacka-Marlowe, G. Crutchfield, R. Khan, R. Londraville and Q. Liu (2016). Krupple-like factors 7 and 6a mRNA expression in adult zebrafish central nervous system. *Gene Expression Patterns* 21:41–53

Bhumika, S., K. Lemmens, P. Vancamp, L. Moons and V. M. Darras (2015). Decreased thyroid hormone signaling accelerates the reinnervation of the optic tectum following optic nerve crush in adult zebrafish. *Molecular and Cellular Neuroscience* 68:92–102

Bibliowicz, J., R. K. Tittle and J. M. Gross (2011). Towards a better understanding of human eye disease: insights from the zebrafish, Danio rerio. *Progress in Molecular Biology and Translational Science* 100:287

Bieker, J. J. (2001). Kruppel-like factors: three fingers in many pies. *Journal of Biological Chemistry* 276:34355–34358

Bilotta, J. and S. Saszik (2001). The zebrafish as a model visual system. *International Journal of Developmental Neuroscience* 19:621–629

Biswas, S. (2012). Role of Protocadherins in Zebrafish Neural Development. The Ohio State University, OH

Biswas, S., M. R. Emond, P. Q. Duy, L. T. Hao, C. E. Beattie and J. D. Jontes (2014). Protocadherin-18b interacts with Nap1 to control motor axon growth and arborization in zebrafish. *Molecular Biology of the Cell* 25:633–642

Biswas, S., M. R. Emond and J. D. Jontes (2010). Protocadherin-19 and N-cadherin interact to control cell movements during anterior neurulation. *The Journal of Cell Biology* 191:1029–1041

Biswas, S., M. R. Emond and J. D. Jontes (2012). The clustered protocadherins Pcdhα and Pcdhγ form a heteromeric complex in zebrafish. *Neuroscience* 219:280–9

Biswas, S. and J. D. Jontes (2009). Cloning and characterization of zebrafish protocadherin-17. *Development Genes and Evolution* 219:265–271

Bitzur, S., Z. Kam and B. Geiger (1994). Structure and Distribution of N-Cadherin in Developing Embryos: Morphogenetic Effects of Ectopic Over-Expression. *Developmental Dynamics* 201:121–136

Blackmore, M. G., Z. Wang, J. K. Lerch, D. Motti, Y. P. Zhang, C. B. Shields, J. K. Lee, J. L. Goldberg, V. P. Lemmon and J. L. Bixby (2012). Krüppel-like Factor 7 engineered for transcriptional activation promotes axon regeneration in the adult corticospinal tract. *Proceedings of the National Academy of*

Sciences 109:7517–7522

Blackmore, M. and P. C. Letourneau (2006). L1, beta1 integrin, and cadherins mediate axonal regeneration in the embryonic spinal cord. *Journal of Neurobiology* 66:1564–1583

Blanco, P., C. A. Sargent, C. A. Boucher, M. Mitchell and N. A. Affara (2000). Conservation of PCDHX in mammals; expression of human X/Y genes predominantly in brain. *Mammalian Genome* 11:906–914

Blanco-Arias, P., C. Sargent and N. Affara (2004). A comparative analysis of the pig, mouse, and human PCDHX genes. *Mammalian Genome* 15:296–306

Blank, M., G. B. Triana-Baltzer, C. S. Richards and D. K. Berg (2004). Alpha-protocadherins are presynaptic and axonal in nicotinic pathways. *Molecular and Cellular Neuroscience* 26:530–543

Blaschuk, O. W., R. Sullivan, S. David and Y. Pouliot (1990). Identification of a cadherin cell adhesion recognition sequence. *Developmental Biology* 139:227–9

Blevins, C., M. Emond, S. Biswas and J. Jontes (2011). Differential expression, alternative splicing, and adhesive properties of the zebrafish delta1-protocadherins. *Neuroscience* 199:523–534

Boggon, T. J., J. Murray, S. Chappuis-Flament, E. Wong, B. M. Gumbiner and L. Shapiro (2002). C-cadherin ectodomain structure and implications for cell adhesion mechanisms. *Science* 296:1308–13

Bollaerts, I., E. Geeraerts, B. Davis, A. Beckers, I. Van Hove, K. Lemmens, L. De Groef and L. Moons (2017). Successful optic nerve regeneration in the senescent zebrafish despite age-related decline of cell intrinsic and extrinsic response processes. *Neurobiology of Aging* 60:1–10

Børglum, A., D. Demontis, J. Grove, J. Pallesen, M. V. Hollegaard, C. Pedersen, A. Hedemand, M. Mattheisen, A. Uitterlinden, M. Nyegaard, T. Ørntoft, M. Wiuf, M. Didriksen, M. Nordentoft, M. Nothen, M. Rietschel, R. Ophoff, S. Cichon, R. Yolken, D. Hougaard, P. Mortensen and O. Mors (2014). Genome-wide study of association and interaction with maternal cytomegalovirus infection suggests new schizophrenia loci. *Molecular Psychiatry* 19:325–333

Bormann, P., V. M. Zumsteg, L. W. A. Roth and E. Reinhard (1998). Target contact regulates GAP-43 and alpha-tubulin mRNA levels in regenerating retinal ganglion cells. *Journal of Neuroscience Research* 52:405–419

Bosze, B., B. Mattes, C. Sinner, K. Stricker, V. Gourain, T. Thumberger, S. Tlili, S. Weber, J. Wittbrodt, T. E. Saunders, U. Strahle, A. Schug and S. Scholpp (2018). Pcdh18a-positive tip cells instruct notochord formation in zebrafish. *bioRxiv*:257717

Bosze, B., Y. Ono, B. Mattes, C. Sinner, V. Gourain, T. Thumberger, S. Tlili, J. Wittbrodt, T. E. Saunders, U. Strähle, A. Schug and S. Scholpp (2020). Pcdh18a regulates endocytosis of E-cadherin during axial mesoderm development in zebrafish. *Histochemistry and Cell Biology*

Bradley, R. S., A. Espeseth and C. Kintner (1998). NF-protocadherin, a novel member of the cadherin superfamily, is required for Xenopus ectodermal differentiation. *Current Biology* 8:325–334

Brasch, J., O. J. Harrison, B. Honig and L. Shapiro (2012). Thinking outside the cell: How cadherins drive adhesion. *Trends in Cell Biology* 22:299–310

Brayshaw, L. L. and S. R. Price (2016). Cadherins in Neural Development. Pages 315–340. *in* Suzuki, ST and Hirano, S, editor. The Cadherin Superfamily. Springer

Breuer, M., L. Guglielmi, M. Zielonka, V. Hemberger, S. Kölker, J. G. Okun, G. F. Hoffmann, M. Carl, S. W. Sauer and T. Opladen (2019). QDPR homologues in Danio rerio regulate melanin synthesis, early gliogenesis, and glutamine homeostasis. *PLoS One* 14:e0215162

Bringuier, P.-P., J. A. Schalken, V. Hervieu and L. A. Giroldi (2015). Involvement of orphan nuclear receptor COUP-TFII in cadherin-6 and cadherin-11 regulation: Implications in development and cancer. *Mechanisms of Development* 136:64–72

Brockerhoff, S. E. and J. M. Fadool (2011). Genetics of photoreceptor degeneration and regeneration in zebrafish. *Cellular and Molecular Life Sciences* 68:651–659

Brockerhoff, S. E., F. Rieke, H. R. Matthews, M. R. Taylor, B. Kennedy, I. Ankoudinova, G. A. Niemi, C. L. Tucker, M. Xiao, F. G. Cilluffo and J. Hurley (2003). Light stimulates a transducin-independent increase of cytoplasmic Ca2+ and suppression of current in cones from the zebrafish mutant nof. *The Journal of Neuroscience* 23:470–480

Brodt, P. (1996). The structure, function and regulation of cadherins. Cell Adhesion and Invasion Mechanisms in Cancer Metastasis. New York: Springer

Bunse, S., S. Garg, S. Junek, D. Vogel, N. Ansari, E. H. Stelzer and E. Schuman (2013). Role of N-Cadherin cis and trans Interfaces in the Dynamics of

Adherens Junctions in Living Cells. *PLoS One* 8:e81517

Bureau, C., N. Hanoun, J. Torrisani, J.-P. Vinel, L. Buscail and P. Cordelier (2009). Expression and function of Kruppel like-factors (KLF) in carcinogenesis. *Current Genomics* 10:353–360

Burrill, J. D. and S. S. Easter (1994). Development of the retinofugal projections in the embryonic and larval zebrafish (Brachydanio rerio). *Journal of Comparative Neurology* 346:583–600

Burzynski, G. M., X. Reed, S. Maragh, T. Matsui and A. S. McCallion (2013). Integration of genomic and functional approaches reveals enhancers at LMX1A and LMX1B. *Molecular Genetics and Genomics* 288:579–589

Caiazzo, M., L. Colucci-D'Amato, M. T. Esposito, S. Parisi, S. Stifani, F. Ramirez and U. di Porzio (2010). Transcription factor KLF7 regulates differentiation of neuroectodermal and mesodermal cell lineages. *Experimental Cell Research* 316:2365–2376

Caiazzo, M., L. Colucci-D'Amato, F. Volpicelli, L. Speranza, C. Petrone, L. Pastore, S. Stifani, F. Ramirez, G. C. Bellenchi and U. di Porzio (2011). Krüppel-like factor 7 is required for olfactory bulb dopaminergic neuron development. *Experimental Cell Research* 317:464–473

Cailliez, F. and R. Lavery (2005). Cadherin mechanics and complexation: the importance of calcium binding. *Biophysical Journal* 89:3895–3903

Y Cajal, S. R., J. DeFelipe and E. G. Jones (1991). Cajal's degeneration and regeneration of the nervous system. Oxford University Press, USA

Cameron, D. A., K. L. Gentile, F. A. Middleton and P. Yurco (2005). Gene expression profiles of intact and regenerating zebrafish retina. *Molecular Vision* 11:775–791

Caroni, P., T. Savio and M. Schwab (1988). Central nervous system regeneration: oligodendrocytes and myelin as non-permissive substrates for neurite growth. *Progress in Brain Research* 78:363–370

Carrasquillo, M. M., F. Zou, V. S. Pankratz, S. L. Wilcox, L. Ma, L. P. Walker, S. G. Younkin, C. S. Younkin, L. H. Younkin, G. D. Bisceglio, N. Ertekin-Taner, J. Crook, D. Dickson, R. Petersen, N. Graff-Radford and S. Younkin (2009). Genetic variation in PCDH11X is associated with susceptibility to late-onset Alzheimer's disease. *Nature Genetics* 41:192–198

Carter-Dawson, L. D. and M. M. Lavail (1979). Rods and cones in the mouse retina. I. Structural analysis using light and electron microscopy. *Journal of*

Comparative Neurology 188:245–262

Centanin, L. and J. Wittbrodt (2014). Retinal neurogenesis. *Development* 141:241–244

Chang, H., N. Hoshina, C. Zhang, Y. Ma, H. Cao, Y. Wang, D. Wu, S. Bergen, M. Landen, C. Hultman, M. Preisig, Z. Kutalik, E. Castelao, M. Grigoroiu-Serbanescu, A. Forstner, J. Strohmaier, J. Hecker, T. Schulze, B. Müller-Myhsok, A. Reif, P. Mitchell, N. Martin, P. Schofield, S. N. M. Cichon, T. S. B. S. Group, M. B. Consortium, H. Walter, S. Erk, A. Heinz, N. Amin, C. van Duijn, A. Meyer-Lindenber, H. Tost, X. Xiao, T. Yamamoto, M. Rietschel and M. Li (2018). The protocadherin 17 gene affects cognition, personality, amygdala structure and function, synapse development and risk of major mood disorders. *Molecular Psychiatry* 23:400

Chapman, N. H., A. Estes, J. Munson, R. Bernier, S. J. Webb, J. H. Rothstein, N. J. Minshew, G. Dawson, G. D. Schellenberg and E. M. Wijsman (2011). Genome-scan for IQ discrepancy in autism: evidence for loci on chromosomes 10 and 16. *Human Genetics* 129:59–70

Chen, B., K. Brinkmann, Z. Chen, C. W. Pak, Y. Liao, S. Shi, L. Henry, N. V. Grishin, S. Bogdan and M. K. Rosen (2014). The WAVE regulatory complex links diverse receptors to the actin cytoskeleton. *Cell* 156:195–207

Chen, J., Y. Lu, S. Meng, M.-H. Han, C. Lin and X. Wang (2009). alpha-and gamma-Protocadherins Negatively Regulate PYK2. *Journal of Biological Chemistry* 284:2880–2890

Chen, M.-W., F. Vacherot, A. de la Taille, S. Gil-Diez-de-Medina, R. Shen, R. A. Friedman, M. Burchardt, D. K. Chopin and R. Buttyan (2002). The emergence of protocadherin-PC expression during the acquisition of apoptosis-resistance by prostate cancer cells. *Oncogene* 21:7861–7871

Chen, W. V. and T. Maniatis (2013). Clustered protocadherins. *Development* 140:3297–3302

Chen, Y., R. Londraville, S. Brickner, L. El-Shaar, K. Fankhauser, C. Dearth, L. Fulton, A. Sochacka, S. Bhattarai, J. A. Marrs and Q. Liu (2013). Protocadherin-17 function in Zebrafish retinal development. *Developmental Neurobiology* 73:259–73

Chhetri, J., G. Jacobson and N. Gueven (2014). Zebrafish—on the move towards ophthalmological research. *Eye* 28:367–380

Cho, E. A., L. T. Patterson, W. T. Brookhiser, S. Mah, C. Kintner and G. R. Dressler (1998). Differential expression and function of cadherin-6 during renal

epithelium development. *Development* 125:803–812

Cho, Y. G., C. J. Kim, C. H. Park, Y. M. Yang, S. Y. Kim, S. W. Nam, S. H. Lee, N. J. Yoo, J. Y. Lee and W. S. Park (2005). Genetic alterations of the KLF6 gene in gastric cancer. *Oncogene* 24:4588–4590

Chu, J. and K. C. Sadler (2009). New school in liver development: lessons from zebrafish. *Hepatology* 50:1656–1663

Cifuentes-Diaz, C., M. Nicolet, D. Goudou, F. Rieger and R. M. Mege (1994). N-cadherin expression in developing, adult and denervated chicken neuromuscular system: accumulations at both the neuromuscular junction and the node of Ranvier. *Development* 120:1–11

Clay, M. R. and M. C. Halloran (2014). Cadherin 6 promotes neural crest cell detachment via F-actin regulation and influences active Rho distribution during epithelial-to-mesenchymal transition. *Development* 141:2506–2515

Clendenon, S. G., S. Sarmah, B. Shah, Q. Liu and J. A. Marrs (2012). Zebrafish cadherin-11 participates in retinal differentiation and retinotectal axon projection during visual system development. *Developmental Dynamics* 241:442–454

Conkright, M. D., M. A. Wani, K. P. Anderson and J. B. Lingrel (1999). A gene encoding an intestinal-enriched member of the Krüppel-like factor family expressed in intestinal epithelial cells. *Nucleic Acids Research* 27:1263–1270

Consortium, E. P. (2011). A user's guide to the encyclopedia of DNA elements (ENCODE). *PLoS Biology* 9:e1001046

Consortium, G. O. (2019). The gene ontology resource: 20 years and still GOing strong. *Nucleic Acids Research* 47:D330–D338

Cooper, S. R. (2017). delta-Protocadherin Function: From Molecular Adhesion Properties to Brain Circuitry. The Ohio State University, OH

Cooper, S. R., M. R. Emond, P. Q. Duy, B. G. Liebau, M. A. Wolman and J. D. Jontes (2015). Protocadherins control the modular assembly of neuronal columns in the zebrafish optic tectum. *The Journal of Cell Biology* 211:807–814

Coughlin, G. M. and D. M. Kurrasch (2015). Protocadherins and Hypothalamic Development: Do They Play An Unappreciated Role? *Journal of Neuroendocrinology* 27:544–555

Cronin, K. D. and A. A. Capehart (2007). Gamma protocadherin expression in the embryonic chick nervous system. *International Journal of Biological Sciences* 3:8

Cuenca, N., L. Fernández-Sánchez, L. Campello, V. Maneu, P. De la Villa, P. Lax and I. Pinilla (2014). Cellular responses following retinal injuries and therapeutic approaches for neurodegenerative diseases. *Progress in Retinal and Eye Research* 43:17–75

Dang, D. T., J. Pevsner and V. W. Yang (2000). The biology of the mammalian Krüppel-like family of transcription factors. *The International Journal of Biochemistry & Cell Biology* 32:1103–1121

Daniel, S., A. Clark and C. McDowell (2018). Subtype-specific response of retinal ganglion cells to optic nerve crush. *Cell Death Discovery* 4:1–16

Darby, J., R. Carr and L. Beazley (1990). Retinal ganglion cell death during regeneration of the frog optic nerve is not accompanied by appreciable cell loss from the inner nuclear layer. *Anatomy and Embryology* 182:487–492

Dasgupta, S., S. M. Vliet, A. Kupsco, J. K. Leet, D. Altomare and D. C. Volz (2017). Tris(1,3-dichloro-2-propyl) phosphate disrupts dorsoventral patterning in zebrafish embryos. *PeerJ* 5:e4156

David, R. and D. Wedlich (2000). Xenopus cadherin-6 is expressed in the central and peripheral nervous system and in neurogenic placodes. *Mechanisms of Development* 97:187–190

Dean, B., D. Keriakous, E. Scarr and E. A. Thomas (2007). Gene expression profiling in Brodmann's area 46 from subjects with schizophrenia. *The Royal Australian and New Zealand Journal of Psychiatry* 41:308–320

Depienne, C., I. Gourfinkel-An, S. Baulac and E. LeGuern (2012). Genes in infantile epileptic encephalopathies. Jasper's Basic Mechanisms of the Epilepsies. Fourth edition. National Center for Biotechnology Information (US), Fourth edition.

Depienne, C., O. Trouillard, D. Bouteiller, I. Gourfinkel-An, K. Poirier, F. Rivier, P. Berquin, R. Nabbout, D. Chaigne, D. Steschenko, A. Gautier, D. Hoffman-Zacharska, A. Lannuzel, M. Lackmy-Port-Lis, H. Maurey, A. Dusser, M. Bru, B. Gilbert-Dussardier, A. Roubertie, A. Kaminska, S. Whalen, C. Mignot, S. Baulac, G. Lesca, A. Arzimanoglou and E. LeGuern (2011). Mutations and deletions in PCDH19 account for various familial or isolated epilepsies in females. *Human Mutation* 32:E1959–75

Derda, A. A., C. C. Woo, T. Wongsurawat, M. Richards, C. N. Lee, T. Kofidis, V. A. Kuznetsov and V. A. Sorokin (2018). Gene expression profile analysis of aortic vascular smooth muscle cells reveals upregulation of cadherin genes in myocardial infarction patients. *Physiological Genomics* 50:648–657

Dezawa, M. and E. Adachi-Usami (2000). Role of Schwann cells in retinal ganglion cell axon regeneration. *Progress in Retinal and Eye Research* 19:171–204

Dibbens, L. M., P. S. Tarpey, K. Hynes, M. A. Bayly, I. E. Scheffer, R. Smith, J. Bomar, E. Sutton, L. Vandeleur, C. Shoubridge, S. Edkins, S. Turner, C. Stevens, S. O'Meara, C. Tofts, S. Barthorpe, G. Buck, J. Cole, K. Halliday, D. Jones, R. Lee, M. Madison, T. Mironenko, J. Varian, S. West, S. Widaa, P. Wray, J. Teague, E. Dicks, A. Butler, A. Menzies, A. Jenkinson, R. Shepherd, J. Gusella, Z. Afawi, A. Mazarib, M. Neufeld, S. Kivity, D. Lev, T. Lerman-Sagie, A. Korczyn, C. Derry, G. Sutherland, K. Friend, M. Shaw, M. Corbett, H. Kim, D. Geschwind, P. Thomas, E. Haan, S. Ryan, S. McKee, S. Berkovic, P. Futreal, M. Stratton, J. Mulley and J. Gécz (2008). X-linked protocadherin 19 mutations cause female-limited epilepsy and cognitive impairment. *Nature Genetics* 40:776–781

Diez-Roux, G., S. Banfi, M. Sultan, L. Geffers, S. Anand, D. Rozado, A. Magen, E. Canidio, M. Pagani, I. Peluso and others (2011). A high-resolution anatomical atlas of the transcriptome in the mouse embryo. *PLoS Biology* 9:e1000582

Dooley, K. and L. I. Zon (2000). Zebrafish: a model system for the study of human disease. *Current Opinion in Genetics & Development* 10:252–256

Doron, N. N. and J. E. Ledoux (1999). Organization of projections to the lateral amygdala from auditory and visual areas of the thalamus in the rat. *Journal of Comparative Neurology* 412:383–409

Dunlop, S., M. Humphrey and L. Beazley (1992). Displaced retinal ganglion cells in normal frogs and those with regenerated optic nerves. *Anatomy and Embryology* 185:431–438

Easter Jr, S. S. and G. N. Nicola (1996). The Development of Vision in the Zebrafish (Danio rerio). *Developmental Biology* 180:646–663

Egusa, S. F., Y. U. Inoue, J. Asami, Y. W. Terakawa, M. Hoshino and T. Inoue (2015). Classic cadherin expressions balance postnatal neuronal positioning and dendrite dynamics to elaborate the specific cytoarchitecture of the mouse cortical area. *Neuroscience Research*

Eisen, J. S. (1996). Zebrafish make a big splash. *Cell* 87:969–77

Ekstrzm, P. and H. Meissl (1997). The pineal organ of teleost fishes. *Reviews in Fish Biology and Fisheries* 7:199–284

El-Amraoui, A. and C. Petit (2010). Cadherins as targets for genetic diseases. *Cold Spring Harbor Perspectives in Biology* 2:a003095

El-Benhawy, S. A., S. A. Ebeid, N. A. Abd El Moneim, R. R. Abdel Wahed and A. R. Arab (2021). Repression of protocadherin 17 is correlated with elevated angiogenesis and hypoxia markers in female patients with breast cancer. *Cancer Biomarkers*:1–10

El-Brolosy, M. A., Z. Kontarakis, A. Rossi, C. Kuenne, S. Günther, N. Fukuda, K. Kikhi, G. L. Boezio, C. M. Takacs, S.-L. Lai, R. Fuuda, C. Gerri, A. Giraldez and D. Stainier (2019). Genetic compensation triggered by mutant mRNA degradation. *Nature* 568:193–197

El-Brolosy, M. A. and D. Y. Stainier (2017). Genetic compensation: A phenomenon in search of mechanisms. *PLoS Genetics* 13:e1006780

Emond, M. R., S. Biswas, C. J. Blevins and J. D. Jontes (2011). A complex of Protocadherin-19 and N-cadherin mediates a novel mechanism of cell adhesion. *The Journal of Cell Biology* 195:1115–1121

Emond, M. R., S. Biswas and J. D. Jontes (2009). Protocadherin-19 is essential for early steps in brain morphogenesis. *Developmental Biology* 334:72–83

Emond, M. R., S. Biswas, M. L. Morrow and J. D. Jontes (2021). Proximity-dependent proteomics reveals extensive interactions of protocadherin-19 with regulators of rho GTPases and the microtubule cytoskeleton. *Neuroscience* 452:26–36

Emond, M. R. and J. D. Jontes (2008). Inhibition of protocadherin-alpha function results in neuronal death in the developing zebrafish. *Developmental Biology* 321:175–187

Etzrodt, J., K. Krishna-K and C. Redies (2009). Expression of classic cadherins and delta-protocadherins in the developing ferret retina. *BMC Neuroscience* 10:1

Fadool, J. M. and J. E. Dowling (2008). Zebrafish: a model system for the study of eye genetics. *Progress in Retinal and Eye Research* 27:89–110

Falcon, J., Y. Gothilf, S. Coon, G. Boeuf and D. Klein (2003). Genetic, temporal and developmental differences between melatonin rhythm generating systems

in the teleost fish pineal organ and retina. *Journal of Neuroendocrinology* 15:378–382

Faulkner-Jones, B., L. Godinho, B. Reese, G. Pasquini, A. Ruefli and S. Tan (1999). Cloning and expression of mouse Cadherin-7, a type-II cadherin isolated from the developing eye. *Molecular and Cellular Neuroscience* 14:1–16

Faura Tellez, G., K. Vandepoele, U. Brouwer, H. Koning, R. M. Elderman, T.-L. Hackett, B. W. Willemse, J. Holloway, F. Van Roy, G. H. Koppelman and M. Nawijn (2015). Protocadherin-1 binds to SMAD3 and suppresses TGF-beta1-induced gene transcription. *American Journal of Physiology-Lung Cellular and Molecular Physiology* 309:L725–L735

Fausett, B. V. (2007). Mechanisms of Retina Regeneration in Zebrafish. The University of Michigan, MI

Ferguson, T. A. and Y.-J. Son (2011). Extrinsic and intrinsic determinants of nerve regeneration. *Journal of Tissue Engineering* 2:2041731411418392

Fernandes, A. M., K. Fero, A. B. Arrenberg, S. A. Bergeron, W. Driever and H. A. Burgess (2012). Deep brain photoreceptors control light-seeking behavior in zebrafish larvae. *Current Biology* 22:2042–2047

Fernández-Monreal, M., S. Kang and G. R. Phillips (2009). Gamma-protocadherin homophilic interaction and intracellular trafficking is controlled by the cytoplasmic domain in neurons. *Molecular and Cellular Neuroscience* 40:344–353

Fero, K., S. A. Bergeron, E. J. Horstick, H. Codore, G. H. Li, F. Ono, J. J. Dowling and H. A. Burgess (2014). Impaired embryonic motility in dusp27 mutants reveals a developmental defect in myofibril structure. *Disease Models & Mechanisms* 7:289–298

Fischer, D., Z. He and L. I. Benowitz (2004). Counteracting the Nogo receptor enhances optic nerve regeneration if retinal ganglion cells are in an active growth state. *The Journal of Neuroscience* 24:1646–1651

Fischer, D. and M. Leibinger (2012). Promoting optic nerve regeneration. *Progress in Retinal and Eye Research* 31:688–701

Fleisch, V. C., B. Fraser and W. T. Allison (2011). Investigating regeneration and functional integration of CNS neurons: Lessons from zebrafish genetics and other fish species. *Biochimica et Biophysica Acta* 1812:364–380

Forsell, J., P. Ekström, I. N. Flamarique and B. Holmqvist (2001). Expression of pineal ultraviolet-and green-like opsins in the pineal organ and retina of teleosts. *The Journal of Experimental Biology* 204:2517–2525

Fraley, S. and S. Sharma (1984). Topography of retinal axons in the diencephalon of goldfish. *Cell and Tissue Research* 238:529–538

Frank, B. D. and J. G. Hollyfield (1987a). Retinal ganglion cell morphology in the frog, Rana pipiens. *The Journal of Comparative Neurology* 266:413–434

Frank, B. D. and J. G. Hollyfield (1987b). Retina of the tadpole and frog: delayed dendritic development in a subpopulation of ganglion cells coincident with metamorphosis. *The Journal of Comparative Neurology* 266:435–444

Frank, M., M. Ebert, W. Shan, G. R. Phillips, K. Arndt, D. R. Colman and R. Kemler (2005). Differential expression of individual gamma-protocadherins during mouse brain development. *Molecular and Cellular Neuroscience* 29:603–616

Frank, M. and R. Kemler (2002). Protocadherins. *Current Opinion in Cell Biology* 14:557–562

Franklin, R. and G. Hinks (1999). Understanding CNS remyelination: clues from developmental and regeneration biology. *Journal of Neuroscience Research* 58:207–213

Fukuda, E., S. Hamada, S. Hasegawa, S. Katori, M. Sanbo, T. Miyakawa, T. Yamamoto, H. Yamamoto, T. Hirabayashi and T. Yagi (2008). Down-regulation of protocadherin-alpha A isoforms in mice changes contextual fear conditioning and spatial working memory. *European Journal of Neuroscience* 28:1362–1376

Gaitan, Y. and M. Bouchard (2006). Expression of the delta-protocadherin gene Pcdh19 in the developing mouse embryo. *Gene Expression Patterns* 6:893–899

Galvez-Ruiz, A., A. Galindo-Ferreiro and A. J. Lehner (2020). CHARGE syndrome: A case report of two new CDH7 gene mutations. *Saudi Journal of Ophthalmology* 34:306

Gao, H., X. Qiao, F. Hefti, J. G. Hollyfield and B. Knusel (1997). Elevated mRNA expression of brain-derived neurotrophic factor in retinal ganglion cell layer after optic nerve injury. *Investigative Ophthalmology & Visual Science* 38:1840–1847

Garg, S., S. Fischer, E. Schuman and E. Stelzer (2015). Lateral assembly of N-cadherin drives tissue integrity by stabilizing adherens junctions. *Journal of The Royal Society Interface* 12:20141055

Garrett, A. M. and R. W. Burgess (2011). Candidate molecular mechanisms for establishing cell identity in the developing retina. *Developmental Neurobiology* 71:1258–1272

Garrett, A. M. and J. A. Weiner (2009). Control of CNS synapse development by gamma-protocadherin-mediated astrocyte-neuron contact. *The Journal of Neuroscience* 29:11723–11731

Gayet, O., V. LaBella, C. E. Henderson and S. Kallenbach (2004). The b1 isoform of protocadherin-gamma (Pcdhgamma) interacts with the microtubule-destabilizing protein SCG10. *FEBS Letters* 578:175–179

Gemberling, M., T. J. Bailey, D. R. Hyde and K. D. Poss (2013). The zebrafish as a model for complex tissue regeneration. *Trends in Genetics* 29:611–620

Gerety, S. S. and D. G. Wilkinson (2011). Morpholino artifacts provide pitfalls and reveal a novel role for pro-apoptotic genes in hindbrain boundary development. *Developmental Biology* 350:279–289

Giefing, M., N. Zemke, D. Brauze, M. Kostrzewska-Poczekaj, M. Luczak, M. Szaumkessel, K. Pelinska, K. Kiwerska, H. Tönnies, R. Grenman, M. Figlerowicz, R. Siebert, K. Szfter and M. Jarmuz (2011). High resolution ArrayCGH and expression profiling identifies PTPRD and PCDH17/PCH68 as tumor suppressor gene candidates in laryngeal squamous cell carcinoma. *Genes, Chromosomes and Cancer* 50:154–166

Glover, G., K. P. Mueller, C. Söllner, S. C. Neuhauss and T. Nicolson (2012). The Usher gene cadherin 23 is expressed in the zebrafish brain and a subset of retinal amacrine cells. *Molecular Vision* 18:2309

Goldberg, J. L., J. S. Espinosa, Y. Xu, N. Davidson, G. T. Kovacs and B. A. Barres (2002). Retinal ganglion cells do not extend axons by default: promotion by neurotrophic signaling and electrical activity. *Neuron* 33:689–702

Goldberg, J. L., V. P. Lemmon, J. Bixby, D. Moore and M. Blackmore (2013). United States Patent - KLF family members regulate intrinsic axon regeneration ability

Goldsmith, P. and W. Harris (2003). The zebrafish as a tool for understanding the biology of visual disorders. Pages 11–18. Seminars in Cell & Developmental Biology

Goodman, K. M., R. Rubinstein, C. A. Thu, F. Bahna, S. Mannepalli, G. Ahlsén, C. Rittenhouse, T. Maniatis, B. Honig and L. Shapiro (2016). Structural basis of diverse homophilic recognition by clustered alpha-and beta-protocadherins. *Neuron* 90:709–723

Grunwald, D. J. and J. S. Eisen (2002). Headwaters of the zebrafish—emergence of a new model vertebrate. *Nature Reviews Genetics* 3:717–724

Guella, I., M. B. McKenzie, D. M. Evans, S. E. Buerki, E. B. Toyota, M. I. Van Allen, S. Adam, C. Boelman, C. Bolbocean, T. Candido and others (2017). De novo mutations in YWHAG cause early-onset epilepsy. *The American Journal of Human Genetics* 101:300–310

Gumbiner, B. M. (2005). Regulation of cadherin-mediated adhesion in morphogenesis. *Nature Reviews Molecular Cell Biology* 6:622–634

Guo, S. (2004). Linking genes to brain, behavior and neurological diseases: what can we learn from zebrafish? *Genes, Brain and Behavior* 3:63–74

Halbleib, J. M. and W. J. Nelson (2006). Cadherins in development: cell adhesion, sorting, and tissue morphogenesis. *Genes & Development* 20:3199–3214

Han, M.-H., C. Lin, S. Meng and X. Wang (2010). Proteomics analysis reveals overlapping functions of clustered protocadherins. *Molecular & Cellular Proteomics* 9:71–83

Harding, P., M. Toms, E. Schiff, N. Owen, S. Bell, I. C. Lloyd and M. Moosajee (2021). EPHA2 Segregates with Microphthalmia and Congenital Cataracts in Two Unrelated Families. *International Journal of Molecular Sciences* 22:2190

Harman, A. and L. Beazley (1989). Generation of retinal cells in the wallaby, *Setonix brachyurus* (quokka). *Neuroscience* 28:219–232

Haruki, S., I. Imoto, K. Kozaki, T. Matsui, H. Kawachi, S. Komatsu, T. Muramatsu, Y. Shimada, T. Kawano and J. Inazawa (2010). Frequent silencing of protocadherin 17, a candidate tumour suppressor for esophageal squamous-cell carcinoma. *Carcinogenesis*:bgq053

Hasegawa, S., M. Kumagai, M. Hagihara, H. Nishimaru, K. Hirano, R. Kaneko, A. Okayama, T. Hirayama, M. Sanbo, M. Hirabayashi, M. Watanabe, T. Hirabayashi and T. Yagi (2016). Distinct and Cooperative Functions for the Protocadherin-alpha,-beta and-gamma Clusters in Neuronal Survival and Axon Targeting. *Frontiers in Molecular Neuroscience* 9:155

Hatta, K., T. Okada and M. Takeichi (1985). A monoclonal antibody disrupting calcium-dependent cell-cell adhesion of brain tissues: possible role of its target antigen in animal pattern formation. *Proceedings of the National Academy of Sciences* 82:2789–2793

Hayashi, S., Y. Inoue, H. Kiyonari, T. Abe, K. Misaki, H. Moriguchi, Y. Tanaka and M. Takeichi (2014). Protocadherin-17 Mediates Collective Axon Extension by Recruiting Actin Regulator Complexes to Interaxonal Contacts. *Developmental Cell* 30:673–687

Hayashi, S. and M. Takeichi (2015). Emerging roles of protocadherins: from self-avoidance to enhancement of motility. *Journal of Cell Science* 128:1455–1464

Heggem, M. A. and R. S. Bradley (2003). The cytoplasmic domain of Xenopus NF-protocadherin interacts with TAF1/set. *Developmental Cell* 4:419–429

Henderson, R. H., Z. Li, M. M. A. El Aziz, D. S. Mackay, M. A. Eljinini, M. Zeidan, A. T. Moore, S. S. Bhattacharya and A. R. Webster (2010). Biallelic mutation of protocadherin-21 (PCDH21) causes retinal degeneration in humans. *Molecular Vision*

Hertel, N., Krishna-K, M. Nuernberger and C. Redies (2008). A cadherin-based code for the divisions of the mouse basal ganglia. *Journal of Comparative Neurology* 508:511–28

Hertel, N. and C. Redies (2011). Absence of layer-specific cadherin expression profiles in the neocortex of the reeler mutant mouse. *Cerebral Cortex* 21:1105–1117

Hertel, N., C. Redies and L. Medina (2012). Cadherin expression delineates the divisions of the postnatal and adult mouse amygdala. *Journal of Comparative Neurology* 520:3982–4012

Heuberger, J. and W. Birchmeier (2010). Interplay of cadherin-mediated cell adhesion and canonical Wnt signaling. *Cold Spring Harbor Perspectives in Biology* 2:a002915

Higuchi, R., C. Fockler, G. Dollinger and R. Watson (1993). Kinetic PCR analysis: real-time monitoring of DNA amplification reactions. *Biotechnology* 11:1026–1030

Hill, E., I. D. Broadbent, C. Chothia and J. Pettitt (2001). Cadherin superfamily proteins in Caenorhabditis elegans and Drosophila melanogaster. *Journal of Molecular Biology* 305:1011–1024

Hirano, S., N. Kimoto, Y. Shimoyama, S. Hirohashi and M. Takeichi (1992). Identification of a neural alpha-catenin as a key regulator of cadherin function and multicellular organization. *Cell* 70:293–301

Hirano, S. and M. Takeichi (2012). Cadherins in brain morphogenesis and wiring. *Physiological Reviews* 92:597–634

Hirano, S., Q. Yan and S. T. Suzuki (1999). Expression of a novel protocadherin, OL-protocadherin, in a subset of functional systems of the developing mouse brain. *The Journal of Neuroscience* 19:995–1005

Hirayama, T. and T. Yagi (2013). Clustered protocadherins and neuronal diversity. *Progress in Molecular Biology and Translational Science* 116:145–167

Hitchcock, P. F. and S. Easter (1986). Retinal ganglion cells in goldfish: a qualitative classification into four morphological types, and a quantitative study of the development of one of them. *The Journal of Neuroscience* 6:1037–1050

Hitchcock, P. F. and P. A. Raymond (2004). The teleost retina as a model for developmental and regeneration biology. *Zebrafish* 1:257–271

Holtzman, N. G., M. K. Iovine, J. O. Liang and J. Morris (2016). Learning to fish with genetics: a primer on the vertebrate model Danio rerio. *Genetics* 203:1069–1089

Homayouni, R., D. S. Rice and T. Curran (2001). Disabled-1 interacts with a novel developmentally regulated protocadherin. *Biochemical and Biophysical Research Communications* 289:539–547

Honjo, M., H. Tanihara, S. Suzuki, T. Tanaka, Y. Honda and M. Takeichi (2000a). Differential expression of cadherin adhesion receptors in neural retina of the postnatal mouse. *Investigative Ophthalmology & Visual Science* 41:546–551

Honjo, Y., S. Nakagawa and M. Takeichi (2000b). Blockade of cadherin-6B activity perturbs the distribution of PSD-95 family proteins in retinal neurones. *Genes to Cells* 5:309–318

Hoon, M., H. Okawa, L. Della Santina and R. O. Wong (2014). Functional Architecture of the Retina: Development and Disease. *Progress in Retinal and Eye Research*

Hoshina, N., A. Tanimura, M. Yamasaki, T. Inoue, R. Fukabori, T. Kuroda, K. Yokoyama, T. Tezuka, H. Sagara, S. Hirano, H. Kiyonari, M. Takada, K. Kobayashi, M. Watanabe, M. Kano, T. Nakazawa and T. Yamamoto (2013). Protocadherin 17 regulates presynaptic assembly in topographic corticobasal

ganglia circuits. *Neuron* 78:839–854

Howe, K., M. D. Clark, C. F. Torroja, J. Torrance, C. Berthelot, M. Muffato, J. E. Collins, S. Humphray, K. McLaren, L. Matthews and others (2013). The zebrafish reference genome sequence and its relationship to the human genome. *Nature* 496:498–503

Hu, L., C. Wu, X. Zhao, R. Heist, L. Su, Y. Zhao, B. Han, S. Cao, M. Chu, J. Dai, J. Dong, Y. Shu, L. Xu, Y. Chen, Y. Wang, F. Lu, Y. Jiang, D. Yu, H. Chen, W. Tan, H. Ma, J. Chen, G. Jin, T. Wu, D. Lu, D. Christiani, D. Lin, Z. Hu and S. H (2012). Genome-wide association study of prognosis in advanced non-small cell lung cancer patients receiving platinum-based chemotherapy. *Clinical Cancer Research* 18:5507–5514

Hu, M. and S. S. Easter (1999). Retinal neurogenesis: the formation of the initial central patch of postmitotic cells. *Developmental Biology* 207:309–321

Hu, X., X. Sui, L. Li, X. Huang, R. Rong, X. Su, Q. Shi, L. Mo, X. Shu, Y. Kuang, Q. Tao and C. He (2013). Protocadherin 17 acts as a tumour suppressor inducing tumour cell apoptosis and autophagy, and is frequently methylated in gastric and colorectal cancers. *Journal of Pathology* 229:62–73

Huang, R., X. Liao, X. Wang and Q. Li (2021). Comprehensive investigation of the clinical significance of long non-coding RNA HOXA-AS2 in acute myeloid leukemia using genome-wide RNA sequencing dataset. *Journal of Cancer* 12:2151

Huberman, A. D., T. R. Clandinin and H. Baier (2010). Molecular and cellular mechanisms of lamina-specific axon targeting. *Cold Spring Harbor Perspectives in Biology* 2:a001743

De la Huerta, I. (2013). Expression and Role of Cadherins in the Mammalian Visual System

De la Huerta, I., I.-J. Kim, P. E. Voinescu and J. R. Sanes (2012). Direction-selective retinal ganglion cells arise from molecularly specified multipotential progenitors. *Proceedings of the National Academy of Sciences* 109:17663–17668

Hughes, A., S. Saszik, J. Bilotta, P. J. Demarco Jr and W. F. Patterson II (1998). Cone contributions to the photopic spectral sensitivity of the zebrafish ERG. *Visual Neuroscience* 15:1029–1037

Hulpiau, P. and F. Van Roy (2009). Molecular evolution of the cadherin superfamily. *The International Journal of Biochemistry & Cell Biology* 41:349–

Hulpiau, P. and F. Van Roy (2011). New insights into the evolution of metazoan cadherins - supplemental material. *Molecular Biology and Evolution* 28:647–657

Inoue, A. and J. R. Sanes (1997). Lamina-specific connectivity in the brain: regulation by N-cadherin, neurotrophins, and glycoconjugates. *Science* 276:1428–1431

Inoue, T., O. Chisaka, H. Matsunami and M. Takeichi (1997). Cadherin-6 expression transiently delineates specific rhombomeres, other neural tube subdivisions, and neural crest subpopulations in mouse embryos. *Developmental Biology* 183:183–194

Inoue, T., T. Tanaka, S. C. Suzuki and M. Takeichi (1998). Cadherin-6 in the developing mouse brain: expression along restricted connection systems and synaptic localization suggest a potential role in neuronal circuitry. *Developmental Dynamics* 211:338–351

Inuzuka, H., S. Miyatani and M. Takeichi (1991a). R-cadherin: a novel Ca 2+-dependent cell-cell adhesion molecule expressed in the retina. *Neuron* 7:69–79

Inuzuka, H., C. Redies and M. Takeichi (1991b). Differential expression of R-and N-cadherin in neural and mesodermal tissues during early chicken development. *Development* 113:959–967

Irizarry, R. A., B. Hobbs, F. Collin, Y. D. Beazer-Barclay, K. J. Antonellis, U. Scherf and T. P. Speed (2003). Exploration, normalization, and summaries of high density oligonucleotide array probe level data. *Biostatistics* 4:249–264

Itaya, S. K. (1980). Retinal efferents from the pretectal area in the rat. *Brain Research* 201:436–441

Ito, S. and D. A. Feldheim (2018). The mouse superior colliculus: an emerging model for studying circuit formation and function. *Frontiers in Neural Circuits* 12:10

Iuchi, S. (2001). Three classes of C2H2 zinc finger proteins. *Cellular and Molecular Life Sciences* 58:625–635

Izuta, Y., T. Taira, A. Asayama, M. Machigashira, T. Kinoshita, M. Fujiwara and S. T. Suzuki (2014). Protocadherin-9 involvement in retinal development in Xenopus laevis. *Journal of Biochemistry*:mvu070

Jeong, K. H., S.-K. Kim, S. Y. Kim and K.-O. Cho (2009). Immunohistochemical localization of Krüppel-like factor 6 in the mouse forebrain. *Neuroscience Letters* 453:16–20

Jontes, J. D. (2016). The Nonclustered Protocadherins. Pages 223–249. The Cadherin Superfamily. Springer

Junghans, D., M. Heidenreich, I. Hack, V. Taylor, M. Frotscher and R. Kemler (2008). Postsynaptic and differential localization to neuronal subtypes of protocadherin beta16 in the mammalian central nervous system. *European Journal of Neuroscience* 27:559–571

Kaczynski, J., T. Cook and R. Urrutia (2003). Sp1-and Krüppel-like transcription factors. *Genome Biology* 4:1

Kanazawa, A., Y. Kawamura, A. Sekine, A. Iida, T. Tsunoda, A. Kashiwagi, Y. Tanaka, T. Babazono, M. Matsuda, K. Kawai, T. Iizumi, T. Fujioka, M. Imanishi, K. Kaku, Y. Iwamoto, R. Kawamori, R. Kikkawa, Y. Nakamura and S. Maeda (2005). Single nucleotide polymorphisms in the gene encoding Krüppel-like factor 7 are associated with type 2 diabetes. *Diabetologia* 48:1315–1322

Kanzler, B., A. Haas-Assenbaum, I. Haas, L. Morawiec, E. Huber and T. Boehm (2003). Morpholino oligonucleotide-triggered knockdown reveals a role for maternal E-cadherin during early mouse development. *Mechanisms of Development* 120:1423–1432

Karlsson, J., J. von Hofsten and P.-E. Olsson (2001). Generating transparent zebrafish: a refined method to improve detection of gene expression during embryonic development. *Marine Biotechnology* 3:522–527

Karthikeyan, S., D. Lantvit, D. Chae and J. Burdette (2016). Cadherin-6 type 2, K-cadherin (CDH6). is regulated by mutant p53 in the fallopian tube but is not expressed in the ovarian surface. *Oncotarget* 7:69871–69882

Kashyap, B., L. Pegorsch, R. A. Frey, C. Sun, E. A. Shelden and D. L. Stenkamp (2014). Eye-specific gene expression following embryonic ethanol exposure in zebrafish: roles for heat shock factor 1. *Reproductive Toxicology* 43:111–124

Kato, S., T. Matsukawa, Y. Koriyama, K. Sugitani and K. Ogai (2013). A molecular mechanism of optic nerve regeneration in fish: the retinoid signaling pathway. *Progress in Retinal and Eye Research* 37:13–30

Kay, J. N., I. De la Huerta, I.-J. Kim, Y. Zhang, M. Yamagata, M. W. Chu, M. Meister and J. R. Sanes (2011). Retinal ganglion cells with distinct directional preferences differ in molecular identity, structure, and central projections. *The*

Journal of Neuroscience 31:7753–7762

Keeler, A. B., D. Schreiner and J. A. Weiner (2015). Protein Kinase C Phosphorylation of a gamma-Protocadherin C-terminal Lipid Binding Domain Regulates Focal Adhesion Kinase Inhibition and Dendrite Arborization. *Journal of Biological Chemistry* 290:20674–20686

Kerstetter, A., E. Azodi, J. Marrs and Q. Liu (2004). Cadherin-2 function in the cranial ganglia and lateral line system of developing zebrafish. *Developmental Dynamics* 230:137–143

Kielczewski, J. L., M. E. Pease and H. A. Quigley (2005). The effect of experimental glaucoma and optic nerve transection on amacrine cells in the rat retina. *Investigative Ophthalmology & Visual Science* 46:3188–3196

Kietzmann, A., Y. Wang, D. Weber and H. Steinbeisser (2012). Xenopus paraxial protocadherin inhibits Wnt/beta-catenin signalling via casein kinase 2beta. *EMBO reports* 13:129–134

Kim, S., J. Mo, S. Han, S. Choi, S. Han, B. Moon, I. Rhyu, W. Sun and H. Kim (2010). The expression of non-clustered protocadherins in adult rat hippocampal formation and the connecting brain regions. *Neuroscience* 170:189–199

Kim, S.-H., A. Yamamoto, T. Bouwmeester, E. Agius and E. Robertis (1998). The role of paraxial protocadherin in selective adhesion and cell movements of the mesoderm during Xenopus gastrulation. *Development* 125:4681–4690

Kim, S.-Y., H. S. Chung, W. Sun and H. Kim (2007). Spatiotemporal expression pattern of non-clustered protocadherin family members in the developing rat brain. *Neuroscience* 147:996–1021

Kim, S.-Y., S. Yasuda, H. Tanaka, K. Yamagata and H. Kim (2011). Non-clustered protocadherin. *Cell Adhesion Migration* 5:97–105

Kita, E. M. (2015). In vivo imaging of the zebrafish retinotectal map

Kita, E. M., E. K. Scott and G. J. Goodhill (2015). The influence of activity on axon pathfinding in the optic tectum. *Developmental Neurobiology* 75:608–620

Kleinjan, D. A., R. M. Bancewicz, P. Gautier, R. Dahm, H. B. Schonthaler, G. Damante, A. Seawright, A. M. Hever, P. L. Yeyati, V. van Heyningen and P. Coutinho (2008). Subfunctionalization of duplicated zebrafish pax6 genes by cis-regulatory divergence. *PLoS Genetics* 4:e29

Kohmura, N., K. Senzaki, S. Hamada, N. Kai, R. Yasuda, M. Watanabe, H. Ishii, M. Yasuda, M. Mishina and T. Yagi (1998). Diversity revealed by a novel family of cadherins expressed in neurons at a synaptic complex. *Neuron* 20:1137–1151

Kolsch, Y., J. Hahn, A. Sappington, M. Stemmer, A. M. Fernandes, T. O. Helmbrecht, S. Lele, S. Butrus, E. Laurell, I. Arnold-Ammer, K. Shekhar, J. Sanes and H. Baier (2021). Molecular classification of zebrafish retinal ganglion cells links genes to cell types to behavior. *Neuron* 109:645–662

Koppelman, G. H., D. A. Meyers, T. D. Howard, S. L. Zheng, G. A. Hawkins, E. J. Ampleford, J. Xu, H. Koning, M. Bruinenberg, I. M. Nolte, C. van Diemen, H. Boezen, W. Timens, P. Whittaker, O. Stine, S. Barton, J. Holloway, S. Holgate, P. Graves, F. Martinez, A. van Oosterhout, E. Bleecker and D. Postma (2009). Identification of PCDH1 as a novel susceptibility gene for bronchial hyperresponsiveness. *American Journal of Respiratory and Critical Care Medicine* 180:929–935

Krishna, K. and C. Redies (2009). Expression of cadherin superfamily genes in brain vascular development. *Journal of Cerebral Blood Flow & Metabolism* 29:224–229

Krishna-K, K., N. Hertel and C. Redies (2011). Cadherin expression in the somatosensory cortex: evidence for a combinatorial molecular code at the single-cell level. *Neuroscience* 175:37–48

Krishna-K, M. Nuernberger, F. Weth and C. Redies (2009). Layer-specific expression of multiple cadherins in the developing visual cortex (V1) of the ferret. *Cerebral Cortex* 19:388–401

Kubota, F., T. Murakami, K. Mogi and H. Yorifuji (2002). Cadherin-6 is required for zebrafish nephrogenesis during early development. *The International Journal of Developmental Biology* 51:123–129

Kubota, F., T. Murakami, Y. Tajika and H. Yorifuji (2008). Expression of protocadherin 18 in the CNS and pharyngeal arches of zebrafish embryos. *The International Journal of Developmental Biology* 52:397

Kumar, R., A. Ciprianidis, S. Theiss, H. Steinbeißer and L. T. Kaufmann (2017). Nemo-like kinase 1 (Nlk1) and paraxial protocadherin (PAPC) cooperatively control Xenopus gastrulation through regulation of Wnt/planar cell polarity (PCP) signaling. *Differentiation* 93:27–38

Kuroda, H., M. Inui, K. Sugimoto, T. Hayata and M. Asashima (2002). Axial protocadherin is a mediator of prenotochord cell sorting in Xenopus.

Developmental Biology 244:267–277

Kuwako, K., Y. Nishimoto, S. Kawase, H. J. Okano and H. Okano (2014). Cadherin-7 regulates mossy fiber connectivity in the cerebellum. *Cell Reports* 9:311–323

Langheinrich, U. (2003). Zebrafish: a new model on the pharmaceutical catwalk. *Bioessays* 25:904–912

Langley, J. N. (1895). Note on Regeneration of Præ-Ganglionic Fibres of the Sympathetic. *The Journal of Physiology* 18:280–284

Larue, L., M. Ohsugi, J. Hirchenhain and R. Kemler (1994). E-cadherin null mutant embryos fail to form a trophectoderm epithelium. *Proceedings of the National Academy of Sciences* 91:8263–8267

Lasky-Su, J., B. M. Neale, B. Franke, R. J. Anney, K. Zhou, J. B. Maller, A. A. Vasquez, W. Chen, P. Asherson, J. Buitelaar, T. Banaschewski, R. Ebstein, M. Gill, A. Miranda, F. Mulas, R. Oades, H. Roeyers, A. Rothenberg, J. Sergeant, E. Sonuga-Barke, H. Steinhausen, E. Taylor, E. Daly, N. Laird, C. Lange and S. Faraone (2008). Genome-wide association scan of quantitative traits for attention deficit hyperactivity disorder identifies novel associations and confirms candidate gene associations. *American Journal of Medical Genetics Part B: Neuropsychiatric Genetics* 147:1345–1354

Laub, F., R. Aldabe, V. Friedrich Jr, S. Ohnishi, T. Yoshida and F. Ramirez (2001a). Developmental expression of mouse Krüppel-like transcription factor KLF7 suggests a potential role in neurogenesis. *Developmental Biology* 233:305–318

Laub, F., R. Aldabe, F. Ramirez and S. Friedman (2001b). Embryonic expression of Krüppel-like factor 6 in neural and non-neural tissues. *Mechanisms of Development* 106:167–170

Laub, F., C. Dragomir and F. Ramirez (2006). Mice without transcription factor KLF7 provide new insight into olfactory bulb development. *Brain Research* 1103:108–113

Laub, F., L. Lei, H. Sumiyoshi, D. Kajimura, C. Dragomir, S. Smaldone, A. C. Puche, T. J. Petros, C. Mason, L. F. Parada and F. Ramirez (2005). Transcription factor KLF7 is important for neuronal morphogenesis in selected regions of the nervous system. *Molecular and Cellular Biology* 25:5699–5711

Lee, R. C., T. R. Clandinin, C.-H. Lee, P.-L. Chen, I. A. Meinertzhagen and S. L. Zipursky (2003). The protocadherin Flamingo is required for axon target

selection in the Drosophila visual system. *Nature Neuroscience* 6:557–563

Lefebvre, J. L., Y. Zhang, M. Meister, X. Wang and J. R. Sanes (2008). gamma-Protocadherins regulate neuronal survival but are dispensable for circuit formation in retina. *Development* 135:4141–4151

Lefkovics, K., M. Mayer, K. Bercsényi, G. Szabó and Z. Lele (2012). Comparative analysis of type II classic cadherin mRNA distribution patterns in the developing and adult mouse somatosensory cortex and hippocampus suggests significant functional redundancy. *Journal of Comparative Neurology* 520:1387–1405

Lei, L., F. Laub, M. Lush, M. Romero, J. Zhou, B. Luikart, L. Klesse, F. Ramirez and L. Parada (2005). The zinc finger transcription factor Klf7 is required for TrkA gene expression and development of nociceptive sensory neurons. *Genes & Development* 19:1354–1364

Lele, Z., A. Folchert, M. Concha, G.-J. Rauch, R. Geisler, F. Rosa, S. W. Wilson, M. Hammerschmidt and L. Bally-Cuif (2002). parachute/n-cadherin is required for morphogenesis and maintained integrity of the zebrafish neural tube. *Development* 129:3281–3294

Lesch, K.-P., N. Timmesfeld, T. J. Renner, R. Halperin, C. Röser, T. T. Nguyen, D. W. Craig, J. Romanos, M. Heine, J. Meyer, C. Freitag, A. Warnke, M. Romanos, H. Schafer, S. Walitza, A. Reif, D. Stephan and C. Jacob (2008). Molecular genetics of adult ADHD: converging evidence from genome-wide association and extended pedigree linkage studies. *Journal of Neural Transmission* 115:1573–1585

Leung, L. C., W. A. Harris, C. E. Holt and M. Piper (2015). NF-Protocadherin Regulates Retinal Ganglion Cell Axon Behaviour in the Developing Visual System. *PLoS One* 10:e0141290

Leung, L. C., V. Urbancic, M.-L. Baudet, A. Dwivedy, T. G. Bayley, A. C. Lee, W. A. Harris and C. E. Holt (2013). Coupling of NF-protocadherin signaling to axon guidance by cue-induced translation. *Nature Neuroscience* 16:166–173

Levkovitch--Verbin, H., C. Harris--Cerruti, Y. Groner, L. A. Wheeler, M. Schwartz and E. Yoles (2000). RGC death in mice after optic nerve crush injury: oxidative stress and neuroprotection. *Investigative Ophthalmology & Visual Science* 41:4169–4174

Li, C., G. Bademci, A. Subasioglu, O. Diaz-Horta, Y. Zhu, J. Liu, T. G. Mitchell, C. Abad, S. Seyhan, D. Duman and others (2019). Dysfunction of GRAP, encoding the GRB2-related adaptor protein, is linked to sensorineural hearing

loss. *Proceedings of the National Academy of Sciences* 116:1347–1352

Li, Q., D. Ritter, N. Yang, Z. Dong, H. Li, J. H. Chuang and S. Guo (2010a). A systematic approach to identify functional motifs within vertebrate developmental enhancers. *Developmental Biology* 337:484–495

Li, S., M. Yin, S. Liu, Y. Chen, Y. Yin, T. Liu and J. Zhou (2010b). Expression of ventral diencephalon-enriched genes in zebrafish. *Developmental Dynamics* 239:3368–3379

Li, W.-H., L. Zhou, Z. Li, Y. Wang, J.-T. Shi, Y.-J. Yang and J.-F. Gui (2015). Zebrafish Lbh-like is required for Otx2-mediated photoreceptor differentiation. *International Journal of Biological Sciences* 11:688

Li, X., J. Montgomery, W. Cheng, J. H. Noh, D. R. Hyde and L. Li (2012a). Pineal photoreceptor cells are required for maintaining the circadian rhythms of behavioral visual sensitivity in zebrafish. *PLoS One* 7:e40508

Li, X., Q. Wang, K. He, Z. Li, J. Chen, W. Li, Z. Wen, J. Shen, Y. Qiang, J. Ji, G. Feng, G. He, H. Lin, Y. Wang and Y. Shi (2014). Common variants in the CDH7 gene are associated with major depressive disorder in the Han Chinese population. *Behavior Genetics* 44:97–101

Li, Y., H. Xiao, C. TT, H. Jin, B. Bonhomme, C. Miralles, N. Pinal, R. Ali, Wvm. T. Chen and A. De Blas (2012b). Molecular and functional interaction between protocadherin-γC5 and GABAA receptors. *The Journal of Neuroscience* 32:11780–11797

Lieschke, G. J. and P. D. Currie (2007). Animal models of human disease: zebrafish swim into view. *Nature Reviews Genetics* 8:353–367

Lilien, J. and J. Balsamo (2005). The regulation of cadherin-mediated adhesion by tyrosine phosphorylation/dephosphorylation of beta-catenin. *Current Opinion in Cell Biology* 17:459–465

Lin, C., S. Meng, T. Zhu and X. Wang (2010). PDCD10/CCM3 acts downstream of gamma-protocadherins to regulate neuronal survival. *Journal of Biological Chemistry* 285:41675–41685

Lin, J., C. Wang and C. Redies (2013). Expression of multiple delta-protocadherins during feather bud formation. *Gene Expression Patterns* 13:57–65

Lin, J., C. Wang and C. Redies (2014). Restricted expression of classic cadherins in the spinal cord of the chicken embryo. *Frontiers in Neuroanatomy*

8:18

Lin, J., X. Yan, C. Wang, Z. Guo, A. Rolfs and J. Luo (2012). Anatomical expression patterns of delta-protocadherins in developing chicken cochlea. *Journal of Anatomy* 221:598–608

Linden, R. and C. E. Esberard (1987). Displaced amacrine cells in the ganglion cell layer of the hamster retina. *Vision Research* 27:1071–6

Liu, B., J. Duff, R. L. Londraville, J. Marrs and Q. Liu (2007a). Cloning and expression analysis of cadherin7 in the central nervous system of the embryonic zebrafish. *Gene Expression Patterns* 7:15–22

Lee-Liu, D., G. Edwards-Faret, V. S. Tapia and J. Larraín (2013). Spinal cord regeneration: lessons for mammals from non-mammalian vertebrates. *Genesis* 51:529–544

Liu, J., C. Zhu, G. Ning, L. Yang, Y. Cao, S. Huang and Q. Wang (2019). Chemokine signaling links cell-cycle progression and cilia formation for left-right symmetry breaking. *PLoS Biology* 17:e3000203

Liu, K., A. Tedeschi, K. K. Park and Z. He (2011a). Neuronal intrinsic mechanisms of axon regeneration. *Annual Review of Neuroscience* 34:131–152

Liu, Q., E. Azodi, A. Kerstetter and A. Wilson (2004a). Cadherin-2 and cadherin-4 in developing, adult and regenerating zebrafish cerebellum. *Developmental Brain Research* 150:63–71

Liu, Q., S. Babb, Z. Novince, A. Doedens, J. Marrs and P. Raymond (2001). Differential expression of cadherin-2 and cadherin-4 in the developing and adult zebrafish visual system. *Visual Neuroscience* 18:923–933

Liu, Q., Y. Chen, F. Kubota, J. J. Pan and T. Murakami (2010). Expression of protocadherin-19 in the nervous system of the embryonic zebrafish. *The International Journal of Developmental Biology* 54:905

Liu, Q., Y. Chen, J. J. Pan and T. Murakami (2009). Expression of protocadherin-9 and protocadherin-17 in the nervous system of the embryonic zebrafish. *Gene Expression Patterns* 9:490–496

Liu, Q., M. Dalman, S. Sarmah, S. Chen, Y. Chen, A. Hurlbut, M. Spencer, L. Pancoe and J. Marrs (2011b). Cell adhesion molecule cadherin-6 function in zebrafish cranial and lateral line ganglia development. *Developmental Dynamics* 240:1716–1726

Liu, Q., R. Ensign and E. Azodi (2003). Cadherin-1,-2 and-4 expression in the cranial ganglia and lateral line system of developing zebrafish. *Gene Expression Patterns* 3:653–658

Liu, Q., R. Frey, S. Babb-Clendenon, B. Liu, J. Francl, A. Wilson, J. Marrs and D. Stenkamp (2007b). Differential expression of photoreceptor-specific genes in the retina of a zebrafish cadherin2 mutant glass onion and zebrafish cadherin4 morphants. *Experimental Eye Research* 84:163–175

Liu, Q., B. Liu, A. L. Wilson and J. Rostedt (2006). cadherin-6 Message expression in the nervous system of developing zebrafish. *Developmental Dynamics* 235:272–278

Liu, Q. and R. Londraville (2003). Using the adult zebrafish visual system to study cadherin-2 expression during central nervous system regeneration. *Methods in Cell Science* 25:71–78

Liu, Q., R. Londraville, E. Azodi, S. Babb, C. Chiappini-Williamson, J. Marrs and P. Raymond (2002). Up-regulation of cadherin-2 and cadherin-4 in regenerating visual structures of adult zebrafish. *Experimental Neurology* 177:396–406

Liu, Q., R. Londraville, J. A. Marrs, A. L. Wilson, T. Mbimba, T. Murakami, F. Kubota, W. Zheng and D. G. Fatkins (2008a). Cadherin-6 function in zebrafish retinal development. *Developmental Neurobiology* 68:1107–1122

Liu, Q., J. A. Marrs, E. Azodi, A. E. Kerstetter, S. G. Babb and L. Hashmi (2004b). Differential expression of cadherins in the developing and adult zebrafish olfactory system. *Journal of Comparative Neurology* 478:269–281

Liu, Q., J. A. Marrs, R. L. Londraville and A. L. Wilson (2008b). Cadherin-7 function in zebrafish development. *Cell and Tissue Research* 334:37

Liu, Q., J. A. Marrs and P. A. Raymond (1999a). Spatial correspondence between R-cadherin expression domains and retinal ganglion cell axons in developing zebrafish. *Journal of Comparative Neurology* 410:290–302

Liu, Q., K. Sanborn, N. Cobb, P. Raymond and J. Marrs (1999b). R-cadherin expression in the developing and adult zebrafish visual system. *Journal of Comparative Neurology* 410:303–319

Liu, Y., C. M. McDowell, Z. Zhang, H. E. Tebow, R. J. Wordinger and A. F. Clark (2014). Monitoring retinal morphologic and functional changes in mice following optic nerve crush. *Investigative Ophthalmology & Visual Science* 55:3766–3774

Livak, K. J. and T. D. Schmittgen (2001). Analysis of Relative Gene Expression Data Using Real-Time Quantitative PCR and the 2-DeltaDeltaCT Method. *Methods* 25:402–408

Lomberk, G. and R. Urrutia (2005). The family feud: turning off Sp1 by Sp1-like KLF proteins. *Biochemical Journal* 392:1–11

Lu, J., R. Liu, A. Miao, X. Chen, W. Xiao, Y. Wang, D. Cao, J. Pan, L. Li and Y. Luo (2020). The role of cldnh during the early retinal development in zebrafish. *Experimental Eye Research* 200:108207

Lucitt, M. B., T. S. Price, A. Pizarro, W. Wu, A. K. Yocum, C. Seiler, M. A. Pack, I. A. Blair, G. A. Fitzgerald and T. Grosser (2008). Analysis of the zebrafish proteome during embryonic development. *Molecular & Cellular Proteomics* 7:981–994

Luckner, R. (2001). Granule cell raphes in the developing mouse cerebellum

Magdaleno, S., P. Jensen, C. L. Brumwell, A. Seal, K. Lehman, A. Asbury, T. Cheung, T. Cornelius, D. M. Batten, C. Eden and others (2006). BGEM: an *in situ* hybridization database of gene expression in the embryonic and adult mouse nervous system. *PLoS Biology* 4:e86

Mah, K. M. and J. A. Weiner (2016). Clustered protocadherins. Pages 195–221. The Cadherin Superfamily. Springer

Mah, S. P., H. Saueressig, M. Goulding, C. Kintner and G. R. Dressler (2000). Kidney development in cadherin-6 mutants: delayed mesenchyme-to-epithelial conversion and loss of nephrons. *Developmental Biology* 223:38–53

Mahler, J., A. Filippi and W. Driever (2010). DeltaA/DeltaD regulate multiple and temporally distinct phases of notch signaling during dopaminergic neurogenesis in zebrafish. *The Journal of Neuroscience* 30:16621–16635

Makarenkova, H., H. Sugiura, K. Yamagata and G. Owens (2005). Alternatively spliced variants of protocadherin 8 exhibit distinct patterns of expression during mouse development. *Biochimica et Biophysica Acta* 1681:150–156

Malicki, J., H. Jo and Z. Pujic (2003). Zebrafish N-cadherin, encoded by the glass onion locus, plays an essential role in retinal patterning. *Developmental Biology* 259:95–108

Manoli, M. and W. Driever (2014). nkx2. 1 and nkx2. 4 genes function partially redundant during development of the zebrafish hypothalamus, preoptic region, and pallidum. *Frontiers in Neuroanatomy* 8:145

Marc, R. E. and D. Cameron (2002). A molecular phenotype atlas of the zebrafish retina. Pages 45–106. Chemical Anatomy of the Zebrafish Retina. Springer

Masai, I., Z. Lele, M. Yamaguchi, A. Komori, A. Nakata, Y. Nishiwaki, H. Wada, H. Tanaka, Y. Nojima, M. Hammerschmidt, S. Wilson and H. Okamoto (2003). N-cadherin mediates retinal lamination, maintenance of forebrain compartments and patterning of retinal neurites. *Development* 130:2479–2494

Matsumoto, N., F. Laub, R. Aldabe, W. Zhang, F. Ramirez, T. Yoshida and M. Terada (1998). Cloning the cDNA for a new human zinc finger protein defines a group of closely related Krüppel-like transcription factors. *The Journal of Biological Chemistry* 273:28229–28237

Matsunaga, E., S. Nambu, M. Oka and A. Iriki (2014). Complementary and dynamic type II cadherin expression associated with development of the primate visual system. *Development, Growth & Differentiation* 56:535–543

Matsunaga, E., S. Nambu, M. Oka and A. Iriki (2015). Complex and dynamic expression of cadherins in the embryonic marmoset cerebral cortex. *Development, Growth & Differentiation*

Matsunaga, M., K. Hatta and M. Takeichi (1988). Role of N-cadherin cell adhesion molecules in the histogenesis of neural retina. *Neuron* 1:289–295

Maximino, C., R. X. do C. Silva, S. de N. dos S. da Silva, L. do S. dos S. Rodrigues, H. Barbosa, T. S. de Carvalho, L. K. R. Leão, M. G. Lima, K. R. M. Oliveira and A. M. Herculano (2015). Non-mammalian models in behavioral neuroscience: consequences for biological psychiatry. *Frontiers in Behavioral Neuroscience* 9:233

McConnell, B. B. and V. W. Yang (2010). Mammalian Krüppel-like factors in health and diseases. *Physiological Reviews* 90:1337–1381

McCurley, A. T. and G. V. Callard (2010). Time course analysis of gene expression patterns in zebrafish eye during optic nerve regeneration. *Journal of Experimental Neuroscience* 2010:17

McDowell, A. L., L. J. Dixon, J. D. Houchins and J. Bilotta (2004). Visual processing of the zebrafish optic tectum before and after optic nerve damage. *Visual Neuroscience* 21:97–106

McGregor, N., C. Lochner, D. Stein and S. Hemmings (2016). Polymorphisms within the neuronal cadherin (CDH2) gene are associated with obsessive-compulsive disorder (OCD) in a South African cohort. *Metabolic Brain Disease*

31:191–196

Meek, H. J. (1990). Tectal morphology: connections, neurones and synapses. Pages 239–277. The Visual System of Fish. The Visual System of Fish

Meunier, I., G. Manes, B. Bocquet, V. Marquette, C. Baudoin, B. Puech, S. Defoort-Dhellemmes, I. Audo, R. Verdet, C. Arndt and others (2014). Frequency and clinical pattern of vitelliform macular dystrophy caused by mutations of interphotoreceptor matrix IMPG1 and IMPG2 genes. *Ophthalmology* 121:2406–2414

Miller, I. and J. J. Bieker (1993). A novel, erythroid cell-specific murine transcription factor that binds to the CACCC element and is related to the Krüppel family of nuclear proteins. *Molecular and Cellular Biology* 13:2776–2786

Miskevich, F., Y. Zhu, B. Ranscht and J. R. Sanes (1998). Expression of multiple cadherins and catenins in the chick optic tectum. *Molecular and Cellular Neuroscience* 12:240–255

Missaire, M. and R. Hindges (2015). The role of cell adhesion molecules in visual circuit formation: From neurite outgrowth to maps and synaptic specificity. *Developmental Neurobiology* 75:569–583

Monesson-Olson, B., J. J. McClain, A. E. Case, H. E. Dorman, D. R. Turkewitz, A. B. Steiner and G. B. Downes (2018). Expression of the eight GABAA receptor alpha subunits in the developing zebrafish central nervous system. *PLoS One* 13:e0196083

Moore, D. L., A. Apara and J. L. Goldberg (2011). Kruppel-like transcription factors in the nervous system: novel players in neurite outgrowth and axon regeneration. *Molecular and Cellular Neuroscience* 47:233–243

Moore, D. L., M. G. Blackmore, Y. Hu, K. H. Kaestner, J. L. Bixby, V. P. Lemmon and J. L. Goldberg (2009). KLF family members regulate intrinsic axon regeneration ability. *Science* 326:298–301

Moore, R., D. Champeval, L. Denat, S.-S. Tan, F. Faure, S. Julien-Grille and L. Larue (2004). Involvement of cadherins 7 and 20 in mouse embryogenesis and melanocyte transformation. *Oncogene* 23:6726–6735

Morcos, P. (2007). Achieving targeted and quantifiable alteration of mRNA splicing with Morpholino oligos. *Biochemical and Biophysical Research Communications* 358:521–527

Morimura, H., F. Saindelle-Ribeaudeau, E. L. Berson and T. P. Dryja (1999). Mutations in RGR, encoding a light-sensitive opsin homologue, in patients with retinitis pigmentosa. *Nature Genetics* 23:393–394

Morishita, H., M. Kawaguchi, Y. Murata, C. Seiwa, S. Hamada, H. Asou and T. Yagi (2004). Myelination triggers local loss of axonal CNR/protocadherin-alpha family protein expression. *European Journal of Neuroscience* 20:2843–2847

Morishita, H., M. Umitsu, Y. Murata, N. Shibata, K. Udaka, Y. Higuchi, H. Akutsu, T. Yamaguchi, T. Yagi and T. Ikegami (2006). Structure of the cadherin-related neuronal receptor/protocadherin-alpha first extracellular cadherin domain reveals diversity across cadherin families. *Journal of Biological Chemistry* 281:33650–33663

Morishita, H. and T. Yagi (2007). Protocadherin family: diversity, structure, and function. *Current Opinion in Cell Biology* 19:584–592

Morrow, E. M., S.-Y. Yoo, S. W. Flavell, T.-K. Kim, Y. Lin, R. S. Hill, N. M. Mukaddes, S. Balkhy, G. Gascon, A. Hashmi, S. Al-Saad, J. Ware, R. Joseph, R. Greenblatt, D. Gleanson, J. Ertelt, K. Apse, A. Bodell, J. Partlow, B. Barry, H. Yao, K. Markianos, R. Ferland, M. Greenberg and C. Walsh (2008). Identifying autism loci and genes by tracing recent shared ancestry. *Science* 321:218–223

Moulton, H. M. and J. D. Moulton (2017). Morpholino Oligomers - Methods and Protocols. Humana Press

Moulton, J. D. (2017). Using Morpholinos to control gene expression. *Current Protocols in Nucleic Acid Chemistry* 68:1–4

Mueller, T. (2012). What is the Thalamus in Zebrafish? *Frontiers in Neuroscience* 6:64.

Müller, K., S. Hirano, L. Puelles and C. Redies (2004). OL-protocadherin expression in the visual system of the chicken embryo. *Journal of Comparative Neurology* 470:240–255

Mullis, K. B. and F. A. Faloona (1987). Specific synthesis of DNA in vitro via a polymerase-catalyzed chain reaction. *Methods in Enzymology* 155:335–350

Munderloh, C., G. P. Solis, V. Bodrikov, F. A. Jaeger, M. Wiechers, E. Málaga-Trillo and C. A. Stuermer (2009). Reggies/flotillins regulate retinal axon regeneration in the zebrafish optic nerve and differentiation of hippocampal and N2a neurons. *The Journal of Neuroscience* 29:6607–6615

Munton, R. P., S. Vizi and I. M. Mansuy (2004). The role of protein phosphatase-1 in the modulation of synaptic and structural plasticity. *FEBS Letters* 567:121–128

Münzel, E. J., C. G. Becker, T. Becker and A. Williams (2014). Zebrafish regenerate full thickness optic nerve myelin after demyelination, but this fails with increasing age. *Acta Neuropathologica Communications* 2:77

Murata, Y., S. Hamada, H. Morishita, T. Mutoh and T. Yagi (2004). Interaction with protocadherin-gamma regulates the cell surface expression of protocadherin-alpha. *The Journal of Biological Chemistry* 279:49508–49516

Murray, M. (1982). A quantitative study of regenerative sprouting by optic axons in goldfish. *Journal of Comparative Neurology* 209:352–362

Mutoh, T., S. Hamada, K. Senzaki, Y. Murata and T. Yagi (2004). Cadherin-related neuronal receptor 1 (CNR1) has cell adhesion activity with beta1 integrin mediated through the RGD site of CNR1. *Experimental Cell Research* 294:494–508

Myers, C. T., J. M. McMahon, A. L. Schneider, S. Petrovski, A. S. Allen, G. L. Carvill, M. Zemel, J. E. Saykally, A. J. LaCroix, E. L. Heinzen and others (2016). De novo mutations in SLC1A2 and CACNA1A are important causes of epileptic encephalopathies. *The American Journal of Human Genetics* 99:287–298

Nadal-Nicolas, F. M., P. Sobrado-Calvo, M. Jiménez-López, M. Vidal-Sanz and M. Agudo-Barriuso (2015). Long-term effect of optic nerve axotomy on the retinal ganglion cell layer. *Investigative Ophthalmology & Visual Science* 56:6095–6112

Nagashima, M., L. K. Barthel and P. A. Raymond (2013). A self-renewing division of zebrafish Müller glial cells generates neuronal progenitors that require N-cadherin to regenerate retinal neurons. *Development* 140:4510–4521

Nakamura, H., F. Chiambaretta, J. Sugar, V. Sapin and B. Y. Yue (2004). Developmentally regulated expression of KLF6 in the mouse cornea and lens. *Investigative Ophthalmology & Visual Science* 45:4327–4332

Nakao, S., A. Platek, S. Hirano and M. Takeichi (2008). Contact-dependent promotion of cell migration by the OL-protocadherin-Nap1 interaction. *The Journal of Cell Biology* 182:395–410

Narla, G., K. E. Heath, H. L. Reeves, D. Li, L. E. Giono, A. C. Kimmelman, M. J. Glucksman, J. Narla, F. J. Eng, A. M. Chan, A. C. Ferrari, J. A. Martignetti and S. L. Friedman (2001). KLF6, a candidate tumor suppressor gene mutated in

prostate cancer. *Science* 294:2563–2566

Narla, G., S. Kremer-Tal, N. Matsumoto, X. Zhao, S. Yao, K. Kelley, M. Tarocchi and S. Friedman (2007). In vivo regulation of p21 by the Kruppel-like factor 6 tumor-suppressor gene in mouse liver and human hepatocellular carcinoma. *Oncogene* 26:4428–4434

Nelson, W. J. and R. Nusse (2004). Convergence of Wnt, beta-catenin, and cadherin pathways. *Science* 303:1483–1487

Nicol, X., M. Bennis, Y. Ishikawa, G. C.-K. Chan, J. Reperant, D. R. Storm and P. Gaspar (2006). Role of the calcium modulated cyclases in the development of the retinal projections. *European Journal of Neuroscience* 24:3401–3414

Niklaus, S., L. Cadetti, C. M. vom Berg-Maurer, A. Lehnherr, A. L. Hotz, I. C. Forster, M. Gesemann and S. C. Neuhauss (2017). Shaping of signal transmission at the photoreceptor synapse by EAAT2 glutamate transporters. *eNeuro* 4

Nollet, F., P. Kools and F. Van Roy (2000). Phylogenetic analysis of the cadherin superfamily allows identification of six major subfamilies besides several solitary members. *Journal of Molecular Biology* 299:551–572

Noonan, J. P., J. Grimwood, J. Schmutz, M. Dickson and R. M. Myers (2004). Gene conversion and the evolution of protocadherin gene cluster diversity. *Genome Research* 14:354–366

Northcutt, R. G. (1983). Evolution of the optic tectum in ray-finned fishes. *Fish Neurobiology* 2:1–42

Northcutt, R. G. and M. F. Wullimann (1988). The visual system in teleost fishes: morphological patterns and trends. Pages 515–552. Sensory Biology of Aquatic Animals. Sensory Biology of Aquatic Animals

Northmore, D. (1991). Visual responses of nucleus isthmi in a teleost fish (*Lepomis macrochirus*). *Vision Research* 31:525–535

Northmore, D. (2011). Optic tectum. *Encyclopedia of Fish Physiology: From Genome to Environment. Elsevier*:131–142

Northmore, D. P. (2017). Holding visual attention for 400 million years: A model of tectum and torus longitudinalis in teleost fishes. *Vision Research* 131:44–56

Nose, A. and M. Takeichi (1986). A novel cadherin cell adhesion molecule: its expression patterns associated with implantation and organogenesis of mouse

embryos. *The Journal of Cell Biology* 103:2649–2658

Novince, Z., E. Azodi, J. Marrs, P. Raymond and Q. Liu (2003). Cadherin expression in the inner ear of developing zebrafish. *Gene Expression Patterns* 3:337–339

Oates, A. C., S. J. Pratt, B. Vail, Y. Yan, R. K. Ho, S. L. Johnson, J. H. Postlethwait and L. I. Zon (2001). The zebrafish klf gene family. *Blood* 98:1792–1801

Obata, S., H. Sago, N. Mori, J. M. Rochelle, M. F. Seldin, M. Davidson, T. St John, S. Taketani and S. T. Suzuki (1995). Protocadherin Pcdh2 shows properties similar to, but distinct from, those of classical cadherins. *Journal of Cell Science* 108:3765–3773

Obst-Pernberg, K., L. Medina and C. Redies (2001). Expression of R-cadherin and N-cadherin by cell groups and fiber tracts in the developing mouse forebrain: relation to the formation of functional circuits. *Neuroscience* 106:505–533

Oda, H. and M. Takeichi (2011). Structural and functional diversity of cadherin at the adherens junction. *The Journal of Cell Biology* 193:1137–1146

Okada, T. S. (1996). The path leading to the discovery of cadherin: In retrospect. *Development, Growth & Differentiation* 38:583–596

Okazaki, N., N. Takahashi, S. Kojima, Y. Masuho and H. Koga (2002). Protocadherin LKC, a new candidate for a tumor suppressor of colon and liver cancers, its association with contact inhibition of cell proliferation. *Carcinogenesis* 23:1139–1148

Olivier, G., M. Corton, D. Intartaglia, S. K. Verbakel, P. I. Sergouniotis, G. Le Meur, C.-M. Dhaenens, H. Naacke, A. Avila-Fernández, C. B. Hoyng and others (2021). Pathogenic variants in IMPG1 cause autosomal dominant and autosomal recessive retinitis pigmentosa. *Journal of Medical Genetics* 58:570–578

Onouchi, T., Y. Kishino-Kaneko, I. Kameshita, A. Ishida and N. Sueyoshi (2015). Regulation of Ca2+/calmodulin-dependent protein kinase phosphatase (CaMKP/PPM1F) by protocadher-gammaC5 (Pcdh-gammaC5). *Archives of Biochemistry and Biophysics* 585:109–120

Osterhout, J. A., N. Josten, J. Yamada, F. Pan, S. Wu, P. L. Nguyen, G. Panagiotakos, Y. U. Inoue, S. F. Egusa, B. Volgyi, T. Inoue, S. Bloomfield, B. Barres, D. Berson, D. Feldheim and A. Huberman (2011). Cadherin-6 mediates axon-target matching in a non-image-forming visual circuit. *Neuron*

71:632–639

Palmblad, M., C. V. Henkel, R. P. Dirks, A. H. Meijer, A. M. Deelder and H. P. Spaink (2013). Parallel deep transcriptome and proteome analysis of zebrafish larvae. *BMC Research Notes* 6:1–8

Pancho, A., T. Aerts, M. D. Mitsogiannis and E. Seuntjens (2020). Protocadherins at the Crossroad of Signaling Pathways. *Frontiers in Molecular Neuroscience* 13:117

Panula, P., Y.-C. Chen, M. Priyadarshini, H. Kudo, S. Semenova, M. Sundvik and V. Sallinen (2010). The comparative neuroanatomy and neurochemistry of zebrafish CNS systems of relevance to human neuropsychiatric diseases. *Neurobiology of Disease* 40:46–57

Park, K.-S. and B. M. Gumbiner (2015). Cadherin-6B is required for the generation of Islet-1-expressing dorsal interneurons. *Biochemical and Biophysical Research Communications* 459:504–508

Paukert, M., S. Sidi, C. Russell, M. Siba, S. W. Wilson, T. Nicolson and S. Gründer (2004). A family of acid-sensing ion channels from the zebrafish: widespread expression in the central nervous system suggests a conserved role in neuronal communication. *The Journal of Biological Chemistry* 279:18783–18791

Pearson, R., J. Fleetwood, S. Eaton, M. Crossley and S. Bao (2008). Krüppel-like transcription factors: a functional family. *The International Journal of Biochemistry & Cell Biology* 40:1996–2001

Peek, S. L., K. M. Mah and J. A. Weiner (2017). Regulation of neural circuit formation by protocadherins. *Cellular and Molecular Life Sciences* 74:4133–4157

Penberthy, W. T., E. Shafizadeh and S. Lin (2002). The zebrafish as a model for human disease. *Frontiers in Bioscience* 7:d1439–d1453

Peng, G. and M. Westerfield (2006). Lhx5 promotes forebrain development and activates transcription of secreted Wnt antagonists. *Development* 133:3191–3200

Peng, J. (2019). Gene redundancy and gene compensation: An updated view. *Journal of Genetics and Genomics* 46:329–333

Perry, V. (1981). Evidence for an amacrine cell system in the ganglion cell layer of the rat retina. *Neuroscience* 6:931–944

Pham, D. H., C. C. Tan, C. C. Homan, K. L. Kolc, M. A. Corbett, D. McAninch, A. H. Fox, P. Q. Thomas, R. Kumar and J. Gecz (2017). Protocadherin 19 (PCDH19) interacts with paraspeckle protein NONO to co-regulate gene expression with estrogen receptor alpha (ERalpha). *Human Molecular Genetics* 26:2042–2052

Phillips, G. R., H. Tanaka, M. Frank, A. Elste, L. Fidler, D. L. Benson and D. R. Colman (2003). gamma-protocadherins are targeted to subsets of synapses and intracellular organelles in neurons. *The Journal of Neuroscience* 23:5096–5104

Pieters, T., S. Goossens, L. Haenebalcke, V. Andries, A. Stryjewska, R. De Rycke, K. Lemeire, T. Hochepied, D. Huylebroeck, G. Berx, M. Stemmler, D. Wirth, J. Haigh, J. van Hengel and F. van Roy (2016). p120 Catenin-Mediated Stabilization of E-Cadherin Is Essential for Primitive Endoderm Specification. *PLoS Genetics* 12:e1006243

Piorkowska, K., K. Zukowski, K. Ropka-Molik, M. Tyra and A. Gurgul (2018). A comprehensive transcriptome analysis of skeletal muscles in two Polish pig breeds differing in fat and meat quality traits. *Genetics and Molecular Biology* 41:125–136

Piper, M., A. Dwivedy, L. Leung, R. S. Bradley and C. E. Holt (2008). NF-protocadherin and TAF1 regulate retinal axon initiation and elongation in vivo. *The Journal of Neuroscience* 28:100–105

Poss, K. D., M. T. Keating and A. Nechiporuk (2003). Tales of regeneration in zebrafish. *Developmental Dynamics* 226:202–210

Powis, Z., I. Petrik, J. Cohen, D. Escolar, J. Burton, C. van Ravenswaaij-Arts, D. Sival, A. Stegmann, T. Kleefstra, R. Pfundt, R. Chikarmane, A. Begtrup, R. Huether, S. Tang and D. Shinde (2018). De novo variants in KLF7 are a potential novel cause of developmental delay/intellectual disability, neuromuscular and psychiatric symptoms. *Clinical Genetics* 93:1030–1038

Prada, C., J. Puga, L. Pérez-Méndez, R. López and G. Ramirez (1991). Spatial and temporal patterns of neurogenesis in the chick retina. *European Journal of Neuroscience* 3:559–569

Presnell, J. S., C. E. Schnitzler and W. E. Browne (2015). KLF/SP transcription factor family evolution: expansion, diversification, and innovation in eukaryotes. *Genome Biology and Evolution* 7:2289–2309

Purves, D., G. Augustine and D. Fitzpatrick (2001). The retina. Neuroscience. Neuroscience

Qian, C. and F.-Q. Zhou (2020). Updates and challenges of axon regeneration in the mammalian central nervous system. *Journal of Molecular Cell Biology*

Que, L., D. Lukacsovich, W. Luo and C. Földy (2021). Transcriptional and morphological profiling of parvalbumin interneuron subpopulations in the mouse hippocampus. *Nature Communications* 12:1–15

Quigley, H. A., R. W. Nickells, L. A. Kerrigan, M. E. Pease, D. J. Thibault and D. J. Zack (1995). Retinal ganglion cell death in experimental glaucoma and after axotomy occurs by apoptosis. *Investigative Ophthalmology & Visual Science* 36:774–786

Radice, G. L., H. Rayburn, H. Matsunami, K. A. Knudsen, M. Takeichi and R. O. Hynes (1997). Developmental defects in mouse embryos lacking N-cadherin. *Developmental Biology* 181:64–78

Rashid, D., K. Newell, L. Shama and R. Bradley (2006). A requirement for NF-protocadherin and TAF1/Set in cell adhesion and neural tube formation. *Developmental Biology* 291:170–181

Rasmussen, J. P. and A. Sagasti (2016). Learning to swim, again: Axon regeneration in fish. *Experimental Neurology*

Rastogi, S. and D. A. Liberles (2005). Subfunctionalization of duplicated genes as a transition state to neofunctionalization. *BMC Evolutionary Biology* 5:1

Rattner, A., J. Chen and J. Nathans (2004). Proteolytic shedding of the extracellular domain of photoreceptor cadherin; Implications for outer segment assembly. *The Journal of Biological Chemistry* 279:42202–42210

Rattner, A., P. M. Smallwood, J. Williams, C. Cooke, A. Savchenko, A. Lyubarsky, E. N. Pugh and J. Nathans (2001). A photoreceptor-specific cadherin is essential for the structural integrity of the outer segment and for photoreceptor survival. *Neuron* 32:775–786

Raymond, P. A. (1985). Cytodifferentiation of photoreceptors in larval goldfish: delayed maturation of rods. *The Journal of Comparative Neurology* 236:90–105

Raymond, P. A., L. K. Barthel and G. A. Curran (1995). Developmental patterning of rod and cone photoreceptors in embryonic zebrafish. *The Journal of Comparative Neurology* 359:537–550

Raymond, P. A. and P. F. Hitchcock (2000). How the Neural Retina Regenerates. *Vertebrate Eye Development*:197–218

Redies, C. (1995). Cadherin expression in the developing vertebrate CNS: from neuromeres to brain nuclei and neural circuits. *Experimental Cell Research* 220:243–256

Redies, C. (2000). Cadherins in the central nervous system. *Progress in Neurobiology* 61:611–648

Redies, C., K. Engelhart and M. Takeichi (1993). Differential expression of N-and R-cadherin in functional neuronal systems and other structures of the developing chicken brain. *Journal of Comparative Neurology* 333:398–416

Redies, C., N. Hertel and C. A. Hübner (2012). Cadherins and neuropsychiatric disorders. *Brain Research* 1470:130–144

Redies, C., H. Inuzuka and M. Takeichi (1992). Restricted expression of N-and R-cadherin on neurites of the developing chicken CNS. *The Journal of Neuroscience* 12:3525–3534

Redies, C., F. Neudert and J. Lin (2011). Cadherins in cerebellar development: translation of embryonic patterning into mature functional compartmentalization. *The Cerebellum* 10:393–408

Redies, C. and M. Takeichi (1993). Expression of N-cadherin mRNA during development of the mouse brain. *Developmental Dynamics* 197:26–39

Redies, C. and M. Takeichi (1996). Cadherins in the developing central nervous system: an adhesive code for segmental and functional subdivisions. *Developmental Biology* 180:413

Redies, C., K. Vanhalst and F. Van Roy (2005). delta-Protocadherins: unique structures and functions. *Cellular and Molecular Life Sciences* 62:2840–2852

Reeves, H. L., G. Narla, O. Ogunbiyi, A. I. Haq, A. Katz, S. Benzeno, E. Hod, N. Harpaz, S. Goldberg, S. Tal-Kremer, F. Eng, M. Arthur, J. Martignetti and S. Friedman (2004). Kruppel-like factor 6 (KLF6) is a tumor-suppressor gene frequently inactivated in colorectal cancer. *Gastroenterology* 126:1090–1103

Reiss, K., T. Maretzky, I. G. Haas, M. Schulte, A. Ludwig, M. Frank and P. Saftig (2006). Regulated ADAM10-dependent ectodomain shedding of gamma-protocadherin C3 modulates cell-cell adhesion. *Journal of Biological Chemistry* 281:21735–21744

Resink, T. J., M. Philippova, M. B. Joshi, E. Kyriakakis and P. Erne (2009). Cadherins in cardiovascular disease. *Swiss Medical Weekly* 139:122–134

Ribeiro, M., K. Levay, B. Yon, A. C. Ayupe, Y. Salgueiro and K. K. Park (2020). Neural Cadherin Plays Distinct Roles for Neuronal Survival and Axon Growth under Different Regenerative Conditions. *eNeuro* 7

Richardson, R., N. Owen, M. Toms, R. M. Young, D. Tracey-White and M. Moosajee (2019). Transcriptome profiling of zebrafish optic fissure fusion. *Scientific Reports* 9:1–12

Riehl, R., K. Johnson, R. Bradley, G. B. Grunwald, E. Cornel, A. Lilienbaum and C. E. Holt (1996). Cadherin function is required for axon outgrowth in retinal ganglion cells in vivo. *Neuron* 17:837–848

Rinner, O., Y. V. Makhankov, O. Biehlmaier and S. C. Neuhauss (2005). Knockdown of cone-specific kinase GRK7 in larval zebrafish leads to impaired cone response recovery and delayed dark adaptation. *Neuron* 47:231–242

Robinson, G. and R. Madison (2004). Axotomized mouse retinal ganglion cells containing melanopsin show enhanced survival, but not enhanced axon regrowth into a peripheral nerve graft. *Vision Research* 44:2667–2674

Robinson, J., E. A. Schmitt and J. E. Dowling (1995). Temporal and spatial patterns of opsin gene expression in zebrafish (Danio rerio). *Visual Neuroscience* 12:895–906

Robinson, S. W., M. Fernandes and H. Husi (2014). Current advances in systems and integrative biology. *Computational and Structural Biotechnology Journal* 11:35–46

Robles, E. (2017). The power of projectomes: genetic mosaic labeling in the larval zebrafish brain reveals organizing principles of sensory circuits. *Journal of Neurogenetics* 31:61–69

Robles, E., E. Laurell and H. Baier (2014). The retinal projectome reveals brain-area-specific visual representations generated by ganglion cell diversity. *Current Biology* 24:2085–2096

Robu, M. E., J. D. Larson, A. Nasevicius, S. Beiraghi, C. Brenner, S. A. Farber and S. C. Ekker (2007). p53 activation by knockdown technologies. *PLoS Genetics* 3:e78–e78

Rodieck, R. (1979). Visual pathways. *Annual Review of Neuroscience* 2:193–225

Rokas, A. (2008). The origins of multicellularity and the early history of the genetic toolkit for animal development. *Annual Review of Genetics* 42:235–251

Rosenberg, U. B., C. Schröder, A. Preiss, A. Kienlin, S. Côté, I. Riede and H. Jäckle (1986). Structural homology of the product of the Drosophila Krüppel gene with Xenopus transcription factor IIIA. *Nature* 319:336

Rossi, A., Z. Kontarakis, C. Gerri, H. Nolte, S. Hölper, M. Krüger and D. Y. Stainier (2015). Genetic compensation induced by deleterious mutations but not gene knockdowns. *Nature* 524:230–233

Van Roy, F. (2012). Cadherins. *Encyclopedia of Signaling Molecules*:211–224

Van Roy, F. and G. Berx (2008). The cell-cell adhesion molecule E-cadherin. *Cellular and Molecular Life Sciences* 65:3756–3788

Ruan, G., D. Wedlich and A. Koehler (2006). Xenopus cadherin-6 regulates growth and epithelial development of the retina. *Mechanisms of Development* 123:881–892

Russek-Blum, N., H. Nabel-Rosen and G. Levkowitz (2009). High resolution fate map of the zebrafish diencephalon. *Developmental Dynamics* 238:1827–35

Sachse, S. M., S. Lievens, L. F. Ribeiro, D. Dascenco, D. Masschaele, K. Horré, A. Misbaer, N. Vanderroost, A. S. De Smet, E. Salta and others (2019). Nuclear import of the DSCAM-cytoplasmic domain drives signaling capable of inhibiting synapse formation. *The EMBO Journal* 38:e99669

Salatino-Oliveira, A., J. P. Genro, G. Polanczyk, C. Zeni, M. Schmitz, C. Kieling, L. Anselmi, A. M. B. Menezes, F. C. Barros, E. R. Polina, N. Mota, E. Grevet, C. Dotto Bau, L. Rohde and M. Hutz (2015). Cadherin-13 gene is associated with hyperactive/impulsive symptoms in attention/deficit hyperactivity disorder. *American Journal of Medical Genetics Part B: Neuropsychiatric Genetics* 168:162–169

Sanchez-Migallon, M., F. Valiente-Soriano, M. Salinas-Navarro, F. Nadal-Nicolas, M. Jimenez-Lopez, M. Vidal-Sanz and M. Agudo-Barriuso (2018). Nerve fibre layer degeneration and retinal ganglion cell loss long term after optic nerve crush or transection in adult mice. *Experimental Eye Research* 170:40–50

Sancisi, V., G. Gandolfi, M. Ragazzi, D. Nicoli, I. Tamagnini, S. Piana and A. Ciarrocchi (2013). Cadherin 6 is a new RUNX2 target in TGF-beta signalling pathway. *PLoS One* 8:e75489

Sano, K., H. Tanihara, R. L. Heimark, S. Obata, M. Davidson, T. St John, S. Taketani and S. Suzuki (1993). Protocadherins: a large family of cadherin-related molecules in central nervous system. *The EMBO Journal* 12:2249

Santana, S., E. P. Rico and J. S. Burgos (2012). Can zebrafish be used as animal model to study Alzheimer's disease? *American Journal of Neurodegenerative Disease* 1:32

Santoriello, C. and L. I. Zon (2012). Hooked! Modeling human disease in zebrafish. *The Journal of Clinical Investigation* 122:2337–2343

Saul, K. E. (2008). Differential Gene Expression in Danio rerio during Optic Nerve Regeneration

Schmalhofer, O., S. Brabletz and T. Brabletz (2009). E-cadherin, beta-catenin, and ZEB1 in malignant progression of cancer. *Cancer and Metastasis Reviews* 28:151–166

Schmidt, R., U. Strähle and S. Scholpp (2013). Neurogenesis in zebrafish - from embryo to adult. *Neural Development* 8:3

Schmitt, E. A. and J. E. Dowling (1996). Comparison of topographical patterns of ganglion and photoreceptor cell differentiation in the retina of the zebrafish, Danio rerio. *Journal of Comparative Neurology* 371:222–234

Schuck, J. B., M. E. Smith, X. Li and N. G. F. Cooper (2008). Microarray analysis of gene expression during auditory hair cell regeneration in zebrafish (*Danio rerio*). *BMC Bioinformatics* 9:P15

Schwab, M. and H. Thoenen (1985). Dissociated neurons regenerate into sciatic but not optic nerve explants in culture irrespective of neurotrophic factors. *The Journal of Neuroscience* 5:2415–2423

Schweitzer, J., D. Gimnopoulos, B. C. Lieberoth, H.-M. Pogoda, J. Feldner, A. Ebert, M. Schachner, T. Becker and C. G. Becker (2007). Contactin1a expression is associated with oligodendrocyte differentiation and axonal regeneration in the central nervous system of zebrafish. *Molecular and Cellular Neuroscience* 35:194–207

Seiler, C., K. C. Finger-Baier, O. Rinner, Y. V. Makhankov, H. Schwarz, S. C. Neuhauss and T. Nicolson (2005). Duplicated genes with split functions: independent roles of protocadherin15 orthologues in zebrafish hearing and vision. *Development* 132:615–623

Sharma, S. (1975). Development of the optic tectum in brown trout. Pages 411–417. Vision in Fishes. Springer

Sharma, T. P., C. M. McDowell, Y. Liu, A. H. Wagner, D. Thole, B. P. Faga, R. J. Wordinger, T. A. Braun and A. F. Clark (2014). Optic nerve crush induces spatial and temporal gene expression patterns in retina and optic nerve of

BALB/cJ mice. *Molecular Neurodegeneration* 9:14

Shibuya, Y., A. Mizoguchi, M. Takeichi, K. Shimada and C. Ide (1995). Localization of N-cadherin in the normal and regenerating nerve fibers of the chicken peripheral nervous system. *Neuroscience* 67:253–261

Shimizu, T., T. Yabe, O. Muraoka, S. Yonemura, S. Aramaki, K. Hatta, Y.-K. Bae, H. Nojima and M. Hibi (2005). E-cadherin is required for gastrulation cell movements in zebrafish. *Mechanisms of Development* 122:747–763

Shin, J. T. and M. C. Fishman (2002). From zebrafish to human: modular medical models. *Annual Review of Genomics and Human Genetics* 3:311–340

Simonneau, L., F. Broders and J.-P. Thiery (1992). N-cadherin transcripts in Xenopus laevis from early tailbud to tadpole. *Developmental Dynamics* 194:247–260

Skene, J. P. (1989). Axonal growth-associated proteins. *Annual Review of Neuroscience* 12:127–156

Slonim, D. K. and I. Yanai (2009). Getting started in gene expression microarray analysis. *PLoS Computational Biology* 5:e1000543

So, K.-F. and H. K. Yip (1998). Regenerative capacity of retinal ganglion cells in mammals. *Vision Research* 38:1525–1535

Soronen, P., H. Ollila, M. Antila, K. Silander, O. Palo, T. Kieseppa, J. Lonnqvist, L. Peltonen, A. Tuulio-Henriksson, T. Partonen and T. Paunio (2010). Replication of GWAS of bipolar disorder: association of SNPs near CDH7 with bipolar disorder and visual processing. *Molecular Psychiatry* 15:4–7

Sotomayor, M., R. Gaudet and D. P. Corey (2014). Sorting out a promiscuous superfamily: towards cadherin connectomics. *Trends in Cell Biology* 24:524–536

Sperry, R. (1948). Patterning of central synapses in regeneration of the optic nerve in teleosts. *Physiological Zoology* 21:351–361

Sperry, R. W. (1944). Optic nerve regeneration with return of vision in anurans. *Journal of Neurophysiology* 7:57–69

Squitti, R., M. De Stefano, D. Edgar and G. Toschi (1999). Effects of axotomy on the expression and ultrastructural localization of N-cadherin and neural cell adhesion molecule in the quail ciliary ganglion: an in vivo model of neuroplasticity. *Neuroscience* 91:707–722

Stainier, D. Y. R., E. Raz, N. D. Lawson, S. C. Ekker, R. D. Burdine, J. S. Eisen, P. W. Ingham, S. Schulte-Merker, D. Yelon, B. M. Weinstein, M. C. Mullins, S. W. Wilson, L. Ramakrishnan, S. L. Amacher, S. C. F. Neuhauss, A. Meng, N. Mochizuki, P. Panula and C. B. Moens (2017). Guidelines for morpholino use in zebrafish. *PLoS Genetics* 13:e1007000

Stenkamp, D. L. (2007). Neurogenesis in the fish retina. *International Review of Cytology* 259:173–224

Stenkamp, D. L., L. L. Cunningham, P. A. Raymond and F. Gonzalez-Fernandez (1998). Novel expression pattern of interphotoreceptor retinoid-binding protein (IRBP) in the adult and developing zebrafish retina and RPE. *Molecular Vision* 4:26

Stewart, A. M., O. Braubach, J. Spitsbergen, R. Gerlai and A. V. Kalueff (2014). Zebrafish models for translational neuroscience research: from tank to bedside. *Trends in Neurosciences* 37:264–278

Stoeckli, E. T. (2014). Protocadherins: Not Just Neuron Glue, More Too! *Developmental Cell* 30:643–644

Stone, K. and D. Sakaguchi (1996). Perturbation of the Developing Xenopus Retinotectal Projection Following Injections of Antibodies against beta 1 Integrin Receptors and N-cadherin. *Developmental Biology* 180:297–310

Stoya, G., C. Redies and N. Schmid-Hertel (2014). Inversion of layer-specific cadherin expression profiles and maintenance of cytoarchitectonic areas in the allocortex of the reeler mutant mouse. *Journal of Comparative Neurology* 522:3106–3119

Strehl, S., K. Glatt, Q. M. Liu, H. Glatt and M. Lalande (1998). Characterization of Two Novel Protocadherins (PCDH8andPCDH9) Localized on Human Chromosome 13 and Mouse Chromosome 14. *Genomics* 53:81–89

Streisinger, G., C. Walker, N. Dower, D. Knauber and F. Singer (1981). Production of clones of homozygous diploid zebra fish (*Brachydanio rerio*). *Nature* 291:293

Stuermer, C. (1988). Retinotopic organization of the developing retinotectal projection in the zebrafish embryo. *The Journal of Neuroscience* 8:4513–4530

Stuermer, C. A. O. (2010). The reggie/flotillin connection to growth. *Trends in Cell Biology* 20:6–13

Stuermer, C., B. Rohrer and H. Munz (1990). Development of the retinotectal projection in zebrafish embryos under TTX-induced neural-impulse blockade.

The Journal of Neuroscience 10:3615–3626

Sun, F. and Z. He (2010). Neuronal intrinsic barriers for axon regeneration in the adult CNS. *Current Opinion in Neurobiology* 20:510–518

Sun, X., J. Yi, J. Yang, Y. Han, X. Qian, Y. Liu, J. Li, B. Lu, J. Zhang, X. Pan and others (2021). An integrated epigenomic-transcriptomic landscape of lung cancer reveals novel methylation driver genes of diagnostic and therapeutic relevance. *Theranostics* 11:5346

Suo, L., H. Lu, G. Ying, M. R. Capecchi and Q. Wu (2012). Protocadherin clusters and cell adhesion kinase regulate dendrite complexity through Rho GTPase. *Journal of Molecular Cell Biology* 4:362–376

Suzuki, S. C. and M. Takeichi (2008). Cadherins in neuronal morphogenesis and function. *Development, Growth & Differentiation* 50:S119–S130

Suzuki, S., K. Sano and H. Tanihara (1991). Diversity of the cadherin family: evidence for eight new cadherins in nervous tissue. *Cell Regulation* 2:261–270

Suzuki, S. T. (1996). Protocadherins and diversity of the cadherin superfamily. *Journal of Cell Science* 109:2609–2611

Suzuki, S. T. (2000). Recent progress in protocadherin research. *Experimental Cell Research* 261:13–18

Suzuki, S. T. and S. Hirano (2016). The cadherin superfamily: key regulators of animal development and physiology. Springer

Tai, K., M. Kubota, K. Shiono, H. Tokutsu and S. T. Suzuki (2010). Adhesion properties and retinofugal expression of chicken protocadherin-19. *Brain Research* 1344:13–24

Takahashi, M. and N. Osumi (2008). Expression study of cadherin7 and cadherin20 in the embryonic and adult rat central nervous system. *BMC Developmental Biology* 8:87

Takeda, M., H. Kato, A. Takamiya, A. Yoshida and H. Kiyama (2000). Injury-specific expression of activating transcription factor-3 in retinal ganglion cells and its colocalized expression with phosphorylated c-Jun. *Investigative Ophthalmology & Visual Science* 41:2412–2421

Takeichi, M. (1977). Functional correlation between cell adhesive properties and some cell surface proteins. *The Journal of Cell Biology* 75:464–474

Takeichi, M. (1987). Cadherins: a molecular family essential for selective cell-cell adhesion and animal morphogenesis. *Trends in Genetics* 3:213–217

Takeichi, M. (1988). The cadherins: cell-cell adhesion molecules controlling animal morphogenesis. *Development* 102:639–655

Takeichi, M. (1990). Cadherins: a molecular family important in selective cell-cell adhesion. *Annual Review of Biochemistry* 59:237–252

Takeichi, M. (1991). Cadherin cell adhesion receptors as a morphogenetic regulator. *Science* 251:1451–1455

Takeichi, M. (2007). The cadherin superfamily in neuronal connections and interactions. *Nature Reviews Neuroscience* 8:11–20

Takeichi, M. (2018). Historical review of the discovery of cadherin, in memory of Tokindo Okada. *Development, Growth & Differentiation* 60:3–13

Tanaka, H., W. Shan, G. R. Phillips, K. Arndt, O. Bozdagi, L. Shapiro, G. W. Huntley, D. L. Benson and D. R. Colman (2000). Molecular modification of N-cadherin in response to synaptic activity. *Neuron* 25:93–107

Tang, R., A. Dodd, D. Lai, W. C. McNabb and D. R. Love (2007). Validation of zebrafish (*Danio rerio*) reference genes for quantitative real-time RT-PCR normalization. *Acta Biochimica et Biophysica Sinica* 39:384–390

Tanihara, H., K. Sano, R. L. Heimark, T. St. John and S. Suzuki (1994). Cloning of five human cadherins clarifies characteristic features of cadherin extracellular domain and provides further evidence for two structurally different types of cadherin. *Cell Communication & Adhesion* 2:15–26

Tarca, A. L., R. Romero and S. Draghici (2006). Analysis of microarray experiments of gene expression profiling. *American Journal of Obstetrics and Gynecology* 195:373–388

Taylor, S. M., K. Alvarez-Delfin, C. J. Saade, J. L. Thomas, R. Thummel, J. M. Fadool and P. F. Hitchcock (2015). The bHLH Transcription Factor NeuroD Governs Photoreceptor Genesis and Regeneration Through Delta-Notch SignalingNeuroD Regulation of Photoreceptor Genesis. *Investigative Ophthalmology & Visual Science* 56:7496–7515

Terakawa, Y. W., Y. U. Inoue, J. Asami, M. Hoshino and T. Inoue (2013). A sharp cadherin-6 gene expression boundary in the developing mouse cortical plate demarcates the future functional areal border. *Cerebral Cortex* 23:2293–2308

Tetreault, M.-P., Y. Yang and J. P. Katz (2013). Kruppel-like factors in cancer. *Nature Reviews Cancer* 13:701–713

Thisse, B., S. Pflumio, M. Fürthauer, B. Loppin, V. Heyer, A. Degrave, R. Woehl, A. Lux, T. Steffan, X. Charbonnier and C. Thisse (2001). Expression of the zebrafish genome during embryogenesis. *ZFIN Direct Data Submission (http://zfin. org)*

Thisse, B. and C. Thisse (2004). Fast release clones: a high throughput expression analysis. *ZFIN Direct Data Submission (http://zfin. org)*

Thornton, M., C. Mantovani, M. Birchall and G. Terenghi (2005). Quantification of N-CAM and N-cadherin expression in axotomized and crushed rat sciatic nerve. *Journal of Anatomy* 206:69–78

Thul, P. J., L. Akesson, M. Wiking, D. Mahdessian, A. Geladaki, H. A. Blal, T. Alm, A. Asplund, L. Björk, L. M. Breckels and others (2017). A subcellular map of the human proteome. *Science* 356

Toth, P. and C. Straznicky (1989). The morphological characterization and distribution of displaced ganglion cells in the anuran retina. *Visual Neuroscience* 3:551–61

Tsonis, P. (2000). Regeneration in vertebrates. *Developmental Biology* 221:273–84

Tuttle, M., M. R. Dalman, Q. Liu and R. L. Londraville (2019). Leptin-a mediates transcription of genes that participate in central endocrine and phosphatidylinositol signaling pathways in 72-hour embryonic zebrafish (*Danio rerio*). *PeerJ* 7:e6848

Uchida, N., Y. Honjo, K. R. Johnson, M. J. Wheelock and M. Takeichi (1996). The catenin/cadherin adhesion system is localized in synaptic junctions bordering transmitter release zones. *The Journal of Cell Biology* 135:767–779

Uemura, M., S. Nakao, S. T. Suzuki, M. Takeichi and S. Hirano (2007). OL-Protocadherin is essential for growth of striatal axons and thalamocortical projections. *Nature Neuroscience* 10:1151–1159

Vaithianathan, T., G. Zanazzi, D. Henry, W. Akmentin and G. Matthews (2013). Stabilization of spontaneous neurotransmitter release at ribbon synapses by ribbon-specific subtypes of complexin. *The Journal of Neuroscience* 33:8216–8226

Vajn, K., J. A. Plunkett, A. Tapanes-Castillo and M. Oudega (2013). Axonal regeneration after spinal cord injury in zebrafish and mammals: differences,

similarities, translation. *Neuroscience Bulletin* 29:402–410

Vanegas, H. (1983). Organization and physiology of the teleostean optic tectum. Pages 43–90. Fish Neurobiology. University of Michigan Press Ann Arbor, MI

VanGuilder, H. D., K. E. Vrana and W. M. Freeman (2008). Twenty-five years of quantitative PCR for gene expression analysis. *Biotechniques* 44:619–626

Vanhalst, K., P. Kools, K. Staes, F. Van Roy and C. Redies (2005). delta-Protocadherins: a gene family expressed differentially in the mouse brain. *Cellular and Molecular Life Sciences* 62:1247–1259

Varshney, G. K., J. Lu, D. E. Gildea, H. Huang, W. Pei, Z. Yang, S. C. Huang, D. Schoenfeld, N. H. Pho, D. Casero, T. Hirase, D. Mosbrook-Davis, S. Zhang, L. Jao, B. Zhang, I. Woods, S. Zimmerman, A. Schier, T. Wolfsberg, M. Pellegrini, S. Burgess and S. Lin (2013). A large-scale zebrafish gene knockout resource for the genome-wide study of gene function. *Genome Research* 23:727–735

Varshney, G. K., W. Pei, M. C. LaFave, J. Idol, L. Xu, V. Gallardo, B. Carrington, K. Bishop, M. Jones, M. Li, U. Harper, S. Huang, A. Prakash, W. Chen, R. Sood, J. Ledin and S. Burgess (2015). High-throughput gene targeting and phenotyping in zebrafish using CRISPR/Cas9. *Genome Research* 25:1030–1042

Veldman, M. B., M. A. Bemben and D. Goldman (2010). Tuba1a gene expression is regulated by KLF6/7 and is necessary for CNS development and regeneration in zebrafish. *Molecular and Cellular Neuroscience* 43:370–383

Veldman, M. B., M. A. Bemben, R. C. Thompson and D. Goldman (2007). Gene expression analysis of zebrafish retinal ganglion cells during optic nerve regeneration identifies KLF6a and KLF7a as important regulators of axon regeneration. *Developmental Biology* 312:596–612

Vesterlund, L., H. Jiao, P. Unneberg, O. Hovatta and J. Kere (2011). The zebrafish transcriptome during early development. *BMC Developmental Biology* 11:30

Vestweber, D. (2015). Cadherins in tissue architecture and disease. *Journal of Molecular Medicine* 93:5–11

Veth, K. N., J. R. Willer, R. F. Collery, M. P. Gray, G. B. Willer, D. S. Wagner, M. C. Mullins, A. J. Udvadia, R. S. Smith, S. W. M. John, R. G. Gregg and B. A. Link (2011). Mutations in zebrafish lrp2 result in adult-onset ocular pathogenesis that models myopia and other risk factors for glaucoma. *PLoS*

Genetics 7:e1001310

Vidal-Sanz, M., G. M. Bray, M. Villegas-Perez, S. Thanos and A. J. Aguayo (1987). Axonal regeneration and synapse formation in the superior colliculus by retinal ganglion cells in the adult rat. *The Journal of Neuroscience* 7:2894–2909

Vina, E., V. Parisi, C. Sanchez-Ramos, R. Cabo, M. C. Guerrera, L. M. Quirós, A. Germanà, J. A. Vega and O. Garc'ia-Suárez (2015). Acid-sensing ion channels (ASICs) 2 and 4.2 are expressed in the retina of the adult zebrafish. *Cell and Tissue Research* 360:223–231

Visel, A., C. Thaller and G. Eichele (2004). GenePaint. org: an atlas of gene expression patterns in the mouse embryo. *Nucleic Acids Research* 32:D552–D556

Vleminckx, K. and R. Kemler (1999). Cadherins and tissue formation: integrating adhesion and signaling. *Bioessays* 21:211–220

Wada, Y., J. Sugiyama, T. Okano and Y. Fukada (2006). GRK1 and GRK7: unique cellular distribution and widely different activities of opsin phosphorylation in the zebrafish rods and cones. *Journal of Neurochemistry* 98:824–837

Wang, F., D. Ren, X. Liang, S. Ke, B. Zhang, B. Hu, X. Song and X. Wang (2019). A long noncoding RNA cluster-based genomic locus maintains proper development and visual function. *Nucleic Acids Research* 47:6315–6329

Wang, K., H. Zhang, D. Ma, M. Bucan, J. T. Glessner, B. S. Abrahams, D. Salyakina, M. Imielinski, J. P. Bradfield, P. M. Sleiman, C. Kim, C. Hou, E. Frackelton, R. Chiavacci, N. Takahashi, T. Sakurai, E. Rappaport, C. Lajonchere, J. Munson, A. Estes, O. Korvatska, J. Piven, L. Sonnenblick, A. Retuerto, E. Herman, H. Dong, T. Hutman, M. Sigman, S. Ozonoff, A. Klin, T. Owley, J. Sweeney, C. Brune, R. Cantor, R. Bernier, J. Gilbert, M. Cuccaro, W. McMahon, J. Miller, M. State, T. Wassink, H. Coon, S. Levy, R. Schultz, J. Nurnberger Jr, J. Haines, J. Sutcliffe, E. Cook, N. Minshew, J. Buxbaum, G. Dawson, S. Grant, D. Geschwind, M. Pericak-Vance, G. Schellenberg and H. Hakonarson (2009). Common genetic variants on 5p14. 1 associate with autism spectrum disorders. *Nature* 459:528–533

Wang, Q., F. Marcucci, I. Cerullo and C. Mason (2016). Ipsilateral and contralateral retinal ganglion cells express distinct genes during decussation at the optic chiasm. *eNeuro* 3:ENEURO–0169

Wang, X., J. A. Weiner, S. Levi, A. M. Craig, A. Bradley and J. R. Sanes (2002). Gamma protocadherins are required for survival of spinal interneurons. *Neuron*

36:843–854

Wang, Y., W. Li, H. Jia, F. Zhai, W. Qu, Y. Cheng, Y. Liu, L.-X. Deng, S. Guo and Z. Jin (2017). KLF7-transfected Schwann cell graft transplantation promotes sciatic nerve regeneration. *Neuroscience* 340:319–332

Ward, A. C. and G. J. Lieschke (2002). The zebrafish as a model system for human disease. *Frontiers in Bioscience* 7:d827–d833

Webb, K. J., M. Coolen, C. J. Gloeckner, C. Stigloher, B. Bahn, S. Topp, M. Ueffing and L. Bally-Cuif (2011). The Enhancer of split transcription factor Her8a is a novel dimerisation partner for Her3 that controls anterior hindbrain neurogenesis in zebrafish. *BMC Developmental Biology* 11:1–19

Weiner, J. A., X. Wang, J. C. Tapia and J. R. Sanes (2005). Gamma protocadherins are required for synaptic development in the spinal cord. *Proceedings of the National Academy of Sciences* 102:8–14

Westerfield, M. (2007). The Zebrafish Book: A Guide for the Laboratory Use of Zebrafish Danio ("*Brachydanio Rerio*"). (Westerfield, M, Ed.). Fifth edition. University of Oregon, Fifth edition.

Wheelock, M. J. and K. R. Johnson (2003). Cadherins as modulators of cellular phenotype. *Annual Review of Cell and Developmental Biology* 19:207–235

Williams, J. S. (2018). The role of pcdh10a and pcdh10b in zebrafish melanocyte migration

Wilson, A. L. (2007). Cadherin4 Function in the Development of Zebrafish Cranial Ganglia and Lateral Line System

Wolverton, T. and M. Lalande (2001). Identification and characterization of three members of a novel subclass of protocadherins. *Genomics* 76:66–72

Wong, M. L. and J. F. Medrano (2005). Real-time PCR for mRNA quantitation. *Biotechniques* 39:75

Wu, J. and D. Kim (2016). Transcriptomics and gene regulation. Springer

Wu, Q. (2005). Comparative genomics and diversifying selection of the clustered vertebrate protocadherin genes. *Genetics* 169:2179–2188

Wu, Q. and Z. Jia (2020). Wiring the brain by clustered protocadherin neural codes. *Neuroscience Bulletin*:1–15

Wu, Q. and T. Maniatis (1999). A striking organization of a large family of human neural cadherin-like cell adhesion genes. *Cell* 97:779–90

Wulliman, M. F., B. Rupp and H. Reichert (2012). Neuroanatomy of the zebrafish brain: a topological atlas. Birkhäuser

Wullimann, M. F. (2020). Neural origins of basal diencephalon in teleost fishes: Radial versus tangential migration. *Journal of Morphology* 281:1133–1141

Wurtz, R. and E. Kandel (2006). The Retina Projects to Subcortical Regions in the Brain

Wyatt, C. (2011). Optic axon guidance during development and regeneration in the zebrafish

Wöhrn, J.-C., S. Nakagawa, M. Ast, M. Takeichi and C. Redies (1999). Combinatorial expression of cadherins in the tectum and the sorting of neurites in the tectofugal pathways of the chicken embryo. *Neuroscience* 90:985–1000

Wöhrn, J.-C., L. Puelles, S. Nakagawa, M. Takeichi and C. Redies (1998). Cadherin expression in the retina and retinofugal pathways of the chicken embryo. *Journal of Comparative Neurology* 396:20–38

Xiang, Y.-Y., M. Tanaka, M. Suzuki, H. Igarashi, E. Kiyokawa, Y. Naito, Y. Ohtawara, Q. Shen, H. Sugimura and I. Kino (1994). Isolation of complementary DNA encoding K-cadherin, a novel rat cadherin preferentially expressed in fetal kidney and kidney carcinoma. *Cancer Research* 54:3034–3041

Xu, L., P. A. Overbeek and L. W. Reneker (2002). Systematic analysis of E-, N- and P-cadherin expression in mouse eye development. *Experimental Eye Research* 74:753–760

Xue, Y., S. Gao and F. Liu (2015). Genome-wide analysis of the zebrafish Klf family identifies two genes important for erythroid maturation. *Developmental Biology* 403:115–127

Yagi, T. (2008). Clustered protocadherin family. *Development, Growth & Differentiation* 50:S131–S140

Yagi, T. and M. Takeichi (2000). Cadherin superfamily genes: functions, genomic organization, and neurologic diversity. *Genes & Development* 14:1169–1180

Yamagata, M., J. A. Weiner, C. Dulac, K. A. Roth and J. R. Sanes (2006). Labeled lines in the retinotectal system: markers for retinorecipient sublaminae and the retinal ganglion cell subsets that innervate them. *Molecular and*

Cellular Neuroscience 33:296–310

Yamashita, H., S. Chen, S. Komagata, R. Hishida, T. Iwasato, S. Itohara, T. Yagi, N. Endo, M. Shibata and K. Shibuki (2012). Restoration of contralateral representation in the mouse somatosensory cortex after crossing nerve transfer. *PLoS One* 7:e35676

Yan, X., J. Lukas, J. Lin, M. Ernst, D. Koczan, M. Witt, G. Fuellen, A. Wree, A. Rolfs and J. Luo (2014). Aberrant expressions of delta-protocadherins in the brain of Npc1 mutant mice. *Histology and Histopathology* 29:1185–1199

Yasuda, S., H. Tanaka, H. Sugiura, K. Okamura, T. Sakaguchi, U. Tran, T. Takemiya, A. Mizoguchi, Y. Yagita, T. Sakurai, E. De Robertis and K. Yamagata (2007). Activity-induced protocadherin arcadlin regulates dendritic spine number by triggering N-cadherin endocytosis via TAO2-beta and p38 MAP kinases. *Neuron* 56:456–471

Yin, K.-J., M. Hamblin, Y. Fan, J. Zhang and Y. E. Chen (2015). Krüpple-like factors in the central nervous system: novel mediators in Stroke. *Metabolic Brain Disease* 30:401–410

Yin, Y., Q. Cui, Y. Li, N. Irwin, D. Fischer, A. R. Harvey and L. I. Benowitz (2003). Macrophage-derived factors stimulate optic nerve regeneration. *The Journal of Neuroscience* 23:2284–2293

Yin, Y., S. De Lima, H.-Y. Gilbert, N. J. Hanovice, S. L. Peterson, R. M. Sand, E. G. Sergeeva, K. A. Wong, L. Xie and L. I. Benowitz (2019). Optic nerve regeneration: A long view. *Restorative Neurology and Neuroscience* 37:525–544

Yoshida, C. and M. Takeichi (1982). Teratocarcinoma cell adhesion: identification of a cell-surface protein involved in calcium-dependent cell aggregation. *Cell* 28:217–224

Yoshida, K. and S. Sugano (1999). Identification of a novel protocadherin gene (PCDH11) on the human XY homology region in Xq21. 3. *Genomics* 62:540–543

Yoshida, K., M. Watanabe, H. Kato, A. Dutta and S. Sugano (1999). BH-protocadherin-c, a member of the cadherin superfamily, interacts with protein phosphatase 1 alpha through its intracellular domain. *FEBS Letters* 460:93–98

Yoshida, K., K. Yoshitomo-Nakagawa, N. Seki, M. Sasaki and S. Sugano (1998). Cloning, expression analysis, and chromosomal localization of BH-protocadherin (PCDH7), a novel member of the cadherin superfamily.

Genomics 49:458–461

Yoshitake, K., H. Tsukano, M. Tohmi, S. Komagata, R. Hishida, T. Yagi and K. Shibuki (2013). Visual map shifts based on whisker-guided cues in the young mouse visual cortex. *Cell Reports* 5:1365–1374

Yu, J., S. Koujak, S. Nagase, C. Li, T. Su, X. Wang, M. Keniry, L. Memeo, A. Rojtman, M. Mansukhani, H. Hibshoosh, B. Tycko and R. Parsons (2008). PCDH8, the human homolog of PAPC, is a candidate tumor suppressor of breast cancer. *Oncogene* 27:4657–4665

Yuan, J. S., J. Burris, N. R. Stewart, A. Mentewab and C. N. Stewart (2007). Statistical tools for transgene copy number estimation based on real-time PCR. Pages 1–12. BMC Bioinformatics

Zang, J., J. Keim, E. Kastenhuber, M. Gesemann and S. C. Neuhauss (2015). Recoverin depletion accelerates cone photoresponse recovery. *Open Biology* 5:150086

Zhang, J., G. J. Woodhead, S. K. Swaminathan, S. R. Noles, E. R. McQuinn, A. J. Pisarek, A. M. Stocker, C. A. Mutch, N. Funatsu and A. Chenn (2010). Cortical neural precursors inhibit their own differentiation via N-cadherin maintenance of beta-catenin signaling. *Developmental Cell* 18:472–9

Zhang, X., J. G. Abreu, C. Yokota, B. T. MacDonald, S. Singh, K. L. A. Coburn, S.-M. Cheong, M. M. Zhang, Q.-Z. Ye, H. C. Hang, H. Steen and X. He (2012). Tiki1 is required for head formation via Wnt cleavage-oxidation and inactivation. *Cell* 149:1565–77

Zhao, X., C. Monson, C. Gao, V. Gouon-Evans, N. Matsumoto, K. C. Sadler and S. L. Friedman (2010). Klf6/copeb is required for hepatic outgrowth in zebrafish and for hepatocyte specification in mouse ES cells. *Developmental Biology* 344:79–93

Zhou, H., X. Wang, J. Lin, Z. Zhao and C. Chang (2020). Distribution of Cadherin in the Parahippocampal Area of Developing Domestic Chicken Embryos. *Experimental Neurobiology* 29:11–26

Zimmer, A. M., Y. K. Pan, T. Chandrapalan, R. W. Kwong and S. F. Perry (2019). Loss-of-function approaches in comparative physiology: is there a future for knockdown experiments in the era of genome editing? *Journal of Experimental Biology* 222

Zou, S., C. Tian, S. Ge and B. Hu (2013). Neurogenesis of retinal ganglion cells is not essential to visual functional recovery after optic nerve injury in adult

zebrafish. *PLoS One* 8:e57280

Zupanc, G. K. H. and R. F. Sîrbulescu (2011). Adult neurogenesis and neuronal regeneration in the central nervous system of teleost fish. *The European Journal of Neuroscience* 34:917–929

ABBREVIATIONS

A	anterior thalamic nucleus
APN	accessory pretectal nucleus
atgMO	translation-blocking morpholino oligo
ATN	anterior tuberal nucleus
BNSM	the bed nucleus of the stria medullaris
BP	biological process (Gene Ontology)
CB	cerebellar body
CC	cerebellar crest
CC	cellular component (Gene Ontology)
CCe	corpus cerebelli
cdh(s)	cadherin(s)
CNS	central nervous system
CO	optic chiasm
CP	central posterior thalamic nucleus
CPN	central pretectal nucleus
Cpop	postoptic commissure
d	day
D	dorsal telencephalic area

Dc	central zone of dorsal telencephalic area
DEG(s)	differentially expressed gene(s)
DIL	diffuse nucleus of the inferior lobe
DiV	diencephalic ventricle
Dl	lateral zone of dorsal telencephalic area
dLGN	dorsal lateral geniculate nucleus
Dm	medial zone of dorsal telencephalic area
DOT	dorsomedial optic tract
DP	dorsal posterior thalamic nucleus
Dp	posterior zone of dorsal telencephalic area
dpf	days post fertilization
dsRGC	direction-selective retinal ganglion cells
E	embryonic (day)
EN	entopeduncular nucleus
ENd	entopeduncular nucleus, dorsal part
ENv	entopeduncular nucleus, ventral part
EC domain	extracellular domain
Fr	fasciculus retroflexus
GC	griseum centrale
gcl	ganglion cell layer
GO	Gene Ontology
Ha	Habenula
Had	dorsal habenular nucleus

HAV	ventral habenular nucleus
Hd	dorsal zone of periventricular hypothalamus
hpf	hours post fertilization
Hv	ventral zone of periventricular hypothalamus
Hy	hypothalamus
I	intermedial thalamic nucleus
IACUC	Institutional Animal Care and Use Committee
IC	intercalated nucleus
IC domain	intracellular (cytoplasmic) domain
IL	inferior lobe of hypothalamus
inl	inner nuclear layer
ipl	inner plexiform layer
Klf(s)	Krüppel-like factor(s)
le	lens
LC	locus coeruleus
LGN	lateral geniculate nucleus
LFB	lateral forebrain bundle
LH	lateral hypothalamic nucleus
LLF	lateral longitudinal fascicle
LX	vagal lobe
MF	molecular function (Gene Ontology)
MO	medulla oblongata (anatomical term)
MO	morpholino oligo

MS	spinal cord
MT	middle temporal visual area (V5)
mTP	migrated nucleus of the posterior tuberculum
nbl	neuroblast layer
NI	nucleus isthmi
NLV	lateral valvular nucleus
OB	olfactory bulb
ON	optic nerve
onl	outer nuclear layer
ONL	optic nerve lesion
opl	outer plexiform layer
OT	optic tract
P	postnatal (day)
pcdh(s)	protocadherin(s)
pg	pineal gland
PGa	anterior preglomerular nucleus
PGl	lateral preglomerular nucleus
Pit	pituitary
PNS	peripheral nervous system
PO	posterior pretectal nucleus
PPa	parvocellular preoptic nucleus, anterior part
PPd	periventricular pretectal nucleus, dorsal part
PPp	parvocellular preoptic nucleus, posterior part

PPv	periventricular pretectal nucleus, ventral part
PSm	magnocellular superficial pretectal nucleus
PSp	parvocellular superficial pretectal nucleus
RGC	retinal ganglion cell
rpe	retinal pigment epithelium
RV	rhombencephalic ventricle
sMO	splice-blocking morpholino oligo
SAC	stratum album central
SC	superior colliculus
SCN	suprachiasmatic nucleus
SFGS	stratum fibrosum et griseum superficial
SGC	stratum griseum central
SM	stratum marginale
SO	stratum opticum
SPV	stratum periventriculare
SR	superior raphe
SRF	superior reticular formation
SY	sulcus ypsiloniformis
Tel	telencephalon
TeO	optic tectum
TeV	tectal ventricle
TF	transcription factor
TH	hypothalamus, pars tuberalis

TL	torus longitudinalis
TM domain	transmembrane domain
TPM	pretectomamillary tract and nucleus
TPp	periventricular nucleus of posterior tuberculum
TSc	central nucleus of torus semicircularis
TSvl	ventrolateral nucleus of torus semicircularis
Vam	medial division of the valvula cerebelli
V1	primary visual cortex, visual cortex 1
V2	secondary visual cortex, visual cortex 2
V5	middle temporal visual area (MT), visual cortex 5
VAO	ventral accessory optic nucleus
Vc	central nucleus of ventral telencephalic area
Vd	dorsal nucleus of ventral telencephalic area
VIII	octaval nerve
VL	ventrolateral thalamic nucleus
VM	ventromedial thalamic nucleus
VOT	ventrolateral optic tract
Vp	posterior nucleus of ventral telencephalic area
Vv	ventral nucleus of ventral telencephalic area
w	week
X	vagal nerve
ZL	zona limitans

APPENDICES

APPENDIX A

THE INSTITUTIONAL ANIMAL CARE AND USE COMMITTEE (IACUC)

APPROVAL OF THE PROTOCOL TO STUDY CDHS AND KLFS IN ADULT

ZEBRAFISH

For IACUC Use Only		
Category:	Special Considerations:	Protocol #: 15-07-08-LFD

REQUEST TO USE ANIMALS

1. PROTOCOL SUMMARY

1. A. Protocol Title:

Study cadherins expression and function in the normal and regenerating adult zebrafish central nervous system

1. B. Principal Investigator's Institution:

University of Akron

1. C. Facility(ies) where animals will be housed: *If animals will be housed in a facility not listed below, please identify the location under "OTHER LOCATION".*

UNIVERSITY OF AKRON	☒	SUMMA HEALTH SYSTEM	☐
KENT STATE UNIVERSITY		YOUNGSTOWN STATE UNIVERSITY	
Cunningham	☐	Cushwa	☐
Kent	☐	DeBartolo	☐
Tuscawaras	☐	Ward Beecher	☐
NEOMED	☐	OTHER	☐

OTHER LOCATION (Institution, building & room OR geographic location for field studies):

N/A

1. D. Source of funding for the project:

INTERNAL ☐
EXTERNAL ☒

For external awards, identify the agency(ies) and award number(s).

National Eye Institute

1. E. Anticipated start date:

Sep. 27, 2015

1. F. Expected animal use over the three year approval period: *Summarize all animal use by species.*

Species	Number	Source
Zebrafsih, Danio rerio	550 adult fish	In house and commercial sources

271

1. G. If this protocol is a continuation of a previously approved protocol, indicate the protocol number and provide a brief summary of the progress made to date. *Your response is limited to the space provided.*   **N/A:**

Previous protocol number:

12-9A

Brief summary of progress/results:

We have been studying expression of two classical cadherins (cdh6 and cdh7) and two protocadherins (pcdh17 and pcdh17) in normal and regenerating adult zebrafish central nervous system (CNS) using in situ hybridization method. Our results show that these cadherins exhibit distinct expression patterns in normal adult zebrafish CNS, with the two classical cadherins (cdhs) showing much restricted expression domains and weak staining intensities, while the two protocadherins (pcdhs) showing wide expression domains and strong staining intensities. Their expression become increased in the retina and some visual structures in the brain following optic nerve crush, with both classical cdhs showing increased expression in the retina, while the two pcdhs showing decreased expression in the retina. We have been working to confirm these results using quantitative real-time RT-PCR (qPCR) method.

We have also been studying cadherin-2 (cdh2) function in the regeneration of the zebrafish optic nerve (cdh2 expression was studied in 2002 by our lab) using morpholino anti-sense oligonucleotide (MO) technology. Our data show that blocking cdh2 function using a zebrafish specific MO severely disrupted the optic nerve regeneration. We have been working on identifying molecular pathways that maybe involved in this cdh2-mediated optic nerve regeneration.

1. H. Project overview. *The response MUST be in lay terminology and understandable to a person with no scientific background.*

(1) Describe the medical condition, scientific question, or teaching value that is being addressed and its importance.

Cadherins are calcium-dependent adhesion molecules that have important roles in tissue development and maintenance throughout the lifespan of an organism in many organisms including humans. More than 100 cadherins have been identified, and they are grouped into several types, based mainly on their amino acid sequences and genomic organization, including classical cadherins and protocadherins. Classical cadherins (e.g. cadherin-1 and cadherin-2) are the most studied and understood, while much less is known about protocadherins (pcdhs, e.g. pcdh9 and pcdh17) expression and function. Even for classical cadherins, efforts have been mostly focused on their functions during embryonic development, knowledge of their expression and function in adult nervous system is very limited. There is even less information on cadherin function during nervous tissue regeneration. Mutations of cadherins contribute to Usher syndrome (deafness and vision loss; e.g. cadherin-23 and pcdh15), epilepsy (e.g. pcdh19), autism (e.g. cadherin-10, pcdh19), bipolar disease and Schizophrenia (e.g. cadherin-7). Therefore information about cadherins expression in adult nervous system is critical for us to study their functions in the system. It has become common knowledge that recovery from central nervous system (CNS) injuries (e.g. to retina and spinal cord) is very limited in humans and other mammals. However, similar injuries in fish and amphibians usually result in complete recovery. One of the key reasons for the difference is that fish and amphibians can drastically increase expression of some developmentally important genes, including cadherins, during CNS regeneration, while there is little or no change in expression of these genes during regeneration in mammals. Identification of differentially expressed genes during CNS regeneration in model organisms (e.g. zebrafish) may lead to development of potential therapeutic strategies. The retina is part of the CNS, and has been used as a model organ (due to its peripheral localization and simpler organization) to study CNS development and function. Zebrafish (Danio rerio) has become a leading model organism to study animal development, physiology and molecular biology due mainly to its experimental advantages such as low cost, ease of maintenance and manipulating gene expression, and fully sequenced and annotated genome. Zebrafish retina is similarly organized as other vertebrate animals including humans. Moreover, studies have shown that similar molecular mechanisms underlying animal development and function.

We have been using this project as an opportunity to train both graduate and undergraduate students doing research. The students learn techniques involved in the project, as well as reasons of conducting the research, anatomy of the vertebrate visual systems. They have also learned how to generate hypothesis, looking up background information, collecting data, critically analyzing the results, making figures, making posters, and learning how to write scientific papers.

274

(2) List the goals of the project.

We propose to study: 1) cadherins expression in normal and regenerating adult zebrafish retina and brain; 2) cadherin function in regenerating zebrafish retina. These goals can be achieved only by using adult zebrafish.

(3) Provide a chronological summary of the animal use from the beginning of the project through its end. *A lay description of the experimental design can be used as the response IF it addresses the intent of the question. Do not provide detailed descriptions of the procedures here.*

The adult zebrafish (550) will come from either our in house colonies or commercial suppliers. The fish will be maintained in 5- or 10-gallon glass tanks (15 fish/tank for 5-gallon tanks, 30 fish/tank for 10-gallon tanks). The animals will be anesthetized in tricain (MS222, 0.03%) before surgical procedures.. After killing the fish (by an overdose of tricain, 0.06% followed by cervical transectioning), eye and brain tissues will be removed and placed on dry ice (for isolation total RNA) or fixed in 4% paraformaldehyde (for in situ hybridization) Standard procedures for tissue sectioning will be used to obtain brain or retinal sections,while Trizol reagent method will be used for isolating total RNAs. For regeneration studies, fish will be anesthetized,in tricain, the left optic nerve will be crushed using a pair of forceps. The operated animals will be returned to their tanks to recover for various time points (e.g. I week). For studying cadherin function during retinal regeneration, a morpholino antisense oligonucleotide (MO), a reagent specifically reduces function of a particular gene (e.g. a cadherin MO), will be introduced into the regenerating retina using electroporation (using current to drive the MO into cells) method. These are established methods for delivering DNA, RNA or MOs to adult animals including zebrafish. After specific time (e.g. 3-day), the animals will be treated as described above (for obtaining retinal and brain tissues from normal fish). Extent of retinal regeneration will be compared between normal regeneration (without cadherin MO) and MO treated regeneration histologically (on tissue sections), immunologically (using retinal markers), and/or molecularly (e.g. reverse transcriptase qPCR, RNA sequencing).

2.   DESCRIPTION OF PROCEDURES INVOLVING LIVE ANIMALS

Please review all parts of this section before answering because there are separate parts for specific types of animal use. Each part will expand to accommodate the response. Mark N/A for sections that do not apply.

2. A. Animal Identification:
Indicate how animals will be identified. Multiple methods may be selected.

CAGE CARD	☐	COLLAR/TAG	☐
EAR PUNCH/NOTCH	☐	EAR TAG	☐
INDELIBLE MARKER	☐	MICROCHIP	☐
TATTOO	☐	OTHER (describe below)	☒

Describe the identification procedure if it involves penetration of the skin. Toe clipping is discouraged and, if it is used, a justification must be provided.

No specific animal ID procedure on individual fish will be needed. Operated fish will be separately kept in labeled tanks.

2. B. Breeding: N/A:
Describe the breeding scheme that will be used. Indicate weaning age of offspring.

N/A

2. C. *Genotyping:*   N/A:
Describe the method used to genotype the animals. Include the amount of tissue taken, age of animals, method of analgesia, and method of instrument sterilization.

N/A

2. D. Experimental manipulations: N/A:
List and describe in detail all nonsurgical experimental manipulations carried out on live animals. Euthanasia is to be described in 2.F. The response must include a statement of the known or expected impact of each procedure on animal well-being.

The anesthetized fish will be caught using a small fish net, placed on a piece of wet paper towel, and partially covered (with the head and eye exposed) by the paper towel.

2. E Surgical manipulations.   N/A:
2.E.(1) Description of surgical procedures:
Describe each surgical procedure under a separate heading. Procedures that are performed on the same animal at the same time may be described as one procedure. IF more than four different surgeries are planned, then similar ones may be combined into a single response.
Surgical procedure #1:
Is the surgical procedure a survival procedure?   **Yes:X**   **No:**

Describe the procedure in detail. Include the pre-operative preparation of the animal, a description of the aseptic technique and how instruments and implantable devices are sterilized. The response must include a statement of the known or expected impact of the procedure on animal well-being.

For each surgery, an anesthetized fish (0.03% tricain) will be placed in a petri-dish (the fish will be partially submerged in fish tank water supplemented with 0.01% tricain) with its right side laying down and the body and tail covered with wet paper towel. The posterior part of the left eye will be partially pulled out of the eye socket to expose the optic nerve. A fine-tipped pair of forceps will be used to crush the optic nerve. This surgery usually takes about 2 min. After the surgery, the animal will be quickly returned to a recovery container with fish tank water supplemented with 0.005% tricain. The next day, the operated fish will be moved to a labeled fish tank. If the fish will be used for studying cadherin gene expression or regenerating marker gene expression, after specific survival time (e.g. 1-week), the fish will be anesthetized again, killed by a cervical transaction for harvesting tissues. If the fish will be used for studying cadherin function in optic nerve regeneration, after 1-3 days of recovery, the fish will be anesthetized again and placed in a petri-dish as described above. A small cut will be made on the cornea, and 0.5 ul of MO will be injected into the left eye using a 5 ul Hamilton syringe. This will be followed by electroporation of the MO into eye cells using a square wave electroporator (67 volts, 2X, 50 ms each, separated by 1 sec pause). Post-surgery treatments will be the same as described above, and the fish will be kept for various periods of survival time (e.g. 1-week). At the end of the survival time, the fish will be anesthetized, killed, tissue harvested as described above. These tissues will be processed for total RNA isolation, in situ hybridization or immunohistochemistry. The optic nerve crush will result in a temporary loss of vision on the left eye. It takes about 1 week for the regenerating retinal axons to reach their brain targets. Operated fish usually adjust quickly and resume feeding within 10 min. of surgery. All surgical tools will be treated with 70% ethanol before each procedure. To study cadherins function in fish optic nerve regeneration, two surgical procedures will be performed. Performing two surgical procedures (optic nerve crush followed by injection of MO and electroporation of the injected MO) on the same animal is necessary because one of the major goals of the project is to find out whether or not cadherins are involved in the optic regenerating process. Application of cadherin MOs (to block cadherins function) via injection and electroporation of MOs to the same eye of the same fish with the optic nerve crushed is a necessary and efficient way to achieve this goal. The fish with its left optic nerve crushed will have one to several days of recovery before the next surgery. Those fish with two surgeries will be allowed to survived one to several (e.g. 3) weeks.

Surgical procedure #2:

Is the surgical procedure a survival procedure?   **Yes:**   **No:**

Description of procedure (instructions as above):

Surgical procedure #3:

Is the surgical procedure a survival procedure?   **Yes:**   **No:**

Description of procedure (instructions as above):

Surgical procedure #4:

Is the surgical procedure a survival procedure?   **Yes:**   **No:**

Description of procedure (instructions as above):

2.E.(2) Multiple major survival surgery:

*Does this project involve multiple major survival surgeries in the same animal?*YES: NO: X
If so, provide a justification.

Optic nerve crush and electroporation are not major surgeries

2. F. Anesthesia/Sedation.   N/A:

List the procedures that require anesthesia or sedation individually below and describe the anesthetic regimen used for each. If multiple procedures use the same anesthetic regimen, then they can be combined into one response.

Anesthesia/sedation procedure #1:

Identify the procedure requiring anesthesia or sedation. List all drugs (including neuromuscular blocking agents) used as part of the anesthetic/sedative regimen; include the dose, route of administration and indicate the frequency of repeat dosing. If animals will be anesthetized with inhalants, indicate the percentage of anesthetic gas, any auxiliary gases used, oxygen flow rate and ventilatory parameters (for mechanically ventilated animals).

The adult fish will be anesthetized in Tricain (0.03%) for anesthetization before each surgery and sacrifice. It usually takes about 5 minutes for the fish to loss its equilibrium and become "non-responsive". Fish used for obtaining normal tissues will be anesthetized once. Fish used for optic nerve crush will be anesthetized twice, while fish used for studying cadherin function in optic nerve regeneration will be anesthetized three times.

Describe the procedures and equipment used to monitor the depth of anesthesia and animal well-being. If neuromuscular blocking agents are used, include techniques that are reliable in paralyzed animals.

An anesthetized fish loses its equilibrium, has much reduced rate of breathing (10-15/min.) and does not respond to touching (with a pair of forceps).

Describe the supportive measures to assure animal well-being while under anesthesia.

Anesthetized fish will be handled with care. They are placed in a wet environment with the head partially submerged in fish tank water supplemented with 0.01% tricain, and body wrapped in wet paper towel. Surgeries will be promptly performed (2 min. for optic nerve crush; 2 min. for MO injection; 1 min. for electroporation) to minimize the animals surgery time. All operated animals will be immediately placed back into a recovery container with low concentration of tricain (0.005%) overnight before returning to labeled fish tanks.

Anesthesia/sedation procedure #2:

Identify the procedure requiring anesthesia/sedation and describe the anesthetic regimen as indicated above.

Procedures and equipment used to monitor the depth of anesthesia and animal well-being:

Supportive measures:

Anesthesia/sedation procedure #3:
Identify the procedure requiring anesthesia/sedation and describe the anesthetic regimen as indicated above.

Procedures and equipment used to monitor the depth of anesthesia and animal well-being:

Supportive measures:

Anesthesia/sedation procedure #4:
Identify the procedure requiring anesthesia/sedation and describe the anesthetic regimen as indicated above.

Procedures and equipment used to monitor the depth of anesthesia and animal well-being:

Supportive measures:

2. G.Building(s) and room number(s) where the procedures will take place:
Nonsurgical Procedures:

ASEC C311, Animal vivarium room 217

Surgical Procedures:

Animal vivarium room 218

279

2. H. Postprocedural care and monitoring:

1) Describe the post-procedural care and monitoring for both surgical (after recovery from anesthesia) and nonsurgical procedures. Identify the parameters being monitored and the frequency and duration of monitoring for each study related procedure. Include how records of the care will be maintained and their location.

Due to the nature of minor surgeries (optic nerve crush, small puncture of the cornea, and/or a brief electroporation), almost all operated fish recover immediately upon returning to their tanks and begin to feed within 5 min. of the operations. The post-operative staying in a recovery tank in low concentration of tricain is a precautionary measure in case the fish experiencing pains. Survival rate for these procedures are almost 100%. Fish swimming and feeding will be monitored: 2 times (5 min. each) the first 12 hours after the surgery, and once a day the remaining survival time. Operated fish will all be kept in animal vivarium room 217.

2) Identify by title who will conduct the care and monitoring.

The operated fish will be cared and monitored by the PI and his graduate students

3) List any analgesics or other medically related pharmaceutical agents that animals may receive. Include a) dose, b) route of administration c) frequency of administration, and d) duration of therapy.

Tricain at a reduced concentration of 0.005% in fish tank water, for 12-, 24 hours

4) List the criteria that will be used to determine that relief from pain or distress is needed and how the adequacy of that relief will be assessed.

If any fish shows discomfort or distress (e.g. swimming abnormally such as in circles, jerky movements, staying near the bottom of the tank, separated from other fish), the fish will be placed in diluted tricain solution (0.005%) until it resumes normal behavior (swimming and feeding).

5) List the humane endpoints that will be used to euthanize an animal or otherwise remove an animal from a study.

The fish will be anesthetized in an increased concentration of tricain solution (0.06% in fish tank water). After no breathing (cessation of opercular movement for more than 10 min.), followed by a cervical transection using a pair of surgical scissors.

2. I. Disposition of animals:

Describe the method of euthanasia including the name, dose, and route of administration of any pharmaceutical agents used. Describe the method(s) that will be used to confirm death. Animals euthanized by an overdose of carbon dioxide must undergo a secondary method of euthanasia to confirm death. If animals will not be euthanized, describe their disposition.

Fish will be treated wtih increased concentration of tricain (0.06%), followed by a cervical transection (see above). Death will be confirmed by lack of mouth/opercular movements for at least 10 min. After removing the retina and brain, the remaining animal will be placed in a plastic bag followed by storing in a -20°C freezer. The bag, once full, will be taken by the University of Akron office of hazardous materials for disposal.

2.J. Chemical/compound administration to live animals

Are all of the chemicals (e.g., test compounds, receptor agonists/antagonists, labeling compounds, anesthetics, analgesics, euthanasia agents, etc.) administered to live animals

commercially available pharmaceutical preparations intended for animal or human use?

                                                            Yes:X   No:

If not, then complete the following for each product.
Identify the chemical/compound and describe how it is prepared and stored to assure appropriate purity, sterility and suitability for administration to animals. Indicate the shelf life of the prepared product.

Are all of the chemicals/compounds listed above pharmaceutical grade? **Yes:X   No:**
If not, then list them and provide a justification for not using a pharmaceutical grade preparation.

3. SPECIAL CONSIDERATIONS
Mark N/A for sections that do not apply.

3.A. Food/ fluid restriction: N/A:X
If the study involves scheduling access to food or fluid OR restricting food or fluid intake beyond that associated with a routine overnight pre-procedural fast or weight control, then describe a) the amount and time of the restriction, b) expected impact on animal well-being, and c) criteria for removal of the restriction.

Describe the record-keeping associated with ongoing restrictions. Indicate where the records will be maintained. At a minimum animal weights must be documented once weekly and food/water consumption noted daily.

3. B. Prolonged restraint: N/A: X
If the project involves more than routine restraint of conscious animals for brief periods, then describe: a) the restraint, b) its duration and frequency, c) how animals will be conditioned to it, and d) how frequently animals will be observed while restrained.

Provide a justification for the restraint.

3. C. Immunologic adjuvants: N/A: X

If the project involves the use of immunologic adjuvants (e.g., Freund's adjuvant, RIBI adjuvant) complete the following.

	First Injection	Second Injection	Subsequent Injections
Adjuvant			
Anatomic site of injection & route			
Number of sites			
Volume per site			
Time interval between injections			

3. D. Dog exercise: **N/A: X**

If the project involves the use of dogs, indicate if any animals will be exempted from the dog exercise program and include the duration of the exemption and a justification for it. If there are no exemptions, enter "no exemptions".

3. E. Environmental enrichment for primates: **N/A: X**

If the project involves the use of nonhuman primates, indicate if any animals will be exempted from the environmental enrichment program for primates and include the duration of the exemption and a justification for it. If there are no exemptions, enter "no exemptions".

3. F. Housing or enrichment restrictions: **N/A: X**

If the project involves the single housing of animals of a social species OR exemption from normal environmental enrichment, then describe and provide a justification for the restriction.

3. G. Hazardous material use: **N/A: X**

If the project involves the administration of any potentially hazardous materials to live animals, complete the following for each material and attach the appropriate hazardous material form(s) required by the institution at which the work will take place.

Name of hazardous agent(s):

Select the appropriate classification of hazard(s)

CARCINOGEN	☐	INFECTIOUS AGENT	☐
RADIOACTIVE ISOTOPE	☐	RECOMBINANT NUCLEIC ACID	☐
TOXIN	☐	HUMAN TISSUE/CELLS	☐
OTHER	☐		

Describe the potential health effects of the hazard and list the possible routes of exposure hazard:

3. H. Genetically modified animals: N/A: X

If the project involves the use, breeding, or creation of genetically modified animals, complete the following for each genotype.

List the animals by genotype and describe the known or expected impact of the associated phenotype on animal well-being:

Describe the measures to relieve or manage pain or distress related to each phenotype that is associated with an adverse impact on animal well-being:

Will any new genetically modified animals be created in the project? **Yes:** **No:**
If so, describe the monitoring associated with the new line to assure adequate provision of humane animal care. Previously undescribed phenotypic conditions that negatively impact animal well-being must be reported to the IACUC:

3.I. Animal housing outside of main animal facility: N/A:X

If animals will be maintained outside of the main animal facility longer than 12 hours for USDA covered species or longer than 24 hours for all others, then complete the following.
Identify the building, room number, species, and number of animals to be housed. Indicate the duration of housing.

Provide a justification for the extramural housing.

Has the IACUC previously approved the location? **YES:** **NO:**

3.J. Field studies: N/A: X

If the project involves the use of animals in a field setting, complete the following.
Identify the occupational health and safety issues associated with studying the species in the wild.

Describe the potential impact of the study on native populations of the species being studied and others that may be affected by the study.

List and attach the permits and other necessary permission documents that are needed to carry out the study.

3.K. Procedures performed at a supplier location: N/A:X

If animals will undergo experimental or surgical procedures at a supplier's location, complete the following and attach a statement from the supplier confirming IACUC approval of the procedure. Identify the procedure and supplier's Public Health Service Animal Welfare Assurance number and USDA registration number (as applicable).

4. **CLASSIFICATION OF PROCEDURES ACCORDING TO LEVEL OF PAIN AND/OR DISTRESS**

Mark the appropriate category for each animal procedure and identify the procedure(s) in the spaces provided. List the number of animals in each pain category in the box provided. If individual animals will undergo procedures in multiple pain categories, then include them in the tabulation for the highest pain category.

☐ - **Category C** - Procedures that involve no more than momentary or slight pain or distress.
List procedures:

Number of animals in category C:

☒ - **Category D** - Procedures that may cause more than momentary or slight pain or distress for which appropriate analgesia, anesthesia or tranquilization is provided.
List procedures:

optic nerve crush and MO electrophorasion. Tricain (0.03%) will be used to alleviate any potential pain or distress the fish may experience during operation. 0.005% Tricain will be used to alleviate discomfort for 12-24 hours or longer after the surgery and during recovery if an animal shows abnormal behavior(s).

Number of animals in category D:

350

☐ - **Category E** - Procedures that may cause pain or distress which are not relieved by analgesia, anesthesia, or tranquilization.

List procedures:

N/A

Number of animals in category E:

None

For Category E procedures: Provide a detailed scientific justification for withholding analgesia, anesthesia, and tranquilization.

5. ALTERNATIVES TO THE USE OF ANIMALS AND PAIN OR DISTRESS PRODUCING PROCEDURES

Provide a written narrative description of the methods and sources that were used to determine that suitable alternatives to the use of animals and to the pain or distress producing procedures described in the protocol are not available. Provide an explanation for alternatives that were identified but deemed unsuitable. Literature searches must include a) databases searched, b) the date of the search, c) the years covered by the search (minimum 10 years), and d) the search strategy including keywords used. At least two acceptable information sources must be used. The response must address the three R's: Replacement models, Refinements in technique, and Reduction in animal numbers. Information sources that are commonly used include http://www.pubmed.gov, http://agricola.nal.usda.gov, http://www.nal.usda.gov/awic, and specifically for teaching activities, http://oslovet.veths.no.

Pubmed web site was searched (key words: cadherin, protocadherin, zebrafish, retinal lesion, optic nerve lesion, alternative methods, and cell culture; years covered, from 1981 to present (June. 10, 2015, date of search)). The searches did not identify any suitable replacement models, refinements in technique to reduce pain or distress, OR any means to reduce the number of animals used. There is no biological alternative to study cadherin expression and function in normal brain and retina, and in regenerating retina of vertebrate animals. The only biological alternative to study in vitro cadherin function is using the cell culture system, but it provides very little relevant information about cadherin function in whole live normal and regenerating animals (i.e. in vivo study). Moreover, in vivo studies on cadherins function can provide more useful insights into cadherin function in humans.

6. JUSTIFICATION FOR THE USE OF ANIMALS

6. A. Provide a rationale for involving animals.

There is no non-biological alternative to study cadherins' in vivo functions in normal and regenerating vertebrate central nervous system.

6. B. What is the basis for selecting the species that you have chosen?

Zebrafish (Danio rerio) has become a leading model organism to study animal development, regeneration, physiology and molecular biology due mainly to its experimental advantages such as low cost, ease of maintenance and manipulating gene expression, and fully sequenced and annotated genome. Zebrafish retina is similarly organized as other vertebrate animals including humans. Moreover, studies have shown that similar molecular mechanisms underlying animal development and function. Finally, the principal investigator has used zebrafish to study cadherins expression and function in developing and adult zebrafish for over 15 years, and our lab has most techniques worked out and reagents available.

6. C. Number of animals requested:

Provide a justification for the number of animals requested. Identify the species, genotypes, strains, and/or stocks of animals. Include other descriptors as relevant (e.g., age or weight, gender, timed pregnant). For research protocols, list the experimental and control groups and indicate the number of animals in each. Include the statistical justification, or other basis, for selecting the number requested. If a research protocol includes the use of animals solely for training (i.e., the training does not occur as part of the experimental use of animals), then include the expected number of animals to be used for training. Animals used for training can be justified by documenting the expected number of persons to be trained and the number that can be trained per animal.

550 adult zebrafish will be obtained either from the in-house colony or from outside suppliers. The number of fish to be used is based on a previous publication by Cameron et al. (2005, Mol. Vis. 11:775-791) using similar experimental approaches. Power analysis was performed to obtain appropriate animal numbers needed for each type of experiment. 40 fish: (8 animals for each cadherin, and we plan to measure 5 different cadherins) for quantitative measurements of cadherin expression levels using qPCR) for studying cadherin expression in normal brain and retina. 100 fish will be used for examining cadherin expression at different stages of regeneration: 1-, 3-, 7-, 10-, and 14 and 21-day; 5 cadherins and 6 animals for each cadherin at each stage. Both spatial (qualitative using in situ hybridization: 5 cadherin X 6 animals X 6 stages=180) and quantitative (using qPCR: 5 cadherins X 6 animals X 6 stages=180) methods will be used. Roles of two cadherin/protocadherins during retinal regeneration will be assessed, which will require additional 150 fish. Retinal regeneration with cadherin MO applied (electroporation or vivo-MO) will be compared with that without MO application at all these six stages (e.g. 3-, 5- and 7-day). In addition to examine histology of unstained retinal tissue sections, numerous retinal markers (e.g. Klf6 and klf7, markers of regenerating retinal ganglion cells; zpr-1 labeles double cone photoreceptors) will be used to assess degrees of regeneration. Considering number of animals for practice and perfecting the techniques, untreat animals for controls, premature removal of animals due to death or surgical complications (see above), the total number of animals (550) is a conservative estimation of the number of fish to be used in this project.

6. D. Provide written assurance that the use of animals described in this protocol does not unnecessarily duplicate previous experiments.

From searching PubMed (1981-present; there was not protocadherin studies before 1981), we found that there is no publication on the types of cadherins/protocadherins (e.g. cadherin-6, pcdh17 and pcdh19) expression in adult zebrafish, and no information on cadherins/pcdhs expression in regenerating vertebrate retina and these molecules function in regenerating CNS. Key words used: brain, cadherin, protocadherin, retina, regeneration, optic nerve, visual system, and zebrafish. Date searched: June, 2015.

7. HOUSING AND HUSBANDRY

7. A. Indicate the approximate number of animals to be housed at one time and approximate duration of housing.

300 adult zebrafish can be used for the entire study period (3 years). The remaining animals can be obtained by raising embryos produced by these fish. It usually takes about 5 months for zebrafish to grow from hatching to adult.

7. B. If rodents are to be housed, is there a preference as to the type of caging (i.e., plastic, wire-bottom, microisolator or other) OR the number of animals per cage?
          YES: NO:

If yes, please specify. Note that the use of wire-bottom cages or single housing of animals requires a justification.

7. C. Will a light cycle other than the standard 12 hours light/12 hours dark be necessary for any of the animals on this protocol?   YES: NO: X

If yes, please specify the light cycle(s) and indicate the group(s) of animals that will require it.

7. D. Will the animals on this protocol have any special temperature or humidity requirements?   YES:X   NO:

If yes, please describe.

26-29°C

7. E. Will the animals on this protocol require a special diet or special water?
          YES: NO: X

If yes, please identify the product, the number of animals receiving it, and who will prepare and administer it.

7. F. Will the animals on this protocol require any other special housing, care, environmental conditions, or other considerations?   YES: NO: X

If yes, please describe.

7. G. Will it be necessary to house animals after they have received any hazardous materials (refer to Part 3.G.)?   YES: NO:

If yes, please identify the material, the number of animals, and the duration of housing. Describe how the housing cages and room will be identified to alert personnel that a hazard is present.

> N/A

8. PROTOCOL APPROVAL

Click "Choose Institution" to select the institution to which the protocol will be submitted.

Protocol approval is indicated by the signatures of the institution-specific individuals identified below. The individuals signing confirm that they have reviewed the protocol and find it to be in compliance with applicable animal care and use regulations and institutional policies.

Choose Institution

Approval Signatures:

_____   Date _____
Facility Director

_____   Date _____
Department Chair/Research Director

University of Akron
_____   Date _____
IACUC Member

Walter L. Horne, DVM   Date 8/6/2015
Attending Veterinarian

[signature]   Date 8/4/15
IACUC Chairperson

INVESTIGATOR ASSURANCE

By signing below I/we agree to:

   A. Employ procedures that will avoid or minimize discomfort, distress, and pain to animals, consistent with sound research design.

   B. Comply with the protocol as approved by the Institutional Animal Care and Use Committee (IACUC) and to obtain the consent of the IACUC before implementing any changes to the protocol.

   C. Comply with the policies of the IACUC of the institution at which this work is conducted, the National Research Council Guide for the Care and Use of Laboratory Animals, the Public Health Service Policy on Humane Care and Use of Laboratory Animals, the regulations of the Animal Welfare Act and other applicable federal, state and local regulations governing the use of animals in research, teaching, and testing.

   D. Maintain adequate records of all animal experimentation procedures.

   E. The provision of emergency veterinary care including euthanasia by the attending veterinarian or his/her designee for animals showing evidence of unbearable pain, distress, or illness with the understanding that an effort will be made to contact me or my designee prior to the initiation of any treatment.

Principal Investigator:

Name: Qin Liu

Department: Biology

Email address: qliu@uakron.edu

Telephone number: 330-972-7558

Signature _____

Date: Aug/1/15

Co-Investigator:

Name:

Department:

Email address:

Telephone number:

Signature _____

Date: _____

Co-Investigator:

Name:

Department:

Email address:

Telephone number:

Signature _____

Date: _____

Consortial protocol 0114.doc   Version 01/14

PARTICIPANT QUALIFICATIONS

Complete this form for the principal investigator, each co-investigator, and each of the individuals who may participate in the animal work described in the protocol. By signing below the participant acknowledges that he/she has read the protocol and agrees to comply with it.

NAME: Qin Liu

TITLE: PI

List the participant's responsibilities on the protocol.

> Supervise the entile project, and participate in most of the proposed experiments.

Describe the participant's experience and/or qualifications relevant to the responsibilities on the protocol. If the participant has no relevant experience then check here ☐ and identify below who will be responsible for training.

EXPERIENCE/QUALIFICATIONS:

> Qin Liu has worked with the zebrafish for about 18 years, with extensive experience in the animal care, zebrafish visual system injury, microinjection, preparation of tissues and variety of histological and molecular techniques.

DESCRIPTION OF FORMAL ANIMAL CARE AND USE TRAINING:

TITLE OR DESCRIPTION OF TRAINING	LOCATION	DATE OF TRAINING
Elective Modules for Investigators, staff and students of the Citiprogram	University of Akron	Feb. 10,2008
Elective Modules for Investigators, staff and students of the Citiprogram	University of Akron	March, 2011
Elective Modules for Investigators, staff and students, and working with zebrafish in research settings of the CITI program	University of Akron	June 9 and June 10, 2015

Liu Qin
PARTICIPANT SIGNATURE

Aug 1, 15
DATE

Consortial protocol 0114.doc   Version 01/14

292

PARTICIPANT QUALIFICATIONS

Complete this form for the principal investigator, each co-investigator, and each of the individuals who may participate in the animal work described in the protocol. <u>By signing below the participant acknowledges that he/she has read the protocol and agrees to comply with it.</u>

NAME: Sunil Bhattarai

TITLE: Research assistant

List the participant's responsibilities on the protocol.

Assist the PI in all aspects of the projects, including animal care, tissue preparation and processing, data collection, analysis and writing of manuscripts

Describe the participant's experience and/or qualifications relevant to the responsibilities on the protocol. If the participant has no relevant experience then check here ☐ and identify below who will be responsible for training.
EXPERIENCE/QUALIFICATIONS:

He has worked with the PI since last 2011, and is familiar with most of the fish care and tissue processing procedures and techniques mentioned in the project. The student will be trained by the PI on techniques that he is not familiar with.

DESCRIPTION OF FORMAL ANIMAL CARE AND USE TRAINING:

TITLE OR DESCRIPTION OF TRAINING	LOCATION	DATE OF TRAINING
CITI training program	University of Akron	September, 2011
CITI training program	University of Akron	June, 2015

PARTICIPANT SIGNATURE   08/01/2015
                                                             DATE

Consortial protocol 0114.doc   Version 01/14

APPENDIX B

THE INSTITUTIONAL ANIMAL CARE AND USE COMMITTEE (IACUC)

APPROVAL OF THE PROTOCOL TO STUDY PCDH17 IN DEVELOPING

ZEBRAFISH

For IACUC Use Only		
Category:	Special Considerations:	Protocol #: 12-9A

REQUEST TO USE ANIMALS

1. PROTOCOL SUMMARY

1. A. Protocol Title:

Using zebrafish as a model organism to investigate cadherins roles in the normal and regenerating adult central nervous system

1. B. Principal Investigator's Institution:

University of Akron

1. C. Facility(ies) where animals will be housed: *If animals will be housed in a facility not listed below, please identify the location under "OTHER LOCATION".*

AKRON GENERAL MEDICAL CENTER ☐	UNIVERSITY OF AKRON ☒
KENT STATE UNIVERSITY	YOUNGSTOWN STATE UNIVERSITY
Cunningham ☐	Cushwa ☐
Kent ☐	DeBartolo ☐
Tuscawarus ☐	Ward Beecher ☐
SUMMA HEALTH SYSTEM ☐	NEOUCOM/P ☐
OTHER ☐	

OTHER LOCATION (Institution, building & room):

NA

1. D. Will this project be submitted for funding to a granting or other agency?
Yes ☒ No ☐ *If so, please identify the agency.*

NEI (National Eye Institute)

1. E. Anticipated start date:

August 27th, 2012

1. F. Expected animal use over the three year approval period: *Summarize all animal use by species.*

Species	Number	Source
zebrafish, Danio rerio	700 adult	in house and commercial sources

1. H. Use lay terminology to describe the value of the project. Include 1) the medical condition or scientific question that is being addressed and its importance, 2) the goals of the research, and 3) how the use of animals will help achieve the goals. *Your response is limited to the space provided.*

Cadherins are Ca^{2+}-dependent adhesion molecules that have important roles in tissue development and maintenance throughout the lifespan of an organism in many organisms including humans. More than 100 cadherins have been identified, and they are grouped into several types, based mainly on their amino acid sequences and genomic organization, including classical cadherins and protocadherins. Classical cadherins (e.g. cadherin-1 and cadherin-2) are the most studied and understood, while much less is known about protocadherins (pcdhs, e.g. pcdh9 and pcdh17) expression and function. Even for classical cadherins, efforts have been mostly focused on their functions during embryonic development, knowledge of their expression and function in adult nervous system is very limited. There is even less information on cadherin function during nervous tissue regeneration. Mutations of cadherins contribute to Usher syndrome (deafness and vision loss; e.g. cadherin-23 and pcdh15), epilepsy (e.g. pcdh19), autism (e.g. cadherin-10, pcdh19), bipolar disease and Schizophrenia (e.g. cadherin-7). Therefore information about cadherins expression in adult nervous system is critical for us to study their functions in the system. It has become common knowledge that recovery from central nervous system (CNS) injuries (e.g. to retina and spinal cord) is very limited in humans and other mammals. However, similar injuries in fish and amphibians usually result in complete recovery. One of the key reasons for the difference is that fish and amphibians can drastically increase expression of some developmentally important genes, including cadherins, during CNS regeneration, while there is little or no change in expression of these genes during regeneration in mammals. Identification of differentially expressed genes during CNS regeneration in model organisms (e.g. zebrafish) may lead to development of potential therapeutic strategies. The retina is part of the CNS, and has been used as a model organ (due to its peripheral localization and simpler organization) to study CNS development and function. Zebrafish (*Danio rerio*) has become a leading model organism to study animal development, physiology and molecular biology due mainly to its experimental advantages such as low cost, ease of maintenance and manipulating gene expression, and fully sequenced and annotated genome. Zebrafish retina is similarly organized as other vertebrate animals including humans. Moreover, studies have shown that similar molecular mechanisms underlying animal development and function.

We propose to study: 1) cadherins expression in normal adult zebrafish brain, normal and regenerating adult zebrafish retina; 2) cadherin function in regenerating zebrafish retina. These goals can be achieved only by using adult zebrafish.

1. I. Use lay terminology to provide an overview of the animal use from the beginning of the project through its end. *Your response is limited to the space provided.*

The adult zebrafish (300) will come from either our in house colonies or commercial suppliers. The fish will be maintained in 5- or 10-gallon glass tanks (15 fish/tank for 5-gallon tanks, 30 fish/tank for 10-gallon tanks). The animals will be anesthetized in tricain (MS222, routinely used anesthetic for aquatic animals). For obtaining retinal or brain tissues, anesthetized animals will be placed in a petridish filled with ice under a dissecting microscope for removing the tissues. An incision will be made to separate the hindbrain from the spinal cord before removing the brain. The removed tissues will be quickly placed in 4% paraformaldehyde or on dry ice. Standard procedures for cryoprotection and tissue sectioning will be used to obtain brain or retinal sections, while Trizol reagent method will be used for isolating total RNAs. For regeneration studies, animals will be anesthetized, placed on a piece of wet paper towel in a peridish. One of the optic nerves will be injured using a fine-pointed tweezer, or the back of an eye will be stabed with a 1-mm sapphire blade. The operated animals will be returned to their tanks to recover. For study cadherin function during retinal regeneration, a morpholino antisense oligonucleotide (MO), a reagent specifically reduces function of a particular gene (e.g. a cadherin MO), will be introduced into the regenerating retina using either electroporation or vivo-MO method. These are established methods for delivering DNA, RNA or MOs to adult animals including zebrafish. After specific time (e.g. 3-day), the animals will be treated as described above for obtaining retinal and brain tissues from normal fish. Extent of retinal regeneration will be compared between normal regeneration (without cadherin MO) and MO treated regeneration histologically (on tissue sections), immunologically (using retinal markers), and/or molecularly (e.g. reverse transcriptase pCR, DNA microarray).

2. DESCRIPTION OF PROCEDURES INVOLVING LIVE ANIMALS

2. A. Nonsurgical manipulations: N/A:
Describe in detail all nonsurgical manipulations carried out on live animals. Euthanasia is to be described in 2.F.

> The fish will be caught using a net, placed on a piece of wet paper towl, and partially covered (with the head and eye exposed) by the paper towl. Short electrical pulses (2, 50 ms each, seperated by 1 sec pause) will be delivered to the dorsal half of the eye (using a square wave electroporator) in some fish to drive MOs into retinal cells.

2. B. Surgical manipulations: N/A:
Provide a description of any surgical procedures (survival or terminal) including the pre-operative preparation.

> All surgical operations will be performed in anesthetized adult zebrafish. For some fish, one of the optic nerves will be crushed by squeezing tips of a fine-pointed tweezer. A different group of fish will have one of their eyes (the back of the eye) stabbed 2-3 times using a double edge sapphire blade (only the tip of the blade will penetrate the tissue, making a small incision about 0.1-0.2 mm in length). A subset of the injured fish will be injected, through a small opening (obtained by using the sapphire blade) in the cornea, with a cadherin MO, a mixture of cadherin MOs or a control MO using a Hamilton syrange (33 gauge blunt tip needle).

1) Does this project involve multiple major survival surgery in animals?   YES: NO: X
If so, please justify.

>

2. C. Anesthesia/Sedation: N/A:
Describe the anesthetic/sedative regimen (include drug[s], dose, and route of administration) and monitoring for each procedure involving anesthesia/sedation.

> The adult fish will be anesthetized in Tricain (also called MS222, 0.05% for anesthetization, and 0.2% for euthanasia) before being sacrificed. After each surgery, the animals will be place in 0.01% MS222 for 24 hours before returning to normal fish tank water

2. D. Building(s) and room number(s) where the procedures will take place:
Nonsurgical Procedures:

> BRC 217 and 218

Surgical Procedures:

> BRC 218

2. E. Postprocedural care and monitoring:
Describe post-procedural care and monitoring for both surgical and nonsurgical procedures.
1) Describe the care and monitoring including the frequency and duration :

> Since the proposed tissue damages will be small (e.g. 0.1-0.2 mm wounds; brief electroporation—2 pulses of 50 ms/each), and the amount of MO is small (about 0.4 ul; MOs at this small amount are non-toxic, there have been no report of death (100% survival) after these manipulations. From our past experience, most fish began swim normally, and resumed feeding minutes after recovering from anesthesia. The operated fish will be placed in diluted MS222 (0.01%) for 24 hours before returning to normal fish tank

water. The operated fish will be observed twice daily to monitor their behavior. Fish showing abnormal swimming behaviors (e.g. circular swimming or little movement) will be anesthetized and killed. Dead fish will also be removed. The operated fish will be house in separate (from unoperated) 5- or 10-gallon tanks.

2) Identify by title who will conduct the care and monitoring :

the principal investigator and the graduate students (research assistants)

3) List any analgesics or other medically related pharmaceutical agents (include the dose, route of administration and frequency) that the animals may receive:

The fish will be anesthetized in Tricain (also called MS222, 0.05%) before and during any surgical operation, 0.01% MS222 for 24 hours after each surgery.

4) List the criteria that will be used to determine that relief from pain or distress is needed and how the adequacy of that relief will be assessed:

Fish can exhibit specific abnormal behaviors such as twiching or unbalanced swimming soon after recovery from anesthesia. We assume that a recovery fish is not experiencing too much discomfort if it swims and feeds like most of unoperated fish. If an operated fish displays any abnormal behavior after returning to normal fish tank water, we will place the fish in 0.01% MS222 for 12-24 more hours. If the abnormal behavior continues, becomes worse or new abnormal behaviors develop, the fish will be killed by overdose of MS222 and cut of the brain stem.

5) List the criteria that will be used to euthanize an animal or otherwise remove an animal from a study for humane reasons:

The animals will be anesthetizd by Tricain (0.2%) and the brain stem will be cut to sacrifice the fish.

2. F. Disposition of animals:

Describe the method of euthanasia including the identification, dose, and route of administration of any pharmaceutical agents used. If animals will not be euthanized, describe their disposition.

After removing the retina and brain, the remaining animal will be placed in a plastic bag followed by storing in a -20°C freezer. The bag, once full, will be taken by the University of Akron office of hazoudous materials for disposal.

3. SPECIAL CONSIDERATIONS

3. A. Prolonged restraint: N/A: X

If the project involves more than routine restraint for brief periods, describe the restraint, its duration and frequency, and how animals will be conditioned to it.

3. B. Neuromuscular blocking agents: N/A: X

If the project involves the use of neuromuscular blocking agents, describe the dose, route, frequency of administration, and how the depth of anesthesia will be monitored.

3. C. Immunologic adjuvants:　　　　　　　　　　　　　　　　N/A: X

If the project involves the use of immunologic adjuvants (e.g., Freund's adjuvant, RIBI adjuvant) complete the following.

	First Injection	Second Injection	Subsequent Injections
Adjuvant			
Anatomic site of injection & route			
Number of sites			
Volume per site			
Time interval between injections			

3. D. Dog exercise:　　　　　　　　　　　　　　　　　　　　N/A: X

If the project involves the use of dogs, indicate if any animals will be exempted from the dog exercise program and include the duration of the exemption and a justification for it. If there are no exemptions, enter "no exemptions".

3. E. Environmental enrichment for primates:　　　　　　　　N/A: X

If the project involves the use of nonhuman primates, indicate if any animals will be exempted from the environmental enrichment program for primates and include the duration of the exemption and a justification for it. If there are no exemptions, enter "no exemptions".

3. F. Hazardous substance use:　　　　　　　　　　　　　　　N/A: X

If the project involves the administration of any potentially hazardous materials to live animals, complete the following for each material __and__ attach the appropriate hazardous substance use form(s) required by the institution at which the work will take place.
Name of hazardous agent:

Underline the appropriate category:　　　Carcinogen　　　Infectious agent　　　Radioisotope

Recombinant nucleic acid　　　Toxin　　　Other

Description of potential hazard:

Number of animals receiving material:

3. G. Genetically engineered animals: N/A: X

If this project involves the use or creation of genetically engineered animals, complete the following for each genotype.

Known or planned phenotype:

Description of measures to relieve or manage pain or distress related to phenotype:

4. CLASSIFICATION OF PROCEDURES ACCORDING TO LEVEL OF PAIN AND/OR DISTRESS

Place an "X" in front of the appropriate category for each animal procedure and identify the procedure in the spaces provided.

- Category C - Procedures that involve no more than momentary or slight pain or distress.

List procedures:

MO injections to the eye of adult fish that are anesthetized.

- Category D - Procedures that may cause more than momentary or slight pain or distress for which appropriate analgesia, anesthesia or tranquilization is provided.

List procedures:

Stabs to the back of the eye, optic nerve crush, MO electrophorasion. Tricain (0.05%) will be used to alleviate any potential pain or distress the fish may experience during operation. 0.01% Tricain will be used to alleviate potential discomfort for 24 hours or longer after the surgery and during recovery.

- Category E - Procedures that may cause pain or distress which are not relieved by analgesia, anesthesia, or tranquilization.

List procedures:

N/A

For Category E procedures: Provide a detailed scientific justification for withholding analgesia, anesthesia, and tranquilization.

N/A

5. ALTERNATIVES TO CATEGORY "D" AND "E" PROCEDURES   N/A: X

For procedures included in Categories D and E in section 4 provide a written narrative description of the methods and sources that were used to determine that alternatives to the procedures are not available. Provide an explanation for alternatives that were identified but deemed unsuitable. If a literature search was conducted identify the <u>databases searched</u>, the <u>date of the search</u>, the <u>years covered by the search (minimum 10 years)</u>, and the <u>keywords used</u>. Information sources that are commonly used include http://www.pubmed.gov, http://agricola.nal.usda.gov, http://www.nal.usda.gov/awic, and specifically for teaching activities, http://oslovet.veths.no.

Pubmed web site was searched (key words: cadherin, protocadherin, zebrafish, retinal lesion, optic nerve lesion, alternative methods, and cell culture; years covered, from 1981 to present (July. 12, 2012, date of search)). There is no biological alternative to study cadherin expression and function in normal brain and retina, and in regenerating retina of vertebrate animals. The only biological alternative to study in vitro cadherin function is using the cell culture system, but it provides very little relevant information about cadherin function in whole live normal and regenerating animals (i.e. in vivo study). Moreover, in vivo studies on cadherins function can provide more useful insights into cadherin function in humans.

6. JUSTIFICATION FOR THE USE OF ANIMALS
6. A. Number of animals:

Provide a justification for the number of animals requested and include a description (e.g., genotype/strain/stock [as appropriate], age or weight, gender, timed pregnant) of them for each species requested.

700 adult zebrafish will be obtained either from the in-house colony or from outside suppliers. The number of fish to be used is based on a previous publication by Cameron et al. (2005, Mol. Vis. 11:775-791) using similar experimental approaches. Power analysis was performed to obtain appropriate animal numbers needed for each type of experiment. 46 fish: 8 for saggital sections and 8 for cross sections, 30 (6 animals for each cadherin, and we plan to measure 5 different cadherins) for quantitative measurements of cadherin expression levels using Q-PCR for studying cadherin expression in normal brain and retina. 180 fish will be used for examining cadherin expression at different stages of regeneration: 1-, 3-, 5-, 7-, 10-, and 14-day; 5 cadherins and 6 animals for each cadherin at each stage. Both spatial (qualitative using in situ hybridization: 5 cadherin X 8 animals X 6 stages=240) and quantitative (using Q-PCR: 5 cadherins X 6 animals X 6 stages=180) methods will be used. Roles of two or three cadherin/protocadherins during retinal regeneration will be assessed, which will require additional 150 fish. Retinal regeneration with cadherin MO applied (electroporation or vivo-MO) will be compared with that without MO application at all these six stages (e.g. 3-, 5- and 7-day). In addition to examine histology of unstained retinal tissue sections, numerous retinal markers (e.g. zpr-1 labeles double cone photoreceptors) will be used to assess degrees of regeneration. Considering number of animals for practice and perfecting the techniques, untreat animals for controls, premature removal of animals due to death or surgical complications (see above), the total number of animals (700) is a conservative estimation of the number of fish to be used in this project.

6. B. Provide a rationale for involving animals.

There is no non-biological alternative to study cadherins' in vivo functions in normal and regenerating vertebrate central nervous system.

6. C. What is the basis for selecting the species that you have chosen?

Zebrafish (*Danio rerio*) has become a leading model organism to study animal development, physiology and molecular biology due mainly to its experimental advantages such as low cost, ease of maintenance and manipulating gene expression, and fully sequenced and annotated genome. Zebrafish retina is similarly organized as other vertebrate animals including humans. Moreover, studies have shown that similar molecular mechanisms underlying animal development and function. Finally, the principal investigator has used zebrafish to study cadherins expression and function in developing and adult

zebrafish for over 15 years, and our lab has most techniques worked out and reagents available.

6. D. Provide written assurance that the use of animals described in this protocol does not unnecessarily duplicate previous experiments.

From searching PubMed (1981-present; there was not protocadherin studies before 1981), we found that there is no publication on the types of cadherins/protocadherins (e.g. cadherin-6, pcdh17 and pcdh19) expression in adult zebrafish, and no information on cadherins/pcdhs expression in regenerating vertebrate retina and these molecules function in regenerating CNS. Key words used: brain, cadherin, protocadherin, retina, regeneration, optic nerve, visual system, and zebrafish. Date searched: Jul, 2012.

7. HOUSING AND HUSBANDRY

7. A. Indicate the approximate number of animals to be housed at one time and approximate duration of housing.

100 adult zebrafish can be used for the entire study period (4 years).

7. B. If rodents are to be housed, is there a preference as to the type of caging (i.e., plastic, wire-bottom, microisolator or other) OR the number of animals per cage?
YES: NO:

If yes, please specify. Note that the use of wire-bottom cages or single housing of animals requires a justification.

7. C. Will a light cycle other than the standard 12 hours light/12 hours dark be necessary for any of the animals on this protocol?   YES: NO: X

If yes, please specify the light cycle(s) and indicate the group(s) of animals that will require it.

7. D. Will the animals on this protocol have any special temperature or humidity requirements?   YES: X   NO:
If yes, please describe.

26-29°C

7. E. Will the animals on this protocol require a special diet or special water?
YES: NO: X

If yes, please identify the product, the number of animals receiving it, and who will prepare and administer it.

7. F. Will the animals on this protocol require any other special housing, care or environmental conditions?   YES: NO: X
If yes, please describe.

7. G. Will it be necessary to house animals after they have received any hazardous materials (refer to Part 3.F.)?   YES: NO: X
If yes, please identify the material, the number of animals, and the duration of housing.

303

8. PROTOCOL APPROVAL

Click on the institution name below (the University of Akron is the default entry) to open the scroll down menu and select the institution to which the protocol will be submitted.

Protocol approval is indicated by the signatures of the institution-specific individuals identified below. The individuals signing confirm that they have reviewed the protocol and find it to be in compliance with applicable animal care and use regulations and institutional policies.

University of Akron
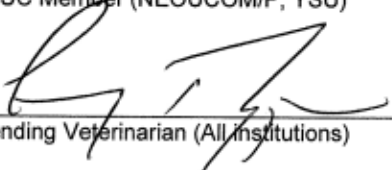
Approval Signatures:

_____
Facility Director (KSU)

Date _____

_____
Manager of Research Safety & Compliance (KSU)

Date _____

_____
Department Chair/Research Director (SHS)

Date _____

_____
IACUC Member (NEOUCOM/P, YSU)

Date _____

_____
Attending Veterinarian (All institutions)

Date 10/1/12

_____
IACUC Chairperson (All institutions)

Date 10/3/12

304

INVESTIGATOR ASSURANCE

By signing below I/we agree to:

A. Employ procedures that will avoid or minimize discomfort, distress, and pain to animals, consistent with sound research design.

B. Comply with the protocol as approved by the Institutional Animal Care and Use Committee (IACUC) and to obtain the consent of the IACUC before implementing any changes to the protocol.

C. Comply with the policies of the IACUC of the institution at which this work is conducted, the National Research Council Guide for the Care and Use of Laboratory Animals, the Public Health Service Policy on Humane Care and Use of Laboratory Animals, the regulations of the Animal Welfare Act and other applicable federal, state and local regulations governing the use of animals in research, teaching, and testing.

D. Maintain adequate records of all animal experimentation procedures.

E. The provision of emergency veterinary care including euthanasia by the attending veterinarian or his/her designee for animals showing evidence of unbearable pain, distress, or illness with the understanding that an effort will be made to contact me or my designee prior to the initiation of any treatment.

Principal Investigator:

Name: Qin Liu   Department: Biology

Email address: qliu@uakron.edu   Telephone number: 3309727558

Signature _____   Date: 7/25/12

Co-Investigator:

Name: Department:

Email address: Telephone number:

Signature _____   Date: _____

Co-Investigator:

Name: Department:

Email address: Telephone number:

Signature _____   Date: _____

Category:	Special Considerations:	Protocol #:

PARTICIPANT QUALIFICATIONS

Complete one of these pages for the principal investigator, each co-investigator, and each of the individuals who may participate in the animal work described in the protocol. By signing below the participant acknowledges that he/she has read the protocol and agrees to comply with it.

NAME: Qin Liu

TITLE: Professor

RESPONSIBILITIES ON THE PROTOCOL:

Supervise the entile project, and participate in most of the proposed experiments.

EXPERIENCE/QUALIFICATIONS:
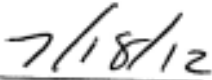
Qin Liu has worked with the zebrafish for about 15 years, with extensive experience in the animal care, zebrafish visual system injury, microinjection, preparation of tissues and variety of histological and molecular techniques.

DESCRIPTION OF FORMAL ANIMAL CARE AND USE TRAINING:

TITLE OR DESCRIPTION OF TRAINING	LOCATION	DATE OF TRAINING
Animal Care and Use Training Workshop	University of Akron	Fall, 2000
Elective Modules for Investigators, staff and students of the Citiprogram IACUCGradebook	University of Akron	Feb. 10,2008
Elective Modules for Investigators, staff and students of the Citiprogram IACUCGradebook	University of Akron	March, 2011

_____
PARTICIPANT SIGNATURE

7/18/12
DATE

Consortial protocol 0108.doc   Version 01/08

PARTICIPANT QUALIFICATIONS

Complete one of these pages for the principal investigator, each co-investigator, and each of the individuals who may participate in the animal work described in the protocol. By signing below the participant acknowledges that he/she has read the protocol and agrees to comply with it.

NAME: Sunil Bhattarai

TITLE: Research assistant

RESPONSIBILITIES ON THE PROTOCOL:

Assist the PI in all aspects of the projects, including animal care, tissue preparation and processing, data collection, analysis and writing of manuscripts

EXPERIENCE/QUALIFICATIONS:

Majored in Biotechnology as undergraduate student. He has worked with the PI since last Fall semester, and is familiar with most of the animal care and tissue processing procedures mentioned in the project

DESCRIPTION OF FORMAL ANIMAL CARE AND USE TRAINING:

TITLE OR DESCRIPTION OF TRAINING	LOCATION	DATE OF TRAINING
CITI training program	University of Akron	September, 2011
...		

PARTICIPANT SIGNATURE

DATE: 7/18/12

PARTICIPANT QUALIFICATIONS

Complete one of these pages for the principal investigator, each co-investigator, and each of the individuals who may participate in the animal work described in the protocol. By signing below the participant acknowledges that he/she has read the protocol and agrees to comply with it.

NAME: Alicja Sochacka

TITLE: Research Assistant

RESPONSIBILITIES ON THE PROTOCOL:

Alicja Sochacka will be involved in most of the proposed experiments and caring for animals, collecting and analyzing data, and writing the manuscripts.

EXPERIENCE/QUALIFICATIONS:

Alica Sochacka majored in B iotechnology as an undergradate and Master degree graduate student. She has worked in the PI lab for one year, is familiar with animal care, day-to-day lab duties, and most of the techniques methoned in the project. She is a co-author in two research manuscripts submitted. One of which is the study of pcdh17 function in embryonic zebrafish retina.

DESCRIPTION OF FORMAL ANIMAL CARE AND USE TRAINING:

TITLE OR DESCRIPTION OF TRAINING	LOCATION	DATE OF TRAINING
CITI trainig program	University of Akron	~~September~~, 2011 August, 2011

_____   07/18/2012
PARTICIPANT SIGNATURE   DATE

Consortial protocol 0108.doc   Version 01/08

308

PARTICIPANT QUALIFICATIONS

Complete one of these pages for the principal investigator, each co-investigator, and each of the individuals who may participate in the animal work described in the protocol. By signing below the participant acknowledges that he/she has read the protocol and agrees to comply with it.

NAME: Ted Bieias III

TITLE: Research assistant

RESPONSIBILITIES ON THE PROTOCOL:

> Ted will be involved in studying cadherins expression in normal (uninjured) adult zebrafish brain and retina: taking care of animals, harvesting tissues, tissue processing, collecting data and writing manuscript.

EXPERIENCE/QUALIFICATIONS:

Ted majored in Biology at University of Akron, and has been working in a microbiology lab of a Pharmaceutical company for years. He joined our lab last fall, and is familiar with most procedures used in our lab including fish care, tissue preparation and processing. He will work with the PI on data collecting analysis and writing of manuscript.

DESCRIPTION OF FORMAL ANIMAL CARE AND USE TRAINING:

TITLE OR DESCRIPTION OF TRAINING	LOCATION	DATE OF TRAINING
CITI trainig program	University of Akron	September, 2011

PARTICIPANT SIGNATURE

DATE 7·25·12
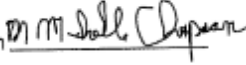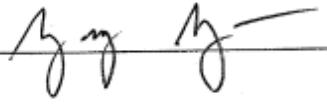
FOR COMMITTEE USE:

Date Proposal Received: _____

Primary Reviewer: _____

Date Reviewed: _____

Project Number: _12-9A_

Project Director: _Liu_

Date Approved: _9/20/12_

Institutional Animal Care and Use Committee (IACUC) members:

X Dr. Gary Riggs DVM _____

4873 Richland Ave.
Barberton, OH 44203

Dr. James Holda _____

Department of Biology

Dr. Brian Bagatto _____

Department of Biology

Dr. Rolando Ramirez _____

Department of Biology

X Ms. Michelle Evancho-Chapman _____

Summa Health System
P.O. Box 2090
Akron, OH 44309-2090

Ms. Emily Njus _____

Department of Research and
Sponsored Services

Dr. Elaine Fisher _____

Department of Nursing

X Dr. Yang Yun _____

Department of Biomedical
Engineering

Dr. Kevin Kaut _____

Department of Psychology

Dr. Wiley Youngs _____

Department of Chemistry

Mr. Robert Zickefoose _____

Supervisor Animal Care Facility

Dr. Leslie Whetstine _____
alt.
Dr. Judy Kreye

Walsh University

310

APPENDIX C

MICROARRAY QA/QC
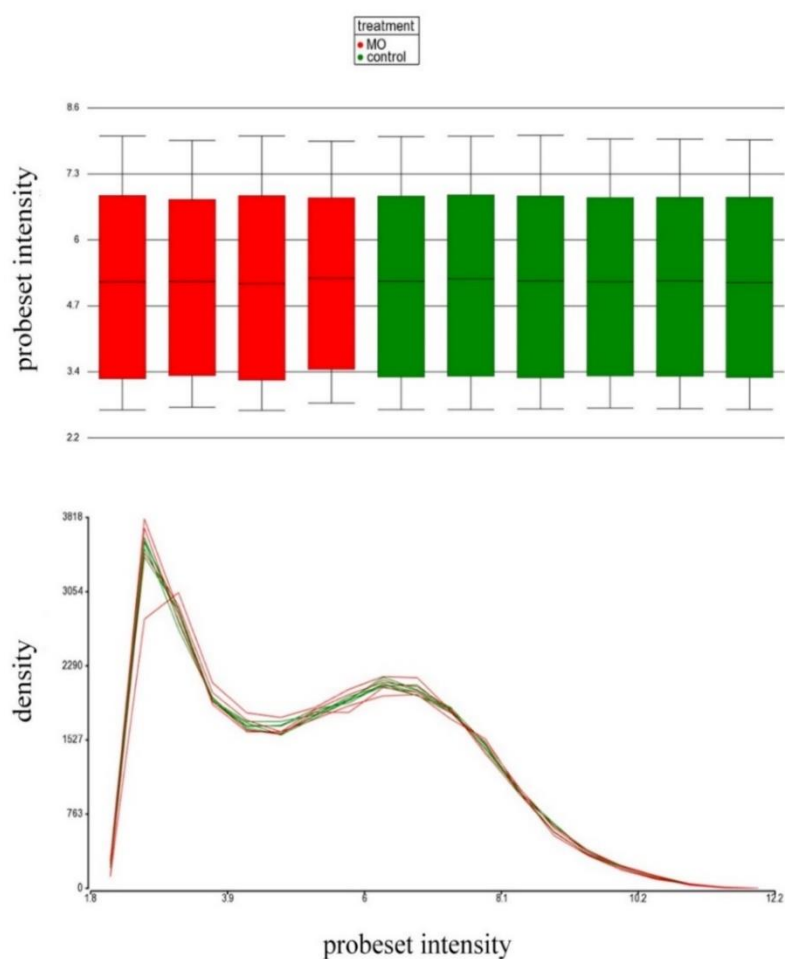
Frequency of detected signal from each microarray sample (n=10) is comparable. Top image: each microarray sample is a box representing first and third quartiles; line inside the box represents second quartile. Whiskers represent 10th and 90th percentile. Bottom image: signal intensity on x-axis and signal density on y-axis. The signals from gene probesets are proportional; the highest peak suggests that intensity of high amount of probes have very low expression, most likely those are probes without matched gene identifier, that were filtered out prior to analysis. The smaller peak has normal distribution of intensities suggesting those are intensities from probes with matched gene identifier.

APPENDIX D

TABLE OF ENRICHED GO TERMS IN *PCDH17* MO WITH P≤0.05

GO ID is a unique identifier assigned by GO consortium. GO type refers to three ontologies, abbreviated as: BP – biological process, MF – molecular function, CC – cellular component. Number of DEGs annotated to each enriched GO term is listed in "DEGs #" column. The percentage of DEGs within the total number of genes in each GO group is listed in "DEGs % in term" column.

GO Term	GO ID	GO Type	Fisher's Exact	DEGs #	DEGs % in term
neuron differentiation	30182	BP	6.98E-06	7	3.33
cone photoresponse recovery	36368	BP	6.88E-05	2	50.00
rhodopsin kinase activity	50254	MF	6.88E-05	2	50.00
cell differentiation	30154	BP	1.06E-04	12	1.21
G protein-coupled receptor kinase activity	4703	MF	3.18E-04	2	25.00
forebrain neuron development	21884	BP	4.08E-04	2	22.22
fructose 6-phosphate metabolic process	6002	BP	5.09E-04	2	20.00
DNA-binding transcription factor activity, RNA polymerase II-specific	981	MF	6.49E-04	11	1.06
response to light stimulus	9416	BP	6.84E-04	4	3.42

transport vesicle membrane	30658	CC	9.75E-04	3	5.26
neuromuscular junction	31594	CC	1.02E-03	2	14.29
DNA-binding transcription factor activity	3700	MF	1.12E-03	11	0.99
neuron development	48666	BP	1.13E-03	4	2.99
ectodermal placode development	71696	BP	1.18E-03	2	13.33
fructose 1,6-bisphosphate metabolic process	30388	BP	1.34E-03	2	12.50
response to radiation	9314	BP	1.52E-03	4	2.76
central nervous system neuron development	21954	BP	1.70E-03	2	11.11
anterior/posterior pattern specification	9952	BP	1.80E-03	4	2.63
RNA polymerase II transcription regulatory region sequence-specific DNA binding	977	MF	2.22E-03	10	0.98
spinal cord motor neuron differentiation	21522	BP	2.32E-03	2	9.52
regionalization	3002	BP	2.81E-03	5	1.76
inner ear morphogenesis	42472	BP	3.03E-03	2	8.33
regulatory region nucleic acid binding	1067	MF	3.12E-03	10	0.93
transcription regulatory region sequence-specific DNA binding	976	MF	3.12E-03	10	0.93

cellular developmental process	48869	BP	3.53E-03	12	0.81
midbrain-hindbrain boundary development	30917	BP	3.55E-03	2	7.69
vesicle docking involved in exocytosis	6904	BP	3.83E-03	2	7.41
sequence-specific double-stranded DNA binding	1990837	MF	3.95E-03	10	0.90
protein dimerization activity	46983	MF	4.32E-03	5	1.59
double-stranded DNA binding	3690	MF	5.17E-03	10	0.87
forebrain development	30900	BP	5.35E-03	2	6.25
transcription regulator activity	140110	MF	5.67E-03	11	0.81
sequence-specific DNA binding	43565	MF	6.52E-03	10	0.84
cell differentiation in spinal cord	21515	BP	6.73E-03	2	5.56
glucose metabolic process	6006	BP	6.73E-03	2	5.56
synaptic vesicle membrane	30672	CC	7.48E-03	2	5.26
exocytic vesicle membrane	99501	CC	7.48E-03	2	5.26
presynapse	98793	CC	7.48E-03	2	5.26
phototransduction	7602	BP	7.48E-03	2	5.26
photoreceptor activity	9881	MF	7.48E-03	2	5.26

cytoplasmic vesicle membrane	30659	CC	7.86E-03	3	2.52
retina development in camera-type eye	60041	BP	8.23E-03	3	2.48
vesicle membrane	12506	CC	8.41E-03	3	2.46
exocytic process	140029	BP	8.67E-03	2	4.88
regulation of neurogenesis	50767	BP	9.39E-03	3	2.36
alcohol transmembrane transporter activity	15665	MF	1.02E-02	1	33.33
retinol transmembrane transporter activity	34632	MF	1.02E-02	1	33.33
fructose 1,6-bisphosphate 1-phosphatase activity	42132	MF	1.02E-02	1	33.33
disaccharide biosynthetic process	46351	BP	1.02E-02	1	33.33
sucrose metabolic process	5985	BP	1.02E-02	1	33.33
sucrose biosynthetic process	5986	BP	1.02E-02	1	33.33
social behavior	35176	BP	1.02E-02	1	33.33
biological process involved in intraspecies interaction between organisms	51703	BP	1.02E-02	1	33.33
regulation of Wnt signaling pathway, planar cell polarity pathway	2000095	BP	1.02E-02	1	33.33
thyroid hormone binding	70324	MF	1.02E-02	1	33.33

optic cup morphogenesis involved in camera-type eye development	2072	BP	1.02E-02	1	33.33
detection of light stimulus	9583	BP	1.08E-02	2	4.35
calcium ion binding	5509	MF	1.13E-02	6	1.08
vesicle docking	48278	BP	1.17E-02	2	4.17
regulation of nervous system development	51960	BP	1.20E-02	3	2.16
integral component of plasma membrane	5887	CC	1.23E-02	7	0.95
central nervous system neuron differentiation	21953	BP	1.27E-02	2	4.00
synapse	45202	CC	1.28E-02	4	1.51
identical protein binding	42802	MF	1.34E-02	3	2.07
retinol binding	19841	MF	1.36E-02	1	25.00
epidermal cell fate specification	9957	BP	1.36E-02	1	25.00
disaccharide metabolic process	5984	BP	1.36E-02	1	25.00
mammillary body development	21767	BP	1.36E-02	1	25.00
bile acid binding	32052	MF	1.36E-02	1	25.00
intrinsic component of plasma membrane	31226	CC	1.41E-02	7	0.93
organelle localization by membrane tethering	140056	BP	1.47E-02	2	3.70
membrane docking	22406	BP	1.47E-02	2	3.70

regulation of cell development	60284	BP	1.60E-02	3	1.94
regulation of cellular macromolecule biosynthetic process	2000112	BP	1.61E-02	13	0.65
syntaxin binding	19905	MF	1.63E-02	2	3.51
regulation of macromolecule biosynthetic process	10556	BP	1.64E-02	13	0.65
pattern specification process	7389	BP	1.64E-02	5	1.15
somatic motor neuron differentiation	21523	BP	1.70E-02	1	20.00
E-box binding	70888	MF	1.70E-02	1	20.00
cranial ganglion development	61550	BP	1.70E-02	1	20.00
cerebrospinal fluid circulation	90660	BP	1.70E-02	1	20.00
GABA-gated chloride ion channel activity	22851	MF	1.70E-02	1	20.00
synaptic transmission, GABAergic	51932	BP	1.70E-02	1	20.00
benzodiazepine receptor activity	8503	MF	1.70E-02	1	20.00
regulation of cellular biosynthetic process	31326	BP	1.80E-02	13	0.64
hexose metabolic process	19318	BP	1.85E-02	2	3.28
regulation of biosynthetic process	9889	BP	1.91E-02	13	0.63

response to abiotic stimulus	9628	BP	1.91E-02	4	1.34
regulation of nucleic acid-templated transcription	1903506	BP	1.93E-02	12	0.65
regulation of transcription, DNA-templated	6355	BP	1.93E-02	12	0.65
regulation of RNA biosynthetic process	2001141	BP	1.94E-02	12	0.65
cellular anatomical entity	110165	CC	1.96E-02	49	0.39
neurogenesis	22008	BP	2.03E-02	2	3.13
6-phosphofructokinase activity	3872	MF	2.04E-02	1	16.67
6-phosphofructokinase complex	5945	CC	2.04E-02	1	16.67
glucose catabolic process	6007	BP	2.04E-02	1	16.67
glycolytic process through fructose-6-phosphate	61615	BP	2.04E-02	1	16.67
glycolytic process through glucose-6-phosphate	61620	BP	2.04E-02	1	16.67
canonical glycolysis	61621	BP	2.04E-02	1	16.67
glucose catabolic process to pyruvate	61718	BP	2.04E-02	1	16.67
NADH regeneration	6735	BP	2.04E-02	1	16.67
olfactory bulb development	21772	BP	2.04E-02	1	16.67

peripheral nervous system neuron development	48935	BP	2.04E-02	1	16.67
olfactory placode development	71698	BP	2.04E-02	1	16.67
oligosaccharide biosynthetic process	9312	BP	2.04E-02	1	16.67
ligand-gated sodium channel activity	15280	MF	2.04E-02	1	16.67
DNA binding	3677	MF	2.13E-02	11	0.67
RNA polymerase II cis-regulatory region sequence-specific DNA binding	978	MF	2.20E-02	7	0.85
monosaccharide metabolic process	5996	BP	2.27E-02	2	2.94
nervous system process	50877	BP	2.28E-02	4	1.27
nuclear receptor activity	4879	MF	2.33E-02	2	2.90
cis-regulatory region sequence-specific DNA binding	987	MF	2.36E-02	7	0.83
sclerotome development	61056	BP	2.37E-02	1	14.29
fructose-6-phosphate binding	70095	MF	2.37E-02	1	14.29
regulation of amyloid precursor protein biosynthetic process	42984	BP	2.37E-02	1	14.29
Wnt signaling pathway, planar cell polarity pathway	60071	BP	2.37E-02	1	14.29

auditory receptor cell development	60117	BP	2.37E-02	1	14.29
cAMP biosynthetic process	6171	BP	2.37E-02	1	14.29
ligand-activated transcription factor activity	98531	MF	2.40E-02	2	2.86
regulation of transcription by RNA polymerase II	6357	BP	2.41E-02	10	0.69
sensory organ development	7423	BP	2.44E-02	3	1.65
detection of external stimulus	9581	BP	2.46E-02	2	2.82
detection of abiotic stimulus	9582	BP	2.46E-02	2	2.82
phosphoric ester hydrolase activity	42578	MF	2.50E-02	4	1.23
ganglion development	61548	BP	2.71E-02	1	12.50
alpha-tubulin binding	43014	MF	2.71E-02	1	12.50
SRP-dependent cotranslational protein targeting to membrane, translocation	6616	BP	2.71E-02	1	12.50
fourth ventricle development	21592	BP	2.71E-02	1	12.50
adenylate cyclase activity	4016	MF	2.71E-02	1	12.50
sarcomere	30017	CC	3.04E-02	1	11.11
proteasome regulatory particle, base subcomplex	8540	CC	3.04E-02	1	11.11

hexose catabolic process	19320	BP	3.04E-02	1	11.11
bile acid and bile salt transport	15721	BP	3.04E-02	1	11.11
dipeptidyl-peptidase activity	8239	MF	3.04E-02	1	11.11
otic vesicle morphogenesis	71600	BP	3.04E-02	1	11.11
fructose metabolic process	6000	BP	3.04E-02	1	11.11
regulation of establishment of planar polarity	90175	BP	3.04E-02	1	11.11
cell junction	30054	CC	3.06E-02	5	0.97
cell-cell signaling	7267	BP	3.07E-02	3	1.51
organophosphate metabolic process	19637	BP	3.10E-02	5	0.97
regulation of cell differentiation	45595	BP	3.14E-02	4	1.15
protein homodimerization activity	42803	MF	3.14E-02	2	2.47
regulation of RNA metabolic process	51252	BP	3.18E-02	12	0.61
multicellular organismal process	32501	BP	3.20E-02	11	0.63
segmentation	35282	BP	3.21E-02	2	2.44
axon terminus	43679	CC	3.37E-02	1	10.00
central nervous system morphogenesis	21551	BP	3.37E-02	1	10.00

diencephalon development	21536	BP	3.37E-02	1	10.00
regulation of glycoprotein biosynthetic process	10559	BP	3.37E-02	1	10.00
regulation of glycoprotein metabolic process	1903018	BP	3.37E-02	1	10.00
detection of visible light	9584	BP	3.37E-02	1	10.00
retinol metabolic process	42572	BP	3.37E-02	1	10.00
morphogenesis of embryonic epithelium	16331	BP	3.37E-02	1	10.00
lysophospholipase activity	4622	MF	3.37E-02	1	10.00
purine-containing compound metabolic process	72521	BP	3.39E-02	3	1.45
phosphate-containing compound metabolic process	6796	BP	3.54E-02	9	0.68
regulation of cation transmembrane transport	1904062	BP	3.66E-02	2	2.27
skeletal myofibril assembly	14866	BP	3.71E-02	1	9.09
proteasome assembly	43248	BP	3.71E-02	1	9.09
monosaccharide catabolic process	46365	BP	3.71E-02	1	9.09
phosphofructokinase activity	8443	MF	3.71E-02	1	9.09

neuron projection terminus	44306	CC	3.71E-02	1	9.09
hindbrain morphogenesis	21575	BP	3.71E-02	1	9.09
otic vesicle formation	30916	BP	3.71E-02	1	9.09
cilium or flagellum-dependent cell motility	1539	BP	3.71E-02	1	9.09
cilium-dependent cell motility	60285	BP	3.71E-02	1	9.09
voltage-gated sodium channel activity	5248	MF	3.71E-02	1	9.09
hormone transport	9914	BP	3.71E-02	1	9.09
dendrite membrane	32590	CC	3.71E-02	1	9.09
inhibitory extracellular ligand-gated ion channel activity	5237	MF	3.71E-02	1	9.09
negative regulation of inflammatory response	50728	BP	3.71E-02	1	9.09
glutathione peroxidase activity	4602	MF	3.71E-02	1	9.09
phosphorus metabolic process	6793	BP	3.82E-02	9	0.67
regulation of nucleobase-containing compound metabolic process	19219	BP	3.85E-02	12	0.59
carbohydrate phosphatase activity	19203	MF	4.04E-02	1	8.33
sugar-phosphatase activity	50308	MF	4.04E-02	1	8.33

gamma-aminobutyric acid signaling pathway	7214	BP	4.04E-02	1	8.33
secretory granule membrane	30667	CC	4.04E-02	1	8.33
glycerophospholipid catabolic process	46475	BP	4.04E-02	1	8.33
signaling	23052	BP	4.23E-02	3	1.33
regulation of transport	51049	BP	4.29E-02	4	1.04
ventral spinal cord interneuron differentiation	21514	BP	4.37E-02	1	7.69
determination of pancreatic left/right asymmetry	35469	BP	4.37E-02	1	7.69
isoprenoid binding	19840	MF	4.37E-02	1	7.69
retinoid binding	5501	MF	4.37E-02	1	7.69
NAD metabolic process	19674	BP	4.37E-02	1	7.69
NADH metabolic process	6734	BP	4.37E-02	1	7.69
axon regeneration	31103	BP	4.37E-02	1	7.69
regulation of postsynaptic membrane potential	60078	BP	4.37E-02	1	7.69
ligand-gated anion channel activity	99095	MF	4.37E-02	1	7.69
pronephric glomerulus morphogenesis	35775	BP	4.37E-02	1	7.69
glomerulus morphogenesis	72102	BP	4.37E-02	1	7.69

cAMP metabolic process	46058	BP	4.37E-02	1	7.69
tube morphogenesis	35239	BP	4.65E-02	3	1.28
PDZ domain binding	30165	MF	4.69E-02	1	7.14
regulation of potassium ion transmembrane transport	1901379	BP	4.69E-02	1	7.14
neuron projection fasciculation	106030	BP	4.69E-02	1	7.14
habenula development	21986	BP	4.69E-02	1	7.14
generation of neurons	48699	BP	4.69E-02	1	7.14
axonal fasciculation	7413	BP	4.69E-02	1	7.14
otolith morphogenesis	32474	BP	4.69E-02	1	7.14
semicircular canal morphogenesis	48752	BP	4.69E-02	1	7.14
phosphatidate phosphatase activity	8195	MF	4.69E-02	1	7.14
SNARE binding	149	MF	4.86E-02	2	1.94
molecular_function	3674	MF	4.89E-02	50	0.38